AN EXPERIMENTAL INVESTIGATION OF HIGH DOSE RATE ELECTRON BEAM IRRADIATION OF PETROLEUM IN A CONTINUOUS FLOW SYSTEM

A Dissertation

By

KUNPENG WANG

Submitted to the Office of Graduate and Professional Studies of
Texas A&M University
in partial fulfillment of the requirements for the degree of

DOCTOR OF PHILOSOPHY

Chair of Committee,	David Staack
Committee Members,	Eric Petersen
	Maria A. Barrufet
	Adolfo Delgado
Head of Department,	Andreas A. Polycarpou

December 2019

Major Subject: Mechanical Engineering

ABSTRACT

High dose rate electron beam (10 MeV, 15 kW, LINAC) irradiation was investigated as a potential technology for heavy oil upgrading. The flow system allows irradiation of crude oils at constant temperature while bubbling natural gas through the oil. Experimental parameters including dose, temperature, shear rate and dose rate were allowed to change in order to find the optimal condition. Pure hydrocarbons were selected and irradiated by the same source at low temperatures. Results revealed that conversion and product yields not only depends on those irradiation conditions, but also relies on the molecular structure of irradiated compounds.

Irradiation of petroleum activates hydrocarbon compounds which subsequently undergo a series of chemical reactions including radical initiation, propagation and termination. Two reaction pathways could be initiated by absorbed energy, then compete inside the irradiated compounds and eventually lead to multiple products. Cracking is due to hydrocarbon chain scission and produces products smaller than the parent molecules. Polymerization is caused by molecule recombination and produces products larger than the parent molecules. Cracking and polymerization could be enhanced or suppressed by altering irradiation conditions such as irradiation temperature and total absorbed energy. To selectively favor one of them and suppress the other one requires detailed investigation of many parameters. In general, higher dose rate and higher temperature favor cracking reactions.

Fundamental studies were conducted by irradiating pure and neat hydrocarbon compounds with the same electron beam source. Responses from irradiating different compounds varied dramatically. Saturated hydrocarbons tended to produce the most products. The presence of rings on a saturated hydrocarbon greatly enhanced its tendency toward polymerized products which are commonly dimers and trimers. Unsaturated hydrocarbons were less reactive with lower yields of products. One unsaturated ring on a molecule will tremendously suppress its reactivity toward chain scission products and only produce detectable polymerized species. Stability of a hydrocarbon compound and its radiation product pattern are closely related to its molecular structure. The saturation degree of a molecule and its average bond strength could be used to characterize the stability and product yields for a compound.

Crude oil is a complex mixture of thousands of hydrocarbon compounds and non-hydrocarbons. Conversion and product yields from irradiating crudes do not simply resemble those from irradiation of pure compounds due to unknown chemical composition and unknown reaction pathways. This explains why it is so challenging to predict heavy oil conversion under electron beam irradiation. Crude oils could be separated into a few fractions, e.g. saturates, aromatics, resin and asphaltene. Irradiation of each fraction may follow the same results obtained from irradiating pure and neat compounds. Saturates should have the highest conversion to light products whereas everything else either is chemically stable or polymerizes. That provides a possibility of improving the total conversion and product yields from crude oil irradiation by separating crudes into different fractions, then selectively irradiating the saturates and avoiding other fractions.

ACKNOWLEDGEMENTS

I would like to thank my graduate advisor Dr. David Staack for his continuous support and guidance through my entire PhD program. His encyclopedic knowledge and passion for doing better research have been a constant source of inspiration. I am also very grateful to my committee members, Dr. Eric Petersen, Dr. Maria Barrufet and Dr. Adolfo Delgado, for their guidance and valuable comments on this dissertation research. I would also like to thank Chevron for their funding of my research and education.

I truly enjoyed the research and work I have been doing in the past five years at the Plasma Engineering and Non-equilibrium Processing Laboratory. Many thanks go to my colleagues and best friends in this lab: Harika, Ilan, Kalissa, Kenneth, John, Matthew, Chris, Xin and others who have graduated. They have created one of the best environment to do research and collaborate with each other. Thank the mechanical department faculty and staff for making my time at Texas A&M University a great experience.

It has been a great pleasure to work with people in the national center for electron beam research at Texas A&M University. I learned a lot from working with them and talking with them. I would like to thank them for everything they have done for me.

Finally, thanks to my mother and father for their unconditional love, encouragement and support. They have always been my heroes while I pursued my dreams.

CONTRIBUTORS AND FUNDING SOURCES

This work was carried out with the assistance of several of my colleagues in the plasma lab. Harika Rao Damarla gave me tremendous help during the test days at the electron beam facility. She also conducted GC and viscosity measurements for treated samples. Ilan Clifford Berman helped design the mobile lab and transported the lab to ebeam facility during test days. Finally, Josef Sebastian, John Lassalle and Kenneth Evans also contributed their efforts to this work and I would like to recognize them.

Much of this work was funded by and supported by grants from Chevron.

TABLE OF CONTENTS

Page

Page

Page

Page

LIST OF FIGURES

Page

LIST OF TABLES

Page

CHAPTER I

INTRODUCTION

1.1 Background

Although heavy and extra heavy oil represents at least half of the recoverable oil resources all over the world, the demand for them has never been significant due to their high viscosity and composition complexity. Their extraction from the subsurface and transport are more difficult. This generally results in a lower recovery rate for the oil in place and higher development and exploitation costs. Its intrinsic low hydrogen to carbon ratio make the processing of them into light and valuable products harder. By 2005, the estimated worldwide production of heavy crude, extra heavy crude and bitumen represented nearly 10% of total crude production, while extra heavy and bitumen production only accounted for 2-3%[1–3].

However, with the quick depletion of the conventional oil resources and continually increasing energy consumption, we already see more exploitation of unconventional crude oils. Both national and international oil companies have realized this and they are investing more in the development of heavy and extra heavy oil resources. The world demand for crude oil has increased from 60 million barrels per day to 84 million barrels per day, in the past 20 years[4].

Oil recovery and refining techniques, such as thermal cracking, catalytic and hydro-cracking have been very successful applied on conventional oils and they are very well adapted to the conventional oil characteristics and the market after over hundred

years' operation and market evolution. Upgrading involves a series of physical and chemical processes and is very commonly used to increase the value of heavy or extra-heavy petroleum products. In particular, bitumen can be extracted and upgraded into synthetic crude oil (SCO), a substitute to conventional oil. However, these resources involve higher CO_2 emissions per unit of energy produced than conventional oil and gas, as they require more energy to be extracted and upgraded. Plus the synthetic crude oil produced by full upgrading directly competes with the dramatically expanding supply of light unconventional oil. Due to multiple reasons not limited to what have been mentioned above, SCO will not be economically or practically produced from a full upgrader. Partial upgrading is defined as any combination of processing steps and reduces diluent to meet the specifications for pipeline transport. Compared to full upgrading which produces SCO, partial upgrader produces a crude oil that has characteristics more comparable to medium or heavy crude. It has both lower capital cost and operation cost per barrel. It therefore might represent a great opportunity to process extra heavy oil or bitumen into a product with higher value, and a product with better market conditions than SCO. The special properties of heavy crude oils require specifically-adapted technical solutions to be used throughout the development chain from upstream to downstream. On one hand, more partial upgrading methods need to be developed to work with higher density and viscosity oils; on the other hand, development of effective and economic technology becomes more and more important. The goal is to decrease exploitation costs and increase the amount of ultimately recoverable reserves, while maintaining acceptable overall energy efficiency for the production-transport-processing system.

Irradiation of petroleum with electron beam is fundamental different from most refining technologies currently used in oil and gas industry, such as catalytic thermal cracking, Visbreaking and coking process. Those process operates at thermal equilibrium with temperatures above 350 ^{o}C and pressures significantly above the ambient pressures. Electron beam radiation method uses high speed electrons and allow them to collide with molecules in the oil sample at ambient conditions. Collision between high energy electrons and molecules result in changes in oil fraction contents and chemical compositions to the sample. Irradiation process is highly non-equilibrium in nature and does not follow classics thermodynamic rules that was applied in equilibrium process. The radiation method in theory could still work at much lower temperature and pressure based on its non-equilibrium property. One of the most prominent advantages is its lower operating temperature and pressure compared to most existing technologies. For example the capital cost of a high pressure system might increase exponentially with the rated pressure, which will make the radiation method much more economically competitive. Ideally radiation processing temperature and pressure could be as low as ambient conditions if other radiation parameters are satisfied.

Radiation processing of petroleum are associated with multiple hydrocarbon transformation process including chain cracking and chain growing process. Production of new compounds and consumptions of preexisting compounds are the results of those process. The key to the success of radiation processing of petroleum compounds is to control parameters that favor desired process such as chain cracking and un-favor process such as polymerization and crosslinking. But it is very important to realize that those

processes coexist and compete during radiation processing. Of course chemical change induced by irradiation on petroleum compounds changes with the compounds. Different fractions present in petroleum vary dramatically in their physicochemical properties, which causes very different, even unique responses from them upon radiation.

1.2 Thesis Statement

This dissertation describes the theory and application of high energy electron beam irradiation of petroleum in both continuous flow system and batch system. Irradiation of heavy crude oils was first experimentally investigated as a potential upgrading technology. Parametric study on the effects of a series of operating parameters such as dose rate, dose, processing temperatures, gas bubbling gas and shear rate on irradiation of crude oils was conducted. Irradiation of the crude oils is able to chemically change the molecule structure and distribution among hydrocarbons, e.g. longer chain molecules convert to shorter chain molecules and smaller molecules may combine through polymerization. Change of irradiated samples are studied by different techniques such as gas chromatography and rheological measurement device. However, Changes in crude oils induced by irradiation are often difficult to characterize due to a large number of chemical compounds with unknown chemical structure. This necessitates the study of irradiating neat hydrocarbons under the same radiation source. Results from irradiating neat materials are more interpretable and possess less uncertainties by its nature. It allows us to more accurately perform fundamental studies on irradiation of petroleum. Petroleum is essentially a mixture of different neat hydrocarbons with small fraction of impurities. Knowledge

learned from irradiating neat hydrocarbons tremendously helped us understand the irradiation process of petroleum.

This dissertation is illustrated in four major sections: the first section provides the basic theory regarding electron beam irradiation of materials and responses from radiating different liquid materials. The second section introduces experimental setup and design of experiment that have been used in this project. Reactor design and function of individual component in the system are discussed in details. The third second describes major experimental findings from irradiation of heavy oil samples with different irradiation parameters. The last section provides insight into the heavy crude processing by analyzing results from irradiating neat and pure hydrocarbons (e.g. mineral oil, neat alkanes, and hydrocarbons with more complex structure).

1.3 Motivation

Since the operating temperatures of LTRC and CRC are below 350 ^{o}C, which is significant lower than that in thermal cracking and thermal catalytic cracking, they represent a more energy efficient process by avoiding huge energy expenses during the feedstock preheating. So in this research only low temperature irradiation method will be investigated and conversion, yields of products and economic analysis associated with this method will be conducted as well. The essential component for this process is an electron accelerator which is used to generate high energy electron beams as reaction initiator when colliding with irradiated molecules. The other unit is a controllable continuous flow system which allows flowing high viscosity crude oils to the irradiation processing reactor.

This system would also allow comparison with conventional refining on the chemical yields, energy consumption and energy cost or overall economics. It could provide insight into the feasibility of radiation processing of crude oils. Primary operating parameters in this irradiation cracking process have been identified in previous work. They include oil processing temperature, dose rate, total absorbed dose, gas bubbling type and the chemical reactor type. Studies were conducted on irradiating pure and neat hydrocarbons to understand the fundamental mechanism of hydrocarbon irradiation. Hydrocarbon with different structure to represent different fractions in crude oils were selectively irradiated. Results from them could be used to establish a correlation between each fraction and conversion and yields. The combination of heavy oil irradiation and fundamental understanding of irradiation of pure compounds will help us find the optimal conditions for heavy oil upgrading by high energy electron beam irradiation.

1.4 Objectives

1. Design and construction of a continuous flow system capable of working with high energy (10MeV) electron beam.
2. Processing heavy crude oil at lower temperatures with desired experimental conditions.
3. Independently evaluating effects of dose (50-1500 kGy), shear rate (0-150 s^{-1}) and temperature (100-300 ^{o}C) on conversion and product yields.
4. Studying the mechanism of high dose rate electron beam irradiation of neat and pure hydrocarbon compounds.

5. Identify parameters that affect conversion and product of petroleum irradiation
6. Evaluation of electron beam irradiation of heavy oil potentials and limitations based on results and understanding.

CHAPTER II

LITERATURE REVIEW

2.1 Refinery Process

Crude oils contain thousands of different compounds that vary in multiple aspects including molecular weight, boiling point and many chemical properties[5–7]. Molecular weight could range very broadly from methane (CH_4, 16) to a few thousands (asphaltene). The corresponding boiling point also varies dramatically from -162.5 ^oC to more than 500 ^oC as seen in figure 1. Refining process involves a series of physical and chemical methods to deal with different feedstock in refinery[8–10]. Specifically those process include different thermal, catalytic and combined processes. The goal is to convert molecules in heavier fractions to smaller molecules in lighter fractions or separate different fractions based on their distinctive properties. A refinery is an integrated network composed with individual unit process that is used to achieve different goals in the refining process. Depending the refined product, unit process was selected and incorporate in the system.

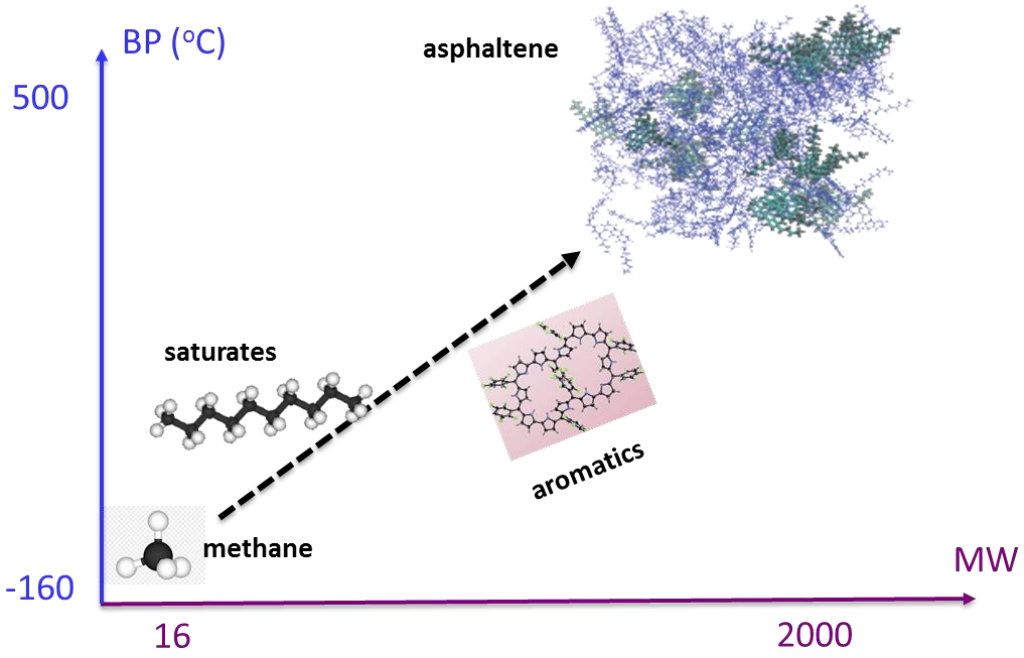

Figure 1: Components in crude oil vary with molecular weight and boiling point

Refining process in a refinery needs to work with specific feedstock and once feedstock is known individual process could be developed. Feedstock might be very different in nature so that each refinery should also be very different. But in general refinery process could be divided into three major categories: Separation, Conversion and Finishing[11].

Separation involves the use of distillation to separate streams from the raw based on a narrow boiling window or treatment with water solutions to remove impurities like salts and dirt[12]. Even though the main purpose of this process might be achieved through a pure physical process, chemistry is often present that could make this process more complex and less controllable. Finishing as it represents is used to purify the product stream and remove impurities. It includes various processes that could be essentially used

to modify the product depending on the need. For example, reforming process to improve gasoline quality could be one of the finishing process. Conversion is fundamentally different from separation since it in essence represents process that could change the molecular structure of hydrocarbons in petroleum[13,14]. Molecular structure of compounds will be changed if the number of carbons or hydrogens per molecule is changed or there is process like isomerization happened which could change the shape of the molecules. In refinery conversion process was normally designed to convert large molecules with higher boiling point to small molecules with lower boiling point. Streams with lower boiling point compounds are more valuable and used more in market, e.g. gasoline and diesel.

2.2 Refining Chemistry

There is complex and different chemistry with regard to each refining process. Nevertheless chemistry in conversion process is ultimately the most important and useful, since the goal of conversion is to convert heavy molecules to light molecules by having the correct chemistry in a refinery.

2.2.1 Thermal Cracking

Cracking reactions plays an important role in processes for upgrading residues, heavy oils as well as bitumen. Cracking refers to a process in which higher boiling point and higher molecular weight constituents in petroleum are converted to lower boiling point and smaller molecular weight constituents. It is the most used techniques in current

petroleum industry. It operates at elevated temperatures (>350 ^{o}C) and relatively high pressures depending on many other parameters such as feedstock and whether gas was used in the process. Reactions such as cleavage of side chains, ring opening of naphthenic and hydro aromatic compounds and dealkylation of alkyl aromatics are primary reactions which are responsible for reducing molecular weight and converting to lighter fractions in the petroleum[15,16]. The development of thermal cracking was largely driven by the demand of gasoline for automobiles. Gasoline derived from the cracking process was believed to be better than that from distillation of unrefined petroleum. And the advancement of engines and cars also require more production of high standard gasoline, which could offer better combustion characteristics and emission property. Visbreaking and delayed coking are still selected by refineries nowadays for partial or bottom of the barrel upgrading, because of their flexibility to handle any type of feedstock and economic advantages without requiring expensive catalysts in the process [17]. They both apply the thermal cracking process and seek to convert heavy molecules to light molecules. Major differences between them include the operation conditions and the fundamental goal of the process. Visbreaking operates at relatively mild thermal conditions and may be applied to both atmospheric residue (AR) and (vacuum residue). The goal is to reduce viscosity of residua to meet specifications. This process uses mild thermal cracking conditions with relatively short residence time to prevent coke formation[18,19]. Figure 2 shows a typical soaker visbreaker unit[20]. Delayed coking is a bottom of the barrel upgrading process that essentially reject all the metals and precursors to coke while partially or completely converting feedstock to naphtha and diesel. It is a combined process with thermal cracking

and condensation reactions, and consumes large amount of high grade energy. It requires high temperatures and longer residence time to secure the complete rejection of metals and coke precursors[21].

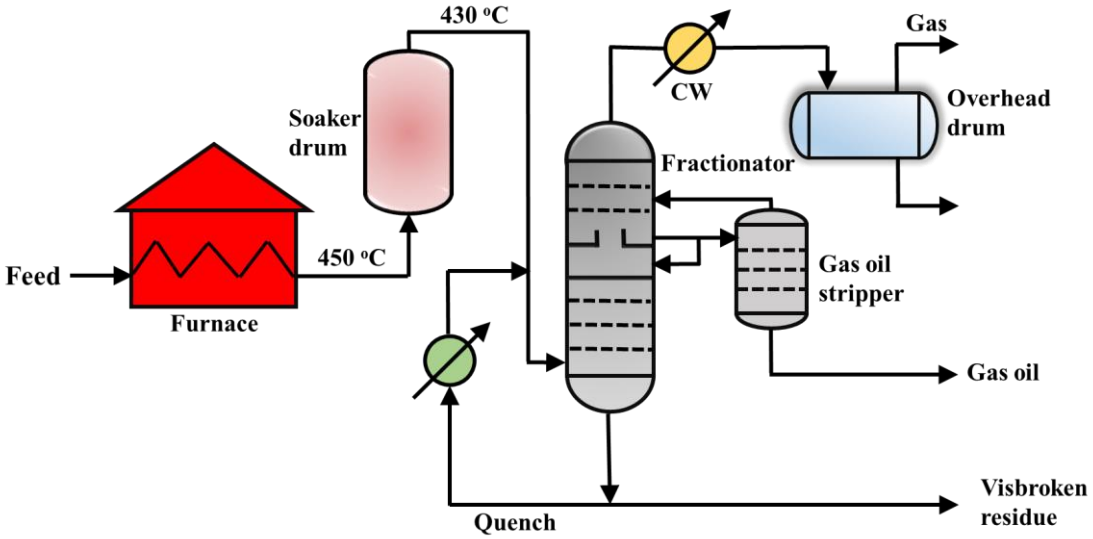

Figure 2: A typical soaker Visbreaking unit

Thermal cracking processes in refinery are essentially processes that convert low value large molecule hydrocarbons to high value small molecules by the addition of heat. Thermal cracking process happens at a thermodynamic equilibrium where not only all compounds are in thermal equilibrium with each other, at microscale all states within a compound are also in thermal equilibrium[22]. It is reasonable to assume that cracking reactions in the chamber are uniform in space. Major variables involved in the process are thermodynamic conditions (temperature and pressure), residence time and feedstock type.

In cracking process, molecules decomposition rate depends on thermodynamic conditions such as temperature and pressure.

Thermal cracking reactions are free radical chain reactions that involves multiple reaction steps: radical initiation that creates free radicals. Radicals are molecules with an unpaired electrons. Free radicals are reactive and have a short life time in nature. They react with other molecules to create new molecules or more radicals. Product distribution largely depends on how radicals interact with other molecules and if they are able to create more free radicals to continue the chain reactions. Propagation is next step after initiation. Once a free radical was created, it will react with other molecules and produce a new radical. This step is the key to cracking process, because to sustain cracking reactions, new radicals have to be created and propagate. Reactions could be terminated through multiple ways. Thermal cracking termination may refer to radical-radical combination, molecules isomerization or polymerization. Reaction pathways in termination are hard to predict and highly dependent on radical behavior and local chemistry.

Behavior of compounds in petroleum vary significantly even in the same thermal environment. Thermal stability largely determines whether a specific hydrocarbon will start to have chemical change[15]. Paraffins with longer straight chain tend to change first under a thermal environment because of a low thermal stability. Olefins with a double bond are also quite reactive because of the double bond. Cycloparaffins with ring structure are more stable against cracking. But they can also be cracked on the side chains which have less bonding with the main ring structure. Aromatics and polycyclic hydrocarbon molecules have the least possibility toward cracking. They are usually not the target

compounds in any thermal cracking refinery. Cracking process in petroleum is probably too complex to study its mechanism simply because the number of compounds is too large. Nevertheless, people have extensively studied cracking reactions based on modelled molecules such as n-hexadecane. Khorasheh[23] studied the reaction mechanism and kinetics of thermal cracking of n-hexadecane under pressures (13.9 MPa) and temperatures (380-450 ^{o}C). He compared two preexisting mechanisms, namely the R-K mechanism and F-S-S mechanism and modified some of their features to account for the formation of large alkane molecules. A kinetic model was developed based on free radical mechanism to more comprehensively predict products in full carbon range[24].

$$n - C_{16}H_{34} \rightarrow R_i^* + R_j^*$$

$$R^* + n - C_{16}H_{34} \rightarrow R - H + C^{16}H_{33}{}^*$$

$$primary\ C^{16}H_{33}{}^* \rightarrow secondary\ C^{16}H_{33}{}^* \qquad (isomerization)$$

$$primary\ C^{16}H_{33}{}^* \rightarrow\ primary\ C^{16}H_{33}{}^* +\ C_2H_4 \qquad (\beta = scission)$$

$$secondary\ \ C^{16}H_{33}{}^* \rightarrow\ C_nH_{2n+1}{}^* +\ C_mH_{2m} \qquad (\beta = scission, m + n = 16)$$

$$C_mH_{2m} +\ C^{16}H_{33}{}^* \rightarrow additional\ compounds$$

$$R^* +\ R^* \rightarrow products$$

A few key features about this mechanism: decomposition of n-hexadecane occurs with first order rate. Both chain scission products and chain growth products are present in products. Parent radical only decompose once to produce a 1-alkene radical and a smaller radical, and the smaller radical then stabilize by abstracting a hydrogen from $n - C_{16}H_{34}$. This mechanism results in an equal molar distribution of alkanes and 1-alkenes and very low gas selectivity. As decomposition steps are increased, the products shift

toward lower carbons and lower selectivity for high alkanes. It is only applied to liquid phase cracking because gas phase cracking involves more than one step decomposition of parent radicals and more $\beta - scission$ reactions. This results in not only larger amount of small molecule products, but also more alkenes than alkanes in the product distribution.

Even though the goal of thermal cracking is to produce light fraction in petroleum by converting heavy fractions under high temperature and high pressure. Reactions that could happen at given conditions, however are not very selective, which not only produce volatile products, but also result in the formation of high weight and high polarity aromatics components. The formation of high weight and high polarity materials always accompany phase separation when their concentration reach a certain level. A process like this may include cracking of side chains from large molecules and removal of hydrogens from a naphthenes to form aromatics as well as condensation of aliphatic structures, then condensation of aromatics to form large molecule aromatics, dimerization, polymerization or oligomerizations [25].

2.2.2 Catalytic Cracking

Catalytic cracking is a process for the conversion of various feedstocks into olefinic gas, high octane gasoline and diesel oil via acidic catalysts such as ZEM-5 zeolites [26,27]. It is also a conversion process similar as thermal cracking for both are thermal equilibrium driven process and requires sever thermal environment such as high temperatures. But catalytic cracking is a catalytic process and involve the usage of catalysts in the cracking process, which adds complexity and more parameters in the

control and operation [28]. Catalytic cracking process has been developed over almost hundred years since the early twentieth century. The incentives of developing this process was to produce high octane number gasoline after a series of methods have been tried and developed including blending gasoline with polymer and reformate or thermal reforming and polymerization [25]. There have been substantial advances in the development of catalytic process in the past 50 years. Significant progress have been made not only in understanding chemistry and physics in catalytic process, but also major achievements in the reactor design and computer aided process simulation, for example, catalysts, which are used to enhance the catalytic reactions, could be used in different shape and form either as a fixed bed, moving bed or fluid-bed configurations.

Fluid catalytic cracking (FCC) is one of the most representative and successful refining technologies. Both the catalytic cracking reaction and the catalyst regeneration are carried out in fluidized beds [29]. Compared to a fixed bed reactor, a FCC unit shown in figure 2 allows microspherical catalyst powders to be conveyed by the hydrocarbon vapors from the bottom to the top of a vertical lift line. The catalysts particles behave like a liquid and flow together into the reaction chamber where the cracking reactions take place. A cyclone located in the top of the reaction chamber was used to separate the cracked vapor and the catalysts powders by centrifugal force. Cracked vapor continue to flow into a bubble tower and fractioned into different components including light and heavy gas oils, gasoline fraction and cracked gases. One challenge of this type of reaction is the successful catalyst regeneration, since catalysts in the reaction chamber were contaminated with coke and need to be continuously withdrawn from the bottom of the

reactor. Normally a stream of fresh air will be blown into the bottom of the chamber and lift the used catalyst into a regenerator where coke is removed by controlled combustion process. Regenerated hot catalysts flow back into the feed line and enter reaction chamber again.

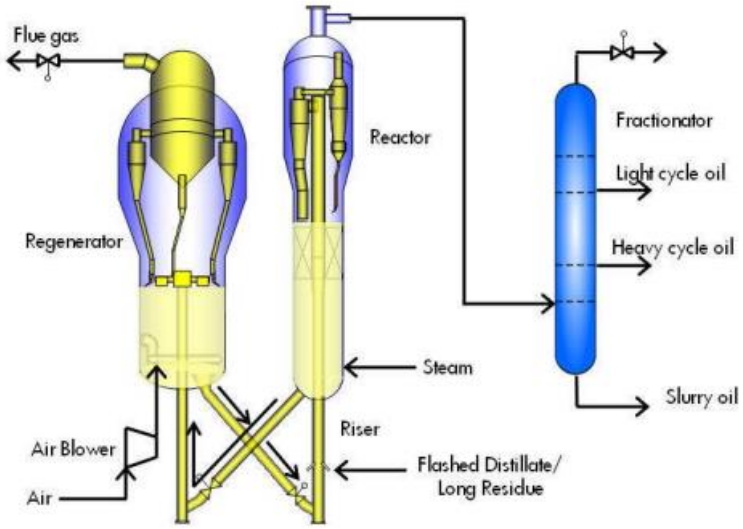

Figure 3: A typical FCC unit

A catalyst needs to have appreciable cracking activity when used in the FCC reaction chamber. The catalysts must have stable properties against physical and thermal impact in the regeneration process. They need to withstand harsh chemical environment under high temperature with different species such as sulfur compounds, air, steam and hydrocarbon vapors. Catalysts typically used in FCC unit are mixtures of porous and highly absorptive anhydrous silica and alumina (SiO_2-Al_2O_3) with a certain amount of water. Catalytic cracking like any other thermal cracking process is highly endothermic

and heat is absorbed by the reactions. As reaction proceeds and more products are being produced, temperature of the reaction mixture may drop significantly. A heat source must be provided to sustain the reaction. External heat is from the combustion of coke during catalyst regeneration process. Cracking reactions inside a FCC chamber are essentially heterogeneous reactions that take place on the catalysts surface in multiple steps: mass diffusion, chemisorption, chemical reaction and desorption[30]. Catalytic cracking mechanism is complex and depends on the type of catalysts and experimental conditions. It is different from thermal cracking which is not selective and results in highly olefinic products. Catalytic cracking produces more branched products and less olefinic species[14]. The main reaction schemes of catalytic cracking are considered to progress with the following reaction mechanism [31]:

Initiation:

$$R_1\text{-}CH_2{=}CH_2\text{-}R_2 + HZ \rightarrow R_1\text{-}CH_2\text{-}CH^+\text{-}R_2 + Z^- \text{ (Brønsted site catalyst)}$$

$$R_1\text{-}CH_2\text{-}CH_2\text{-}R_2 + L^+ \rightarrow R_1\text{-}CH_2\text{-}CH^+\text{-}R_2 + HL \text{ (Lewis site catalyst)}$$

Proton exchange:

$$R_1\text{-}CH_2\text{-}CH^+\text{-}R_2 + R_3\text{-}CH_2\text{-}CH_2\text{-}R_4 \rightarrow R_1\text{-}CH_2\text{-}CH_2\text{-}R_2 + R_3\text{-}CH_2\text{-}CH^+\text{-}R_4$$

Cracking:

$$R_3 \overset{\beta}{-} CH_2 \overset{\alpha}{-} CH^+ - R_4 \rightarrow R_3^+ + CH_2 = CH - R_4$$

Carbenium ions include $R_1\text{-}CH_2\text{-}CH^+\text{-}R_2$, $R_3\text{-}CH_2\text{-}CH^+$ and R_3^+. This cracking mechanism is called β scission, because the scission of the carbon bond occurs at the β position to the carbenium ion.

Carbenium ions undergo various reactions besides cracking as follows:

CH_3

Isomerization:

$$R - CH_2 - CH_2 - \mathrm{CH}^+ - CH_3 \rightarrow R - CH_2 - \overset{|}{C}^+ - CH_3$$

Hydrogen transfer:

$$3C_nH_{2n} + C_mH_{2m} \rightarrow 3C_nH_{2n+2} + C_mH_{2m-6}$$

The hydrogen transfer reactions explain why there is large amount of aromatic products.

2.2.3 Hydrocracking

Hydrocracking is another refining technology in modern petroleum refineries for converting a variety of feedstock to more value products such as gasoline, diesel and jet fuel [32–34]. It is a highly flexible process that could be utilized with other cracking process such as catalytic cracking or coking to break down high boiling aromatics from them. The concept of hydrocracking inside a refinery is to produce lower molecule weight compounds with higher hydrogen to carbon ratio and less yield of coke. It typically operates at high temperature and pressure (above 400^{o}C and 1000psi)[25]. Since hydrogen was heavily used in the reaction chamber under high pressure, that results in significant reactor design and heat transfer challenges due to the extremely thick wall thickness. Due to the nature of this process, the products of it are saturates to aromatics, no olefins are found. Probably because olefins are all saturated with hydrogen or cracked under an environment in the hydrocracking unit. Gasoline made in hydrocracking process are normally high quality with higher octane numbers. Challenges encountered in this process are similar to many other refineries when dealing with complex, heavy and viscous feedstock. Pretreatment like dewater and desalt as well as preheating are necessary.

Despite high temperature and high pressure in the process, hydrogen to oil ratio and catalysts are another two important parameters that may determine the conversion and product quality. For example, catalysts used in this process need to be bi-functional to promote both cracking and hydrogenation. Zeolite based catalysts are generally used in hydrocracking process and they are responsible for high cracking activity. Then metal elements such as nickel, tungsten, platinum and palladium could be supported by zeolites and they provide the hydrogenation function. Most zeolites based catalysts are synthesized from a mixture of silica and alumina through well controlled procedure and treatment. They possess good thermal and hydrothermal stability, and better resistance to nitrogen and sulfur compounds tan amorphous catalysts. In addition to the chemical or thermal properties of the catalysts, physical properties like the pore size and porosity are also important during the catalytic process, especially when it involves multiple phases and heterogeneous reactions. The main reason that might cause issues in a heterogeneous reaction is due to facts that gas and liquids phase have very different mass diffusion ability near the catalyst surface and mass transfer and reaction kinetics are not happening at the same rates. Usually reaction rates are much faster than diffusion rates and concentration gradients can develop within the pore of catalysts. When catalysts are not selected with correct geometry and porosity, efficiency and selectivity toward a certain reaction in this process will be negatively affected [35].

The mechanism of hydrocracking differs from thermal cracking in two fundamental ways. Thermal cracking is basically a pyrolysis to achieve thermal decomposition of large molecules in the absence of any added solvent or gas. The outcome

of this process is formation of light products such as gasoline and gas and a certain amount of polymerized heavier products like residuum or coke. Hydrocracking is also a thermal decomposition process but with the presence of hydrogen at very high pressure and a catalyst. The addition of those two in the process makes it very unique. First of all, the existence of a catalyst enhances the production of carbonium ions via intermediate species. The enhancing effect depends on the catalysts as well as operation conditions. Then the intermediates are quickly hydrogenated by hydrogen with a very high partial pressure. This hydrogenation process prevents the absorption of olefins on the catalysts surface and ultimately prevents coke formation and catalyst fouling because of dehydrogenation. The prevention of coke formation results in an increased light distillate production and the necessity of catalysts regeneration. Hydrocracking of saturated hydrocarbons can proceed by heterogeneous reactions on solid surface.

Hydrocracking catalysts for heavy feedstock are usually bi-functional and comprise a hydrogenation/dehydrogenation component, often a noble metal and a strong acid component, Bronsted or Lewis acid. Main function of metal is to dehydrogenate saturated hydrocarbon molecules to alkenes and to hydrogenate olefinic intermediates desorbed from the acid sites. Cracking reactions start from the attack of a strong acid on a paraffin chain to form a carbonium ion. Then reactions such as skeletal rearrangements and carbon-carbon bond scission may take place from there. The intermediates formed on two acid sites might be different because carbon cations would be different when active sites are different. In details, the proton in Bronsted acids can add to an olefinic double bond to form a carbon cation. While a Lewis acid can abstract a hydride from the

corresponding paraffins to generate another intermediate. Detailed hydrocracking mechanism on a long chain n-alkane molecule shown in figure 3 was proposed to account for the full spectrum of different products[36]. Catalysts used here are bi-functional which comprises a metal-based component that is involved in hydrogenation/dehydrogenation process and an acid component that is responsible for cracking and rearrangement.

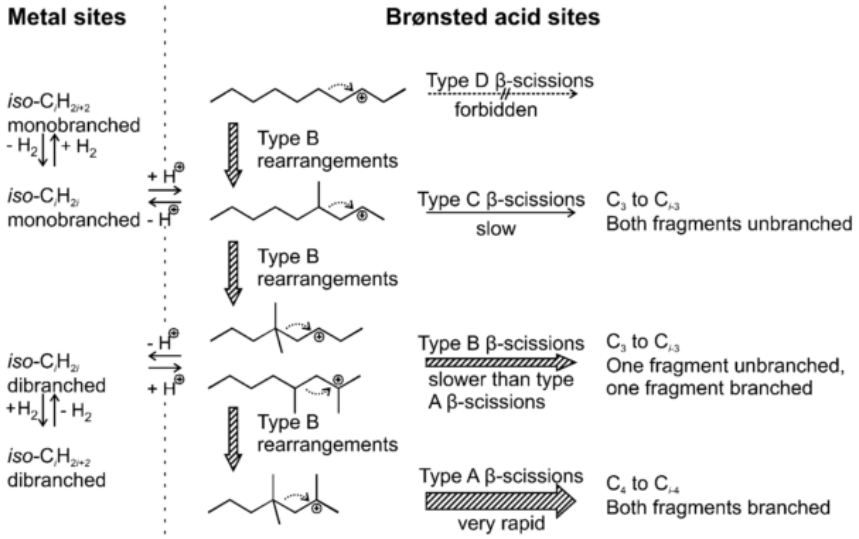

Figure 4: Hydrocracking mechanism on long chain alkane molecule

This mechanism assumes a long chain n-alkylcarbenium ion can experience three skeletal isomerization and the triply branched iso-alkylcarbenium ion undergoes a very rapid type A β-scission. Type B and type C β-scission of dibranched and monobranched

iso-alkylcarbenium ions are minimal compared to type A. It also assumes that elementary steps on the metal sites including mass transfer of alkenes between both two types of catalytic sites and the desorption of carbenium ions from the acid sites are much faster than the rearrangement and β-scission at the acid sites. Therefore the rate limited steps are on the acid sites.

2.2.4 Product Improvement (Finishing Process)

Finishing processes in petroleum include reforming, isomerization, polymerization as well as alkylation. These processes are applied very specifically to different streams obtained either from separation or cracking to achieve different goals.

2.2.4.1 Reforming

Reforming was first developed in the 1930s with an aim to improving the octane number of gasoline fractions[25]. Because straight-run gasoline and the desulfurized light fractions of crude oils have low octane numbers. It is often necessary to treat those fractions and meet the demand for higher quality gasoline. Reforming is essentially a process that converts n-paraffins to iso-paraffins, olefins and aromatics. Product distribution in a reforming process largely depends on the composition of the feedstock but shows very similar results as the gas oil cracking process. Parent molecule size will be reduced and species like olefins and aromatics will be produced[37–39]. Reforming could take the forms of thermal reforming and catalytic reforming to achieve a similar goal. Thermal reforming resembles the thermal cracking and crack long chain paraffins to high octane olefins, which will increase the octane number of gasoline. It is commonly carried

out at 500 ^{o}C to 600 ^{o}C with pressures from 400 to 1000 psi in a furnace. Outcome of thermal reforming primarily depends on the process temperature and gas additives. For example, higher temperatures favor higher octane products but reduce the yields of those products. Unsaturated hydrocarbon gases such as propylene and butylene could help this process because they could convert to liquid products under the temperature and pressure conditions used in thermal reforming.

Catalytic reforming is another method to increase the octane number of the gasoline pool. It is more efficient compared to thermal reforming on generating higher octane components in gasoline[39–41]. Typical feed to catalytic reforming is a mixture of straight run naphtha including light naphtha (C5 and C6), medium naphtha (C7-C9) and heavy naphtha (C9 and C12). This process is usually carried out by feeding the naphtha and hydrogen mixture to a furnace where the mixture was heated to the desired temperatures 450 ^{o}C to 520 ^{o}C. Then the hot mixture passed through a fixed bed catalytic reactor at hydrogen pressures of 100-1000 psi. Although this process may have certain degree of conversions by cracking reactions, the boiling point distribution does not change much. Hydrogen as a product during this process was produced in large quantities. Hydrogen is recycled through the reactors where reforming takes place. Like hydrocracking, hydrogen will help prevent coke formation on the catalysts surface. Unlike hydrocracking, hydrogen is produced as a by-product in catalytic reforming. Hydrogen could also be used in other process such as hydrotreating and hydrocracking[42]. Sulfur and nitrogen compounds are converted into hydrogen sulfide and ammonia, respectively, under catalytic reforming conditions. Those two species are both poisons for catalysts used

in this process. They need to be removed in order make the catalytic reforming more efficient. For example, sulfur is generally removed from the feedstock by using a conventional desulfurization over cobalt-molybdenum catalyst. Nitrogen removal requires high hydrogen pressure and with the aid of nickel-cobalt-molybdenum catalysts.

Since carbonaceous materials and coke might be deposited on the catalysts surface as byproducts and the amount of deposits increase with time of operation, feed quality and the catalysts state[43], regeneration of catalysts is necessary and encountered as a challenge during catalytic reforming. There are different types of process configurations to accommodate the regeneration of catalysts. Reforming process are usually classified as semi-regenerative, fully regenerative and continuous regenerative process based on the mode of regeneration. Semi-regenerative process operates at relatively low severity by a combination of units and catalysts management to extend the cycle length or time between catalyst regeneration. Operation will be stopped at the end of the cycle for catalyst regeneration. The regeneration process could be conducted in situ or ex situ by following a specific procedures. Fully regenerative reformers are more flexible on regenerating the catalysts because it can temporarily switch off one reactor for regeneration while keeping the rest of reactors continue to run. Work conditions are harder for catalysts since they need to maintain the throughput while a portion of them are being selectively regenerated. Continuous regenerative reformers allow non-stop regeneration of catalysts in a moving-bed process or fluid-bed process. For example in a moving-bed reformer, catalysts moves downward through the reactor by gravity flow and is returned to the top by means of a solids-conveying technique. Feedstock and recycled gas move upward countercurrent to

the catalyst and regeneration of catalysts could be accomplished. A fluidized solid catalyst bed could also continuously regenerate catalysts inside the reactor and remain the catalyst activity. Continuous regeneration process allows higher throughput because of its non-stop operation mode. This increases the severity of the process and may result in faster coking rate. In this case more frequent regeneration will be required.

2.2.4.2 Isomerization

Isomerization process in refinery is very important and being used to achieve various goals including gas to liquid conversion and improving gasoline quality[44–46]. It has been used in converting butane to isobutene, then further converting it to gasoline range product by alkylation. This process can also be used to improve the octane number of gasoline by converting n-paraffins to their isomers isoparaffins[37,47–51]. Isomerization process involves the use of catalysts and allow contact between them and feedstocks in the reactor. Various chemistry may happen on the catalysts surface despite isomerization such as fragmentation, disintegration and polymerization. Undesired reactions may be suppressed or controlled by adding inhibitors to the hydrocarbon feed or by creating an reaction environment with the presence of hydrogen[25]. Reaction conditions vary widely depending on the feedstocks and the process, 50 ^{o}C to 480 ^{o}C and 150 psi to 1000 psi with a 10-40 min residence time in reactor.

For hydrocarbons with more than 4 carbon atoms, isomerization process proceeds with the formation of the skeletal branching of the carbenium ion intermediate and then the intermediate undertake a monomolecular isomerization[47]. In contrast to paraffins with five or more carbon atoms, butane isomerization generally goes through a

bimolecular reaction pathway assuming the formation of C8 intermediates. Larger paraffins isomerize with more ease but the disproportionation reaction also increases. Olefins comparted to paraffins are more readily isomerized. Reaction pathways involves either the movement of double bond or the shift of methyl group shift. If double bond is a terminal on the molecule, olefins are the easiest to isomerize. Reaction pathways vary with the type of catalysts used to activate the reactions: acid catalysts and solid acids located with transition metals. In both cases, carbenium ions are considered to be responsible for the skeletal rearrangements. Therefore, the most important steps in the isomerization are the formation of carbenium ions and its rearrangement on the catalyst surface. Some specific isomerization process: Butomerate process, designed to isomerize n-butane to produce alkylation feedstock. This process operates with hydrtogen recycle to eliminate coke deposition on the catalysts. Feedstock in this process should be dry and comparatively free of sulfur and water. Operating conditions range from 150 ^{o}C to 260 ^{o}C and 150 psi to 450 psi; Isomerate process, a process designed to convert pentane and hexanes into branched isomers. Operating conditions are typically mild below 400 ^{o}C and 750 psi. Hydroisomerization is another process that convert n-paraffins to branched paraffins to produce high octane gasoline blending components[52,53]. It involves catalytic isomerization of light hydrocarbons in the presence of hydrogen. Addition of hydrogen in this process helps prevent coke deposition on catalysts surface. Typical operating temperatures are 400 ^{o}C-480 ^{o}C. Isomerization reactions are reversible and reach a thermodynamic equilibrium at low temperatures. High temperatures favor side reactions such as cracking and polymerizations. To achieve a high selectivity of isomerization

against all side reactions, temperatures should be controlled below a certain value. But to maintain a fast reaction kinetics and accomplish a certain degree of isomerization, catalysts are necessary to ensure the rate of reactions at a low temperature.

2.2.4.3 Polymerization

Polymerization in petroleum industry represents a process in which higher molecular weight compounds are formed by transforming lower molecular weight compounds while maintaining the same atomic arrangement in the basic molecule[54]. Olefin polymerization is an important reaction to convert small olefinic molecules to liquid condensation products in the gasoline range. Other products such as detergents and oil additives are also produced through olefin polymerization[55]. Polymerization of propene and butene from cracking processes could be accomplished thermally without catalysts under temperature 500-600 ^{o}C and pressure 1000-2000 psi[54–62]. Catalytic polymerization process is faster compared to thermal process and can happen at lower temperatures and pressures (150-220 ^{o}C and 150-1000 psi). Acid catalysts such as sulfuric acid, copper pyrophosphate or phosphoric acid are commonly used to treat feedstocks in the polymerization process. Because of this reason, feedstocks for the polymerization process needs to be pretreated to remove sulfur and nitrogen compounds[25].

2.2.4.4 Alkylation

Alkylation reaction in petroleum refining is a process that combines an olefin (ethylene, propylene, or butene) with iso-butane to produce branched-chain hydrocarbons with higher octane number in the gasoline range. Feedstock of olefins are from catalytic cracker and iso-butane could be made from isomerization of butane[63–67]. Typically

alkylation process are catalyzed with strong acids such as sulfuric acid at very low temperature (2-20 ^{o}C) to prevent polymerizations of the olefins. Around 13-15% of the global gasoline consumption consists of alkylation gasoline which represents 100 million tons production rate per year. Sulfuric acid (H_2SO_4) and hydrofluoric acid (HF) have widely been used in commercial alkylation process to synthesize high-grade petrol via the addition reaction of light alkanes and alkenes[68].

2.3 Electron Beam Irradiation of Materials

Most common forms of radiation employed in industry are electromagnetic radiation (gamma) from the radioisotopes cobalt-60 and cesium-137, and electron beams generated by electron accelerators. Heavy particles like ions and neutron beams may be used for special purposes[69]. Compared to gamma radiation, electron beams represents a series of advantages including more compact design, improved reliability, more steady radiation sources as well as less shielding materials and cost[70]. The key advantages, however, are higher power and directional beams. Higher power accelerators above 300 kW has been constructed and are able to process materials with high throughput. Directional beams allow for greater efficiency and better flexibility in radiation energy utilization efficiency than gamma sources, which emits electromagnetic radiations uniformly in all directions. Electron beam radiation applications for material processing have been evolving for more than half a century since the introduction of this technology[71,72]. Since it provides an efficient way of delivering energy to targeted molecules (generating radicals), while avoiding transferring energy to the bulk materials

in other forms. A similar processes occurs in non-thermal plasma process. Today it has matured to engulf a broad range of materials from simple molecules to complex composites. The effects of radiation are utilized in numerous technologies including food preservation[73–75], polymerization initiation[76–80], medical device sterilization[81–83] as well as waste water treatment[84].

2.3.1 Radiation Sources (e-beam)

Electrons are from a thermionic cathode and accelerated toward the anode at the ground potential. Cathode is typically a heated tungsten wire which releases free electrons from its surface when temperatures is above a certain level. Electron emission number density could be controlled by the temperature of cathode[85]. High energy electrons gain energy in electrostatic or electromagnetic field and accumulate the energy without colliding with other particles in vacuum. Devices used to transfer energy to electrons are accelerators. There are many type of electron accelerators in radiation processing, although they have features in common. Classification of electron accelerators could be based on either their operation mode or the energy level of electrons produced in the accelerators. Accelerators could operate on direct current (DC) or AC current (microwave and radio frequency)[86,87]. DC accelerators accelerate electrons by using a DC voltage, either applied directly between the electron source and an electrode as electrostatic device, or building an inductor to transfer energy to electrons. The energy of electrons is equal to the potential difference between the acceleration tubes and solely depends on applied DC voltage. Accelerating tubes could vary from a single gap to multiple gaps. Potentials are

applied on each gap to achieve the desired electron energy. DC accelerators were successful and still used today in several applications, but suffer from many limitations. For example, potential in the accelerating tube is limited below a certain value by a lot of factors which prevents the electron energy from becoming higher. Radio frequency electron accelerators use a single or several large resonant cavities to generate strong, alternating electric fields. Electron pass across a pattern of electromagnetic fields with controlled frequency. Electrons can gain kinetic energies ranging from 0.8 to 10 million electron volts with average beam power ratings from 20 to 700 kilowatts. Linear accelerators (Linac) are representative of the RF electron accelerators that inject electrons into a straight and segmented tube by pulses and accelerate them in the electric field [88].

According to the electron energy ranges, accelerators are usually divided into three groups: low energy range which is from 80 to 300 keV; medium energy range extending from 300 keV to 5 MeV; high energy range that covers above 5 MeV-10 MeV, very high > 10 MeV (not used industrially). Low energy accelerators usually employ a long linear cathode or multiple cathodes to distribute the electrons over a wide region on the materials under the beam. Electrons acceleration is done inside a long evacuated tube connected to a direct current high voltage power supply. Because of the low energies of electrons, accelerators like this could be self-shielded by high density metals such as steel or lead. DC high voltage is generated by using transformers and rectifier and shielded by high voltage cables. Applications of low energy accelerators are expanding rapidly in multiple areas such as coatings, curing of inks and adhesives[89]. Most of the medium energy accelerators use high current DC voltage to accelerate electrons inside the tube. But its

insulation is different from low energy accelerators, because high voltage cables alone are not practical at such a higher voltages above 800 kV. One way to achieve better insulation is to combine the high voltage generator and the acceleration tube within the same enclosure which was filled with sulfur hexafluoride gas at elevated pressures of 6-7 atm. Accelerators in this range are mainly used for crosslinking of wire and cables as well as heat shrinkable tubing. They are also used to generate X-rays for medical device sterilization and curing thick composite products. High energy accelerators use radio frequency power to accelerate electrons in AC field. They are predominately linear accelerators giving pulsed beams at powers above 50 kW. Electrons emitted from the electron gun are accelerated down the waveguide by the electric field created by the RF waves, and the accelerated beam is scanned over the product. The accelerated electrons from a linear accelerator are delivered in pulses of micro or nanosecond duration, each pulse consisting of a sequence of shorter picosecond pulses[69].

Electron accelerators are certainly the key components of the electron beam irradiation system, but there are important design and safety considerations during building and operating the system. Material handling system is used to transport, irradiate and protect materials to be irradiated. Usually conveyors with belts or rollers may be used to handle the materials. Temperature rising or dose may be controlled by external cooling or irradiation in multiple passes. Lead or steel could be used to provide compact shielding to electrons less than 1 MeV. Concrete, sand or soils are commonly used for higher energy electrons because of cost reasons. Shielding walls are typically more than 3 m thick for high power and high energy accelerators. There are protective equipment and devices for

personnel to access and exit zones affected by radiation. Byproducts from irradiating air including ozone and nitrogen oxides are dissipated into exhaust system with large capacity. Radioactivity may be induced in heavy materials like metals inside the material when electrons are highly energetic. This effect is negligible when irradiating materials like plastic, food and liquids with electrons less than 10 MeV.

2.3.2 Interaction of Ebeam Radiation with Matters

Electron beam radiation induced chemical changes are brought by the interaction of high energy radiation with matter. Interaction include elastic and inelastic collisions associated with different energy transfer mechanism depending on the irradiated materials and particle energy. Figure 5 shows how high speed electrons interact with atoms or molecules in irradiated materials. Elastic scattering happens when an electron is an incident particle and it is diffracted in the Coulomb potential of atoms or molecules. Energy loss in elastic scattering depends on the incident electron energy, scattering angle and the mass ratio of electron to the molecule[90]. Since most molecules are orders of magnitude heavier than electrons, the energy loss is regarded to be zero. Inelastic scattering is the only one of the processes that causes ionization and excitation in the material, so it is responsible for the radiation chemistry. The kinetic energy of electrons is lost in inelastic collisions that produce ionization or excitation energy. The rate of energy transfer from electrons to materials is described as linear energy transfer (LET) of the radiation. Electron beam radiation with energies in the range of keV to a few MeV are typical of low energy transfer which deposit energy predominately in small clusters of

ions and excited molecules[11]. The typical energy loss for incoming electron beam of a couple MeV is about 2 MeV/cm in water or similar materials. The energy loss rate because of collisions depends on the electron energy and on the electron density of materials being irradiated. The rate of energy loss per gram per square centimeter sample ($MeV/g^{-1}cm^{-1}$) is larger for low atomic number materials than for high atomic number materials because high atomic number materials have less number of electrons per unit mass than lower atomic number materials. High atomic number materials also present less number of electrons available for this type of interaction. While slower electrons and large positively charged ions (helium ion and heavier particle beams) transfer energy much faster and are considered high LET radiations.

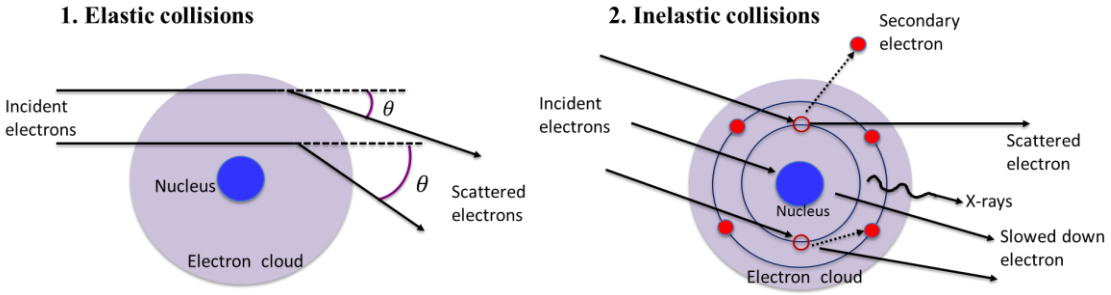

Figure 5: High speed electrons interaction with atom or molecules in materials

High energy electron beams are able to penetrate the outer electron shells and interact with the inner shell electrons. If energy transferred to the inner shell electrons is high enough, those electrons might be ejected and leave a hole in the inner shell. Atom at this state is ionized. Almost immediately another electron from outer shell will fill in the

missing electron in the inner shell and help the atom return to its ground state. At the same time, an X-ray will be emitted. The energy of the X-ray is equal to the difference of the two electron shells. Since beam energy at MeV is significantly larger than the critical ionization energy (<20kV) in almost all of the materials, this type of X-rays will be seen and detected in devices such as transmission electron microscopy. Cross section area for ionization of electrons in different shells are pretty constant and does not vary much as incident electron energy changes. This is by taking into account the overvoltage U, which is the ratio of beam energy to the critical ionization energy of electrons at different shells.

If the electrons in the beam completely penetrate the electron shell they will directly interact with the nucleus. Coulomb field of the nucleus can decelerate the electrons and this might result in emission of X-rays. Depending on the interaction strength between nucleus and incident electrons, energy of X-rays can range very widely from below detect limit to the beam energy. Such X-rays produced as the electron decelerates are known by their original German name of Bremsstrahlung. Cross section of Bremsstrahlung radiation could be derived by Kramers's law[91].

Secondary electrons are ejected from the atom due to collision with incident electron beams. They are involved in almost all of the physico-chemical phenomena underlying radiation chemistry and play central roles in the effect of ionizing radiation chemistry[92]. Secondary electrons could be classified into three groups based on the mechanism how they are produced[93,94]: slow secondary electrons are ejected from the conduction or valence bands in the atom and their energies are typically below 50 eV. Slow secondary electrons are free electrons and not associated with any atom. They are

weak and cannot escape the specimen unless they are near the surface; fast secondary electrons are produced if incident electron beams knock out electrons from inner shell of the atom. The produced electrons could gain a significant fraction of the beam energy. Because of this high energy, fast secondary electrons are able to travel longer distance in the specimen and produce more secondary electrons and X-rays. Compared to slow secondary electrons, fast secondary electrons are more probably to be produced during the ebeam irradiation of materials due to a larger cross section area; Auger electrons are another type of secondary electrons ejected from inner shell, which are produced when an ionized atom returns to its ground state.

When electron beams with MeV energies encounter a target. Energy transfer happens between the incident electrons and the targets through all inelastic collisions and radiations which are discussed previously. Most of the interactions only transfer tiny fraction of the incident electron's energy. Therefore this process could be assumed to happen gradually and continuously until the incident electron energy drop to a certain level. It is referred to as the continuous slowing down approximation (CSDA). Several advantages about this: CSDA simplified and speeds up transport calculations. The statistical fluctuations of energy losses in successive inelastic collisions are disregarded. Energy losses only depends on the stopping power and material properties[95–97]. The energy loss per unit path length due to collisions is known as stopping power. Mass stopping power is energy loss per unit mass of materials:

$$S/\rho = -dE/dl \times \frac{1}{\rho}$$

Where S is the stopping power and ρ is the density of the material. Total mass stopping power includes collision stopping power $(S/\rho)_{col}$ and radiation stopping power $(S/\rho)_{rad}$ due to different inelastic scattering mechanisms. The collision stopping power predominates at low and intermediate energies, and the radiative stopping power at high energies. Radiative stopping power is also favored by the high atomic number materials. Collision and radiative stopping powers are equal at an energy that depends on the material. For example, this critical energy is close to 90 MeV for water or most hydrocarbon materials, and 10 MeV for lead. Stopping powers could be calculated based on theoretical formula or experiments. In CSDA approximation, another important parameter is the cross section areas of different collisions. It governs the electron interactions with the atoms that make up the medium. Fundamental processes such as excitation and ionization are of great interests in many fields but to predict energy transfer process due to them require reasonably accurate cross section area data over a wide range of energies. Similar to the stopping power, cross section area for different process could also be found in two different ways: theoretical calculation and experimental determination[95].

Monte Carlo simulation codes have been developed and used for the calculation of the transport of electrons and photons through extended media[98,99]. This method was able to simulate event by event slowing down of electrons in different medium and has become a valuable tool in elucidating radiation action at the molecular level. There are many individual elastic and inelastic Coulomb interactions that occur during the passage of a high energy electron through the matter. It is not practical to simulate all of them

directly. Instead, in a Monte Carlo code the electron trajectories are divided into many segments in each of which numerous interactions occur. For each segment, the net angular deflection and the net energy loss are sampled from relevant multiple-scattering distributions. The accuracy of simulation like this depends on a series of things. For example how comprehensive and complete the electron scattering processes have been included in the code and whether the cross section areas for different scattering process is up to date. Errors in simulation results also arises from various causes: uncertainties of the single scattering cross sections used as input and the approximations made in the various sampling procedures as well as coding errors[95].

2.3.3 Radiation Dosimetry

Chemical effects caused by exposure to ionizing radiation are roughly proportional to the amount of energy transferred from the radiation to the absorbing material. Chemical changes in the material being irradiated are generally the result of free radical reactions that are complete within a few minutes or less in gaseous and liquid system. Reaction is much slower in most solid system because of the limited mobility of any radicals. With Continuous slowing down approximation we are able to estimate the mass stopping power of a certain material electron beam is interacting with and more importantly the dose distribution inside the material could be estimated as well[100,101]. The dependence of mass stopping power on electron energy in different medium was shown in figure 6. The first thing to notice is collision stopping power is much larger than radiation stopping power in three materials including water, hexadecane and aluminum when electron energy

is below 100 MeV. Water and hexadecane has very similar mass stopping powers because of similar atoms and density. Aluminum compared to both water and hexadecane has smaller mass stopping power because of higher density, but difference is not significant within a factor of two. Note that stopping power data was originally found the National Institute of Standards and Technology (stopping power and range tables for electrons).

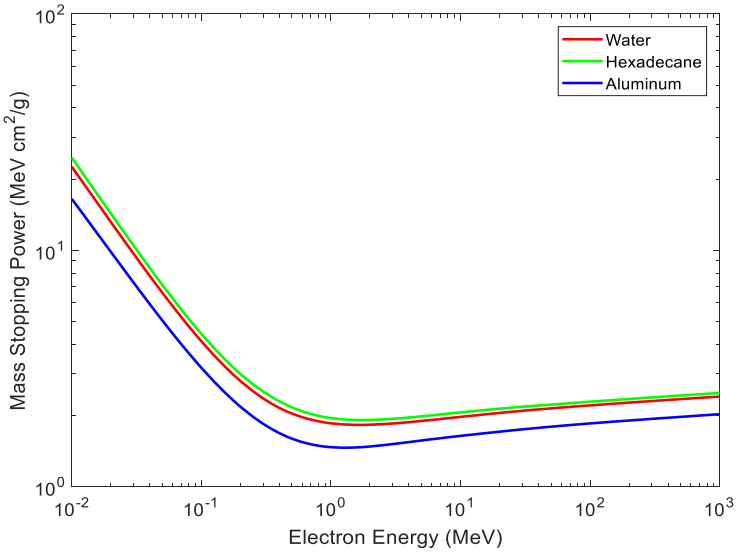

Figure 6: Ebeam mass stopping power of water, hexadecane and aluminum

With known mass stopping power of irradiating materials, it is straightforward to calculate the electron energy loss as a function of penetration depth in the medium. Electron beam dosimetry in water has been investigated extensively to study irradiation dose distribution as a function of both depth and electron energy. Typically a 10 MeV electron beam could penetrate 5-6 cm water before it slows down to a negligible level[102]. Dose distribution inside a known chemical composition material could be

calculated based on its density and mass stopping power. Dose distribution is important because it connects with the radiation chemistry and radiation yields. SI unit of absorbed dose is joules per kilogram of irradiating material (J/kg^{-1}), which is commonly used as gray (symbol Gy). More fundamentally, absorbed dose is a measure of the energy transferred to the irradiated material that may cause physical and chemical change to the material by creating reactive species such as ions, excited species, and radicals.

Absorbed dose in irradiating material could be determined by various techniques and principles. There are physical and chemical dosimetry depending on the method and device used. Physical dosimetry based on the temperature change of irradiated material or ionization product[69]. When using temperature change to indicate absorbed dose, metal or graphite are commonly used and they need to be thick enough to absorb all the energy of radiation. Therefore the rate of temperature increase measured within the materiel is related to the intensity of the beam. Ionization is measured by means of an ionization chamber consisting of two electrodes separated by a selected gas. When electron beam comes to interact with the gas, ionization produces ions. Under the applied potential on the two electrodes and known distance, current is monitored. This method requires the knowledge of radiation yields of the ion for the selected gas. Air is normally used in this method because of its well-known radiation response from multiple resources.

Chemical methods to measure dose in the material are based on the chemical change produced by irradiation. A relationship must be established between the absorbed dose and the radiation product yields (G value)[103]. This could be implemented by comparing with another well-known dosimeter through a calibration process. Measured

dose by this method is the average dose over the entire volume of the dosimeter. Therefore dosimeter volume and its location in the irradiating material affect the measured value. Absorbed dose measured in one material could be converted to the dose in another material with different density and atomic composition[104]. Gas phase dosimeters were developed and used, e.g. N_2O, but are difficult to handle compared to liquid and solid dosimeters. Liquid dosimeters are widely used nowadays. For example, the ferrous sulfate dosimeters. Oxidation of ferrous ions to ferric ion will take place upon irradiation and could be measured by absorption spectroscopy. Other liquid dosimeters include ferrous cupric sulfate dosimeters, dichromate dosimeters, glucose dosimeters and so on. Solid dosimeters possess advantages over liquid dosimeters because they are easier to store and measure. Some commonly used ones include PMMA dosimeters, which are based on radical's generation after absorbing radiation and associated absorption spectroscopy change and alanine dosimeters, which trap the produced radicals inside its solid matrix. The radicals could be measured by electron paramagnetic resonance.

When using dosimeters to determine the dose inside an irradiating materials, two questions are always encountered. One is related to the difference between the irradiating material and the dosimeter. Since absorbed dose depends on the material properties such as density and stopping power, it is necessary to convert the measured dose in dosimeters to the absorbed dose in irradiating materials under the sample irradiation conditions.

$$Dose_{sample} = Dose_{dosimeter} \times \frac{(S/\rho)_{sample}}{(S/\rho)_{dosimeter}}$$

The other one is because of the chemical composition change. When a mixture rather than a pure elements are being irradiated, the average mass stopping power needs to be used. One way to calculate the average mass stopping power is by:

$$(S/\rho)_{mix} = \sum_{i}^{n} w_i (S/\rho)_i$$

Where w_i is the mass ratio of each element.

2.3.4 Radiation Yields

Ionizing radiations initiate a number of processes that contribute to the physical-chemical change of molecules inside the materials. Interaction of high speed electrons with molecules are characterized by excitation and ionization and result in formations of radiation intermediates including secondary electrons, free radicals, ions and excited molecules[105]. Intermediates are super-reactive and react with other species or with each other. This result in their short life time and difficulties to quantitatively study them. Their successive reactions may produce stable or final products directly, which are more easily to study in a quantitative way, but most final products are produced through the formation of intermediates.

Radiation yields of intermediates and final products are characterized by the G values which are the number of particles produced per 100 eV of absorbed energy or mol/J. G values represent the efficiency of production of the products in the radiation system and depend on various parameters. Methods and techniques used to quantify G values of radiation products vary dramatically and primarily depend on the nature of the

species, e.g. its life time, chemical or optical property. Final radiation products due to their stable property and long life time are easier to study. Practical applications to study radiation yields of stable products are very broad including electron beam irradiation induced decomposition of pollutants in aqueous solutions or exhaust emissions as well as degradation of organic materials from different resources[106–108]. Radiation yields of the same material at different phase vary significantly because of the reaction pathways and electron behavior. The radiolysis of liquid phase fundamentally changes its behavior from gas phase radiation in the sense that the primary species (ions and excited molecules) tend to react with surrounding molecules because of higher medium density, whereas in gas phase, those species separate and react independently[109]. Reaction chemistry and associated physics will be discussed more in chapter 4. For example radiolysis of water vapor produces larger quantity of hydrogen and oxygen compared to other products. Liquid water as the most rebound medium in aqueous solutions was extensively studied on radiation yields of both stable products such as H_2 and H_2O_2 and intermediates such as H, OH, H_3O and hydrated electrons e_{aq} [110]. G values of those species were studied and quantified in the following equation:

$$H_2O \rightarrow 0.28\, OH^* + 0.27\, e_{aq} + 0.06 H^* + 0.05\, H_2 + 0.07\, H_2O_2 + 0.27\, H^+$$

Toluene, Xylene and phenol as pollutants in industrial effluents are removed very efficiently by electron beam irradiation through a serious of oxidation process. G values for each different species were experimentally determined and distributed in the range of 0.002-0.1 mol/J [108]. Hydroxyl radicals and hydrated electrons reactions with organics

in aqueous solutions are believed to be responsible for most of decomposition and degradation process in the electron beam radiolysis.

Ionizing radiation yields of organic systems have been studied for decides with early interest on insulators and lubricants in electrical industry. Gaseous hydrocarbons (C1-C3) from natural gas are investigated in gas to liquid process in petroleum industry. Yields of those hydrocarbons have very broad distribution in carbon number and primarily depends on the parent molecule length and hydrogen to carbon ratio. Liquid hydrocarbons radiolysis gives lower yields of products than irradiation in the gas or vapor phase and with less proportion of low molecules weight products. This is due to the shorter life time of excited ions and molecules in the dense medium, where energy transfer is very efficient, so that there is a smaller probability that excited species will dissociate in the liquids than in gas. Yields are lower in dense medium partially because of the greater probability that radicals formed by the dissociation of excited molecules will be trapped, not be able to propagate and eventually recombine or polymerize. In general saturated hydrocarbons with simple structure tend to be less stable upon irradiation and have higher yields, while unsaturated and cyclic structure hydrocarbons are more radiation resistant and produce less products.

Radiation yields of final products are relatively straightforward to characterize by using varieties of techniques. It does not require special design and modification of the radiation device or radiation chamber. Sample analysis could be completed either on-line by using techniques such as mass spectroscopy or gas chromatography, or off line by using chemical methods to quantitatively characterize the radiation products. Radiation yields

of final products are important in a sense that it will determine whether this technology is applicable to a certain application. For example irradiation of aqueous solutions to remove organic pollutants, if removal of such species are not significant, this technology may not be viable for large scale application. However it is important to know that ionizing radiation of medium is a complex phenomenon that involves physical, chemical or even biological process that happen in multiple stage at multiple time scale. What is essentially important is the radiation intermediates formed by electron collisions with molecules. Intermediates from ionizing radiation include ions, secondary electrons, excited species and radicals, all of which drive the reaction chemistry in different pathways. Different chemical reactions and pathways produce different final products. To initiate study of reaction chemistry and pathway, knowledge of radiation yields of intermediates are necessary.

Pulse radiolysis provides a very powerful technique for identification of short-lived intermediates generated by ionizing radiation in its primary energy deposition stage. In practice, a short pulse (10^{-15}-10^{-9} s duration) of electrons irradiates the substance, and the intermediates produced are investigated with fast response method[105,109]. The absorbed dose per pulse depends on the pulse duration, beam current and the irradiating medium, and is usually in the range of 1-20 Gy. Different methods are applicable to this process including optical spectroscopy, electron spin resonance and conductivity analysis. Hydroxyl radical is one of the primary species that are produced in irradiation of aqueous solutions. It participates in many chemical reactions that are responsible for reduction or decomposition of a series of organic pollutants in aqueous solutions. Extensive research

have been conducted to understand how it is generated in aqueous solutions and how it is involved in chemical reactions with organic molecules[111,112]. Picosecond pulse radiolysis of pure water was well studied and the time-dependent yields of hydroxyl radical (OH) was measured by UV-absorption spectra. The radiation yield of OH at 10 ps was found to be around $4.8 \times 10^{-7}\ {}^{mol}/_{J}$. Usually the radiation yields of a species is higher initially upon radiation and decay rapidly in time. The rate of decline largely depends on all the chemical reactions and kinetics where this species is involved.

Irradiation of aqueous solution to remove organic pollutants at ppm level is mainly focused on water radiolysis and the radiation yields of a water molecule. Because water molecules received almost all radiation energy and its yields is much higher than all pollutants. Certain functional groups in organics are particularly susceptible to water radiolysis radicals (H, OH and e_{aq}). For example, both saturated hydrocarbons ($-CH_2-$) and alkenes ($C=C$) will quickly react with H and OH, but stay inert with hydrated electrons; hydrogen ions only react with hydrated electrons; aromatics react with all three them, although H and OH react more rapidly with aromatics. Reactions of hydroxyl radicals with aromatic hydrocarbons have been studied with pulse radiolysis. Hydroxyl radical is electrophilic and reacts readily with aromatic compounds. Depending on the environmental conditions, hydroxyl radical may attack aromatic compounds either through hydrogen abstraction or addition to the ring structure[110,113]. Radicals attack the aromatics from various sites. For example, the attack could happen on the ring or on the side chain. When air is present in the solutions, reactions may be different because of

the formation of hydrogen peroxide, phenolic products and small yields of dimeric products[104].

Radiation yields of hydrocarbons are not as well understood as for water or aqueous solutions. This is due to the facts that hydrocarbon molecules represent more complex structures and upon irradiation intermediates (ions, excited species and radicals) have broad distribution and unknown behaviors. Response of different type of hydrocarbons to irradiation varies significantly in terms of yields. In general, most hydrocarbons give complex mixture of products that include hydrogen and broad distribution of hydrocarbons molecules ranging from gaseous species such as methane and ethane to molecule of the same size as parent molecule as well as those of twice the size of original molecule. It is also likely very large polymeric molecule may be formed from irradiating unsaturated hydrocarbons or polymers. Radiation yields of vapor phase are higher than liquid and solid phase with more low-molecular weight products. Saturated hydrocarbons tend to produce higher yields of products than unsaturated hydrocarbons. In particular, branched alkenes with a long chain produce the most amount of low molecular weight products. Aromatics shows very good resistance to irradiation and give low yields of radiolysis products[114–116]. Protection effect in aromatics and saturated hydrocarbon mixture have been observed and studied. Addition of aromatics can dramatically lower the yields of low molecular weight products in a mixture of aromatic with cyclohexane/n-dodecane. This is due to the energy transfer from the saturated hydrocarbons to the aromatics. The interaction of aromatic additive with radiation intermediates was believed to be responsible for this phenomenon[117,118]. Radiation yields of polar liquids such as

alcohols and non-polar liquids (most hydrocarbons) might shift dramatically because of the existence of solvation effects. Electrons and ions might be trapped in polar compounds and loss the activity to react with other reactive species. This may result in the reduced reactions in bulk liquids such as ion recombination. In this sense, irradiation of alcohol and other polar compounds resemble that of water because they are polar molecules. Non-polar compounds such as saturated hydrocarbons will not get delayed by solvation so that recombination of ions will proceed much faster and yields of radiation will be higher.

As previously stated, radiation yields of different solutions depends, despite the type of material, on the phase of irradiation (vapor or liquids) and processing temperature and pressure. In general, high temperature and low pressure will favor the radiation yields of products. There is also a large increase in radiation yields with the dose rate which is proportional to LET (linear energy transfer), especially for hydrogen formation, because hydrogen formation is a second order process[118]. Reasons for the increased yields are due to facts that when radicals are produced with high concentrations, they might interact with a rate that overtake their interaction with parent molecules. It might un-favor radiation induced reactions such as polymerization since propagation of radicals might be interfered by termination. Nevertheless the same mechanism might favor radiation induced chain scission reactions such as large hydrocarbons cracking to produce low molecular weight molecules.

2.4 Radiation Chemistry of Hydrocarbons

2.4.1 Theory of Electron Beam Radiation Chemistry

Radiation processing of hydrocarbons or radiolysis of hydrocarbons have been studied for many years with different radiation sources. Radiation mechanism and chemistry of hydrocarbons change significantly with the type of hydrocarbons and experimental conditions including radiation source, temperature, pressure and phase of irradiating materials. Response of different type of hydrocarbons to irradiation varies significantly in terms of yields. In general, most hydrocarbons give complex mixture of products that include hydrogen and broad distribution of hydrocarbons molecules ranging from gaseous species such as methane and ethane to molecule of the same size as parent molecule as well as those of twice the size of original molecule[116,119]. Radiation yields and products are the results of different chemistry pathways that radiation intermediates participate after they are created by ionizing radiation in primary stage. Applications of hydrocarbon irradiation were selected based on the radiation response, for example, radiation induced cracking preferably occurs on long chain saturated hydrocarbons but polymerization normally happens when irradiating ethylenic hydrocarbons or polymers[120]. To understand or predict the radiation response of a certain type of hydrocarbon or hydrocarbon mixture, radiation chemistry is ultimately important.

Understanding the nature of radiolysis mechanism in hydrocarbons requires knowledge of fundamental physics about ionizing radiation and chemistry. It is essential to realize that reactions happen in different time scales inside and outside the spurs. Keeping those in mind will help us tremendously on interpreting the diversity of products. Though the mechanism of hydrocarbon radiolysis is still not completely understood and research is still being conducted, a few statements could be made from previous work with

decent confidence. First, the wide distribution of products from hydrocarbon radiolysis is largely driven by free radical reactions. The nature of free radicals reactions give rise to chain reactions and trigger a sequence of radical reactions before the radical center is lost. Normally chain reactions offer a large yield of products for small amount of energy input. Most of the products are formed by the reactions of free radicals diffusing outside of the track with thermal energies[104]. Free radicals must abstract hydrogen, disproportionate or dimerize to give hydrocarbons of all molecular length up to twice that of the parent molecule. This statement have been proved by electron spin resonance studies[121]. This is not possible if all those reactions only happen within the spurs. Electron spin resonance provided solid evidence for free radicals in irradiated hydrocarbons. Second, small molecules including hydrogen and short chain hydrocarbons are not all produced outside the track due to diffusions of species such as free hydrogen and methyl radicals. This statement was well proved by addition of radical scavenger such as iodine in the bulk liquids[120]. No hydrogen iodine is produced under irradiation. Hydrogen may come from a unimolecular decomposition of a hydrocarbon molecule. Similarly, methane formed from mixture of C_2H_6 and C_2D_6 contains little CH_3D and CD_3H, proving that free methyl radicals are not the main path producing methane.

Electron beam induced radical chain reactions are the success keys to many ebeam applications including crosslinking, polymerization, degradation and cracking. Radical chain reactions corresponding to the chain length change are divided into two groups: chain growth and chain scission. Crosslinking and polymerization are resulted from chain growth by successive addition of radicals, while degradation and cracking are the opposite

and produce short chain products. Electron beam induced radical chain reactions for cracking are believed to follow the same mechanism as thermally induced cracking reactions[122]. In terms of kinetics, the chain reactions could be broken down into three steps: chain ignition, propagation and termination. Chain initiation involves the production of radicals from the substrate through thermal effect or ionizing radiation. The radical production rate is characterized by its G value of the radical. It depends on the temperature and material if it is thermally generated and the dose rate if it is radiation activated. Propagation is the step that produce a product and generate another radical, so that the chain reactions could proceed. Termination could undergo by multiple reactions, e.g. radical-radical combination, radical isomerization or polymerization. Radiation assisted thermal cracking of hydrocarbons (RTC) takes advantage of the facts that ionizing radiation generates radicals, ions and excited states as primary species in the sample and they are all very reactive and could potentially participate in the chain reactions. Due to very short lifetimes, ions and some excited species are not included in the chain reactions despite their formation in the primary process. This greatly simplify the radiation reactions and the radiation chemistry. It also makes it possible to study the radiation effect and thermal effect simultaneously on hydrocarbon cracking reactions.

Radiation thermal cracking exerts both the thermal and radiation effects on the materials, therefore, its activation energy is much smaller than thermal cracking alone, because both the thermal activation and radiation activation can contribute to cracking initiation[123,124]. The chain cracking rate and the yield of the products are usually higher due to the synergistic effects. Radiation effect on samples is complex and varies

with other parameters including temperature, type of sample, phase and so on. Radiation cracking affects the radiation yields and product distribution through total absorbed dose and dose rate. Both of them affect the cracking reactions kinetics through radical chain reactions. Dose rate is believed to be the major source of radical initiation when temperature is not high enough to initiate the chain reactions[125,126]. If radical chain reactions could proceed further by thermal activation, the dependence of an individual product on dose rate could be derived based on the reaction kinetics. Usually dependence shows a nonlinear behavior and changes with temperature and sample type. If radiation temperature is too low to initiate the chain reactions, both of the chain initiation and propagation will have to be activated by radiation. Radiation cracking can still happen at low temperatures only when the dose rate is high enough. Because the temperature is not high enough to activate the chain reaction and there has to be another chain reaction activation mechanism, which is radiation in this case. What's more, the radiation dose rate has to be at least above a critical value. The concept of cracking reaction at low temperatures relays on the facts that radiation alone could create unstable excited states that are capable of propagating radical reactions. In this case, radiation effects are more significant and complex since it is involved in more steps in the kinetics and non-linear behavior is expected to be even stronger.

Dr. Zaikin and Dr. Zaikina developed very detailed kinetic models to describe radiation cracking reactions and the relationship between dose rate and temperature. Temperature and dose rate together determine the cracking reaction rate. Critical temperature and critical dose rate are coupled within a nonlinear relationship. For a

specific feedstock, this critical dose rate value depends on temperature and can be qualitatively shown in figure 7. The region on the left of the curve has no cracking reactions indicated by non-cracking region, while the region on the right of the curve is cracking reaction region. Detailed derivation can be found in the book[126].

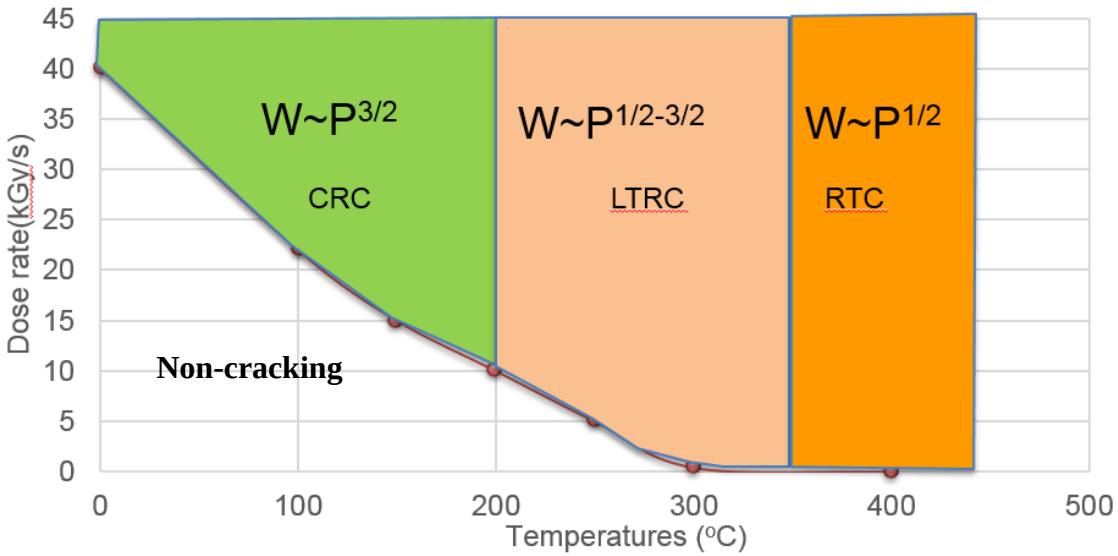

Figure 7: Critical dose rate and reaction rate dependence

Classification of radiation chain cracking reactions based on different temperature intervals and mechanism of radiation cracking are: radiation cracking (RTC) in the temperature range between 350 and 450 °C, low temperature radiation cracking in the temperature range between 200 and 350 °C and cold radiation cracking in the temperatures below 200 °C. Reaction rate dependence on dose rate differs in different reaction zones. In the case of RTC at higher temperatures, the reaction rate and dose rate correlation would be $W \sim P^{1/2}$, since radiation only contributes to the cracking initiation, while it is $W \sim P^{3/2}$ for

CRC at much lower temperatures, because radiation contributes both to the initiation and propagation. Dose required for a given degree of feedstock conversion also depends on dose rate and the dependence are different in different radiation cracking reaction region. Since at lower temperatures the dependence of reaction rate on dose rate is stronger, it is reasonable that dose rate of ionizing irradiation should be much higher at lower temperatures, e.g. 10 kGy/s below 200 ^{o}C and 5 kGy/s between 200 and 350 ^{o}C. In other words, there is a lower dose rate threshold that determines the start of the low temperature cracking reaction. Electron irradiation could operate in two different modes: Pulsed or Continuous. Dose rate we mentioned above are time averaged values. It was found that light cracking products are always higher in the case of continuous irradiation provided the dose rate of ionizing irradiation exceeds the threshold dose rate for the start of low temperature cracking.

2.4.2 Radiation Induced Polymerization and Crosslinking

Polymerization requires the monomer molecules to react with active sites at the end of growing polymer chains. Active sites are either free-radical centers, positive ions or negative ions. Depending on the intermediates grow the molecules, polymerization is classified as radical polymerization, anionic polymerization and cationic polymerization[54]. The mechanism, however is the same and follows a series of chain reactions comprising initiation, propagation and termination. Ionizing radiation could initiate polymerizations by creating both radicals and ionic molecules and allow them to polymerize with different mechanism. Radiation induced radical polymerization depends

on the monomer, dose rate, absorbed dose and temperature. The polymerization process could be illustrated by the following steps:

$$M \rightarrow 2R^{*} \qquad \textit{radical initiation}$$

$$R^{*} + M \rightarrow RM^{*} \qquad \textit{propagation1}$$

$$RM_{n-1}{}^{*} + M \rightarrow RM_{n}{}^{*} \qquad \textit{propagation2}$$

$$2RM_{n}{}^{*} \rightarrow R - M_{2n} - R \qquad \textit{termination}$$

Parent molecule M could be hydrocarbons such as butane, propylene and any other olefinic molecules.

When hydrocarbon monomers are irradiated, multiple fundamental processes will be initiated and the results of the process depends on all of them: polymerization, crosslinking, chain scission, long chain branching and grafting. Different polymers have different responses to electron beam irradiation. The response to radiation is related to the chemical structure of the polymers and the radiation sources. For example, crosslinking and chain scission are two elementary process that always coexist during irradiation of not only polymers but also most of long chain hydrocarbons[127]. Typically, crosslinking structure is formed only when the number of crosslinking points are at least two times larger than that of the main chain scission. Crosslinking rate and chain scission rate depend on, despite the polymer type, radiation dose, dose rate and temperature. Radiation induced crosslinking of hydrocarbons is a chemical process to form a three dimensional network structure from a linear polymer. The crosslinking process could be simplified as figure 8. Usually it starts with a polymer such as polyethylene and proceed by recombination of

polymer radicals. It is important to know that crosslinking and main chain scission occurs simultaneously [127–129].

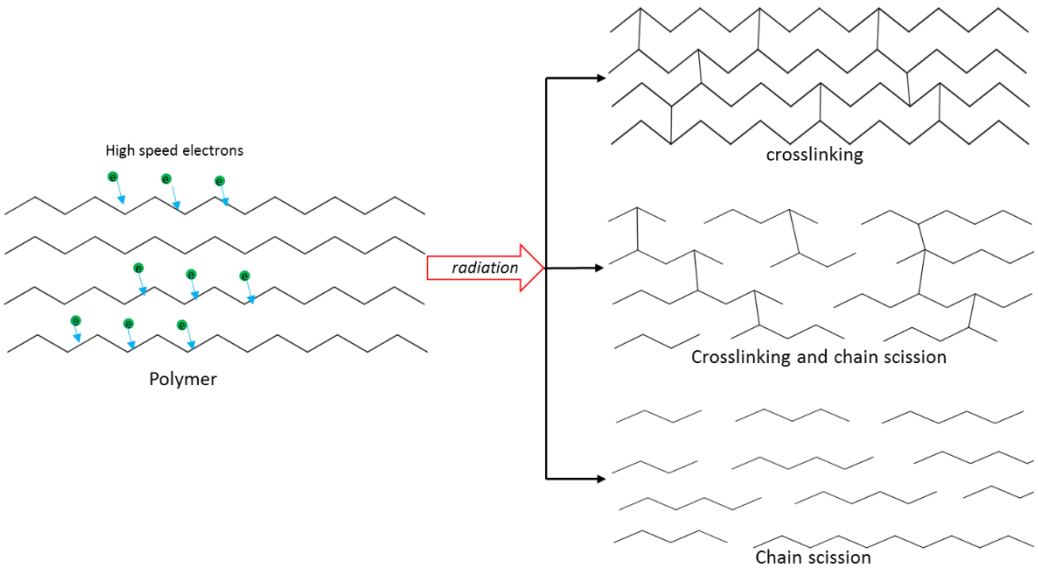

Figure 8: Ebeam irradiation induced crosslinking process

2.4.3 Irradiation of Saturated Hydrocarbons

Irradiation of saturated hydrocarbons with different structure and different chain length have been experimentally studied by many researchers[104,130]. Methane as the simplest saturated hydrocarbon was irradiated by high speed electrons in a flow type reactor. The effect of irradiation temperature, dose and dose rate were studied on product yields[131,132]. First of all, when methane was irradiated with high speed electrons, both saturated and unsaturated hydrocarbons are produced in the range of C2-C6 alone with

hydrogen. Table 1 is the distribution of yields of major products (G-values) from irradiating methane.

Table 1: Product Yields of Irradiation of Methane at 69 ºC

H_2	C_2H_4	C_2H_6	C_3H_8	n-C_4H_{10}	i-C_4H_{10}	n-C_5H_{12}	i-C_5H_{12}	Neo-C_5H_{12}
7.1	0.16	2.25	0.34	0.092	0.037	0.004	0.048	0.006

Secondly, G values of alkane products are found to be independent of the dose and dose rate in a broad range of dose distribution, while alkene products are both dose and dose rate dependent. Thirdly, temperature effect on G values of different products are more complex and depends on the reaction pathways. Most products yields increase with the temperature over a temperature range 50-280 ºC. High temperature above 150 ºC favors the production of olefins. Irradiation of methane follows a simpler reaction scheme compared to all other hydrocarbons, especially at ambient pressure. Key species of methane radiolysis are methyl and hydrogen radicals which are produced as intermediates after fundamental processes such as ionization and excitation. Those intermediates will undergo reactions via free radicals. Other species including ions and excited species are important in the early stage of irradiation of materials. Then they are either quickly neutralized by electrons or transferred to another stable states before they could react to form other long life species. Based on those assumptions the reaction pathways of irradiation of methane could be illustrated as follows:

$$CH_4^+ + CH_4 \rightarrow CH_5^+ + \dot{C}H_3$$

$$\dot{C}H_3 + \dot{C}H_3 \rightarrow C_2H_6^*$$

$$H + C_2H_4 \rightarrow \dot{C}_2H_5$$

$$H + \dot{C}_2H_5 \rightarrow C_2H_6^*$$

$$C_2H_6^* \rightarrow C_2H_6$$

$$C_2H_6^* \rightarrow C_2H_4 + H_2$$

$$\dot{C}H_3 + \dot{C}_2H_5 \rightarrow C_3H_8^*$$

$$C_3H_8^* \rightarrow C_3H_8$$

$$C_3H_8^* \rightarrow C_3H_6 + H_2$$

$$\dot{C}_2H_5 + \dot{C}_2H_5 \rightarrow n - C_4H_{10}^*$$

$$n - C_4H_{10}^* \rightarrow n - C_4H_{10}$$

$$n - C_4H_{10}^* \rightarrow 2C_4H_8 + H_2$$

Olefins formed above are consumed by reactions with hydrogen atom to produce species like ethylene. Alkyl radicals are formed by adding hydrogen to olefins. Both of the reactions consume olefins. As temperatures increases, one significant effect is the production of thermal hydrogen which is not reactive at room temperature. Thermal hydrogen react with methane molecule very rapidly and produce hydrogen gas and methyl radical:

$$H + CH_4 \rightarrow H_2 + \dot{C}H_3$$

The increase of methyl radicals is largely responsible for the increased yields of a lot of saturates.

Electron beam radiation yields of higher saturated hydrocarbons in gas phase resembles that of methane in many ways. For example, irradiation of ethane and propane give very similar yields on multiple products. For liquid or solid hydrocarbons, one distinctive feature of liquid hydrocarbons irradiation above pentane is more chain growth products after sufficient irradiation because radicals become linked or combined together. Chain scission products are still in the same range, even though irradiation of same hydrocarbons at vapor phase gives more yields than liquid and solid phase on chain scission products. Table 2 includes radiation product yields of various straight alkanes. Irradiation of liquid hydrocarbons by ionizing radiation results in energy deposition in the form of ionized and excited molecules concentrated alone the track of ionizing particles. The ions and excited molecules are clustered into groups as spurs that contain a number of ion pairs and larger number of excited molecules. Yields and change of irradiating materials are the results of reactions of the radiation produced ions and excited species. One could try to understand the reactions based on the time scale each reaction might take. After the passage of the high speed electrons, ions and excited species are created alone the tracks of the electrons. Reaction such as ionizations, ion dissociation to give a radical, ion-molecule reactions, geminate recombination of ions, solvation of charged species, dissipation of excited species and recombination of caged radicals, etc. are very fast and will complete before species in the spur diffuse into the bulk. After 10^{-10} seconds following the passage of electrons, expansion and diffusion become important, reactions such as ion neutralization, hydrogen abstraction, radical recombination as well as radical disproportionation are dominate. Since each species is active in multiple reactions, it is

hard to predict its fate, for example, ion may take part in geminate recombination with an electron, or may undergo dissociation or ion-molecule reactions. Radicals may undergo dissociation or combine and produce dimers. But in general, ions in non-polar liquids such as most hydrocarbons will more likely undergo geminate recombination reactions within the spur. Excited states created in molecule such as liquid or solid aromatics may dissipate their energy very quickly without dissociation.

Table 2: Radiation Yields of Various Straight Hydrocarbons (Organic Radiation Chemistry Handbook, 1989, Edited by V. K. Milinchuk and V. I. Tupikov)

Molecule/100eV	Butane,C_4H_{10}	Pentane,C_5H_{12}	Hexane,C_6H_{14}	heptane,C_7H_{16}	hexadecane,$C_{16}H_{34}$
H_2	4.73	5	5	3.43	4.5
CH_4	0.52	0.26	0.14	0.11	0.038
C_2H_2	NA			0.011	0.126
C_2H_4	0.78	0.37	0.24	0.092	
C_2H_6	0.99	0.61	0.31	0.28	
C_3H_4	NA				
C_3H_6	0.2	0.35		0.058	0.06
C_3H_8	0.16	0.58	0.34	0.3	
C_4H_8	1.86	0.2	0.2	0.062	0.025
C_4H_{10}			0.4	0.325	
C_5H_{10}		2.76	0.1		
C_5H_{12}					
C_6H_{12}					
C_7			0.06		
C_8			0.29		
C_9			0.22		0.075
C_{10}			0.16		0.069
C_{11}			0.17		0.072
C_{12}					0.072
C_{13}					0.073
C_{14}					0.075
C_{18}					0.012
dimers					1.5
Polymers					
chain scission	2.65	2.37	1.73	1.238	0.685
chain growth			0.9	1.0	1.512

Wu and his partners investigated the radiation effect on the thermal cracking of n-hexadecane[122,133]. They analyzed the products distribution and proposed reaction scheme to find the reaction rate constants and activation energies. This is so far probably the most comprehensive study on radiation cracking of saturated hydrocarbons. Assumptions made in this study include: radiation initiation is temperature independent and reactions follow the Arrhenius kinetics. Such reactions are carbon bond rupture, H abstraction, β-scission and production of alkenes from radical reaction. Reaction mechanism of liquid phase hexadecane cracking due to irradiation are proposed in the following scheme:

Initiation

$$M \rightarrow M^* \rightarrow R_i^* + R_j^* \; and \; H + M^*$$

Propagation

$$R^* + M \rightarrow RH + M^*$$

$$M^* \rightarrow \; R^* + 1 - alkene$$

Radical addition

$$M^* + 1 - alkene \rightarrow \; {R_{18^+}}^*$$

Termination

$$M^* + M^* \rightarrow \; product \; \rho_1$$

$$R^* + M^* \rightarrow \; product \; \rho_2$$

$$R^* + R^* \rightarrow \; product \; \rho_3$$

M represents parent molecule hexadecane and M^* the parent radical; R^* is small radicals $C_1^* - C_{15}^*$; $\rho_1 - \rho_3$ are probable termination products. Reaction rate constants and

activation energy for each step was assumed in this scheme. If the limiting step is chain propagation, cracking reaction rate could be derived for hexadecane decomposition. With a model like this, a lot of kinetic parameters can be estimated. For example, activation energy of carbon-carbon bond dissociation in the initiation of radicals is estimated based on the Arrhenius plot. Hydrogen abstraction and radical addition as competing reactions are estimated based on the assumed kinetics.

2.4.4 Irradiation of Unsaturated Hydrocarbons

The yields of products formed on irradiation of unsaturated hydrocarbons including cyclic alkanes and ethylenic hydrocarbons differ from those from straight saturated hydrocarbons. The main difference between the radiolysis of straight pentane and hexane and cyclopentane and cyclohexane is the reduced number of products of C1-C5. This is in part due to the fact that only one radical was created by losing one hydrogen atom from a cyclohexane, while three isometric radicals were created by losing one hydrogen atom from hexane. Also C-C bond structure is stronger and more resistant to rupture. Ethylenic hydrocarbons give relatively high yields of high molecular weight products (polymers) and less hydrogen and other small weight molecules. For example, radiolysis of hexene produces three times less chain scission products than hexane, but the chain growth products are two times higher. The reason for less hydrogen production from ethylenic hydrocarbons is that hydrogen atom addition competes with hydrogen abstraction and the latter reaction makes hydrogen molecules. Hydrogen addition cannot happen to saturated hydrocarbons. High yields of large molecules in radiolysis of ethylenic

hydrocarbons could be explained by the fact that unsaturated hydrocarbons are efficient radical scavengers. Once a radical is created, it will react with the substrate rather than with other radicals. Polymeric products are formed by repeated addition of alkenes to a radical following the ionic polymerization mechanism. Ionic polymerization will not be inhibited by low temperature or radical scavengers. For example, isobutylene is polymerized by radiation in good yield at -80^{o}C. Chain scission products of radiolysis of alkenes are greatly reduced compared to alkanes. This could be explained by the fact chain scission products are believed to originate from free radicals chain reactions, at least it is true for straight alkanes. Since alkenes are good radical scavengers and will consume most of the radicals in polymerization reactions.

Radiation yields of acetylenic hydrocarbons are even higher than compounds containing double bonds towards polymerization. Irradiation of acetylene produces large amount of solids that does not dissolve in any solvents. The mechanism was similar as irradiation of ethylenic hydrocarbons and followed ionic polymerization. After an ion or radicals were created by radiation they are immediately surrounded by neutrals. Polymerization proceed from there.

Table 3: Radiation Yields of Various Cycloalkanes (Organic Radiation Chemistry Handbook, 1989, Edited by V. K. Milinchuk and V. I. Tupikov)

Molecules/100 eV	Cyclopentane, C_5H_{10}	Cyclohexane, C_6H_{12}	Pentene	hexene	Cyclopentane	cyclohexene
H_2	5.35	5.2	0.83	0.09	1.2	1.19
CH_4		0.016	0.47	0.03		
C_2H_2	0.05	0.155	0.8	0.091	0.06	0.021
C_2H_4	0.45		1.26	0.133	0.15	0.14
C_2H_6			0.4	0.028		
C_3H_4			1	0.113	0.16	0.006
C_3H_6	0.12	0.051				
C_3H_8	0.08		0.3	0.043		
C_4H_8		0.04	0.26	0.044		0.067
C_4H_{10}			0.035	0.035		
C_5H_{10}	0.74			0.007		
C_5H_{12}	0.14		2.66	0.001		
C_6H_{12}	cyclopentene 2.97	0.34				C6 0.25
C_7	bicyclopentane1.29	cyclohexene 2.8				2,2-dicyclohexenyl 1.9
C_8	cyclopentylcyclopentene 0.11	dicyclohexyl1.7				3-cyclohexylcyclohexene 0.58
C_9						dicyclohexyl 0.21
Dimers			3	1.7		
Polymers						
chain scission	1.58	0.262	4.49	0.525	0.37	0.234
chain growth	4.37	4.5	3	1.7	0	2.69

Aromatic hydrocarbons are more radiation resistant than alkanes and alkenes and give lower yields of products. Radiolysis products from benzene and toluene are mainly polymers with minor amount of hydrogen and acetylene. One important step responsible for polymers is the recombination of one positive aromatic ion and one negative aromatic ion. Negative ions are formed when an aromatic molecule captures one electron. Biphenyl, higher polyphenyls and hydrocarbons with polyaromatic structures are more stable under radiation. The reason for higher resistance to radiation is that electronic structure of aromatics allows energy transfer from higher excited energy states to lower excited energy

states that have a lower probability of dissociation. Especially in liquid phase, the excited molecules do not decompose immediately, but dissipate their energy by colliding with molecules. It is because the excitation energy is associated with the electrons moving in non-localized π orbitals, therefore energy is not sufficient to lead to dissociation. Aromatics can act as energy sink when mixed with other materials and reduce the damage of radiation.

Aromatics with alkyl group give yields of gas products and the chain scission product yields are higher when alkyl groups are larger. But the chain scission yields is much lower than the case without the aromatic structure. The addition of an aliphatic side chain with progressively from one to six carbon lengths to benzene increases the H_2 yield, but the yield seems to reach a plateau far below that found from a simple aliphatic such as cyclohexane. There is a large increase in H_2 with LET (linear energy transfer) for all of the substituted benzenes, which indicates that the main process for H_2 formation is a second-order process and dominated by the aromatic entity[118]. It also indicates that there is a strong interaction between the alkyl group and aromatic group that reduce the possibility of chain scission. This is because energy absorbed by the side chain will transfer to the aromatic group and get dissipated without causing bond rupture.

Table 4: Radiation Yields of Aromatics (Organic Radiation Chemistry Handbook, 1989, Edited by V. K. Milinchuk and V. I. Tupikov)

Molecules/100 eV	Benzene	Toluene	propylbenzene	butylbenzene
H_2	0.039	0.14	0.23	0.27
CH_4		0.012	0.014	0.015
C_2H_2	0.02	0.0023	0.997	0.088
C_2H_4				
C_2H_6				
C_3H_4			0.019	0.146
C_3H_6				
C_3H_8				
C_4H_8				0.018
C_4H_{10}				
C_6	cyclohexadiene,0.028	benzene 0.0188		benzene0.018
C_7	phenylcyclohexene 0.022	ethylbenzene 0.0012		toluene0.019
C_8	biphenyl 0.072	xylenes 0.0034		ethylbenzene 0.023
C_9	m-terphenyl 0.022			
C_{10}	p-terphenyl 0.021			
Dimers		0.179		
Polymers	0.92	1.28		
chain scission	0.02	0.0143	1.03	0.267
chain growth	1.057	1.4636	NA	NA

2.4.5 Irradiation of Hydrocarbon Mixtures

Radiation chemical yields are generally not as well established for hydrocarbon and non-hydrocarbon mixtures as for pure substances. The complexity becomes significantly large when dealing with mixtures of compounds that are fundamentally different in terms of their response to irradiation. This is due to the facts that a huge number of excited states and different radicals will be formed when electrons collide with organic molecules, and that there will be significant interactions between them.

When a mixture of hydrocarbon compounds was irradiated with high speed electrons, the response is usually not a linear accumulation of the irradiation yield of individual compound, except that the mixture was composed of similar compounds, for example alkane or alkene mixture. For the case of similar compounds in a mixture, the radiolysis of a mixture could be simulated by a formula:

$$G\ (P) = \sum_{i=1}^{n} G(P)_{A_i} * \epsilon_i$$

It predicts that total yield of a product P is equal to the sum of yield of individual compound A times its electron fraction ϵ_i under the same irradiation conditions. This mixture law assumes that ionization and excitation process happened to each compound are not intervened by another compound and the yields of a product is independent of the addition of another compound except the absorbed energy in each compound has to be reduced based on its mass ratio and stopping power. In reality, most of the hydrocarbon mixtures are not composed of closely-related compounds, therefore the abovementioned mixture law will not hold to predict the product yields. In fact there is always significant

deviation from this law if two compounds in the mixture are different in their irradiation nature.

When liquid alkane such as hexadecane is mixed with aromatic compounds including naphthalene, phenanthrene and hydroaromatics (95% alkanes -10% additives) and exposed to radiation. Less alkane degradation and reduction of radiolysis products including hydrogen and most chain scission products are observed. Since the number of aromatic molecules in the systems is much smaller than the number of alkane molecules, the radiation energy is mainly absorbed by alkane molecules. The absorbed energy generates excitation and ionization of the alkane molecules. Because aromatic and hydroaromatics compounds have a lower excitation and ionization potential than those of most alkanes, excitation energy and charge transfer from the excited state of the alkanes molecules and alkane's cation to the aromatic molecules takes place. These two processes lead to the reduction of alkane decomposition, and induce selective degradation of the aromatic additives[134]. The protection effect of aromatic on other hydrocarbons under irradiation was believed to follow a charge scavenging and energy transfer mechanism. It could be illustrated in the following steps:

$$n - C_{16}^{+} + A \rightarrow n - C_{16} + A^{+}$$

$$A^{+} + e^{-} \rightarrow A^{*}$$

$$A + e^{-} \rightarrow A^{-}$$

$$A^{-} + A^{+} \rightarrow A^{*} + A$$

$$n - C_{16}^{+} + A^{-} \rightarrow n - C_{16} + A^{*}$$

Specifically, chain scission products were reduced by addition of aromatics in the mixture and the reduction of those products was proportional to not only the concentration but also the degree of aromaticity of the additives. In addition to the reduction of final products, fast pulsed radiolysis could be used to verify the charge transfer and energy transfer between aromatic and alkane molecules. Reactive intermediate species such as excited alkane molecule and radical could be identified and their reaction pathways could be studied as well. Absorption spectra analysis by using pulsed technique proved that aromatic molecules has strong reactivity toward radical cations of alkanes and electrons. Since chain scission products are believed to be produced from free radical chain reactions, the reactivity of aromatics towards radical cations of alkanes might be responsible for the reduced scission products.

2.4.6 Irradiation of Crude Oils

Crude oils are unrefined petroleum product and comprised of hydrocarbons, other organic compounds and impurities including metal and salt. Hydrocarbons are usually the primary component of crude oils. Organic compounds like nitrogen, oxygen, and sulfur typically make-up between 6%-10% of crude oil while metals such as copper, nickel, vanadium and iron account for less than 1% of the total composition. Crude oils are more difficult to process due to higher contents of asphaltenes, heteroatoms and metals. Chemical compositions of crude oils are important because they determine the type of refining techniques that need to be used and what the products distribution will be after refining. Techniques such as simulated distillation and SARA are used to separate

saturates, aromatics, resins and asphaltenes[135]. Elemental analysis could be used to determine the contents of metal such as Vanadium and Nickel and heteroatoms such as sulfur, nitrogen and oxygen[136]. More detailed characterizations of crude oils could be done by chromatographic and spectroscopic analysis to study the large molecule structure in crude oils[7].

The study of irradiation of crude oils in many sense is based on the results of hydrocarbon irradiation. Irradiation of crude oils, however are more complex than that of normal hydrocarbons mixtures because of the large number (thousands) of compounds and large volume of unknown molecules with poly-aromatic structure as well as the effect of impurities including metals and heteroatoms. The complexity of irradiating crude oils are largely due to the facts that: First, as mentioned in the previous section, there is no simple mixture law that can predict the radiolysis of such a complex mixture like crude oils. When the number of hydrocarbons in a mixture is more than a few and the type of them varies from saturates to aromatics, the radiolysis yields and products are impossible to predict based on current understanding of this process; second, the existence of large quantities of non-hydrocarbons (impurities) in crude oils including water, salt, metal and heteroatom compounds add more complexity and unpredictability to the radiolysis yields and products. Very few research or results could be found on irradiation of hydrocarbons with impurities like metal or salt. In generally irradiation of a mixture of organic and inorganic compounds are not well studied and lack of theory and experimental data.

Despite undeveloped theory and very limited data regarding irradiation of crude oils with many impurities, there are still important aspects that might help us understand or at least give us a sense what might be going on when irradiating crude oils.

Metal and metalloid constituents could be naturally found in crude oils or they could be added during production and transportation. Those elements are present in crude oils in the form of organometallic compounds of Ca, Mg, Fe, Ni, V and Zn adsorbed in water oil interface[137,138]. The presence of them could be deleterious to the refining process due to corrosion on processing equipment or catalysts poisoning. Among them, vanadium and nickel are found to be most abundant in crude oils. Very few literature have been found on the effect of those elements on irradiation of crude oils. It is reasonably possible that those elements may not play important role in irradiations since their concentrations are at ppm scale, which means the possibility of them contacting with a hydrocarbon radical or excited states is below 1% by estimation. Catalysts are not necessary in any irradiation processing unit which further reduces the concern of metals.

Irradiation of Water and oxygen give rises of large number of reactive species including OH, O, H_2O_2 and O_3. Those species attack hydrocarbons very efficiently and form other organic compounds mainly via oxidations. Water and oxygen might not be present in crude oils, but once they are, radiation induced hydroxylation and oxidation reactions may occur and produce hydroxyl-aromatic structures like phenols and hydroxylated biphenyls.

A series of sulfur compounds could add to alkenes through radiation initiated chain reactions[104]. Sulfur compounds commonly found in crude oils are hydrogen sulfide,

sulfur dioxide, bisulfide ions and so on. For example, hydrogen sulfide gives HS radial and H radical upon radiation. HS radicals can react with an ethane molecule to form another radical and propagate the chain reactions. A bigger molecules will be formed after the chain termination step.

$$H\dot{S} + CH_2 = CH_2 \rightarrow \dot{C}H_2 - CH_2SH$$

$$\dot{C}H_2 - CH_2SH + H_2S \rightarrow CH_3 - CH_2SH + \dot{S}H$$

Other sulfur compounds could add to alkenes in a similar manner. The final product size largely depends on the sulfur compound size and irradiation conditions such as dose rate and dose. But any product that contains sulfur compounds is not desired in crude oil refining.

Unlike sulfur compounds that can add to alkenes through chain reactions, nitrogen oxides including nitric oxide and nitrogen dioxide are effective radical scavengers and can react with hydrocarbon radicals to form nitrogen compounds as a chain termination step. For example:

$$C_{12}\dot{H}_{25} + NO_2 \rightarrow C_{12}H_{25}NO_2$$

Possible reactions in irradiation of crude oils are not limited to those mentioned above, others include sulfoxidation, carbonylation, halogenation and many reactions with phosphorus compounds. Please note that the reason why those reactions are introduced is not that they are dominate in irradiation of crude oils, but that the compounds involved in those reactions are present in crude oils with significant quantity. Because of their quantities and potential effect on radiolysis of hydrocarbons, we should not ignore them.

In this context we treat all non-hydrocarbon compounds as impurities. Based on possible reactions brought by all impurities in crude oils, the main mechanism that an impurity could change the irradiation process is reacting with a radical intermediates to remove the radicals or form a more stable radical that is unable to carry on the chain reactions. The effect of the impurity on irradiation response depends on its concentration and the type of compounds it is attached to. The Oxygenated species and aromatics, for example, react with other hydrocarbon radicals to form stable species and therefore inhibit many other chain reactions.

In summary, Irradiation of crude oils faces unpresented challenges and tremendous uncertainties due to factors discussed in early part of this section. It could be treated as irradiation of thousands of different type of hydrocarbon compounds with significant amount of impurities. This is due to the nature of crude oil and does not deviate much between crude oils except significant variation on fractions of each crude oil. What is changing though is the responses of each fraction under radiation when it is mixed with many other fractions. Despite the difficulties and complexity of irradiation of crude oils, there are unique features and advantages regarding irradiation of petroleum. This is why electron beam radiation methods for upgrading and refining high-viscous crude oils and petroleum products are investigated by researchers at various conditions. The advantages of radiation technology include simple configuration of radiation facilities, low capital and operational costs, processing at lowered temperatures and nearly atmospheric pressure without the use of any catalysts, high production rates, relatively low energy consumption, and flexibility to the type of oil feedstock[139–143]. Deactivation and poison of catalysts

due to coke and metal deposition as well as sulfur content has been a big issue in the petroleum industry, so avoiding catalysts will significantly benefit this industry. The benefits of lower temperature process are that it will avoid runaway chemistry due to chemical instabilities at very high temperature at local hot spots which will lead to the formation of C(s) and H_2. Also the non-uniformity of temperature will favor the formation of coke precursors and precipitation of asphaltene causing problems such as transportation rate reduction and coking generation.

Based on the current theory and understanding of the irradiation of crude oils, reasonable expectations on the results should be: first, radiolysis of crude oils and products are not the same from that of hydrocarbon mixtures without impurities. Impurity effect might be significant enough and cause the overall results of radiation processing not to follow the law of irradiation of hydrocarbons. Yields of irradiation of crudes might not be comparable with yields of hydrocarbons; second, it might not be clear which compound has larger effect on irradiation response because of the larger number of them. Third, all radiation induced reactions can happen at the same time and compete. Some of them lead to chain scission products via cracking reactions. Some of them lead to chain growth products via polymerization or crosslinking. Forth, parameters such as conductivity, viscosity and density have not been well understood on their effects on radiation yields and radiation products. It is not surprising that one or all of them play import roles in the radiation process. Take conductivity for example, it affects the behavior of charged species inside the irradiated sample and charged species are believed to contribute to the radiation yields. Last but not the least, radiation yields and products distribution may also depend

on the reactor design and flow type, especially in the refining industry, reactor design does not only change the efficiency of the process, it could also change the quality of products to make the process totally economically viable or not. The key is controlling the experimental conditions to favor desired reactions and suppress side reactions.

CHAPTER III

RESEARCH METHODOLOGY AND APPROACH

This research topic will be mainly composed of three parts: Design and building of the experimental setup, flow condition and irradiation condition determination (flow rate, velocity distribution and resident time, dose rate and dose) and oil property characterization with devices including rheometer, density meter and GC.

3.1 Experimental Setup

3.1.1 Ebeam Facility

The ebeam irradiation of crude oil tests were performed at the National Center for Electron Beam Research (NCEBR), which is located on the campus of Texas A&M University, College Station. There are two vertically mounted 10 MeV, 18 kW commercial scale high energy linear accelerator and a single horizontally mounted 5 MeV, 15 kW X-Ray linear accelerator. This research facility was designed for food processing and it utilizes a single conveyance system to deliver the product in and out of the process chamber. It has been approved for commercial use as well as for research projects. Two operation modes are available but will not run at the same time, which means during commercial irradiation, research irradiation will not take place and vice versa. Regarding to this project, special fixture was designed and built for oil sample irradiation. Figure 9 shows the oil sample irradiation experimental setup in the cell. The oil samples were irradiated with one of the vertically mounted accelerator from the top with an average pulse current of 1.5 mA, pulse rate of 256 pps, pulse duration of 10 μs, instaneous current

0.7 A and scan frequency of 4.2 Hz.

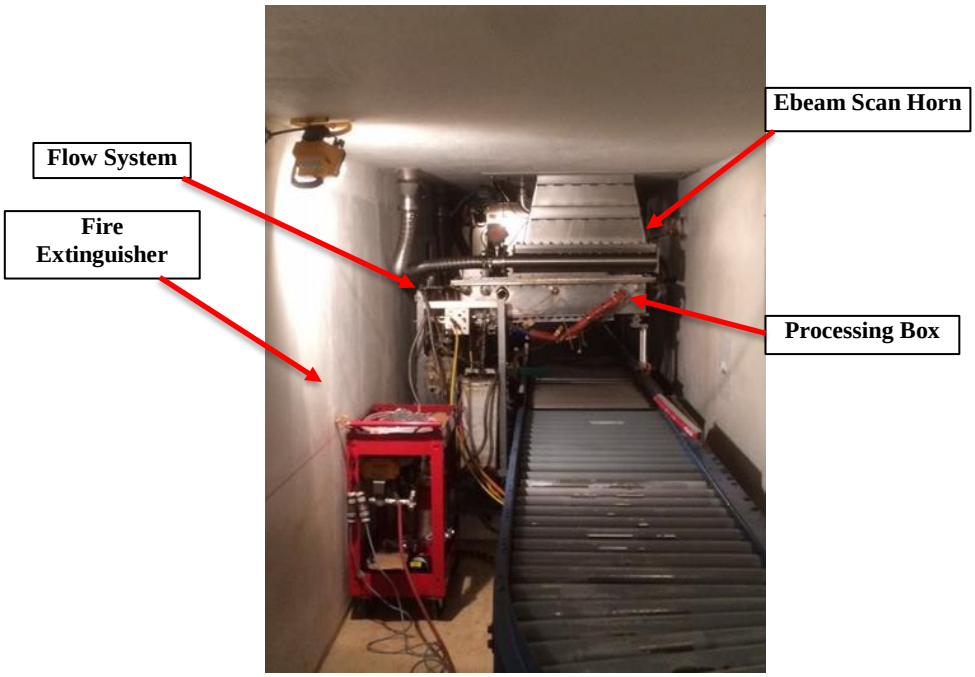

Figure 9: Crude Oil Sample Irradiation Setup in the Cell

3.1.2 Continuous Flow Reactor

The flow reactor was supported by a steel base with rolling wheels that can handle over 200lbs. Strut channels typical 1 5/8-inch aluminum are used to provide extra support to all devices on the rolling cart. The overall dimension and size is constrained by the pass-through doors and hallways to the testing area of the ebeam vault. Important components include a 3 phase AC motor, a Chemsteel gear pump, electrical band heaters and fiber glass heating tapes, oil storage and collectors, a closed processing box, aluminum U-shape

channel and electrical inputs. Figure 10a is the continuous flow oil testing system. Oil starts from the storage tank and get pressurized in the pump, then enter the processing box. Inside the box is an aluminum channel that allows oil flow through it as seen in Figure 8b. Treated oil will be stored in the collector. It depends on whether the treated oil was sent back to the processing box and got further irradiated, there will be two processing modes: multi-pass and single pass. It is very important that all the oil transport lines upstream of the processing box are preheated and insulated to maintain its temperature in order to transport highly viscous crude oils without clogging.

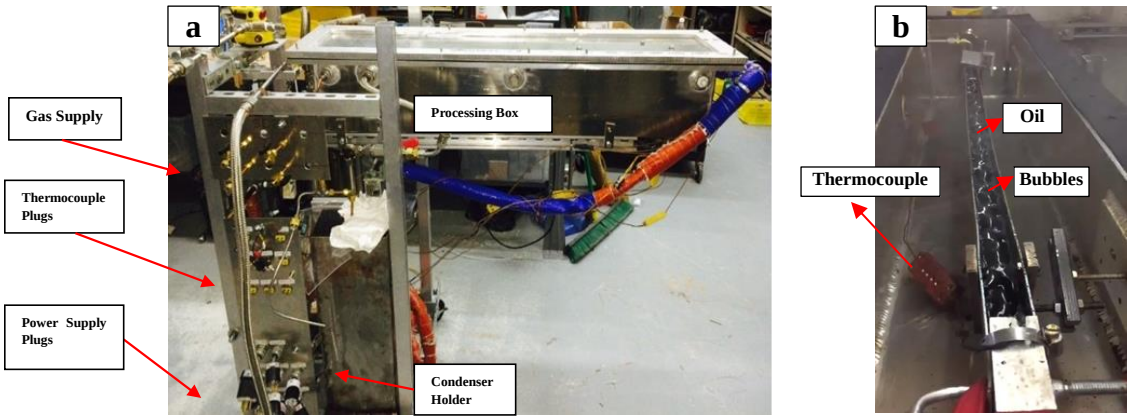

Figure 10: Experimental setup (a) and crude oil with gas bubbling (b)

The Oil collector and condenser are High-Polish Quick-Clamp Sanitary Straight Tube Fittings 3in OD x 18in in length with both ends sealed by sanitary tube caps and clamps. Both were made of 304 stainless steel and have a capacity of 2L. Viton gaskets are used here to work with high temperature oils. The storage tank is 4in OD x 15in in

length and has 3L capacity. One three phase AC motor and one gear pump are connected coaxially through a shift coupler. The motor-pump combination is powered by a VFD (variable frequency drive). The VFD intakes normal power supply 120AC, at constant 50 Hz and outputs power to the motor with varying frequency and voltage. In this way we will be able to continuously control the oil flow rate by adjusting the VFD output to the motor. A rectangular shape aluminum box 45x8x8-inch with wall thickness 1/8 in and flange 2.5-inch long and 0.5-inch thick was designed to provide space for the electron beam irradiation of crude oil. Aluminum allows less loss of electron beam energy due to its small density so that electrons still preserves its original energy and there is no significant energy deposition to the wall. Therefore, temperatures on aluminum surface will not be significantly higher than the processed oil. Holes are used for oil inlet and outlet, gas inlet and outlet, cooling water inlet and outlet, thermocouples monitor and sight windows.

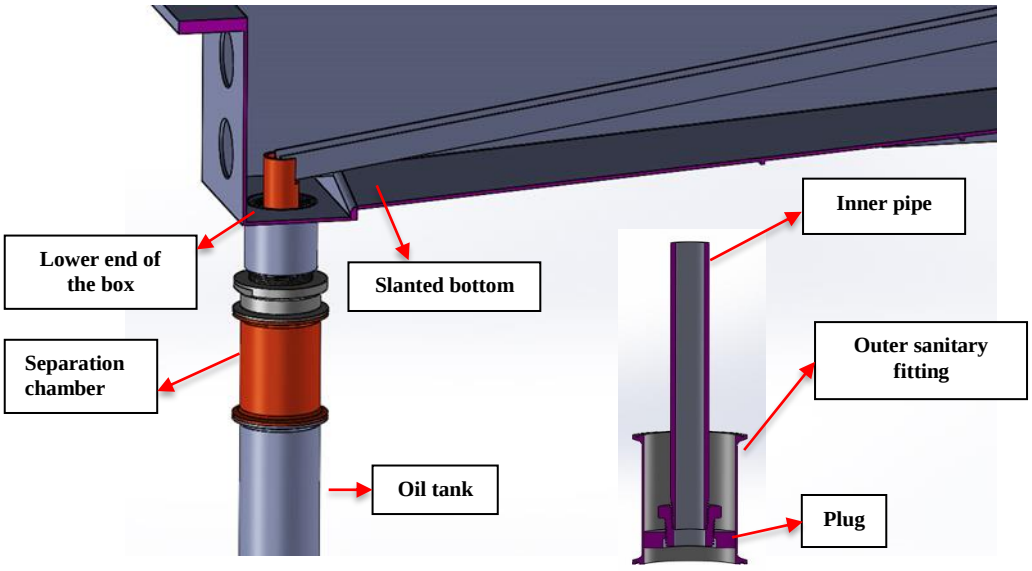

Figure 11: Separation chamber located below the channel inside the box

Note that there is an optional separation chamber seen in Figure 11 connected between the box and the tank. The function of it is to separate the condensed light components inside the box from the main stream and that will prevent those from being irradiated again. The idea behind this originated from the results that produced lights are a desired products and should not be further processed. This takes advantage of the localized beam nature of the process and effectively evaporative selectivity (only those components which are still heavy and high density (liquid phase) are processed). A competing theory, which would indicate that the separation chamber is bad, is that lights should be recycled back into the oil being processed. This assumes that the lights are hydrogen rich and can act as hydrogen donors to the hydrogen deficient heavier

hydrocarbons. Another possible effect though is that these lights are polymerized when stored with the hydrogen deficient oils.

Important parts in experimental setup except the separation chamber include oil flow channel, processing box as well as condenser. Design details such as function and capability for each of them will be discussed in chapter IV. Performance of different design will also be evaluated.

Two testing modes will be available with the current setup and only a small adjustment needs to be made: single-pass (Figure 12a) and multi-pass (Figure 12b). Single-pass test will be conducted in a way that oil starts from the storage tank and stops at the collector after being irradiated in the processing box. Multi-pass test combines the storage tank with the collector. Oil flows in closed loops and get treated repeatedly with a longer time. Both of the testing modes are shown below in Figure 5.

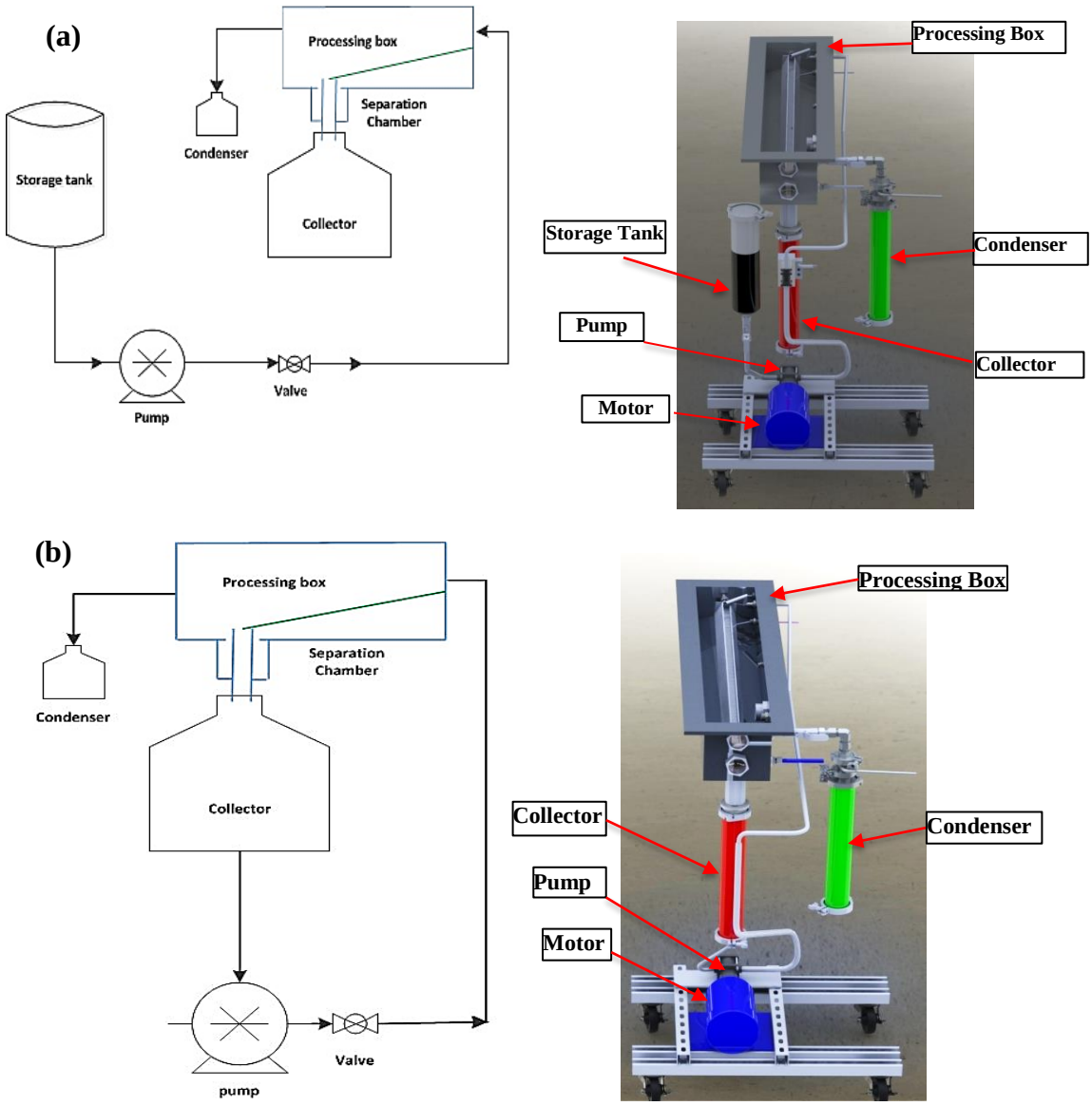

Figure 12: Oil Flow Testing Configuration: (a), Single-pass and (b), Multi-pass

3.1.3 Fire Monitoring System

A fire monitoring system in Figure 13 with two fire extinguishers, remote control pneumatic valves and a camera was designed and assembled to work with the continuous

flow reactor during the oil irradiation experiments in the cell. The camera will be setup about 8-10 feet far from the testing cart and will provide a real time view of what is happening on the testing cart to a monitor on the control table. Nozzles of fire extinguishers target at the spots that may cause fire, e.g. the top of the box very closed to the beam horn and band heaters on the storage tank. The pneumatic valves controlling the extinguishers could be switched on/off from the control table.

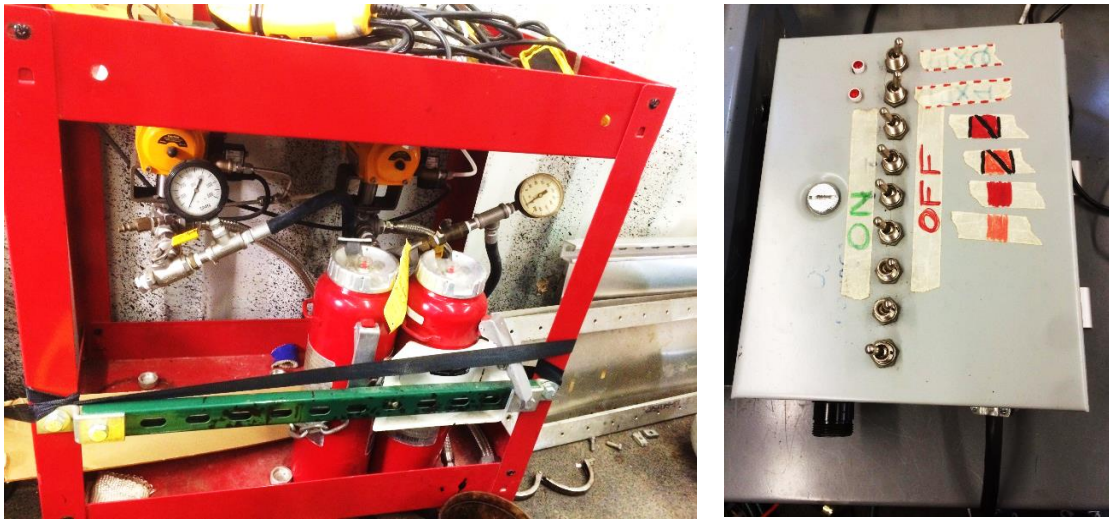

Figure 13: Fire extinguishers and control box

3.1.4 Remote Control Table

The control and monitor process during the irradiation experiments were conducted on a rolling table seen as figure 14 which houses a main control laptop, a PC

monitor, VFD, NI data acquisition system, thermometers, camera system, power supply and control as well as an air compressor. The remote control system is connected with the experimental setup inside the cell through 100 ft of wiring. This table is 30in x 60in steel welded and capable of loading over 1500lbs. NI LabVIEW and DAQ on the laptop are the platform to do the process control and data acquisition. 7 solid state relays were connected with NI device and together they will provide a closed loop control on the heaters to maintain required oil temperature.

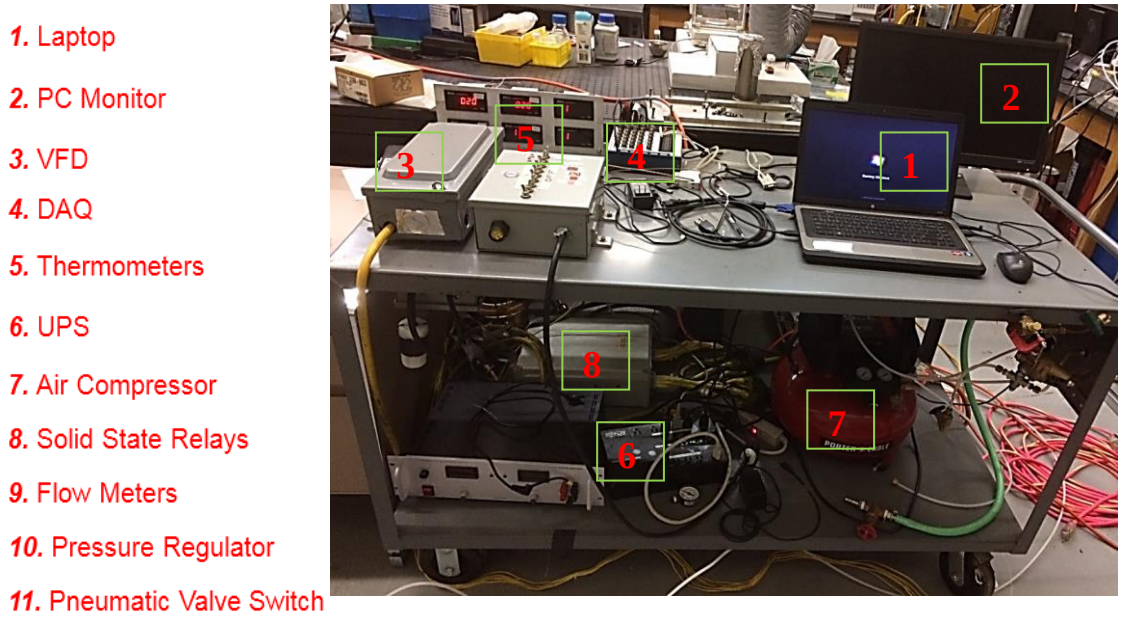

Figure 14: Remote control table that houses all control and display units for irradiation experiments

3.1.5 Mobile Lab Trailer / Portable Walk-In Hood

A mobile lab trailer in figure 15 to provide a continuously air-purge environment for reactor testing was built and tested. It consists of several components including an 8'x8'x20' steel container, a trailer with four wheels, two upblast ventilators (one constant speed and one variable speed), a gasoline-powered power generator and the lighting system. The ventilators (on the top) together are able to provide a total air flow rate to the trailer in the range of 1500-7000 CFM at a small static pressure. Divided by the cross section area, the air flow still moves at 25-100 feet per minute. Such air flow, face velocity, classifies it as a walk in hood. A gasoline fueled power generator (on the bottom) with rated power at 17500 watts provides electricity to all the devices working inside the trailer, such as ventilator, AC motor, flow pump, lights, such that the system can be tested in a standalone configuration in a safe manner prior to testing in the e-beam facility. The mobile lab will be primarily used when we are dealing with any potentially flammable and toxic volatile species and need to work in a continuously air-purge environment. Being portable the facility can be used during shake-down test and control test at the plasma lab and during real testing at the e-beam facility.

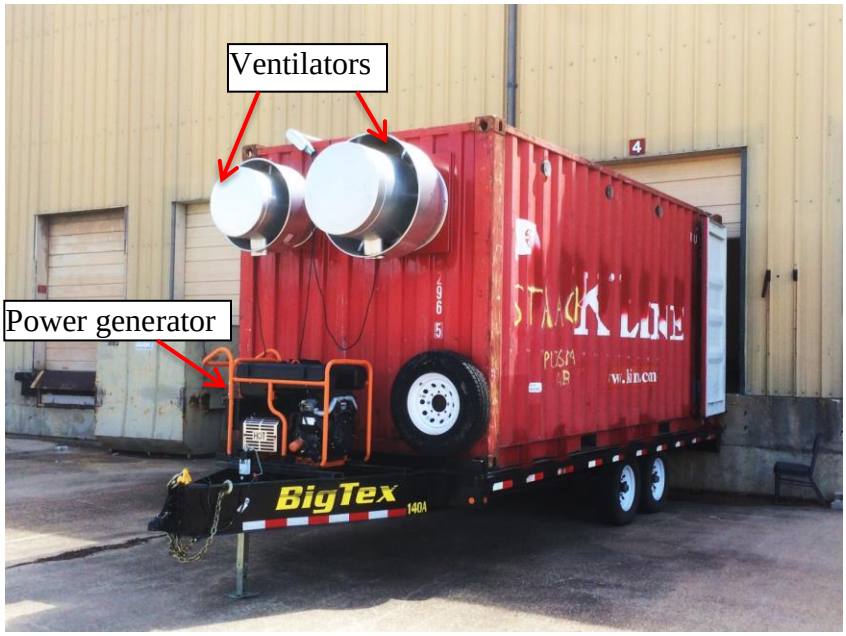

Figure 15: Mobile lab trailer assembly that is used to transport all equipment to ebeam facility

3.2 Flow Modeling and Irradiation Simulation

Oil flows on a 1-inch wide and 7/8-inch deep aluminum channel in figure 16a under the electron beam radiation. To quantify the specific energy input (or dose) to oil samples in the flow system requires both velocity profile and dose distribution inside the oil film. The residence time, oil flow thickness, and oil velocity were experimentally measured in the flow system as a function of channel angle, total flow rate, and temperature in a set of control experiments outside of the vault. Generally the Reynolds number for the flow ranges from 100 to 500 and the oil flow is laminar. In the absence of gas bubbling the velocity profile can be derived assuming flow on an open channel driven by gravity and a shear-free surface at the oil-air interface. Only friction on the flow was

from the wall and depending on the viscosity of the oil. Those boundary conditions result in a parabolic velocity distribution in the oil film shown in figure 16b. Therefore more parameters such as average velocity, oil residence time and oil film thickness are derived. Oil film thickness and flow velocity were also found from experiments. The thickness of oil film on the channel was measured directly with rulers. Oil free surface velocity was found by using high speed camera. Difference between modeling results and experimental results was within 10%. Theses modeling results assume a constant temperature oil, due to the water cooling here this assumption is applicable. Based upon laminar flow modeling there would be a significantly higher dose on the near wall oil than the free surface. The gas bubbling through the bottom of the open channel mixing boundary layer with free oil surface oil.

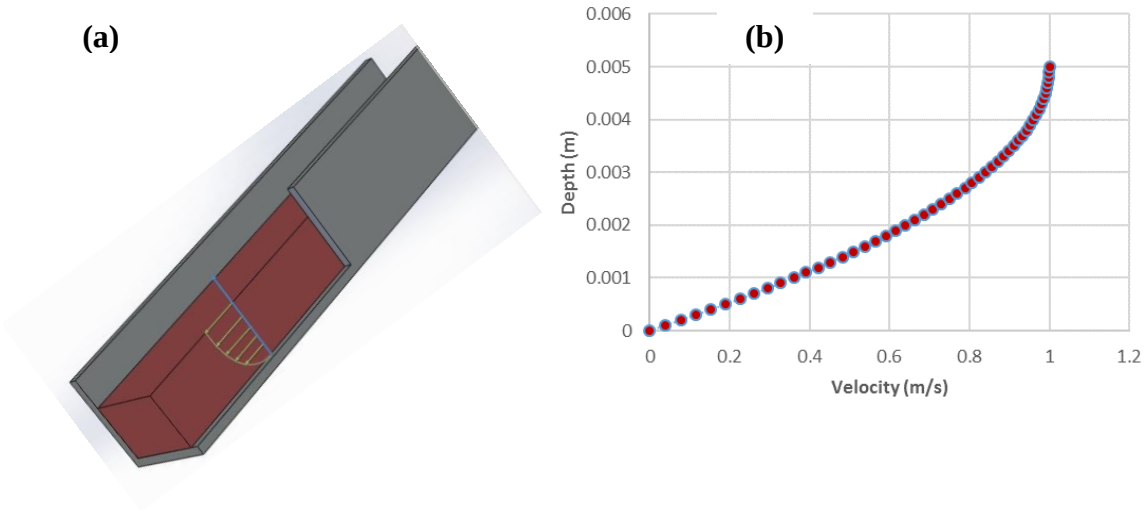

Figure 16: Oil film (a) and velocity distribution (b) in oil thickness

Knowing residence time of the fluid, dose rate is needed to calculate the dose received during each pass of the oil under the beam. Dose rates in both beam scan direction and width direction were found by using solid alanine dosimeters. Alanine tablets are irradiated for 2-3 seconds (measured by monitoring the EMI from the beam, which correlated with beam current) under the electron beam and after that EPR (Electron Paramagnetic Resonance) was used to find the dose inside the tablets. EPR probes are calibrated quarterly at the NCEBR using standard dosimeters calibrated by Nordion.

Five dosimeters along 5 cm in this direction were exposed for about 2.5 seconds and the dose was measured. A Gaussian distribution fits the measured data very well. The FWHM of the beam is about 2.5 cm which is equal to the width of the channel. The average dose rate over the width of the channel is calculated based on the distribution. This calculation has some uncertainty but is indicative of the average dose received. Dose

distribution along the beam through the oil film was estimated based on known distribution in water for a 10 MeV electron beam[102,144]. Figure 17 represents a calculated dose distribution in mineral oils. This calculation took into account the density effect. As we can see, its penetration depth in mineral oil is more than 4 centimeters. Because oil film thickness on the channel is less than 1 centimeter, it is reasonable to assume that dose rate difference in oil depth direction is less than 15%.

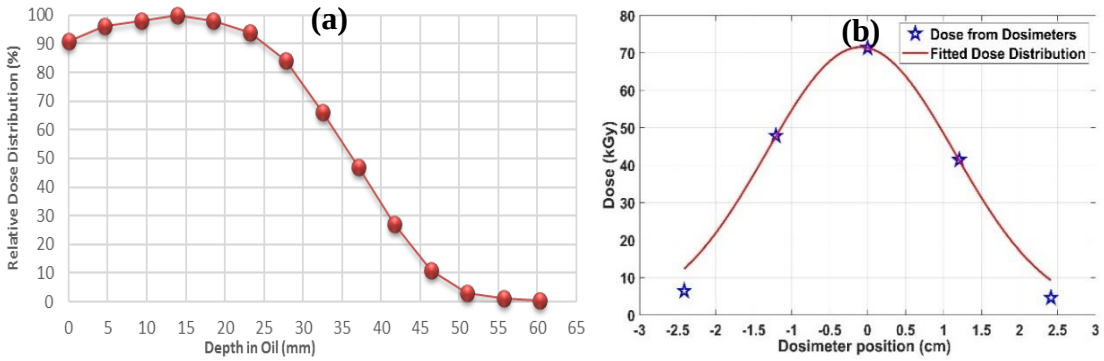

Figure 17: Solid dosimeters and dose distribution in depth (a) and width (b) direction

When gas was injected into the oil film during irradiation, there were bubbling jets along the irradiation length with an overall gas flow rate of 5 L/min. Flow visualization with and without bubbles indicate that the bubbling causes laminar mixing on length scales on the order of the spacing between the jets. On average with this regular mixing the residence time and dose for all oil is about the same. The overall residence time of the oil is about the same for bubbling and non-bubbling cases since the relative momentum of the gas flow is about 1% of that of liquid.

3.3 Oil Property Characterization

One of the most important goals of processing crude oils for transportation application are increasing API gravity and reducing the bulk fluids viscosity. Viscosity of a crude oil sample depends on the ratio of all compounds that compose it and the viscosity of each compound. Typically if crude oil has high light fractions it will show a low viscosity and high API gravity. This indicates that viscosity reduction could be achieved by converting heavy fractions to light fraction in the oil after ebeam treatment.

Many crude oil contain dissolved impurities and asphaltenes that can precipitate when the temperature falls below a critical value. Those substances will force the crude oil to transition its rheological behavior from its original simple Newtonian to a much more complex behavior and can exhibit a high yield stress and time dependent characteristics under different shear stress and shear rate. In this research oil rheological characteristics at relatively high temperatures will be studied before and after the irradiation. The difference will be contributed to the electron beam treatment.

3.3.1 Mass Balance

Mass balance of treated samples was recorded to account for all different hydrocarbons found in different locations after the test. Volatile hydrocarbon compounds in the oil evaporate when oil is being heated or irradiated, then they will condense on cold surface and wet the surface, for example lighter hydrocarbons condense and become liquids when contacting the wall of the processing box and inside the condenser. The mass

of those need to be measured or estimated. Oil also remains on the bottom of the channel and the box after flowing through them. The weight of the remaining oils will also need to be known. All those components will add up to the total mass of the treated sample. Ideally this cumulative mass should be very close to the initial mass of sample before the irradiation experiment. Most of the crude oil is concentrated in the storage tank (collector; for the purpose of this discussion). However, a moderate portion of liquids are found in the condenser, separation chamber, the channel and at the bottom of the box. All these different liquids are collected and mixed in the same mass ratios to obtain the treated sample. This section talks briefly about the different liquid products and their properties

Mass balance results are critical and indicate whether the experiments are successful and whether the experimental results (viscosity change and conversion) will be applied. For processing of oils at industrial scale, mass balance is typically close to 100%, whereas the mass balance of oil processing at laboratory scale with less than 2kg sample is expected in the range of 95-100%. The mass ratio of individual component within the total mass balance varies as experimental parameters change. One goal of the research was to increase the yields of light fractions in the crude oil.

Mass balance uncertainty impose larger uncertainties on viscosity results because viscosity depends on the mass ratio of each component following either a power law or exponential law, for example 5% mass change might cause a viscosity change as high as 50%. What's more, the dependence of the treated oil viscosity on each component deviates significantly because of the drastic viscosity difference. Lighter fractions which have a viscosity thousands of times smaller than that of heavy fractions will have much bigger

impact on the crude viscosity. That implies that if there is 5% mass loss due to light compounds, it could lead to a 70% increase in viscosity. But if the 5% was heavy residue, it would only decrease the viscosity by about 10%.

To reduce the uncertainty due to mass balance, the mass balance should be in the range of 95-105%, so that viscosity of the resulting oil mixture due to mass loss or mass gain will not be significant. Since the irradiation system is a continuous flow system with energy addition, control tests need to be done without ebeam. Control test will be used as reference to study the net effect of ebeam irradiation. Control tests will also be used to study the repeatability of the system. Tests with and without ebeam should yield similar results.

3.3.2 Viscosity

Two crude oil samples were investigated in this dissertation research and their raw sample properties are attached in Table 5. API gravity and viscosity indicate that they are both extra-heavy crude oils. They all have significant amount of metal, nitrogen and sulfur contents. Oil B is heavier and much more viscous than Oil A. Other major differences between them are the sulfur content and H/C. Oil A has higher sulfur content and hydrogen to carbon ratio H/C.

Table 5: Properties of two Crude Oils

Oil	Density (g/ml) 15 ºC	API gravity	Asphaltene (%)	C (%)	H (%)	N (%)	S (%)	V (ppm)	Ni (ppm)	H/C	Viscosity (cP) 50 ºC	100 ºC	150 ºC
Oil A	1.021	7.8	7.14	82.95	10.28	0.48	5.10	79	213	1.49	9400	240	25
Oil B	1.036	5.2	8.7	84.12	10.02	0.68	4.3	110	478	1.42	86000	1920	129

All ebeam irradiated oil samples were measured on their viscosity. Viscosity results were compared with the raw sample viscosity. A rheometer seen in figure 18a is used to measure the oil viscosity. It is a rotational device with accurate motor speed control that allows to monitor the torque and power. Together with the motor, a rigid air bearing allows very good drift stability and low torque capabilities. Oil sample is heated up with controlled temperature inside a housing. Sample loading is easy and fast.

Anton Paar MCR Physica 101 rheometer has been used for obtaining rheological properties of oil A and oil B. Both cone-plate and plate-plate measuring systems were used though cone-plate measuring system is favored in order to obtain constant shear rate over the sample. The cone has a diameter of 50mm and angle of 2°. Two sets of parallel plates with diameters 50mm and 25mm have been used. The cone-plate measuring system requires a sample of 1.14ml whereas the plate-plate configuration requires 1.96ml (for 50mm diameter and 1mm gap). The instrument has automatic thermal expansion compensation and a thermal insulating cover to avoid any thermal gradients and positioning errors. The instrument is limited by a maximum torque of 0.125 Nm. This

corresponds to a maximum shear stress of 3830 Pa or 8955 s-1 (whichever comes first) for the cone-plate system and 5093 Pa or 7854 s-1 for plate-plate system.

To do the test, shear rate is controlled by changing the speed of the motor. This will result in a torque due to shear stress from the oil. With both shear stress and shear rate known, viscosity of the sample will be derived.

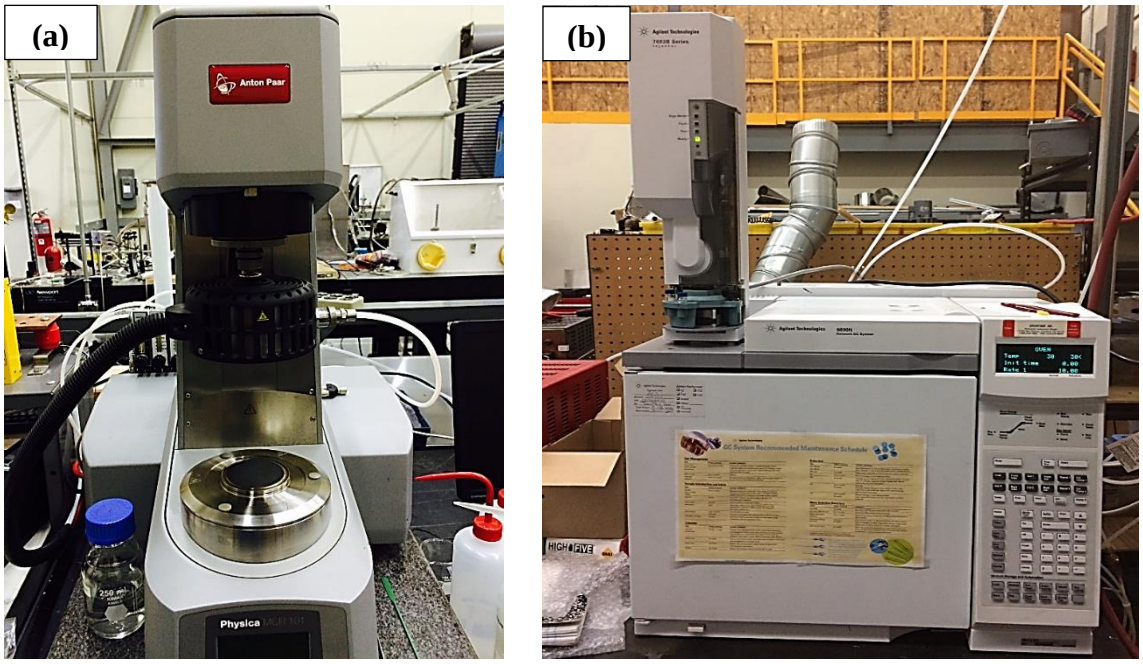

Figure 18: Rheometer (a) and GC equipment (b) in plasma lab

3.3.3 Simulated Distillation

The simulated distillation results provided by the project sponsor are given in figure 19. By definition, Oil A has less than 10% residue, while Oil B has 30% residue with the applied method. Neither of them has significant fractions less than C_{20}.

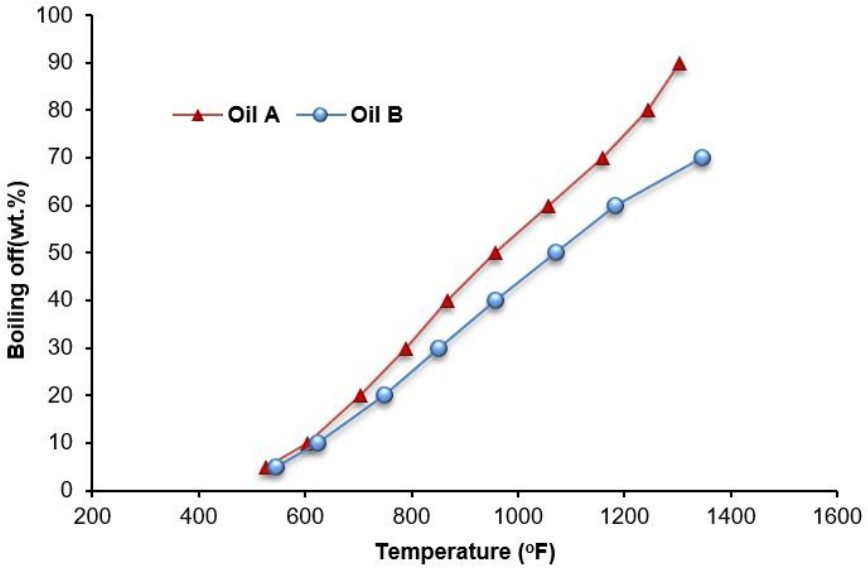

Figure 19: Simulated distillation results of Oil A and Oil B

Simulated distillation method is an alternative to the physical distillation method which could be applied in laboratory with small sample quantity. It belongs to the separation process and could be used to study the distribution of each fraction in the crudes. It will be carried out on a gas chromatograph with a goal to separate hydrocarbon species because of different elution time in the GC column. Simulated distillation uses methods defined by the American Society for Testing and Material (ASTM). Methods

vary by temperatures profiles and the oil sample that applies this method, for example light crude and heavy crude use different methods. Oil A and Oil B are both extra heavy crudes with large fractions of heavy compounds. To analyze them with simulated distillation, a method with high temperature will be used. ASTM D6352 is used to study the petroleum distillate fractions having an initial boiling point greater than 174^{o}C and a final boiling point of less than 700^{o}C.

Agilent 6890N series gas chromatograph is used for simulated distillation analysis to quantify conversion in all ebeam treated oil samples. Figure 18b is the GC equipment. It is equipped with an auto-sampler (Agilent 7683B series) and a flame ionization detector. A 5 µL micro-syringe with a 23 gage stainless steel needle has been used for injection. The instrument comprises of a cool-on-column (COC) injection system. A high temperature non-polar simulated distillation metal column of length 5m and diameter 0.53mm has been employed. The capillary column has a stationary phase composed of 100% bonded dimethylpolysiloxane and the film thickness is 0.09µm. The oven is capable of reaching high temperatures of 450°C and programs up to 35°C/min. The data acquisition can acquire signals in the range of 5-30 Hz. Ultra-high purity Helium is used as a carrier gas along with hydrogen and air for the detector. Along with using high purity gases, additional gas purifiers are set in place to prevent any minute amount of83 contamination possible. The gas chromatograph is equipped with electronic pneumatic controls to achieve and maintain the flow rates necessary.

To perform simulated distillation on a GC requires a series of other devices under standard ASTM methods such as ASTM D2887 and D6352.

3.3.3.1 GC-FID configuration and signal processing

Column: high temperature distillation method requires thin film of stationary phase to obtain the resolution within the specified range. Typical film thickness range from 0.09 to 0.15 μm and can elute components equivalent to n-C110. Even though glass, fused silica and stainless steel columns are recommended, metal tubing is preferred as fused silica cannot withstand the high temperatures of the order of 430°C required for analysis.

Detector: multiple detectors can work with GC including FID (flame ionization detector), TCD (thermal conductivity detector) as well as mass spec detectors. FID detectors are more robust and sensitive with low concentration compounds in the sample. It is used with the GC.

Injector: auto injection system was installed on the top of the GC. It works with accurate sequence controlled by the GC software. Injection was done by a glass syringe with stainless steel needles. Sample was directly injected into the column. It is called cool-on-column.

Oven: temperature programmable oven is used for the GC to precisely control the temperature profile in the column. It is capable of ramping temperature to a certain value within specified time.

Sample preparation and injection: sample was diluted in a glass vial by a ratio of 1 gm of sample to100 ml of solvent. The mixture is shaken vigorously to ensure enough dissolution. Then 1.5-2 ml of diluted sample / solvent mixture was transferred to a GC vial

with Teflon lined lids. A concentration of 1:100 m/v is chosen in order to obtain a good signal without overloading the column. Samples are placed in the injection tray of the auto sampler according to the injection sequence. Baseline and blank (solvent only) run are first performed to make sure there is no residual left on the column. After the blank run was a sample injection. At least two blank runs are performed between two sample injections to reduce the residues in the column.

GC signal integration: An important assumption with usage of Sim Dist methods is that all hydrocarbons have the same relative response factors regardless of the composition or retention time. A computer program constructs a calibration curve from the hydrocarbon retention times and their atmospheric boiling points, then uses this curve to calculate the boiling range distribution of the petroleum fractions. Sample area is integrated into area "slices" vs. retention time, then the boiling point for each cumulative area % wt. is determined by the computer program. Since the chromatographic area of importance is only due to the oil sample, solvent-only injection should be subtracted from the sample chromatogram. Baseline subtraction needs to be performed to remove the effect of background and solvent. The area slices during the first second are noted and average, and standard deviation computed. Any of the slices during the first second which are out of one standard deviation are thrown out and the average recomputed. The average computed in this manner is subtracted from the chromatogram. Any negative signals are made zero. After blank subtraction, total sample area is found by adding all the area slices between initial and final points. Initial area point is the end of solvent elution and final area point is when the signal level reaches the baseline. In order to obtain the % wt. off,

cumulative area slices spanning over the time of temperature ramp are calculated and divided by the total sample area. This gives the plot of wt. % off versus retention time. Retention time is correlated with atmospheric boiling point using retention time calibration. Once, the retention time-boiling point relation is obtained, % wt. off vs BP can be plotted and boiling point distribution obtained. Code used to obtain Sim Dist is attached in Appendix A. It should be noted that % wt. off is calculated only till the end of temperature ramp. However, residue plays a role in the total sample area.

3.3.3.2 GC-FID calibration

The accuracy of Sim Dist data depends on both the gas chromatography (GC) and flame ionization detector (FID). FID detects the number of ions inside a hydrogen flame with the eluted compounds from a column. The number of ions are assumed to be proportional to the concentration of compounds in the sample. One way to make sure FID works well is to check its linear response to injected samples. A linear response check has been performed on the detector to verify its proper working. One gm of oil crude has been dissolved in 100 ml DCM (dichloromethane) and a series of different volume between 0.5- 1.5µl was injected into the GC system. Good correlation between total area and injection volume was found indicating a good linear response from the detector. Qualitative calibration is performed by using a mixture of known n-alkanes with the Sim Dist (simulated distillation) method used for crude oil studies. Since compounds in the calibration mixture are different and known, the retention time corresponding to each compound is different. Also, with the boiling points of each of the n-alkanes in the mixture known, relation between peaks and boiling points is obtained and the

retention time (RT) vs boiling point plot generated. Since crude oil A and crude oil B are both heavy, elution at high temperatures is required (400-430°C). A typical calibration standard used for this range is Polywax 655 which contains a mixture of known n-alkanes from C20 to C100. Polywax 655 has been used with the method D6352 for the GC-FID calibration. One of the challenges using this waxy mixture is their insolubility in most solvents. However, it dissolves in toluene at moderate temperatures. Polywax 655 in toluene was warmed up by a heat gun prior to injection. Figure 20 gives the chromatograph of Polywax 655 using ASTM standard D6352. All peaks corresponding to each compound are identifiable with known carbon number and boiling point.

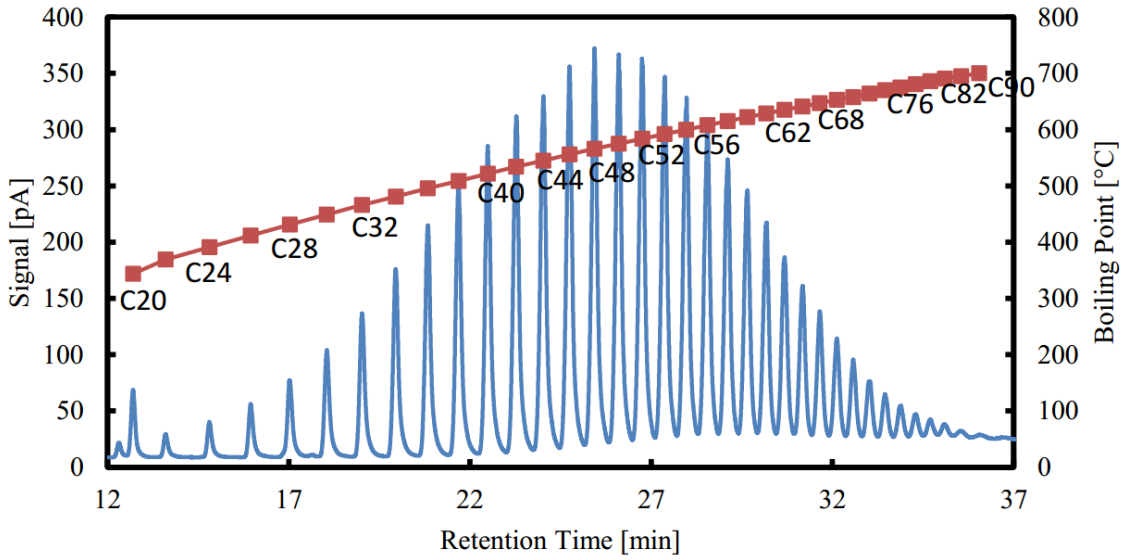

Figure 20: GC-FID responses of Polywax 655 with carbon number and boiling point by using ASTM D6352

To complete the calibration curve at carbon number below C20, another calibration standard in the range of C5 to C44 was used with the same method. Use of this standard

helps in calibrating the lower carbon number range. Additionally, it helps to verify the peaks overlapped between the new standard and the Polywax 655. Figure 21 showed a combined calibration curve that covers a carbon number from C5 to C100.

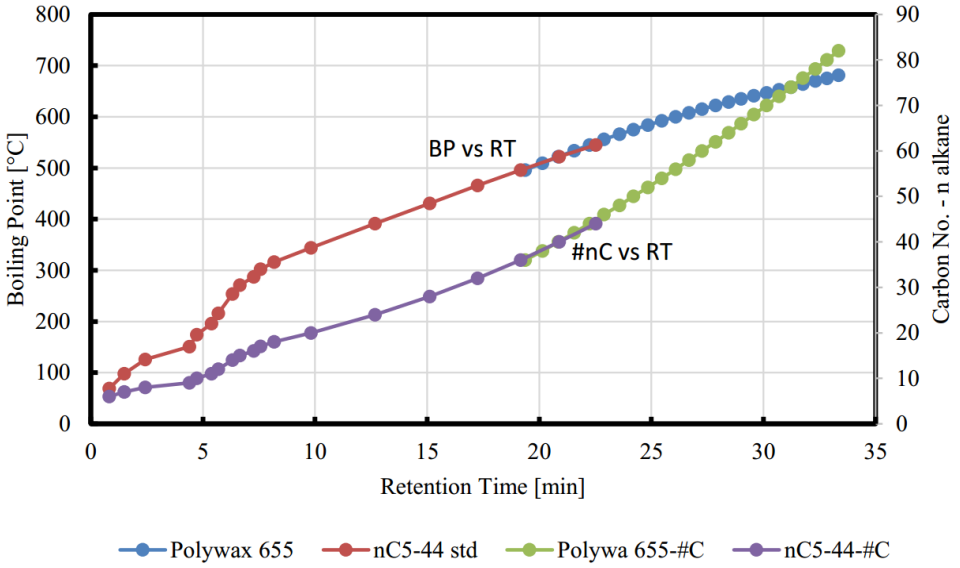

Figure 21: Calibration curve by using combined Polywax 655 and low carbon number standard

3.3.3.3 Sim Dist of irradiated oil

One dimensional gas chromatography system was not able to resolve tens of thousands of compounds in crude oils. It is further complicated because heavy fractions from the resins or asphaltene do not elute with the used method. Due to those reasons, the GC-FID signals of two crude oils do not show many individual peaks but all overlapped and form one large hump. Simulated distillation techniques which do not require resolution of individual components are employed to obtain the boiling point distribution. For this specific GC, oil samples was injected on the top of the column. There is a risk of

contaminating the column by residue from injection. To reduce that a hold time was added at the end of the method to help elute any residue on the column. Figure 22 are GC-FID signals of both heavy oils and the derived Sim Dist signals of two crude oil samples by using ASTM D6352 method.

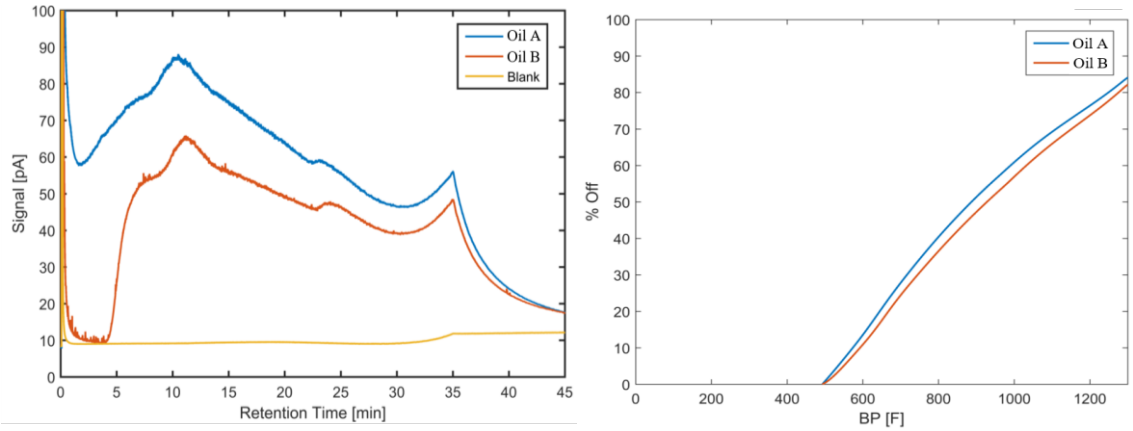

Figure 22: Raw GC-FID signal and Sim Dist signal of oil A and B by using ASTM D6352

Both A and oil B have a significant amount of weight that cannot be eluted before 35 min which corresponds to an atmospheric boiling point of 700°C (1292°F). This portion is called residue which is the non-eluting sample and should not be confused with the industrial definition of residue which is typically at 1000°F. Oil A has about 15% and oil B has about 18% with boiling points greater than 700°C. At 800°F (427°C) about 40% of oil A and 37% of oil B eluted whereas at an even lower temperature 600°F (315°C) there is only 15% of oil A and 12% of oil B eluted. If applying industry standard, oil A has 38% residue and oil B has about 42% residue both of which are extremely high. One noticeable difference between two oils is the amount of light fractions before 5 min. Oil

A has a significant portion of light fraction corresponding to retention time smaller than 5 min, while oil B has no light fraction in the same time window.

GC-FID signal of irradiated samples has different components belonging to each mass fraction. Figure 23a showed signals of each mass fraction from irradiated oil B. Raw oil A and weighted oil mixture were compared on this plot. After integration, the Sim Dist of each fraction was plotted on figure 23b.

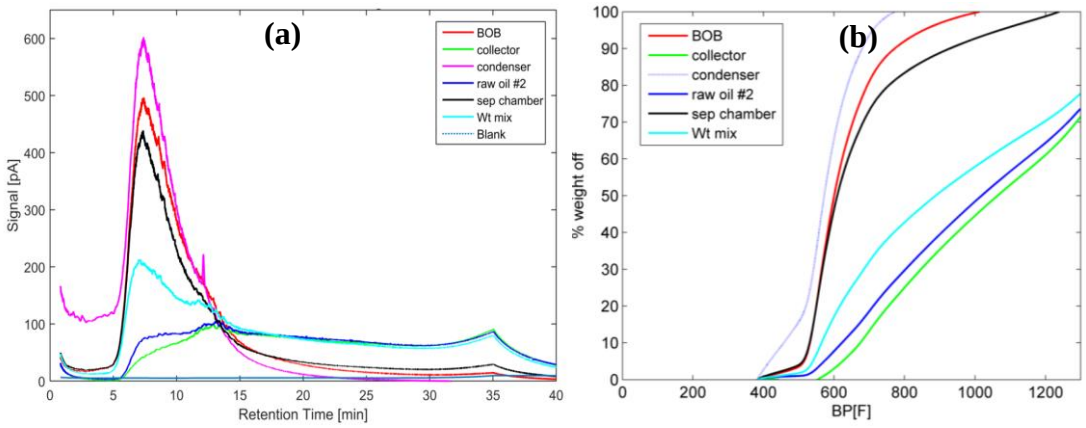

Figure 23: GC-FID signals of each mass fraction from irradiated oil A, raw oil A as well as the weighted mixture

Repeatability of the GC-FID system with two oil samples were performed. Simulated distillation of both oil A and oil B has been carried out several times according to method ASTM D6352 with a sample injection of 1 µL. Results were compared to study the difference between the Sim Dist curves. Average differences between different runs was smaller than 5% for both oils.

3.3.3.4 Conversion and yields

Conversion and yields were estimated from GC-FID data based on the same calibration curve. Hydrocarbon conversions depend on the carbon number. It also relates to the composition of one specific hydrocarbon mixture. FID signal vs. time is baseline subtracted and then integrated from retention time corresponding to C_{10} to C_{60}, and normalized to weight percentage from the total integral in this range. Our definition of conversion, C, is defined as the weight percentage (wt. %) change after treatment in any range of C_{N1}-C_{N2}, N_1 and N_2 are hydrocarbon numbers. It is calculated by the following equation (1):

$$C_{N1-N2} = \sum_{N=N1}^{N2} (wt.\%(treated)_N - wt.\%(raw)_N) \qquad (1)$$

Where $\boldsymbol{C_{N1-N2}}$ is conversion in a certain carbon number range; $\boldsymbol{wt.\%(treated)_N}$ and $\boldsymbol{wt.\%(raw)_N}$ are the weighted percentage of hydrocarbon with N carbon number in treated sample and raw sample, respectively. Conversion could be used in multiple hydrocarbon ranges to study different products and yields when a mixture of hydrocarbon was processed. Yields and reduction of each hydrocarbon number were estimated in equation (2):

$$R_N \; or \; Y_N = \frac{C_N}{MW_N \cdot SE} \qquad (2)$$

Where $\boldsymbol{R_N \; or \; Y_N}$ are reduction and yields at each carbon number; $\boldsymbol{MW_N}$ and $\boldsymbol{SE}$ are the molecular weight of hydrocarbon with $\boldsymbol{N}$ carbon number and specific energy input (equivalent to dose), respectively. Total yields (TY) and mass selectivity (S) are represented by equation (3) and (4):

$$TY_{N1-N2} = \sum_{N=N_1}^{N_2} Y_N \qquad (3)$$

$$S_{lights} = \frac{C_{10-21}}{C_{10-21} + C_{26-60}} \quad (4)$$

Where $\boldsymbol{TY_{growth}}$ and $\boldsymbol{TY_{scission}}$ are total yields of chain growth products and chain scission products, respectively. Conversion is calculated here for $C_{10\text{-}21}$ for lighter ends and chain scission, $C_{22\text{-}25}$ for the bulk of the mineral oil, and $C_{26\text{-}60}$ for the heavier ends and chain growth. Selectivity, S_{lights}, and total yields, TY, are calculated using the same ranges. High yield indicates a more efficient, lower energy cost, chemical conversion. High selectivity indicates more of the products are light hydrocarbons. Not accounted by these methods is conversion or reactants to products that are in the same boiling point range.

3.4 Standard Operating Procedure (SOP) Development

Since these experiments are the first of their kind in Texas A&M University. Special attentions were given to develop the operating procedures and safety analysis. The irradiation system was pretested with water and mineral oil first in the electron beam facility before switched to crude oils. At the same time standard operating procedure (SOP) and project safety analysis (PSA) were developed in parallel. There are multiple goals on doing these: 1, to make sure that all devices used in the irradiation reactor and operating procedures are safe; 2, to check the flow system under electron beam irradiation; 3, acquire correct signals from different devices closed to the ebeam horn; 4, to check the fire monitor and control system; 5, to make sure the heaters and insulation materials work properly; 6, to match the timing of liquids flow and ebeam on and off.

The standard operating procedure and project safety analysis were developed in collaboration with MKO process safety center in the chemical engineering, Texas A&M University. Both of them are living documents which will be reviewed and updated as the project proceed with experiments and tests in the future. The main hazards in the ebeam crude oil test include lighter hydrocarbons, ozone and H2S, etc. Most of the condensable species from the processing box will be condensed and stored in the condenser. One ozone detector was used to identify if the concentration level has been too high. Ozone generation in the ebeam facility is unavoidable since electron beam has to travel out of the scan window and shoot on the sample. Ozone was produced when electrons collide with oxygen molecules in the air. The best way to avoid any harm to personnel is to leave enough time for the gas to get diluted by the air purge below a safety value. One additional H2S detectors and one multiple gas detector (CO, CH4 and so on) were placed at the personnel entry point.

3.5 Neat and Pure Hydrocarbons Irradiation

Although this dissertation started with irradiating heavy crude oils at various conditions, the application of high energy electron beam irradiation of petroleum is not limited on heavy oil processing. Another application might be ebeam induced conversion of low value gas hydrocarbons such as methane or propene to liquid product such as C6 or higher carbon numbers.

It is known from literature that ebeam irradiation of hydrocarbons causes cracking and polymerization or crosslinking at the same time. Whether it is more favorable towards

the cracking reactions or polymerization depends on the experimental conditions and reactor design. Heavy oil upgrading by using ebeam technology largely depends on big hydrocarbon molecules cracking and polymerization suppression. While the gas hydrocarbon conversion to liquid by ebeam requires more polymerization or crosslinking and less cracking. Similarly its conversion depends on all experimental parameters and reactor design.

To strengthen our understanding of the ebeam irradiation of different hydrocarbons, we also designed experiments to irradiate neat and pure hydrocarbons with different structure and study the radiation product distribution and quantify yields. These experiments are conducted in a batch reactor that will be introduced later. Irradiation of neat and pure hydrocarbons with the ebeam source allows us to investigate the most fundamental aspect of irradiation of petroleum. Compared to irradiation of crude oils, neat or pure hydrocarbons are very well characterized with known chemical structure, results from them will be more easily interpreted by using similar techniques. Pure hydrocarbons are selected to be highly representative compounds present in crude oils, including straight alkanes, unsaturated alkanes, aromatics and polyaromatics. It will help us determine what should be the targeted compounds in petroleum for radiation processing.

CHAPTER IV

DESIGN OF EXPERIMENTS

4.1 DOE (Design of Experiment)

Irradiation of crude oils represents a very complicated process and involves multiple factors (hydrocarbon structure, processing temperature, irradiation dose rate, total irradiation dose, flow shear rate, bubbling gas type, reactor type, separation chamber, etc.). Irradiation response for the project interest regarding heavy oil processing is heavy oil conversion and bulk fluids viscosity reduction. The complexity of the heavy oil irradiation process lies in two areas. First of all, the interaction between high energy electrons and crude oil molecules is a highly nonlinear process, it depends on several parameters such as electron energy, oil type, temperature, residence time and so on. Secondly, the Visbreaking process that results from blending generated lighter fractions with heavier fractions is also a nonlinear process which depends on not only the mass ratio of both the lighter ones and heavier ones but also the quality of them, like viscosity and boiling range. For example, if 10% mass conversion was achieved and viscosity of blended mixture was reduced by 30%. This does not necessarily mean that a 20% mass conversion will bring us a higher than 30% viscosity reduction, even though we have seen a positive dependence of viscosity reduction on mass conversion. So the knowledge of Visbreaking helps us understand that in order to achieve desired viscosity reduction, we have to manage the electron beam oil processing in a way that we should convert a

reasonable amount without turning the remaining oil into ‘solids’. This requires to carefully study each parameter and its influence on the outcome.

For a nonlinear process with complexity like this one, it is better to design the experiment in advance and systematically examine each parameter to avoid randomly performing experiments and random results[145,146]. Design of experiments with the use of statistical principles ensure that the experiments are designed economically, that they are efficient, and that individual and joint factor effect can also be evaluated. A complete factorial experiments need at least 2^n tests if n is the number of factors and assume there are only two levels for each factor, e.g. a lower temperature and a higher temperature. But complete factorial experiments cannot always be conducted because of economic, time, or other constraints. Fractional factorial experiments are important alternatives to complete factorial experiments when budgetary, time, or experimental constraints preclude the execution of complete factorial experiments. In addition, experiments that involve many factors are routinely conducted as fractional factorials because it is not necessary to test all possible factor-level combinations to estimate the important factor effects, generally the main effect and low-order interactions.

In this research project, we couldn’t even apply factorial experimental design, since it is still too time consuming and budget limited, what’s more, it couldn’t incorporate an evolving experimental setup as the project proceeds. Our experimental method tried to follow an incremental approach and address one factor at a time. Further we added more capability to the system as we introduced more controls and extended the operating range.

For example, we started from only investigating the effect of shear rate in the single pass mode under similar dose rate and dose and ignoring other effects. Later on we started testing in a multi-pass mode and then we started bubbling gas into the oil stream. Then, a separation chamber was applied to the system and its function was studied. After that water cooling was used to control the treated oil temperature. The recent test was targeted with a longer residence time to see if that helps the cracking process. Factors such as temperature, dose rate, dose, separation chamber and shear rate will be studied primarily. The following list was made to introduce our incremental method for running experiments.

A. Single-pass, laminar flow, high shear rate, starting temperature control, inert gas environment, flow rate control, dose rate~10 kGy/s
B. Higher dose rate~17 kGy/s
C. Multiple-pass, higher dose rate
D. Inert gas bubbling into oil
E. Separation chamber application
F. Hydrogen-rich gas bubbling
G. Water cooling, processing temperature control
H. Single-pass, long residence time, high dose

Table 6 specify the experimental parameters being investigated in this project and their ranges: Temperature (100-280 ^{o}C), Dose Rate (15 or 20 kGy/s), Dose (0-1000 kJ/kg), Bubbling Gas Type (methane or hydrogen) and Shear Rate (20-150 1/s). The selected values of those parameters are based on economic consideration and physical limit of the

testing device. For example, irradiation dose above 1000 kJ/kg will make the process uneconomical. Dose rate beyond 20 kGy/s is not accessible as of now in the electron beam facility.

Table 6: Important Experimental Parameters in Irradiation of Heavy Oils

Parameters	Range	Units
Dose	0-1000	kJ/kg
Dose Rate	8-20	kGy/s
Temperature	100-300	^{o}C
Shear Rate	8-150	1/s
Gas Bubbling	CH_4 or H_2	LPM

4.2 Reactor Design

4.2.1 Processing Box

The primary purpose of this box was to provide a reaction space that allows the petroleum to interact with the ebeam during the oil irradiation process. Phase change will also happen inside this box. Therefore it is very important to seal this box and isolate air. For example, as the oil was heated up to a certain temperature, phase equilibrium was destroyed and species stared to separate. A few experimental and safety considerations when designing and building this box includes: the box material needs to be high temperature rated with good strength; material should be small density or wall thickness should be very small; its shape and size should be enough to house components such as

different oil channels and water cooling parts but be limited by the overall space we have in the irradiation cell; the geometry of the box largely depends on how gas and oil was supplied to the box. There are multiple feed through holes distributed on different places of the box including the oil inlet and oil drain. To satisfy the experimental and safety requirements on the box, we chose aluminum instead of other metal because of its low density and less ebeam energy loss on the wall. Its overall dimension and design specifications were shown in Table 7.

Table 7: Design and Construction Details of Processing Box

Length	Width	Height	Wall thickness	Flange width	Flange thickness	Material	Shape	Lid thickness	Sealing gasket
50 in	8 in	8 in	1/16 in	2 in	1/16 in	Aluminum	Rectangular	1/32 in	Viton

A three dimensional drawing of the box with feed through holes was given in figure 24. Note that the bottom of the box was made with slopes in both beam direction and the direction perpendicular to the beam. The slopes allows oil to quickly move outside of the beam region and hot metal surface, prevents it from being over irradiated.

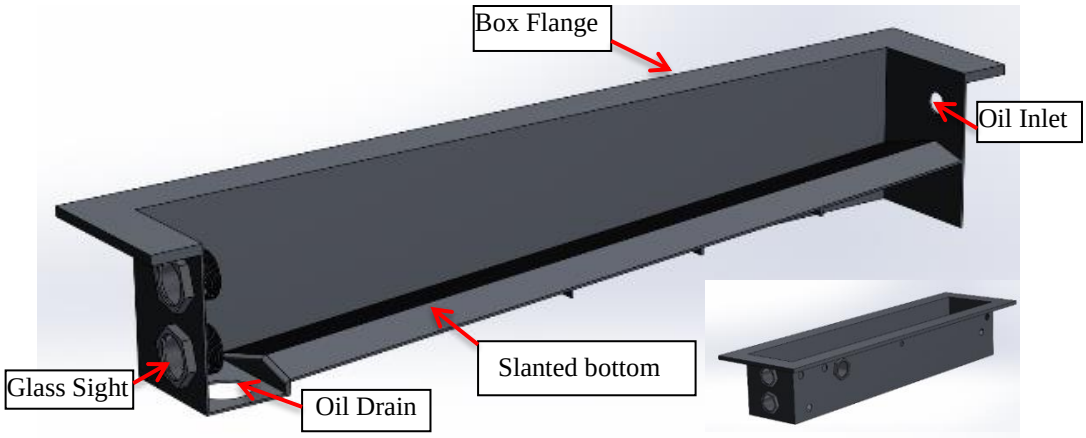

Figure 24: Processing box with glass sight and feed through

4.2.2 Oil Channels

Several aluminum channels have been designed and tested as the oil flow bed. Aluminum was selected because of its low density. It absorbs less energy from the incident electrons and improve the utilization efficiency of electron beams. Thin aluminum wall was another key to reduce the energy loss of electrons. Thermal effect on the channel, however might be an issue, since aluminum has a significantly larger electron stopping power than oil and that will result in a temperature gradient between those two different materials. Each of them had a different design and function to be used during the ebeam irradiation experiment.

4.2.2.1 Channel with Gas Bubbling

Figure 25 is one channel configuration with gas bubbling from the bottom. Oil flows on the top channel which is 1 inch wide and around 38 inches long. Bubbling gas flows into the second channel which is one inch shorter on both ends and exit through the holes on the bottom of the first channel. Holes are 1/32 inch in diameter. This

configuration allows gas bubbling into the oil during electron beam irradiation. It was designed to investigate the effect of different gas, e.g. Methane and Hydrogen. The drawback of this design is no temperature control on the channel, therefore the temperature of the aluminum channel might be too high after absorbing energy from electrons. Oil on the interface will be heated up as well and that brings thermal effect despite the irradiation effect.

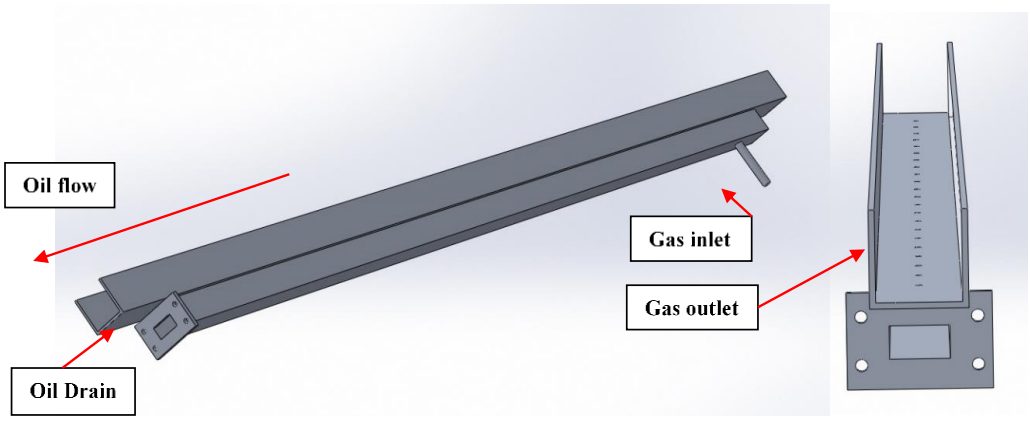

Figure 25: Oil channel with gas bubbling from the bottom

4.2.2.2 Channel with Water Cooling

In order to control the oil temperature during irradiation processing, we attached a ½ inch tubing on the bottom of the oil flow channel, then flowed water through it. This configuration shown in figure 26 has a limited cooling surface area between oil flow channel and water tubing. It was not able to provide enough cooling on both the channel

and oil. In addition to that, there was no gas flow into the oil with this configuration. A new design was required to satisfy desired experimental conditions.

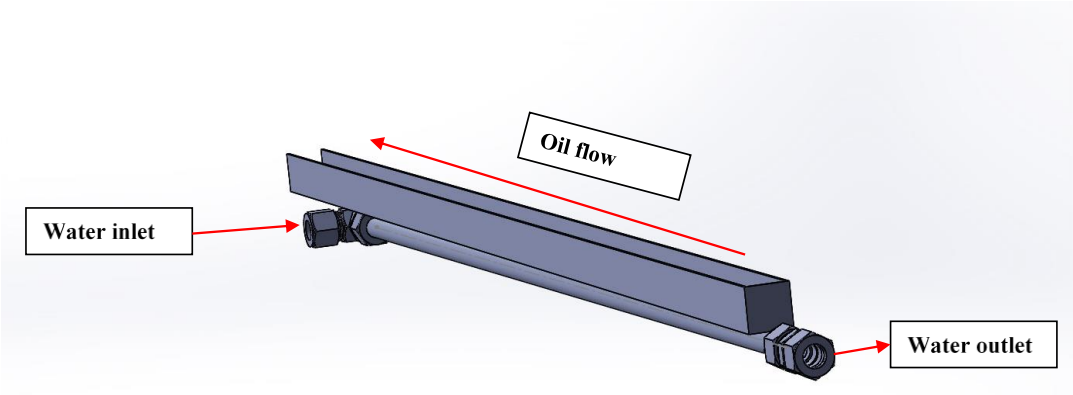

Figure 26: Oil channel with water cooling through a tube

4.2.2.3 Water Cooling Jacket

The new design will need to be more cooling effective and should incorporate gas bubbling function on the channel. A new channel was built in SolidWorks as seen in figure 27. It is essential a water cooling jacket that encloses two channels for oil flow and gas bubbling. Water enter the jacket from a tube inlet on one end of the jacket and exit on the other. Gas bubbling channel also has a tube inlet on its bottom. This configuration was maximized in its cooling surface area and should be able to provide much more effective cooling effect.

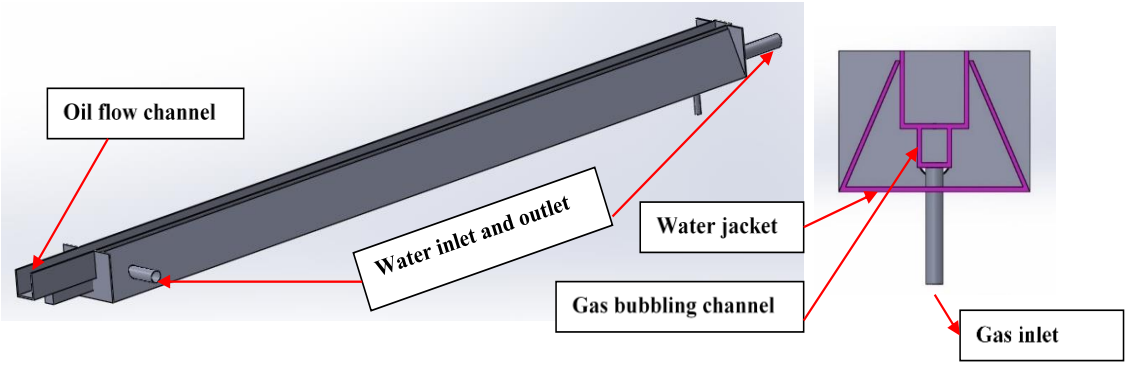

Figure 27: Oil channel with a water cooling jacket

4.2.2.4 Channel with Deeper Wall for Longer Residence Time

Residence time under the beam might be an important parameter during irradiation processing. We designed another channel with deeper wall to allow oil to stay in the irradiation region longer for a larger residence time. The oil channel was 2 inch tall and 1 inch wide. Oil enters the channel from one side and exits on the other. Depth of oil was around ¾ inch. The estimated residence time was about 1 minute at a flow rate of 1 LPM. Gas bubbles channel was still attached on the bottom of the oil channel. There was no water cooling function added to this design. Consequently the processing temperature will be higher. Design of this channel was shown on figure 28.

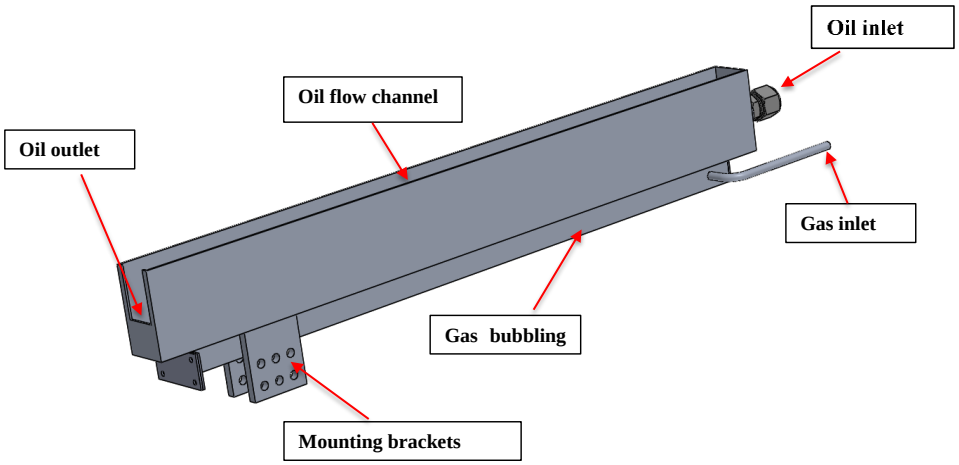

Figure 28: Longer residence time oil channel

4.2.3 Condenser

Electron beam irradiation of hydrocarbons is able to crack big molecules and produce smaller molecules. The number of produced species depends on the experimental conditions. If the species are light enough, they will travel with the gas flow and leave our system. Temperature favors the production of light species, since light species evaporates and separates from heavy species faster under higher temperatures. Therefore it is very important to capture those in the exhaust that separate from the main stream. To achieve that, we designed a condenser that could use liquid nitrogen or dry ice as coolant to condense hydrocarbon species. The condenser assembly was shown in figure 29

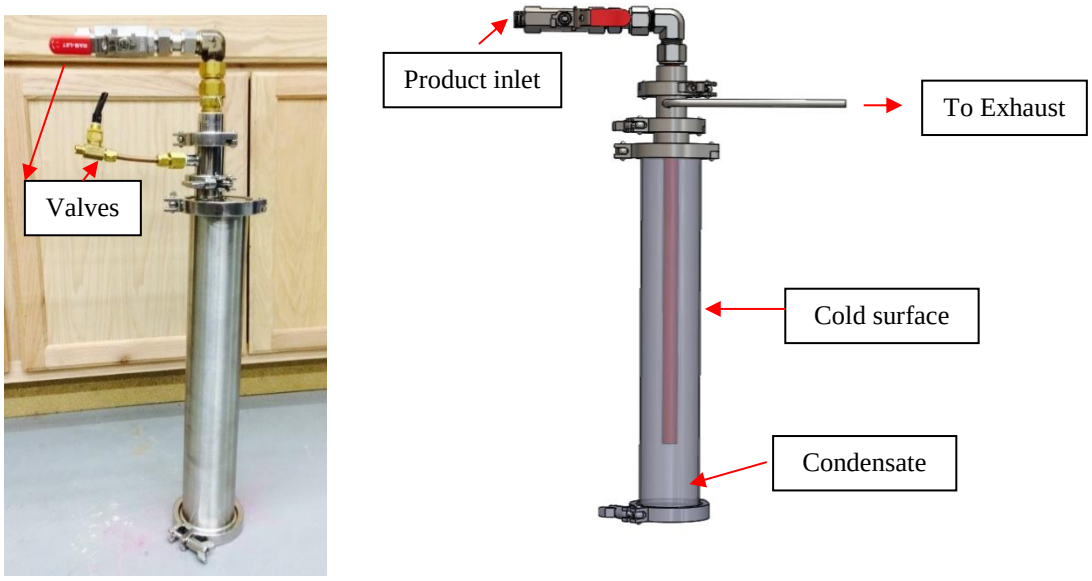

Figure 29: Condenser used to trap evaporated hydrocarbons

CHAPTER V

RESULTS AND DISCUSSION- LOW DOSE

5.1 Irradiation parameters of Crude oil A

Three irradiation experiments with crude oil A in single pass mode were completed successfully. The goal was to study the effect of shear rate under low energy inputs (low dose). Irradiation conditions were shown in Table 8. Note that conditions such as flow rate, separation chamber, dose rate, temperature are either monitored or controlled. Other conditions including residence time, shear rate and dose are calculated based on an open channel flow model. Those experiments were conducted without water cooling or bubbling gas. The key to vary shear rate without causing too much change on other major parameters like temperature and dose rate was to change the oil flow rate and the angle of the oil channel. For example, higher flow rate and larger slope of the change both increased the shear rate of oil. Shear rate also depends on the density and viscosity of the oil sample. Oil density and viscosity was correlated with oil temperature in the flow model and we used real time oil temperature in the model. To achieve desired shear rate, temperature was slightly varied to change the oil sample density and viscosity. Since our focus was to study the effect of shear rate, we ignored the effect of temperature. Irradiation time was varied in order to change the specific energy input to the treated oil sample (dose).

Table 8: Crude Oil A Irradiation Experimental Conditions

Test Number	Flow mode	Flow rate (LPM)	Average Residence time (s)	Separation chamber	Bubbling gas	Average shear rate (s^{-1})	Dose rate (kGy/s)	Dose (kGy)	Temperature range (^oC)	As planned?
1	Single-pass	1	3.6-3.7	NO	NA	30-32	7	24.8	160-165	Yes
2	Single-pass	2	1.53-1.59	NO	NA	82-89	7	10.85	200-210	Yes
3	Single-pass	1	5.2-6.1	NO	NA	11-15	6.9	36.8	200-230	Yes

5.2 Mass balance and viscosity change

Mass balance and Viscosity of crude oil A before and after irradiation tests were given in Table 9. Majority of the treated oil sample was collected into three places: collector, separation chamber and condenser. But there might be small fraction of oil sample found on the channel and box surface. Oils found on all different places account for the total recovery. The accounted weight also includes mass that are not collected or recovered but could be estimated. Mass balance uncertainty was assumed in the range of ±5% when initial mass was in the range 1500 to 2500 grams. Viscosity measurement was conducted at two temperatures 50 ^oC and 100 ^oC. Raw sample was measured before the irradiation test. To measure the viscosity of irradiated samples, we have to make a treated oil mixture by mixing collected samples from different places. Mixing was completed by hand in a jar following a weight-proportion rule. Then we measured the viscosity of a weighted mixture and compared with the raw sample viscosity.

Table 9: Crude Oil A Mass Balance and Viscosity Change

Test Number	Initial mass (g)	Collector %	Separation %	Channel %	Box %	Condenser %	Total Accounted %	Total recovered %	Viscosity reduction (%)		As planned ?
									50 °C	100 °C	
1	1950	96.67	0	0.62	0.77	0.30	98.35	94.89	0.06	-1.28	Yes
2	2370	94.73	0	0.21	0.19	0.21	97.05	94.94	0.26	-4.88	Yes
3	2760	100.54	0	0.52	0.47	0.18	104.44	100.72	6.2	2.06	Yes

Mass recovery on each individual section varies significantly, but the variations in total accounted mass were all below 5%, which indicates that mass balance was in an acceptable range. Viscosity of irradiated samples under temperatures 50 °C and 100 °C showed slightly change when varying the shear rates. However the viscosity change is less than 5% which is very close to the rheometer uncertain level during measurement. Shear rate and shear stress were believed to exert effect on irradiated heavy oil sample, especially highly non-Newtonian fluids by changing the oil particle structure. Shear rate is the velocity gradient in the oil film flowing in the irradiation region. Shear stress is the force acting on the oil particle because of the viscosity and velocity gradient. Supposedly a large enough shear stress is able to change the oil particle structure and enhance the irradiation effect. The facts that we did not see the effect could be attributed to two possible reasons: shear rate and shear stress are not big enough to change the particle structure so they remained the same, or the oil sample being irradiated is already a Newtonian fluid, therefore its structure is independent of the shear stress and shear rate.

CHAPTER VI

RESULTS AND DISCUSSION- HIGH DOSE WITHOUT TEMPERATURE CONTROL

Following the low dose tests discussed in the previous chapter, we slightly updated the testing system by adding a separation chamber and irradiating samples with longer time for higher energy input. Longer irradiation time and higher dose makes the separation chamber more necessary because a larger quantity of lighter species are expected to evaporate or boil off from the main oil stream. Instead of using two oil tanks, one tank was used to allow treated oil and untreated oil to mix when oil flows in a loop. A three way valve was used to drain the oil tank after the irradiation test. Figure 30 shows the oil testing flow loop for higher dose. Red arrows represent the oil flow direction.

For any petroleum refining technology such as Visbreaking or thermal catalytic cracking, conversion primarily depends on residence time and the reaction severity (temperature and pressure) in the reaction region. For example, longer residence time in the tower will result in a higher conversion or species separation. In order to increase the residence time, we increased the number of circulations of oil in the flow system by passing it multiple times through the radiation region. Note that temperature of the oil sample also depends residence time. Longer residence time inevitably caused the oil temperature to rise. At this stage of our experiments, we did not have a good control on oil temperature. Its effect on irradiation results was discussed in the next chapter.

Figure 30: High dose oil irradiation in a flow loop

6.1 High Dose Irradiation of Crude Oil A

Eight irradiation tests were complete on crude oil A. The primary experimental goal was to study the effects of higher dose. Different gas was also tested bubbling into the oil during irradiation. Temperature was not the focus of this set of experiments, even though we have seen it is varying positively in response to dose. Table 10 shows the experimental conditions for those eight tests. Independent and varying parameters are gas bubbling and dose. All tests were conducted with the same flow rate and around the same dose rate. Slight change in dose rate is due to the lineup variation between the setup and electron beam. Shear rate and residence time were calculated based on the flow model. Six tests were finished as planned and considered successful. Two were finished but not successfully. One encountered a beam issue and the other lost significant amount of mass.

Table 10: Crude Oil A Irradiation Experimental Conditions

Test Number	Flow mode	Stages	Flow rate (LPM)	Average Residence time (s)	Separation chamber	Bubbling gas	Average shear rate (s^{-1})	Dose rate (kGy/s)	Dose (kGy)	Temperature range (°C)	As planned?
4	Multi-pass	3	2	1.41-1.66	NO	NO	73-106	15	525	178-225°C	NO[1]
5	Multi-pass	1	2	1.07-2.07	Yes	Helium	48-181	17	348	175-310°C	Yes
6	Multi-pass	1	2	1.25-2.07	Yes	Helium	48.6-134	18.5	270	177-278°C	Yes
7	Multi-pass	1	2	1.16-3.4	Yes	Hydrogen	18-155	17.68	605	130-300°C	Yes[3]
8	Multi-pass	1	2	1.26-3.71	NO	Hydrogen	15-134	14.75	691	120-260°C	Yes
9	Multi-pass	1	2	1.88-2.62	Yes	Hydrogen	30-60	19	198	150-215°C	Yes[4]
10	Multi-pass	2	2	1.08-2.48	Yes	Hydrogen	21-130	20	1308	140-280°C	NO[2]
11	Multi-pass	1	2	1.01-2.26	Yes	Methane	25-126	21.65	648	140-280°C	Yes[5]

1, Ebeam technical issues, run was extended into stages; 2, bad mass balance; 3, oil leaking between channel and separation chamber; 4, hydrocarbon leaking from a fitting on the box; 5, coke on the bottom of the box

Table 11: Crude Oil A Mass Balance and Viscosity Change

Test Number	Initial mass (g)	Collector %	Separation %	Channel %	Box %	Condenser %	Total Accounted %	Recovered %	Viscosity reduction (%)		As planned ?
									50 °C	100 °C	
4	2350	90.89	0	0.09	2.1	0.17	94.09	92.07	-21.9	-5.49	NO
5	1613	86.4	8.4	0.62	2.54	0.6	99.99	97.26	20.73	12.58	Yes
6	1550	89.03	4.8	0.67	2.41	0.59	97.48	95.44	7.49	2.04	Yes
7	1785	80.32	15.32	0.62	2.89	0.85	103.66	99.39	17.09	9.19	Yes
8	1673	94.62	0	0.9	3.32	3.71	102.54	101.35	2.36	-0.53	Yes
9	1584	96.05	3.64	1	2.16	1.01	102.87	101.61	16.27	14.52	Yes
10	1575	41.01	15.04	3.19	23.9	3.24	86.4	80.15	72.4	49.8	NO
11	1604	81.62	12.1	0.93	2.85	3.11	100.61	98.67	37.56	24.63	Yes

Table 11 showed the mass balance results and viscosity change for all eight irradiation tests at different conditions. An ebeam technical issue was encountered during test 4, and that resulted in a non-continuous irradiation in several stages. Each stage irradiation was a few minutes long. Oil temperature was cooled down to its initial temperature before restarting the experiment again. This significantly extended the time when oil sample stayed in the system. Viscosity of treated oil sample from this test was also measured. Its viscosity compared to the raw sample increased by 25% and 5%, respectively. One possible explanation for this viscosity increase could be due to polymerization that happened in the sample during the over-extended time between different irradiations. Polymerization is another major reaction pathway in ebeam irradiation of hydrocarbons except cracking reactions. It combines hydrocarbon chains through different radical reactions and results in larger molecules. This process was favored under conditions where ebeam source is not present and radicals are more prone to combination instead of propagation. A more detailed description of what happened in this test: radicals were created when beam was on and they participate in both combination and propagation which later might result in processes including cracking and polymerization. But when beam was shut off, no radicals were produced from interaction with electrons, the remaining radicals continue to interact with each other and with other particles. This process in general favors polymerization over cracking.

Test 10 had a mass recovery lower than 90%. Dose was more than 1000 kGy and overall irradiation time was more than 40 minutes. During this test oil sample leaked between the channel and separation chamber. This explains why more than 20% of oil

sample was found at the bottom of box and collector only recovered 40% of the treated oil sample. Mass loss in this run might be due to hydrocarbon leaking from an unidentified place and the longer irradiation time favors this process. Another possible reason is the lower oil temperature when we collect treated samples on the surface of the tank and box, so that more oil samples still stay on the surface because of higher viscosity. Despite this erroneous mass balance, viscosity showed significant reduction of 70% at 50 ^{o}C and 50% at 100 ^{o}C. Since the uncertainty of this test is too high, we will not seriously consider its results.

Test 7, 8 and 9 were conducted with hydrogen as the bubbling gas. Dose was controlled at 200 kGy (test 9) and 600 kGy (test 7 and 8). Test 8 had no separation chamber to separate lighter hydrocarbons from the crude mixture, which means they were processed alone with the heavy hydrocarbons. Processed oil sample from test 8 showed lower viscosity reduction than those from test 7 and 9, although there was a higher energy input in test 8. This proves again the positive effect of a separation chamber during the heavy oil irradiation. Oil sample in test 7 absorbed more energy (600 kGy) than that (200 kGy) in sample from test 9. All other parameters were similar during the irradiation process. Viscosity change of those two tests did not show significant difference.

Hydrogen and methane as bubbling gas or donor gas were compared in test 7 and 11. Energy input in both oil samples was around 600 kGy. Samples from test 11 with methane shower higher viscosity reduction than samples from test 7 with hydrogen. It has great implications since methane is more abundant and a cheaper resource near the oil

field. Inert gas helium was also tested as bubbling gas during test 5 and 6. Since helium is chemically stable, we did not expect it to interact with hydrocarbon molecules in the same way as hydrogen or methane does. Hydrogen and methane once irradiated by electron beam will produce hydrogen radicals that interact with large hydrocarbon molecules. This might involve hydrogen transfer from them to those large molecules and the oil property largely depends on the hydrogen to carbon ratio. But when helium was used as bubbling gas, interaction was different since no mass or atom transfer is possible between an inert gas and hydrocarbon molecules. Therefore helium as a bubbling gas should not bring chemical effects. The reason it still helps the process could be due to the facts that helium bubbling created bubbles inside the oil film and improved the beam molecules interaction.

6.2 Conversion of Crude Oil A

GC-FID analysis was first conducted on irradiated samples from test 4. Figure 31 showed the raw GC-FID signal as well as the Sim Dist signal. As the figure showed, treated sample has less fractions than the raw sample before 30 min and more fractions after 30 min. Its Sim Dist showed that about 3% of light fractions was converted to heavy fractions before 1000 F. Conversion to lights from heavies was normally due to polymerization. Viscosity of this irradiated sample increased significantly from the raw due to the production of heavy fractions. Conversion results were consistent with viscosity change.

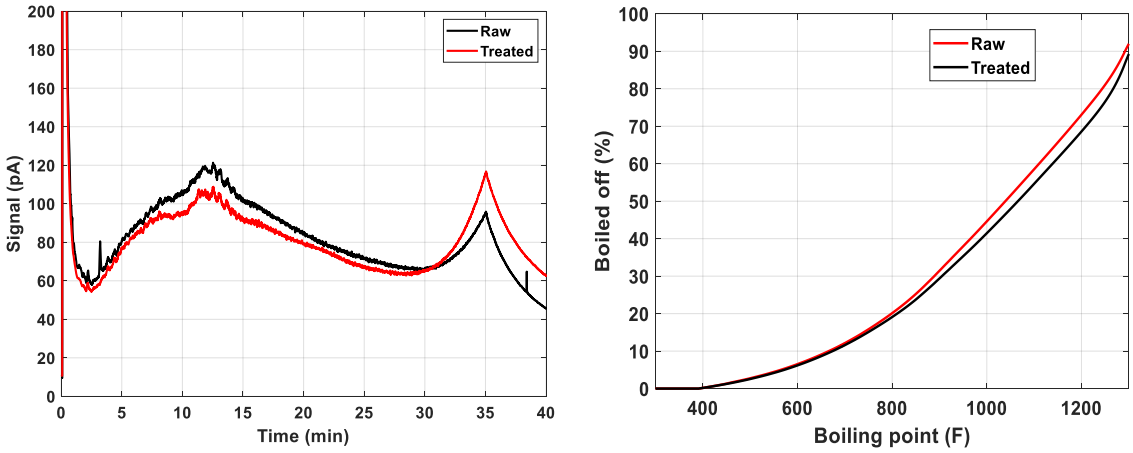

Figure 31: Raw GC-FID signal and Sim Dist signal of irradiated oil A from test 4

Conversion in test 5 and test 6 was compared in figure 32 at similar specific energy input. Irradiated oil A from Test 6 was identical with the raw sample whereas sample from test 5 showed significant changes. Comparison between Sim Dist curves of irradiated oil from test 6 and the raw indicated that heavy fractions were converted to light conversions. Conversion in irradiated oil A from test 5 was about 4% before 1000 F and 3% before 1300 F. Conversion to light fractions in test 5 explains why viscosity was reduced by 21% at 50 ^{o}C and 13% at 100 ^{o}C.

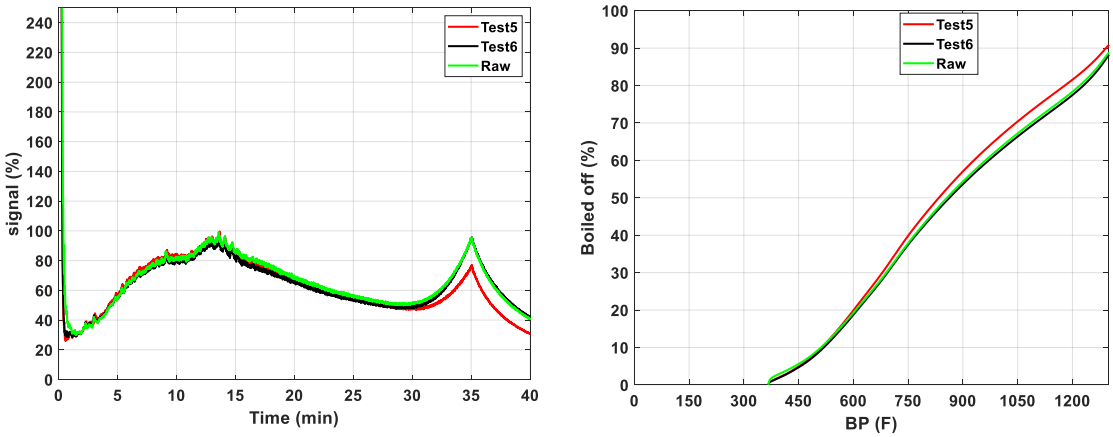

Figure 32: Raw signal and Sim Dist signal of oil A from test 5 and test 6

GC-FID analysis was also performed on irradiated samples from test 9-11. Results were shown figure 33. Raw GC-FID signals of irradiated samples were higher than that of raw sample before 15 minutes and lower than that of raw sample after that. This indicates that there are more light fraction and less heavy fraction in irradiated samples. Sim Dist signals proved that heavy fractions were converted to light fractions in test 10 and test 11. Irradiated sample from test 10 had the highest conversion to light fraction close to 7% at 1000 F. Conversion in sample from test 11 was about 4% at the same temperature. Sample from test 9 was very close to the ram sample and no significant conversion was detected. Higher conversion in test 10 helped reduce the viscosity by more than 70% at 50 ^{o}C and 30% at 100 ^{o}C. However the total mass recovery from this test was extremely below the acceptable range and the conversion results here are not very meaningful. Results from test 11 are more reliable and also showed significant conversion and viscosity reduction (37% at 50 ^{o}C and 25% at 100 ^{o}C). Comparing test 9 with 200 kGy and test 11 with 600 kGy, we might be able conclude that higher dose favors conversion to light fractions.

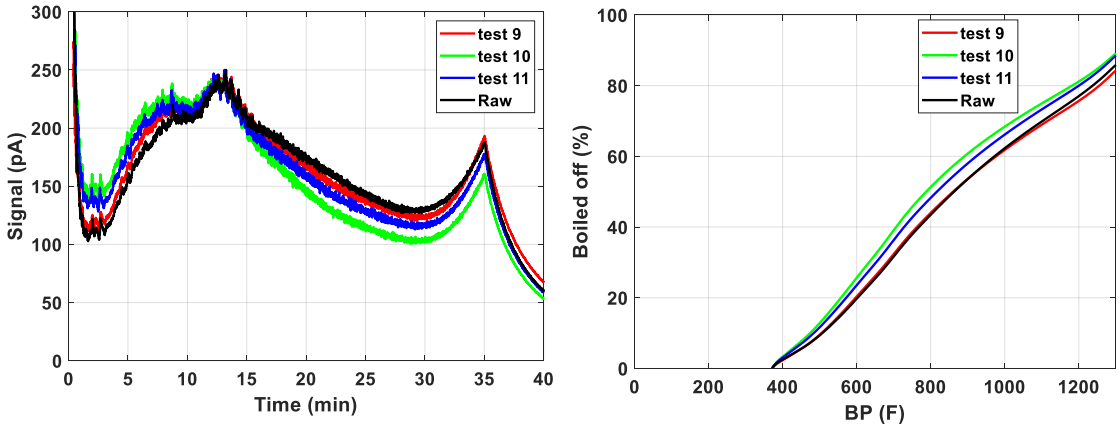

Figure 33: Raw signal and Sim Dist signal of irradiated oil A from test 9-11

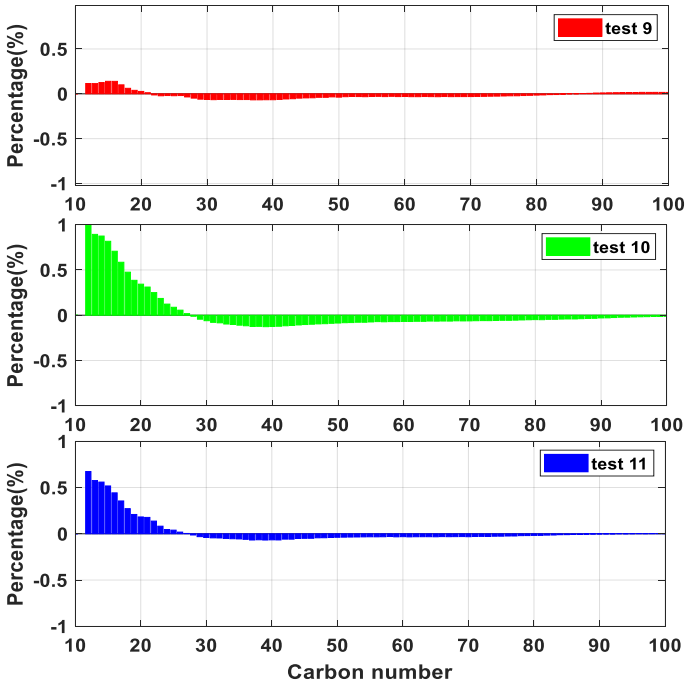

Figure 34: Conversion of irradiated oil A from test 9-11

Conversion and yields were also studied based on known specific energy input and conversion corresponding to each hydrocarbon number in the range of C10-C100.

Conversion was shown in figure 34. It is clearly shown that larger hydrocarbons above C30 was converted to smaller hydrocarbons below C25 in all three irradiated samples. Sample from test 10 had the most accumulated conversion in the range of C10-C25 compared to samples from test 9 and test 11. Yields (molecules/100eV) of products in irradiated samples were calculated and shown in figure 35. Because heavy fraction was converted to light fraction by electron beam irradiation, yields of light products (C10-C25) are positive and yields of heavy products (>C30) are negative. Indeed the number here are lower by one order of magnitude than that found in literature which irradiated a pure compounds. However, yields here are products resulted from irradiating heavy crude oils with significantly more complex chemical compositions. Total yields of light products are about 1.9, 2.4 and 3 molecules/100eV for all three tests. Note that the trend of yields is different from conversion. Test 10 which has the highest conversion does not represent the highest yields because of higher energy input. Test 9 with very low conversion still showed decent yields number due to low energy input. This indicates that conversion and yields are both required to fully characterize products from the irradiation process.

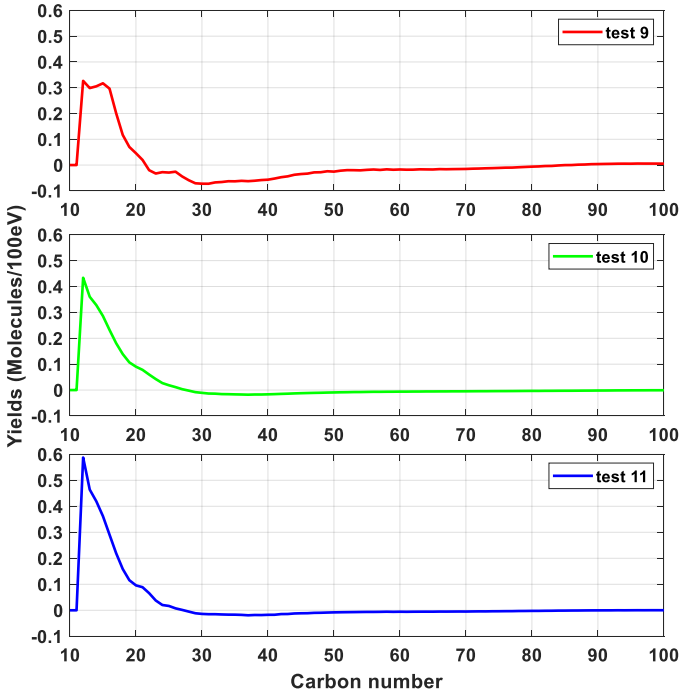

Figure 35: Yields of products in irradiated oil A from test 9-11

6.3 High Dose Irradiation of Crude Oil B

Following the same experimental strategy used in irradiation of crude oil A, we finished eight irradiation tests on crude oil B. This type of crude has a higher API gravity and viscosity. Its simulated distillation curve shows very negligible light fraction below C20. This crude oil well represents the extra heavy oils which are widely found in Venezuela and Canada. Due to their large reserve volume and low market value, industry has shown a tremendous interest in upgrading them to increase its value. A series of novel technology and techniques have been researched and developed to improve the recovery or achieve better upgrading. Irradiation of this oil was conducted with methane under higher dose 500-1000 kGy. Since temperature was not controlled through any external

device, e.g. water cooling, tests with energy input close to or larger than 1000 kGy had to be run in more than one stage to prevent overheating the oil. Table 12 concludes important experimental conditions for those eight tests. Independent and varying parameters are dose only. All tests were conducted with the same oil flow rate and the same dose rate. Shear rate and residence time were calculated based on the flow model. Seven tests were finished as planned and considered successful. Gasket was broken during one test and it might have led to a product leak. Therefore this test was marked finished but not successful.

Table 12: Crude Oil B Irradiation Experimental Conditions

Test Number	Flow mode	Stages	Flow rate (LPM)	Average Residence time (s)	Separation chamber	Bubbling gas	Average shear rate (s^{-1})	Dose rate (kGy/s)	Dose (kGy)	Temperature range (°C)	As planned?
1	Multi-pass	1	2	1.8-3.3	Yes	Methane	12-44	19.5	583	189-290°C	Yes
2	Multi-pass	2	2	1.8-3.3	Yes	Methane	12-44	19.5	1100	175-289°C	Yes[1]
3	Multi-pass	2	2	1.7-3.3	Yes	Methane	12-44	20	1100	174-305°C	NO[2]
4	Multi-pass	2	2	1.7-3.3	Yes	Methane	12-44	20	1100	174-295°C	Yes[3]
5	Multi-pass	1	2	1.77-3.36	Yes	Methane	12-44	20	1100	172-305°C	Yes
6	Multi-pass	1	2	1.36-2.2	Yes	Methane	28-74	20	738	188-298°C	Yes
7	Multi-pass	1	2	1.36-1.9	Yes	Methane	37-73	20	1487	200-290°C	Yes[4]
8	Multi-pass	1	2	2.24-2.89	NO	Methane	22-37	20	648	200-240°C	Yes[5]

1, coking at the bottom of the box, two stages run; 2, broken gasket on the oil tank, two stages run; 3, funnel leak into box, two stages run; 4, mass balance error; 5, one heater broke

Table 13: Crude Oil B Mass Balance and Viscosity Change

Test Number	Initial mass (g)	Collector %	Separation %	Channel %	Box %	Condenser %	Total Accounted %	Recovered %	Viscosity reduction (%)		As planned ?
									100 °C	150 °C	
1	1831	92.3	5.05	0.8	0.91	1.32	100.36	99.01	56.82	38.97	Yes
2	1832	75.9	13.54	0.54	1.77	3.28	98.42	96.66	83.42	69.63	Yes
3	1832	85.4	11.85	0.02	2.3	2.94	102.47	98.52	-3.65	-0.23	NO
4	1803	32.3	15	0.21	43.23	4.15	95.75	92.95	35.8	21.8	Yes
5	2131	59.4	13.5	0.27	19.8	3.5	96.5	93	-27	-22.5	Yes
6	1812	89.6	4.84	0.19	1.59	3.16	99.56	97.83	16.7	10.5	Yes
7	1850	93.7	9.13	0	2.02	6.49	111.36	109.6	27.25	15.7	Yes
8	2105	97.2	0	0.02	1.99	2.82	102.14	101.17	16	10	Yes

Mass recovery was estimated in the same way as what has been done in crude oil A. Viscosity of treated oil sample at two temperatures 100 °C and 150 °C were measured. Mass balance and viscosity results were shown in table 13. Viscosity was measured at higher temperatures because of its Non-Newtonian fluids property at temperatures below 100 °C. It has been observed that viscosity of crude oil B depends on hear rate or shear stress at a temperature below 100 °C. To make the comparison simpler between treated and untreated samples, we chose to measure the viscosity when oil was a Newtonian fluid.

Test 3 was not considered successful because of a broken gasket. Photo after the test shown leaked oil traces on the wall of the tank. Viscosity of the treated oil sample did not show significant change. Mass balance of all tests were below the uncertainty level. Viscosity change in test 5 is not consistent with other tests since it showed a viscosity increase. Argon was injected into the oil tank to help mixing the oil instead of methane.

What argon could have done to the irradiated oil is not very clear at this point. But we believe that it is related to the property of argon as an inert gas. It is a larger molecule and known to be able to act as radical scavenger. We also noticed the oil temperature was rising slower than test 2 to 4 which had similar conditions. There was a significant energy transfer between argon and the oil molecules.

Test 2-4 are repeating tests with about 1000 kGy energy input. They were all two stages run to prevent overheating the oil above 300 ^{o}C. Treated oil samples from both test 2 and test 4 showed significant viscosity reduction, 87% and 35%, respectively, at 100 ^{o}C. These are the highest viscosity reduction we have been able to achieve in all ebeam irradiation experiments. But please note that test 2 produced cokes on the bottom of the box because a small quantity of oil was over irradiated at the bottom of the box. Coking process with longer residence time and higher energy input produces produce both cokes and light products, but the process is typically not economical due to its high energy input. Test 4 was successful with good mass balance, even though it had a funnel leak issue in the box, but there was no coking and product leak. Its viscosity showed 35% and 22% reduction at 100 ^{o}C and 150 ^{o}C, respectively.

Energy input was reduced in test 6 and test 8 and other parameters remained identical. Mass recovery of both tests were good. Viscosity reduction were also similar. A major difference between those two tests was the use of a separation chamber. But test 6 with separation chamber and test 8 without separation chamber had no effect on viscosity reduction. What's different between them was the mass recovery on each component. Certainly separation chamber contributes to the light fraction production in the mixture.

Energy input in test 6 and test 8 was nearly half of that in test 2 and test 4. Viscosity reduction in test 6 and test 8 was also less than that in test 2 and test 4. It seems that viscosity reduction was consistent with the energy input. Test 7 had bad mass balance because untreated oil was not completely drained during a prior test run. But viscosity results should be correct.

6.4 Conversion of Crude Oil B

GC-FID analysis was conducted on three irradiated samples from test 1, test 2 and test 4 which had higher viscosity reduction. Figure 36 showed Sim Dist signals of those three with the raw sample. As the figure showed, all treated samples are above the raw sample in the temperature range, which indicates that there are more light fraction and less heavy fractions in all treated sample compared to the raw sample.

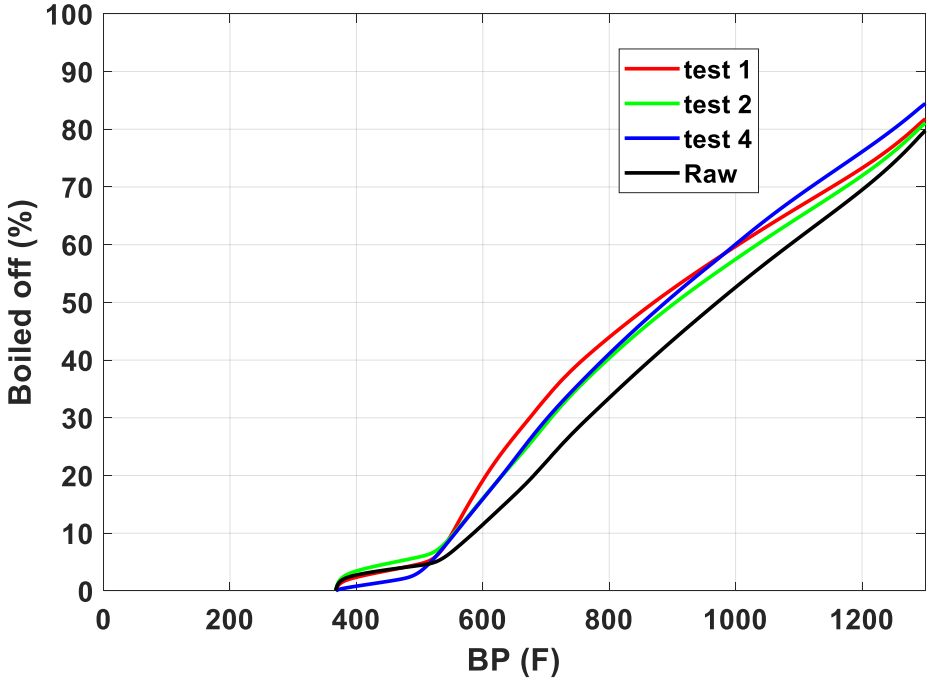

Figure 36: Sim Dist of irradiated crude oil B from test 1, 2 and 4

Viscosity of those irradiated samples was significantly smaller than that of the raw sample due to conversion to light fraction. Conversion results were consistent with viscosity change.

Conversion in three irradiated samples was calculated based on the Sim Dist curves in the carbon range of C10-200. Conversion was estimated based on two methods: mass-based and mole-based. Results were shown in figure 37. Similarly, conversion to hydrocarbons in the range C10-C25 was observed and responsible for the viscosity reduction. Total conversion in this range was estimated by summing up conversion at each carbon number. Total mass-based conversion in test 1was about 11.6% which is the

highest among all three. This number in test 2 and 4 are 6.3% and 9.8%, respectively. Mole-based conversion for three tests were 15%, 8.7% and 13%, respectively. Conversion based on moles was higher than conversion based on mass, because light hydrocarbons have lower molecular weight.

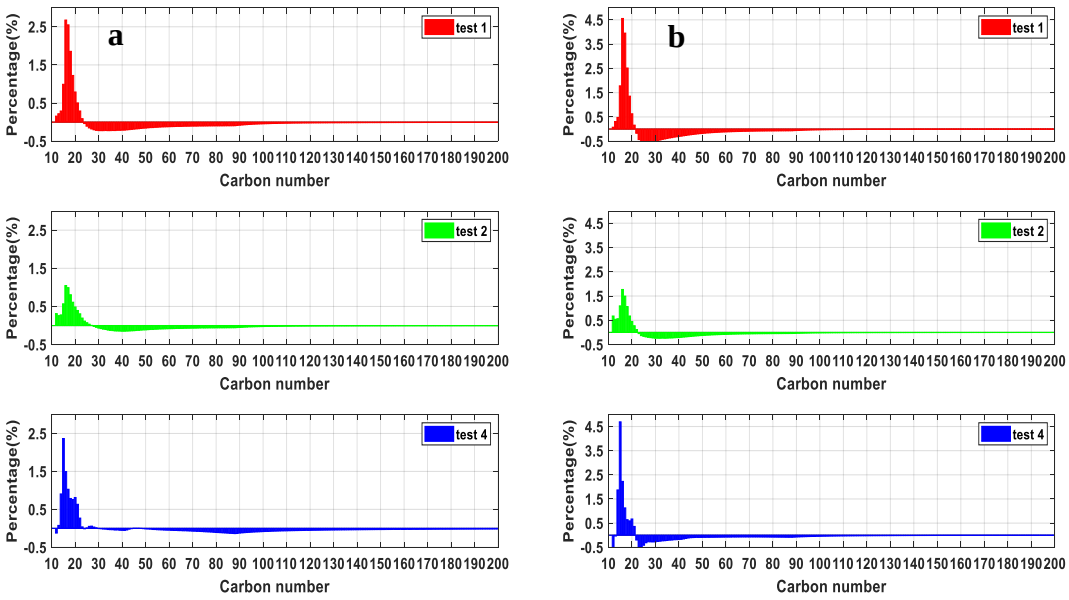

Figure 37: Conversion in crude oil B from test 1, 2 and 4: (a) mass-based conversion and (b) mole-based conversion

Yields of products (molecules/100eV) in three samples were estimated and showed in figure 38. Yields of light products are in the range of 0-2 mol/100eV, significantly higher than that of heavy fraction consumption. This is due to the facts that hydrocarbons from heavy fractions are much bigger than the light products. One heavy compound might

be able to product multiple light compound. It seems that yields of light products from irradiating crude oil B are higher than those from crude oil A. This could be attributed to the difference of oil property. Since there were no light fractions in the range of C10-C20 in crude oil B before irradiation. It might be more suitable for irradiation processing. Total yields of light products are estimated by adding yield at each carbon number. In test 1 about 7.7 molecules were produced with 100 eV input while only 2.2 and 3.5 molecules were produced in test 2 and test 4 , respectively, by spending the same amount of energy.

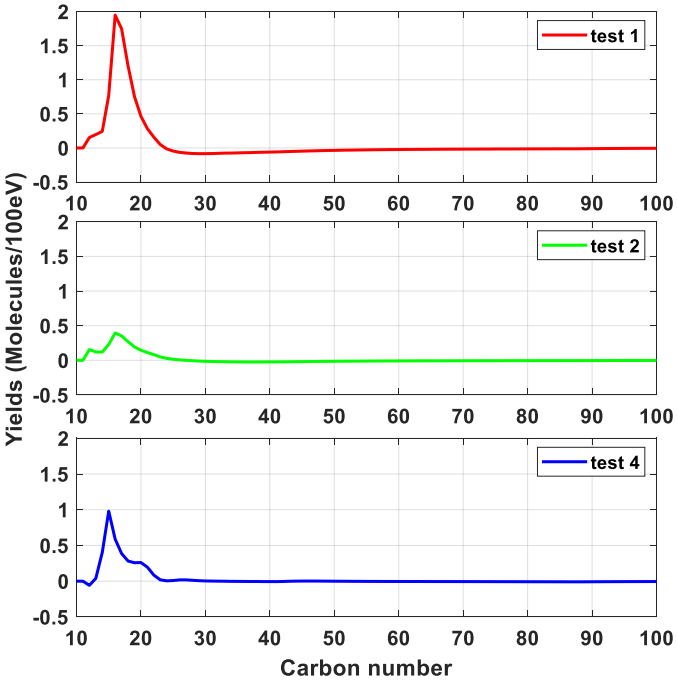

Figure 38: Yields of products in irradiated crude oil B from test 1, 2 and 4

CHAPTER VII

RESULTS AND DISCUSSION- HIGH DOSE WITH TEMPERATURE CONTROL

Temperature as an important parameter needs to be controlled when studying other parameters such as dose and shear rate. Its influence on radiolysis of hydrocarbons have been discussed in previous chapters. Generally temperature effect on irradiation of petroleum is complex and is coupled with irradiation dose rate. As dose rate changes, temperature effect will also change accordingly. Therefore decoupling those two parameters becomes necessary in order to investigate them more accurately. The other reason temperature needs to be controlled is because we have to prevent irradiation processing from approaching thermal conditions (>350 ^{o}C). Under thermal conditions, radiation effect might become less dominant than thermal cracking does. Therefore the goal of temperature control is to achieve constant temperature irradiation of heavy oils below 300 ^{o}C.

7.1 Temperature Control with Water-Cooling Jacket

Temperature control during irradiation was achieved by using a water-cooling jacket. The cooling jacket was specially designed to reduce the thermal effect on treated oil by maximizing the contact area between cooling water and hot metal surface. It resembles a counter-flow heat exchanger. Water flows into the jacket at the lower end of the channel at around 10 L/min. Oil enters the channel from the other end. Cold water surrounds the oil channel from three sides with only one side open to the beam. This

significantly increased the heat exchange surface area compared to the previous channel. The other advantage of this cooling jacket is the incorporation of gas bubbling into oils films. One of the challenges regarding to the use of this channel is installation of it in the processing box. It needs to connect with more than five different fitting that are used to transport gas, water and oils. Figure 39 shows the configuration of the new channel inside the processing box including a few inlets and outlets for gas and water. Since oil flows on this water jacket and gets irradiated, it is very important to lineup this 4 ft long channel with the beam region. Our strategy was to line up the channel with the center line of the box. It was easier to know whether beam pathway has been overlapped with the center line of the box even after box was closed.

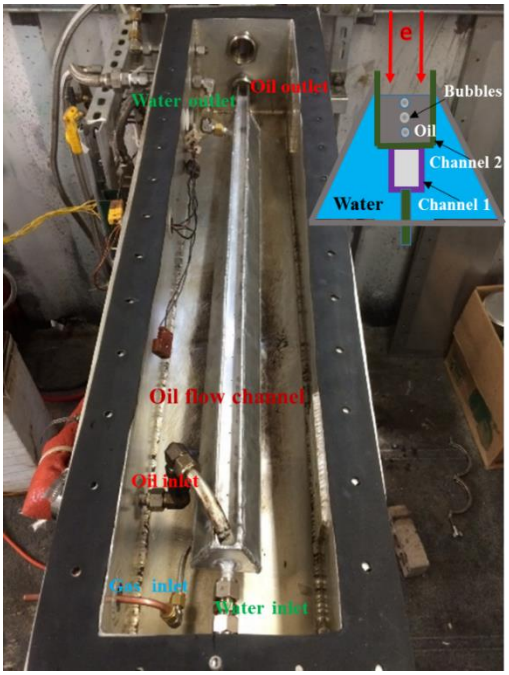

Figure 39: Configuration of oil flow on the cooling jacket inside processing box

7.2 Cooling Effect in Irradiation Tests

Six irradiation tests with temperature control were completed on crude oil A. The goals of conducting those tests include: test the new cooling channel under desired experimental conditions; verification of new design; study the effects of dose at constant temperatures. Table 12 shows the detailed experimental conditions during the test. All tests were performed in a multi-pass mode with methane bubbling into oil at 1 LPM. Dose rate was constant during those tests. Oil temperature during irradiation test was controlled by flowing cooling water into the jacket. Temperature rise during all the irradiation process were smaller than 30 °C whereas the temperature variations from previous experiments with old design were close to or above 100 °C. This indicates the success of this design by optimizing the cooling surface area and that temperature as an important parameter could be isolated and studied independently from absorbed dose.

Oil temperatures from each irradiation experiment were recorded on multiple locations inside the box. Three temperature values including the oil temperature in tank, oil temperature before entering the ebeam zone and after the ebeam zone were monitored for all six tests. Oil was warmed up to a desired temperature by external heating in the system before beam and water were turned on. Then beam and water were turned on at the same time once initial temperature was reached. Energy deposition from beam competes with energy loss due to water cooling. If water cooling is effective enough, all thermal effects from the beam will be removed.

Figure 40 showed the oil temperature during all 6 experiments. Two temperature ranges were investigated in those tests: <150 ^{o}C and >250 ^{o}C. Temperatures lower than 150 ^{o}C is possible to achieve with this channel, e.g. test 3 and test 4. As more energy was added to the oil, temperature tend to increase above 150 ^{o}C and may reach a steady state between 150 and 160 ^{o}C. We did not try to irradiate oil at a temperature below 100 ^{o}C because the density and viscosity at this temperature might be too high, which might cause overflow on the channel or line clog due to high viscosity. Temperature control with this water cooling channel was more effective at relative high oil temperature due to higher heat transfer coefficient. In test 2 we were able to irradiate oil A at a temperature range of 260 $\pm$ 5 ^{o}C. In general, water cooling was able to balance the beam power and maintain the oil temperatures in a narrow window during all tests. Cooling effect depends on the water flow rates and water temperature. In those experiments, water was supplied from a source on the wall. The cooling system has a potential to further reduce the oil temperature during irradiation if colder water or higher flow rate are provided.

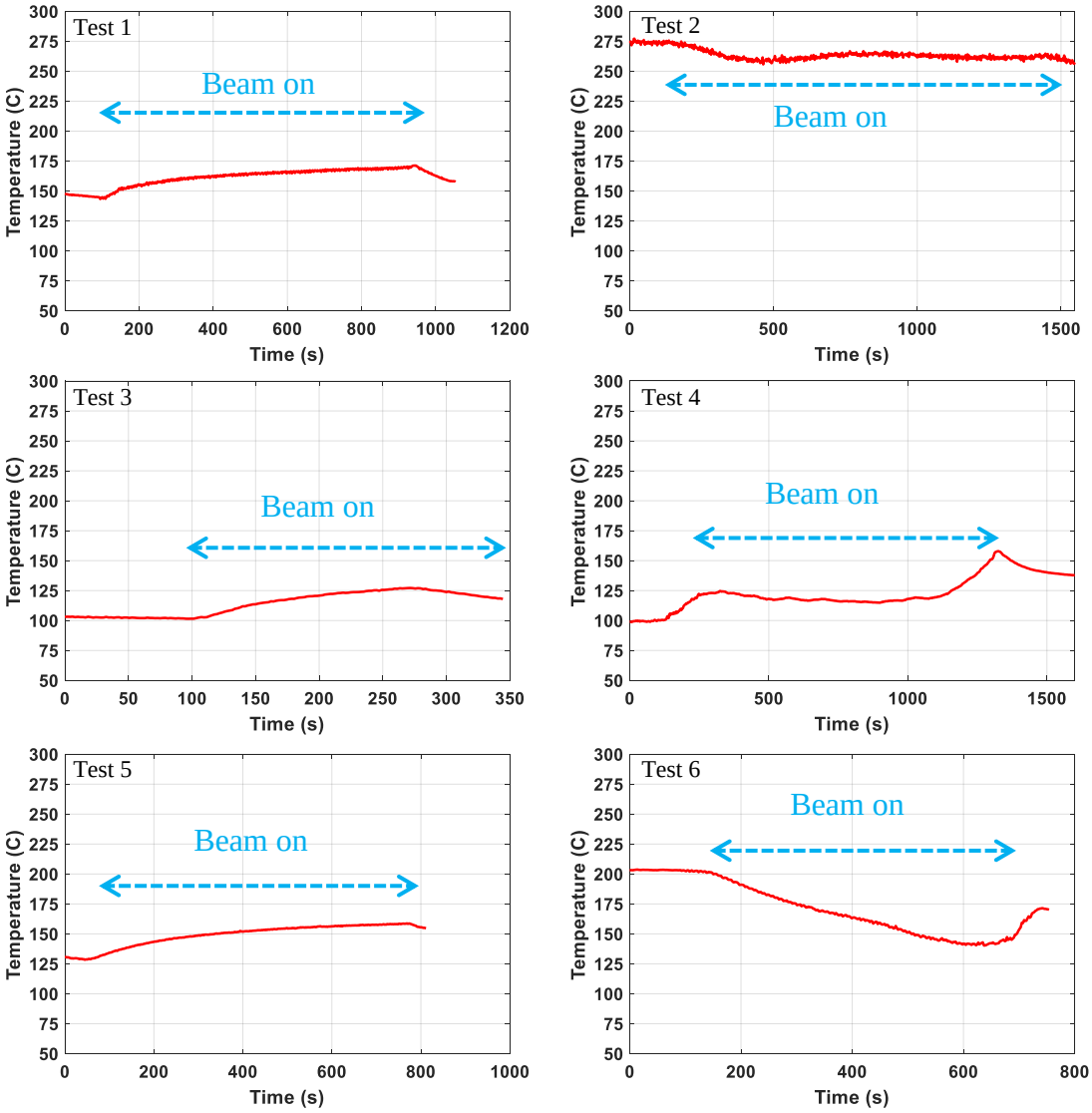

Figure 40: Oil temperatures with water cooling in six irradiation tests of oil A

Cooling effect from test 4 was investigated with more detains and shown in figure 41. During this test water was turned on and off when ebeam was on to study the dynamic effect of water cooling on oil sample. Water was turned on during the first ten minutes and oil temperature was close to 120 ^{o}C with less than 3 degree variations. Then water

was turned off for about 4 minutes. Oil temperature during this period increased by more than 40 ^{o}C. When water was turned on again, oil temperature quickly dropped below 135 ^{o}C within 5 minutes. This test proves the best evidence and effectiveness of water cooling with this design.

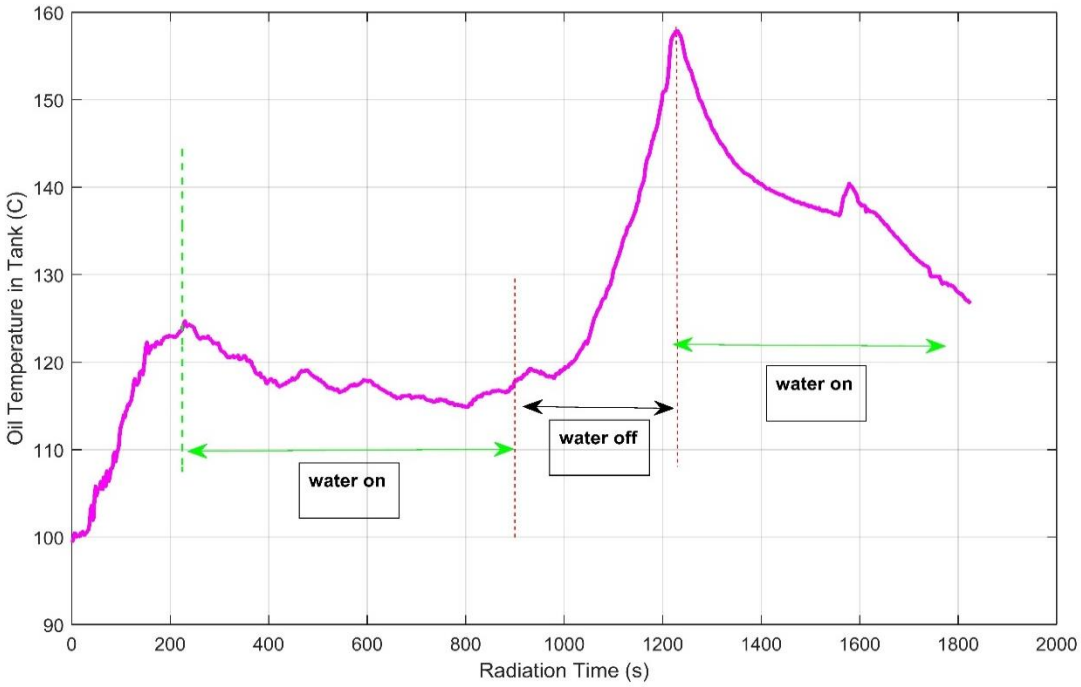

Figure 41: Water cooling effect on oil temperature during irradiation test

A few considerations on the design and operation of this water-cooling jacket. Compared to previous channels without water cooling or less effective cooling, this water cooling jacket is much more effective due to its large surface area in contact with cold water. Cooling power is driven by two factors: surface area and water flow rates. Increasing either one of them will make the cooling more effective. Due to the constrain

of space inside the box under the beam, this jacket probably maximized the surface area which means that it will not provide more cooling power unless by flowing water at higher rate or at lower temperature. During test water source is from the sink and its temperature is constant. Water flow rates are adjusted by a flow meter. When both water and beam are on during the test, temperature profile on this channel will be slightly different from that on the previous channels. Metal surface temperature will be higher because of its higher absorbing power and low heat capacity. Typically aluminum beam absorbing power is about three times higher than that of crude oils and its heat capacity is smaller. So overall metal surface temperature will be much higher than the oil temperature. Oil film near the metal surface will have higher temperature than the bulk liquid due to this effect. If temperature is above 300 ^{o}C, thermal effect of oil conversion may become significant. It is difficult to measure the metal surface temperature under the beam, but it could be simulated with a fluids flow analysis. With water cooling metal surface has a lower temperature than oil and heat conducts from oil to metal, eventually dissipated into water. Since metal is very thin and highly thermal conductive, it is reasonable to assume that its temperature is uniform and its value resides between water temperature and oil temperature.

7.3 Irradiation of Crude Oil A at Constant Temperatures

Irradiation tests at constant temperatures were conducted on crude oil A in two temperature zones: 150 °C zone and 250°C zone including six tests. Another major variable in those tests is the total absorbed dose. Three dose values were compared in the temperature zones and they are 150 kGy, 500 kGy and 750 kGy. The goal of those tests

was to verify the cooling effect with the new design and to study the effect of dose on crude oil A irradiation. Only test 4 was not run as planned due to water leakage in the box. Parameters including dose rate, shear rate and separation chamber are not the interest of the test here and they are only changing in a very narrow window.

Table 14: Irradiation Experiment Conditions of Crude Oil A

Test Number	Flow mode	Flow rate (LPM)	Average Residence time (s)	Separation chamber	Bubbling gas	Average shear rate (s^{-1})	Dose rate (kGy/s)	Dose (kGy)	Temperature range (°C)	As planned?
1	Multi-pass	1	2.3-3.4	NO	Methane	15-27	19.5	757	140-156°C	Yes
2	Multi-pass	1	1.7-1.8	NO	Methane	61-68	19.5	362	257-279°C	Yes
3	Multi-pass	1	4.3-7.3	NO	Methane	5.9-16.7	19.5	147	98-131°C	Yes
4	Multi-pass	1	NA	NO	Methane	NA	19.5	NA	178-225	NO*
5	Multi-pass	1	2.9-4.9	NO	Methane	13-37	19.5	385	121-157°C	Yes
6	Multi-pass	1	1.9-2.1	NO	Methane	67-80	19.5	562	150-200	Yes

*, water leaked into box and mixed with oil

Table 15: Mass Balance and Viscosity Reduction of Crude Oil A

Test Number	Initial mass (g)	Collector %	Separation %	Channel %	Box %	Condenser %	Total Accounted %	Recovered %	Viscosity reduction (%)		As planned?
									50 °C	100 °C	
1	1889	85.73	0	1.47	6.31	1.2	94.72	89.00	-0.71	-1.79	Yes
2	1851	89.61	0	1.98	1.93	1.24	94.76	93.63	-1.31	-0.35	Yes
3	1938	94.16	0	1.75	0.78	0.26	97.72	95.55	-3.39	0.35	Yes
4	1882	69.06	0	7.24	17.36	6.64	107.68	94.21	-21.9	-15.22	NO
5	1911	88.09	0	1.49	2.63	0.77	95.86	91.62	-7.00	-5.27	Yes
6	1917	80.61	0	2.45	3.0	4.43	91.79	89.14	-14.05	3.37	Yes

Table 15 includes the mass balance and viscosity change results corresponding to each of the tests above. Note that test 4 was not a planned test because cooling water leaked into the processing box and mixed with oil. That caused a significant gain on the mass recovery which ended up to be 107.68 %. Consequently the viscosity results on this run will not be considered. All other tests showed relatively good mass balance in the range of 94% to 98% except test 6 which had a low mass recovery. None of them showed positive viscosity reduction with recovered oil mixture from multiple locations.

It is quite possible that the lost mass is responsible for the increased viscosity because mass loss is more likely due to the lighter species in the oil. The contribution of lighter species to viscosity is much larger than that of heavier species. Therefore a 5% mass loss on lighter species may cause more than 20% increase on viscosity in the oil mixture. Note that both temperature and specific energy input to samples in those tests were not high. To achieve a certain conversion or viscosity reduction may require higher energy input or at higher temperature. Another possibility would be oil property related. The oil samples that was irradiated was too complex and chemically stable in terms of its hydrocarbon molecules structure and distribution.

7.4 Effect of Temperature, dose and condensed liquids on viscosity reduction

With all the results regarding viscosity reduction by irradiation of both oil A and oil B, we studied the effect of average oil temperature, total absorbed dose and total condensed liquids on viscosity reduction. Temperature was first investigated as an independent parameter and its effect on viscosity reduction was shown in figure 40a and

40b. It seems that higher temperature helped reduce viscosity in irradiated oil A, except those points not as planned. The enhancing effect of temperature on viscosity reduction was significant between 200 and 250 ºC. A clear trend was observed in this range. Temperature effect in irradiation of oil B was not clear due to very limited number of runs. The other reason is temperature of oil B had a narrower window compared to oil A irradiation, therefore effect of it was difficult to see.

Dose as another parameter was also evaluated on its effect on viscosity reduction. Results were shown in figure 42c and 42d. For both oils, dose was varied with a wide range between 100 kGy to 1500 kGy. No trend was observed.

Condensates produced in the irradiation process are the most important products. They are produced by converting heavy fractions to light fractions. Two sources to find the condensates are separation chamber and condenser. Their mass ratio in irradiated oil determine the oil viscosity change. Figure 42e and 42f showed the relationship between total condensates and viscosity reduction. Viscosity reduction in irradiated oil A was directly related to the total condensates. More condensates in the irradiated oil means a higher viscosity reduction and vice versa. Trend was less clear between total condensates and viscosity reduction in irradiated oil B. But we can still see a weak correlation between them. Again this weak correlation might be due to a limited number of experiments that have been competed on oil B.

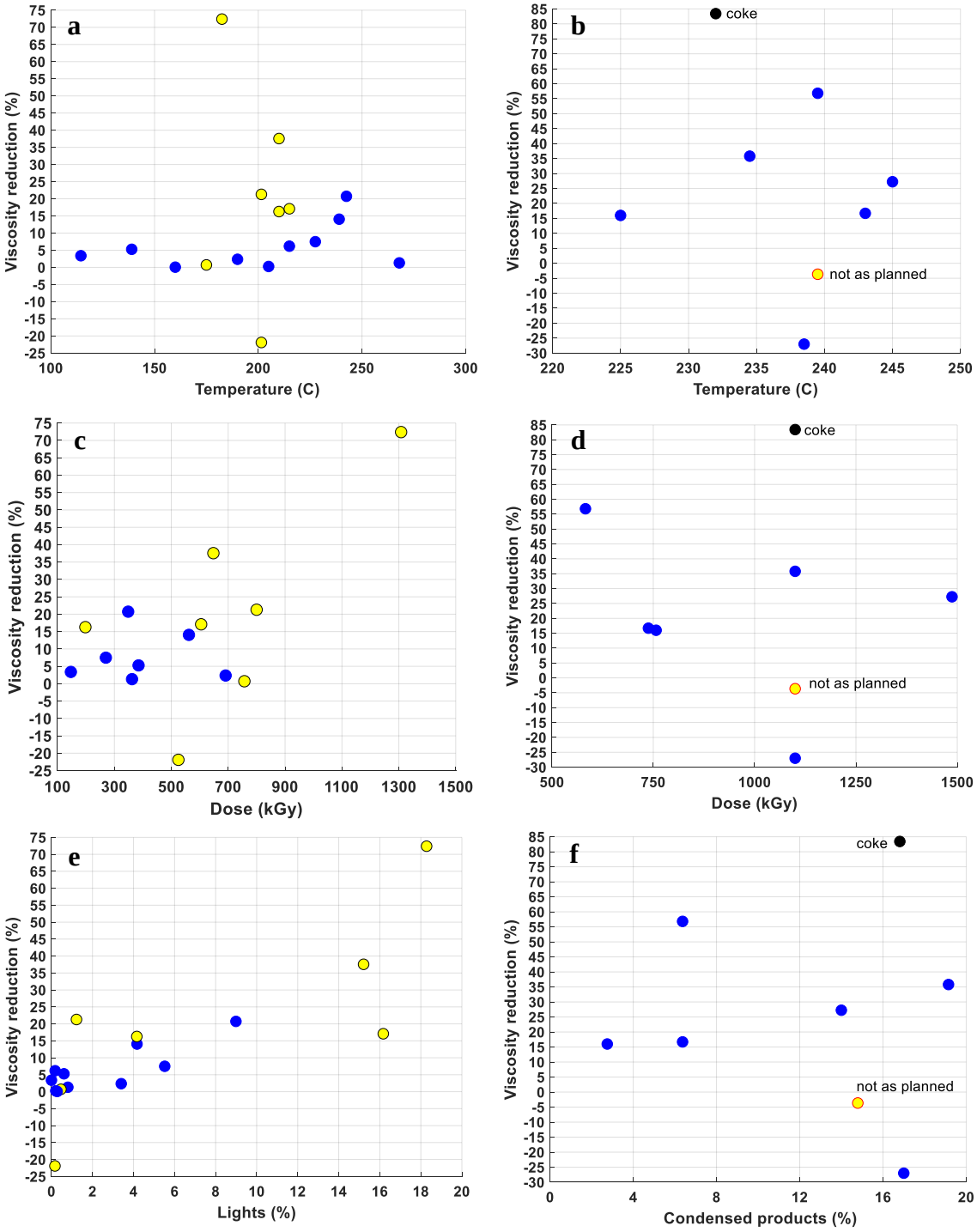

Figure 42: Effect of Temperature, dose and condensed liquids on viscosity reduction for oil A and oil B. blue means runs are as planned and yellow means runs are not as planned

CHAPTER VIII

IRRADIATIION OF NEAT HYDROCARBONS

Irradiation of crude oils is a complex process and faces tremendous challenges due to various factors. First, parameters that affect the radiolysis of crude oils are not only limited to hydrocarbon groups but also some other impurities such as trace metals and many non-hydrocarbons groups (nitrogen and sulfur based groups). The effect of impurities on irradiation of petroleum is largely unknown. Based on theory and current literature some of the impurities in petroleum are important and will change the irradiation results. However it is not possible to completely remove impurities in a crude oil before irradiating it. Arguably one can mix tens of hundreds of different hydrocarbon compounds including saturated and unsaturated ones to mimic crude oil contents but without any non-hydrocarbon impurities, but it is not practical and cost effective.

For research purposes, it is necessary to isolate the effects of impurities and only focused on irradiation of hydrocarbons with well-known property. In chapter II, radiolysis and radiation effect on individual hydrocarbon were discussed form multiple literature resources. Undoubtedly they provide a fundamental theory basis for this dissertation and guide us through the course of this work. However it is crucial to realize that there are aspects on this research that are significantly different from information found from existing literatures, for example the energy of electron beam are much higher (10 MeV) and irradiation system is a continuous flow system rather than a batch system. This largely justify the importance of irradiating neat hydrocarbons in this continuous flow system and compare results with those from prior literature. For this purpose, we first irradiated

mineral oils which represent a heavy hydrocarbon mixture without impurities and heteroatomic systems such as sulfides.

8.1 Irradiation of Light Mineral Oil

Light mineral oil was purchased from McMaster-Carr and irradiated with the flow system. It has a boiling point larger than 250 ^{o}C and a specific gravity ~0.81 at 15 ^{o}C. It is a clear liquid with petroleum odor. Viscosity was 16.75 cP at 30 ^{o}C and 8.25 cP at 50 ^{o}C. It is a mixture of saturated alkanes and cycloalkanes which are in the range of C15-C25 by boiling point [147]. The distillation curve and hydrocarbon distribution specific to the oil used were measured and are shown in figure 49.

8.1.1 Experimental Parameters

Various parameters are known to affect electron beam irradiation of hydrocarbons. Those parameters include: specific energy input, dose rate, temperature, electron beam energy, type of hydrocarbon, type of gas bubbled, as well as if vaporization occurs. Parameters evaluated in this research include temperature, bubbling gas and specific energy input. Beam energy was 10 MeV, dose rate was 17 kGy/s, and only mineral oil was tested here. Helium and methane were used as bubbling gas for the experiments. Helium is an inert gas and no chemical reactions are expected to happen between the gas and liquid hydrocarbons. Methane could potentially act as hydrogen and methyl group donor, which play substantial roles in many radiation induced reactions. Processing temperatures were 80 ^{o}C and 150 ^{o}C and may exert influence on irradiation of hydrocarbons because it affects process such as mass transfer and many chemical reactions. For example higher temperature will favor the diffusion of reactive species

which might change the reaction selectivity between cracking and polymerization. Specific energy input into samples mainly controls overall conversion percent and not process chemistry, particularly at relatively low conversions when the composition is mainly reactant. Treated samples were analyzed shortly after irradiation (in 2016) and again 2.5 years later (in 2019) after storage in a sealed stainless steel container at HVAC controlled lab conditions (20^{o}C to 24^{o}C). All processing was done in 2016.

8.1.2 Data Analysis Method

Responses of irradiation of mineral oils are focused on the physiochemical change of treated samples such as appearance, optical properties (FTIR), viscosity, hydrocarbon conversions and yields of products. Average viscosity of each sample was calculated in the shear rate range of 1-100 s^{-1} at a given temperature. Viscosity of three treated samples was compared to that of the raw sample. Absolute viscosity values were reported as well as the percentage change with respect to raw. Conversion and yields were estimated by using GC-FID based on the method introduced in Chapter 3.

8.1.3 Mass Balance

Mass balance was performed on all treated samples. Table 14 shows detailed mass balance results for the three experiments. It was used to validate the experimental results and bound the uncertainty. For example a 5% unaccounted mass could change viscosity by 40%[148,149]. For valid results total mass balance should be in the range of 99%-101% of the initial mass. The total mass has contributions from mass collected in various locations in the flow system. Sample was collect from four locations: the collector, the condenser, the bottom of the box (using a syringe and squeegee) and the channel. There

was oil left on the channel and the condenser was able to collect some hydrocarbons. They are all part of the total mass balance. For the channel and condenser they were weighted before and after the experiment. Coke is also quantified and is defined as any insoluble solids which stick to the channel or bottom of box. No coke was observed in these experiments (but had been observed during failed experiments with a flat box bottom). Mass balance of all three experiments are very close to 100% indicating small experimental uncertainty. Over 99.3% of the total mass was found in the collector for all three experiments. Mass fraction in condenser was higher when processing temperature was higher. This is probably due to increased evaporations caused by higher temperature. Whereas the factions from channel and bottom of box were lower when processing temperature was lower. Measurement uncertainty for values in table 16 are less than 0.3% of the measured percentage.

Table 16: Mass Balance of Treated Samples

Accounted Mass %	H80	H145	M85
net mass put in [g]	971.45	1825	1830
collector %	99.38	99.56	99.32
bottom of box (outside of beam) %	0.38	0.16	0.16
condenser %	0.21	0.52	0.41
coke %	0	0	0
channel %	0.21	0.11	0.11
total %	100.18	100.35	100.78

8.1.4 Oil Temperature Profiles

Oil temperature during irradiation experiment was controlled to achieve constant temperature irradiation processing. It was measured from multiple locations to ensure the accuracy of temperature values. Three locations were selected to measure the temperature: inside the tank, near channel inlet and channel outlet. Temperature on channel inlet and outlet are more likely to be interfered by the electron beam since they were closer to the ebeam region. Oil temperature in tank was much further from the ebeam region and well

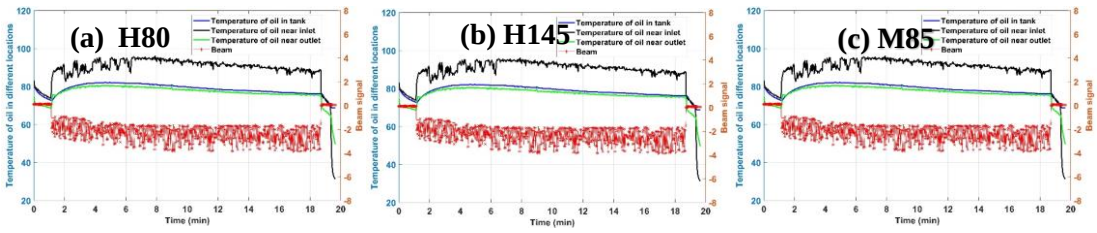

Figure 43: Temperature profiles measured from three locations: (a), H80; (b), H145; (c), M85.

insulated, it should more accurately represent real oil temperature. Therefore, this temperature was used in the flow model to estimate oil property and velocity distribution.

Figure 43 showed the oil temperature time traces from each irradiation experiment. In general, oil temperatures in all locations were quite stable and deviate in the range of ± 10 ℃. Oil processing with electron beam at constant temperature were achieved at both warm conditions (H80 and M85) and hot conditions (H145). Specifically, oil temperature in tank only deviated with ± 5 ℃ over 20-60 minutes. But temperature in

channel inlet sometimes showed a spike, that was due to shaking of the thermocouple by oil flow and it was directly exposed to ebeam after it was moved. Electron beam status was monitored by an antenna wire and sent to the DAQ device. Red line is the ebeam signal. It showed negative values when beam was on and returned to zero when beam was off. It had a very quick response and could be potentially used in situations that require less time delay.

8.1.5 Appearance

Color of a liquid hydrocarbons is an important indicator of its chemical compositions and states. One way to change the color of liquid hydrocarbon is by creating a new color center. Color centers could be created by irradiation in almost all type of hydrocarbons spanning from very small molecules like CH_4 to very large molecules such as polymers [150–152]. Irradiation induced color change could be understood in terms of formation of two type of color centers: annealable color center and permeant color change [153]. Annealable color change is due to the creation of radicals that are trapped in the matrix. This commonly happens to polymers and aromatics once irradiation applies, because they are more likely to trap radicals due to their large molecular size and low reactivity [152]. Annealing the color centers is possible by increasing temperature or providing reactive species such as oxygen to react with those radicals. Permeant color centers are due to the formation of chromophores such as conjugated double bond and a lot of aromatic systems. Typically this color center contributes less to the color change

initially with low dose, but is more significant at high doses. A trace concentration (<0.1%) of color centers can significantly change the observable color.

The second way to change hydrocarbon color is by adding impurities such as soot. Soot were produced in refining processes such as thermal cracking [154,155]. Suspended soot will change the color of the original liquid because of their low solubility in the liquids, which brings strong scattering effect.

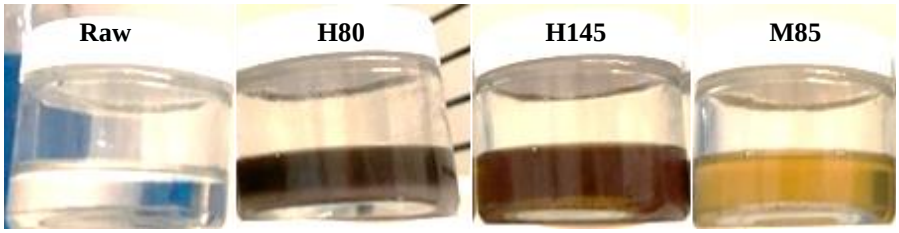

Figure 44: Appearance of treated samples

After the ebeam irradiation, samples showed significant color change as seen in Figure 44. The raw sample is a clear and transparent liquid. Treated samples became yellow to brown depending on the experimental conditions. Sample H80 and H145 are brown, while sample M85 is yellow. It seems that there are more color centers created in the first two samples treated with helium and less color centers in sample treated with methane. This could be explained by different gas response under high energy electron beam irradiation. Since helium is a small inert gas molecule, it does not react with color

centers during irradiation. Methane, however, produces methyl and hydrogen radicals that could potentially react with color centers and mitigate their effect in the liquids.

8.1.6 Viscosity Change after Two Years

Viscosity of a neat hydrocarbon depends on parameters such as molecular structure, molecule volume as well as its thermodynamic conditions (temperature and pressure)[156–158]. Typically hydrocarbons with longer chain or more branches will have larger viscosity. Position of a side chain has little effect on viscosity. Cyclic compounds have larger viscosity than straight compounds[159].Viscosity at elevated temperature is lower, but becomes higher when pressure increases[160]. Viscosity of a known hydrocarbon mixture generally follows mixing rules that could be represented by density and viscosity of each individual species as well as its mass ratio. This indicates that there is a strong correlation between the mixture viscosity and mass ratio of each hydrocarbon species. Hydrocarbons with smaller viscosity has more significant effect on the viscosity of a mixture. Hydrocarbons with larger viscosity has less effect on the viscosity of a mixture. Therefore viscosity could be used as an indicator of species inside a hydrocarbon mixture. Viscosity of hydrocarbons might also depend on the applied shear stress and shear rate due to its non-Newtonian behavior. But the oil sample we study here is a Newtonian fluid and viscosity is independent of both shear stress and shear rate in the temperature range we are interested in.

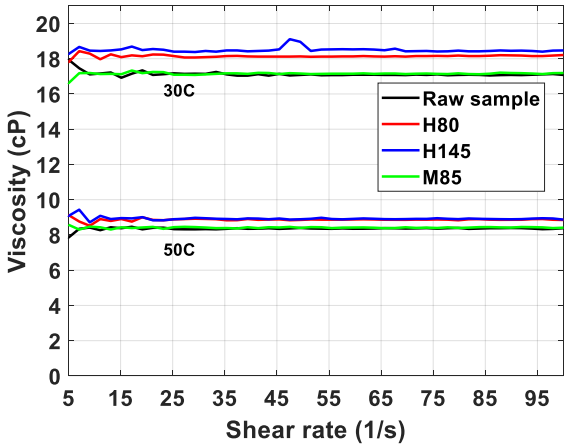

Figure 45: viscosity change after two years

Viscosity as a function of shear rate at 30 ^{o}C and 50^{o}C were shown in figure 45 for each treated oil sample together with the control sample. Uncertainty is 2% for each sample. Control and treated sample with methane have almost the same viscosity, while treated samples with helium have significantly increased viscosity. Increased viscosity was very likely due to the increased contents of larger molecules which have higher viscosity. Sample H145 has more than 8% viscosity increase compared to 6% on sample H80, it indicates H145 might have more contents of larger molecules produced by irradiation. Viscosity change of treated samples are consistent with the color change. In this case, more color change indicates more increased viscosity. This correlates with the use of helium. Sample M85 with unchanged viscosity had less color change correlated with the use of methane.

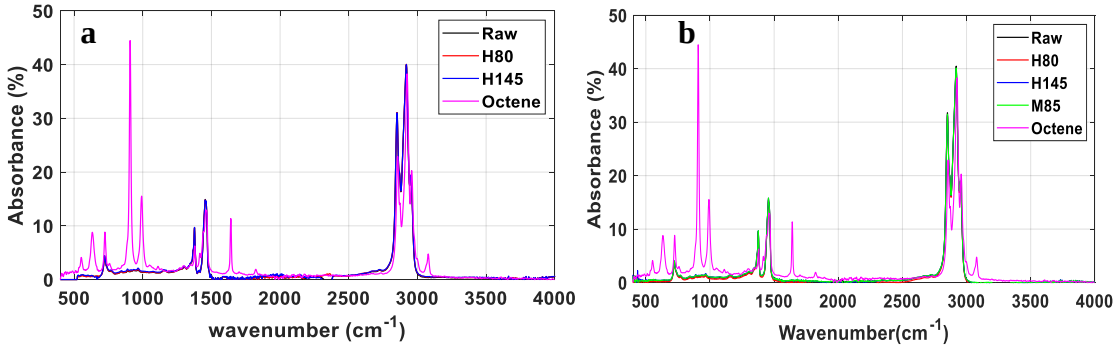

Figure 46: FT-IR analysis of samples within two years: (a) 2016 and (b) 2019

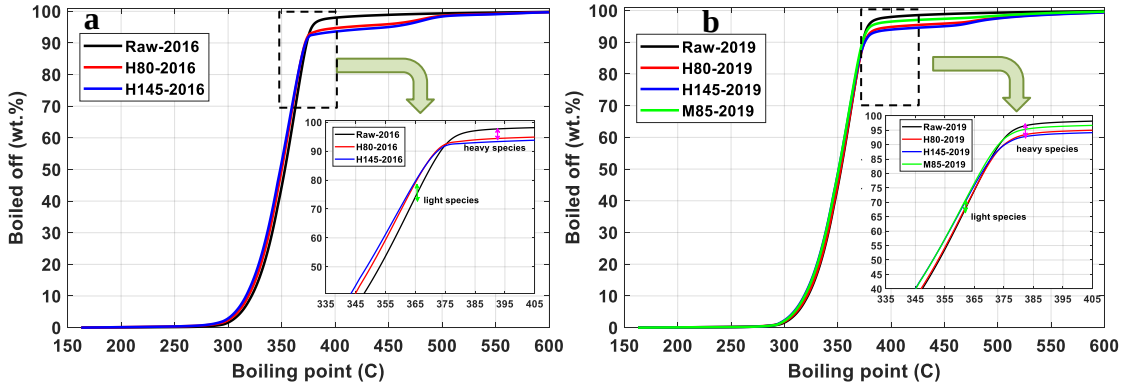

Figure 47: Simulated distillation curves of treated samples measured in 2016 (a) and 2019 (b)

FTIR analysis was performed on samples treated with helium to analyze carbon-carbon and carbon-hydrogen bonds change induced by irradiation. Octene was used as a reference to qualitatively study double bond change in the treated sample. Figure 46a shows the results measured in 2016 shortly after irradiation, Figure 46b shows results measured in 2019 after aging. IR spectra of raw mineral oil and treated mineral oil are

very identical. Octene peaks corresponding to 917 and 1004 cm^{-1} are for H-C= bending. Octene peak at 1640 cm^{-1} is for C=C stretching and peak at 3083 cm^{-1} corresponds to H-C= stretching. None of those peaks was found in treated sample in a two years period, which indicates that no significant amount of olefins were made in the process. Level of detection of this technique is ~1%.

8.1.7 Conversion, Yields and Selectivity

Simulated distillation curve and hydrocarbon distribution of irradiated mineral oil samples were studied and compared with raw mineral oil by using GC-FID. Simulated distillation curve derived from the GC-FID signals were plotted in figure 47. It simulated the boiling curve of a hydrocarbon sample as temperature increases until all the samples were completely boiled off. It also measures the hydrocarbon distribution based on boiling point. Its shape is important because the shape change indicates the composition change in a hydrocarbon mixture. For example, to boil off 98% of all treated samples in 2016 the required temperature is close to 500 ^{o}C which is 100 ^{o}C higher than the raw sample. This indicates that there are heavy species in the treated sample that were produced during the irradiation process. On the other hand, treated samples were boiled off more before 375 ^{o}C. This indicates that there were light species in treated samples. Distillation curve of the treated samples measured in 2019 all shifted towards the raw sample. This was a result of the reduction of products created in irradiation in 2016.

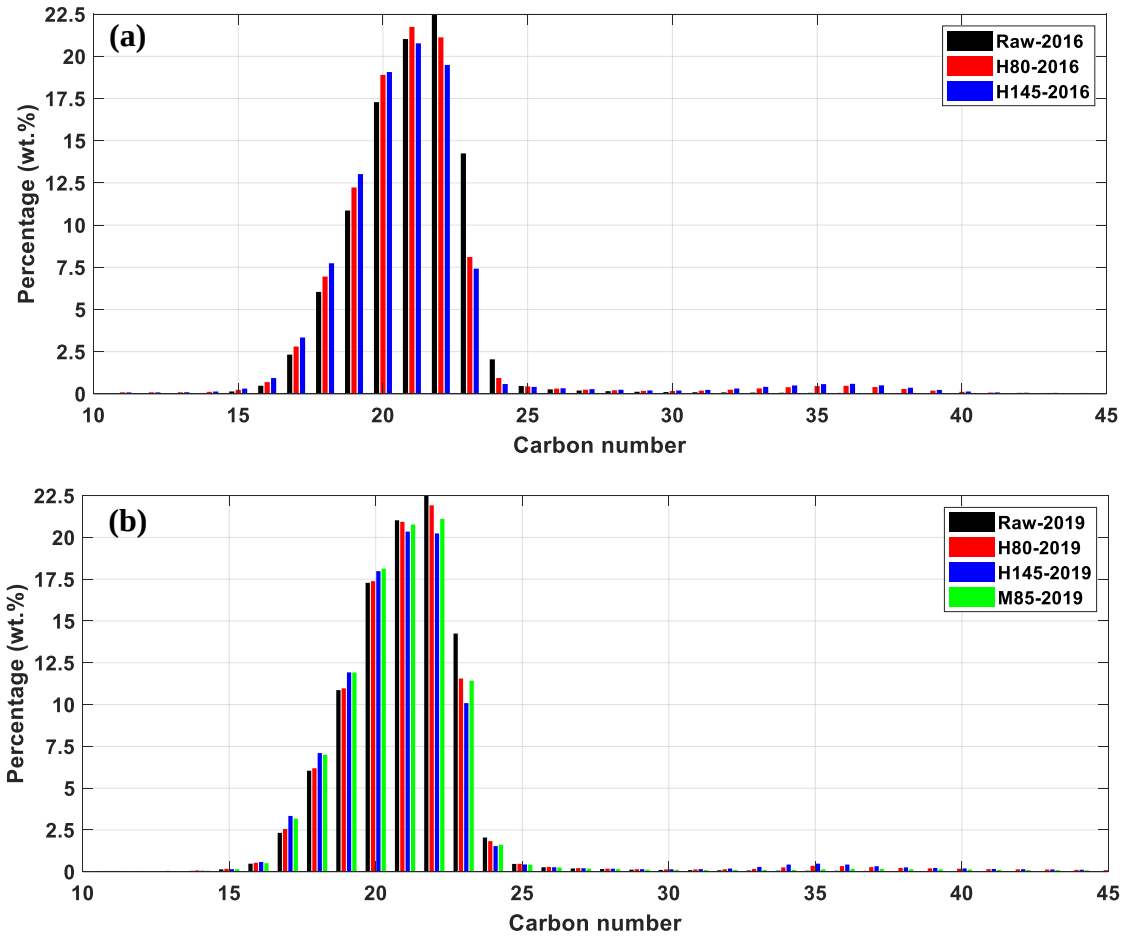

Figure 48: Hydrocarbon distributions in all samples measured in 2016 (a) and 2019 (b)

Hydrocarbon distribution in the range of C10-C60 in all samples were compared. Results were in shown in figure 48. Change above C45 were small and aren't shown in the plot to focus on other regions. More than 95% of hydrocarbon species in all samples were distributed in the range of C15 to C25 and the rest of them were distributed in the range of C10-14 and C24-45. Hydrocarbon distribution in all treated samples were changed by

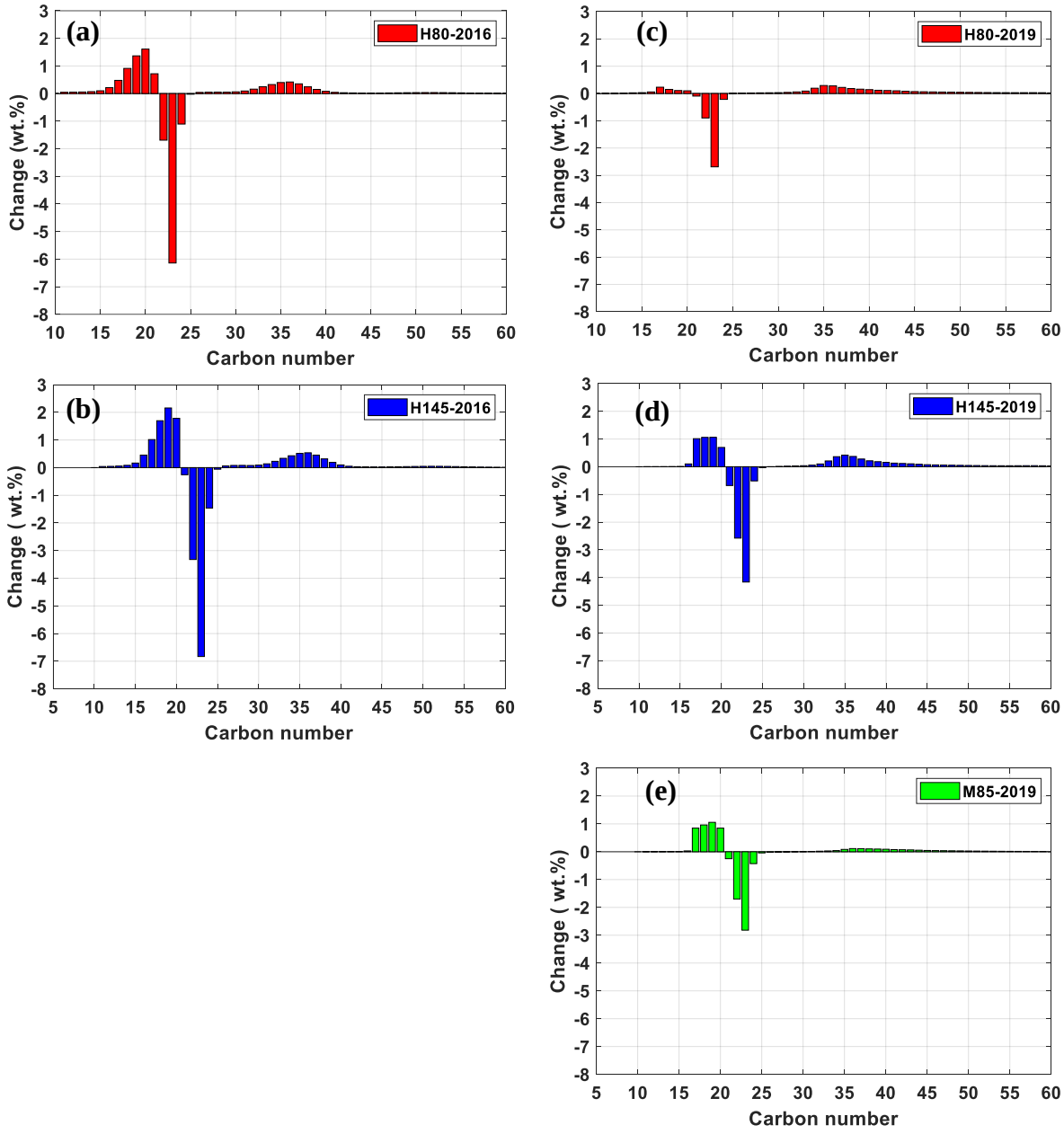

Figure 49: Hydrocarbon distribution change in treated samples measured in 2016 (a and b) and 2019 (c, d and e). For low temperature (a, c, and e), and high temperature (b and d) processing conditions. And for methane (e) and helium (a-d) processing gas.

irradiation. More hydrocarbons were seen in the range of C25-20 and C25-45. Compounds in middle range C21-24 were consumed and converted to hydrocarbons in the previous two ranges. Distribution measured before and after aging showed significant difference and will be explained in figure 49.

Hydrocarbon distribution changes in treated samples compared to the raw was measured at two different times and was plotted in figure 50. Hydrocarbon distribution changes in H80 measured in 2016 showed that 8.5-9% hydrocarbons in the range of C21-

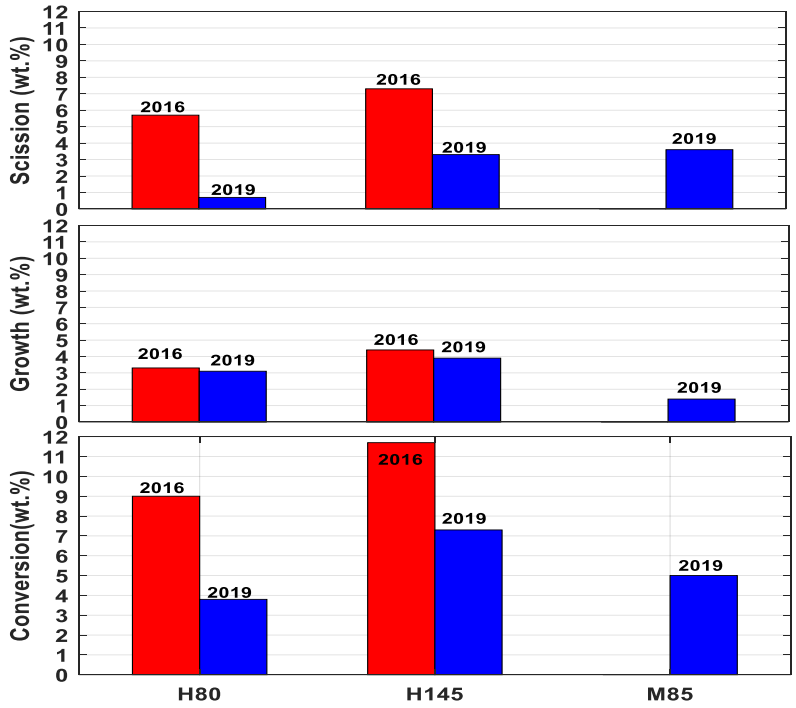

Figure 50: Hydrocarbon product stability in all treated samples measured in 2016 and 2019

24 were converted to other compounds. Specifically, 5.7% of those species was converted to light products smaller than C21 and 3.3% converted to heavy products larger than C25. Product selectivity of converted hydrocarbons to light products is 63%. In sample H145, conversion to smaller products and larger products were 7.3% and 4.4%, respectively, which results in a 62% product selectivity towards light hydrocarbons. Conversions to both products in H145 were higher than those in H80 with similar specific energy input. This could be attributed to the temperature effect. Higher temperature irradiation favors conversion by producing more chain scission and chain growth products. Hydrocarbon distribution in H80 sample measured in 2019 showed 3.8% total reduction in the range of C21-24, among which 0.7% was converted to chain scission products and 3.1% converted to chain growth products. Product selectivity is close to 18% towards light hydrocarbons. Conversion to smaller products and larger products in H145 measured in 2019 were 3.3% and 3.9%, respectively. Product selectivity drop to 46%. Again conversions to both products in H145 were higher than those in H80 due to higher irradiation temperature. More importantly, conversion was found to be highly dependent on time. Sample M85 was irradiated with methane at lower specific energy input. Conversion in this sample was measured only in 2019 and there was 3.6% conversion to chain scission products and 1.4% conversion to chain growth products. Product selectivity was close to 72%. It was irradiated at a similar temperature as H80 but with less dose, conversion was higher with methane and more chain scission products were found. Table 17 and 18 summarized hydrocarbon distributions in all samples as well as conversion in treated samples.

Table 17: Hydrocarbon Distribution and Conversion measured in Dec, 2016

Samples	Distribution			Conversion		
	C_{10-21}	C_{22-25}	C_{26-60}	C_{10-21}	C_{22-25}	C_{26-60}
Raw	58.3%	39.6%	1.9%	0	0	0
H80	64%	30.6%	5.2%	5.7%	-9.00%	3.30%
H145	65.6%	27.9%	6.3%	7.3%	-11.70%	4.40%

Table 18: Hydrocarbon Distribution and Conversion measured in Jan, 2019

Samples	Distribution			Conversion		
	C_{10-21}	C_{22-25}	C_{26-60}	C_{10-21}	C_{22-25}	C_{26-60}
Raw	58.3%	39.6%	2.1%	0	0	0
H80	59%	35.8%	5.2%	0.7%	-3.8%	3.1%
H145	61.6%	32.3%	6%	3.3%	-7.3%	3.9%
M85	61.9%	34.6%	3.5%	3.6%	-5.0%	1.4%

Conversion to different products changed over time in all treated samples because of stability of irradiated hydrocarbons. Stability of treated samples with helium was studied. Both conversion to chain scission products and conversion to chain growth products were compared over two years. Results were shown in figure 50. Chain scission products in sample H-80 were almost completely lost after two years, decreased from 5.7% in 2016 to 0.7% in 2019. Only about half of the chain scission products were lost in the H-145 sample, which indicates a significant effect of temperature on radiation products

stability. It would seem these lights converted to the mid-range. Higher temperature seems to increase the stability of chain scission products created in helium-mineral oil environment. Chain growth products in both samples, however, remained unchanged over

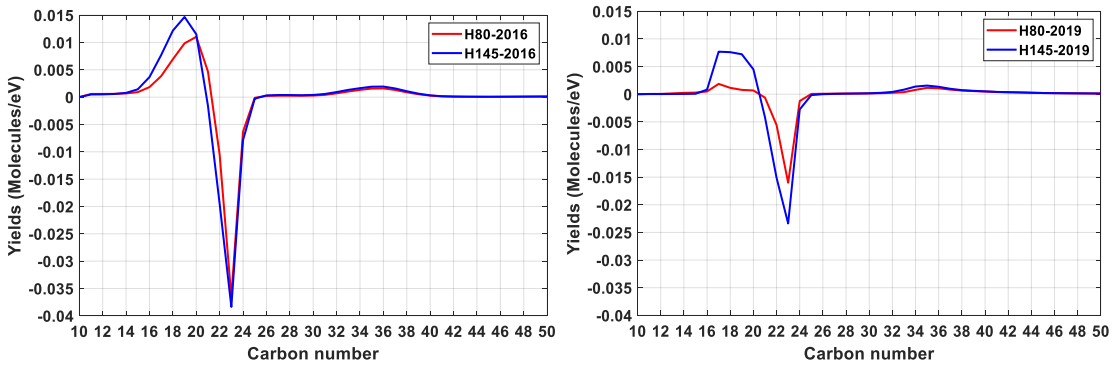

Figure 51: Hydrocarbon product yield in helium gas treated samples

two years. Those heavier products seem to have better stability. Total conversion decreased in both samples predominately because chain scission products decreased.

Yields (molecules/eV), Y in equation 2, of irradiated mineral oil samples with helium were estimated based on the hydrocarbon distribution and conversion before and after aging. Higher yields indicate a more efficient chemical conversion. Yields include chain scission products in the range of $C_{10\text{-}21}$ and chain growth products in the range of $C_{26\text{-}50}$. Reduction of original molecules (molecules/eV), R in equation 2, was also calculated in the range of $C_{22\text{-}25}$. Product selectivity, S in equation 4, represented by the ratio of scission products and growth products and was evaluated based on the conversion results. Figure 51 shows the yields and reduction of different hydrocarbons in the range of

$C_{10\text{-}C50}$ for all treated samples. Negative yields indicate reactant reduction. Yields of chain scission products varied in the range of 0-0.015 molecule/eV, while yields of chain growth products varied in the range of 0-0.002 molecules/eV. Yields of products from this research agrees with results from multiple literatures[105]. Yields in those two samples measured in 2016 were very similar except that H145 has higher yields on chain scission products. This is ascribed to higher irradiation temperature in H145. Yields in both samples measured in 2019 were significantly reduced after two years. More importantly, yields change of chain scission products and chain growth products showed dramatically different pattern. Chain growth products in two samples only showed minor decreases. Yields of chain scission products were reduced by a factor of two or more. In particular, yields in H145 decreased by a factor of two. Yields in H80 decreased by a factor of 8. This almost consumed all the light products created in irradiation process. Yields and selectivity results imply that even though irradiation temperature has marginal effect on conversion and yields immediate after the irradiation experiment, it does exert a huge influence on product yields and selectivity over time. Primarily because chain scission products created in the irradiation process at low temperature are less stable species. Yields and selectivity results are summarized in table 19 and 20.

Table 19: Total Yields (molecules/eV) and Selectivity (%) Estimated in Dec, 2016

Samples	Total Yields	Total Reduction	Total Yields	Selectivity Lights
	TY_{10-21}	TR_{22-25}	TY_{26-60}	S
H80	0.042	-0.054	0.012	63%
H145	0.052	-0.066	0.016	62%

Table 20: Total Yields (molecules/eV) and Selectivity (%) Estimated in Jan, 2019

Samples	Total Yields	Total Reduction	Total Yields	Selectivity Lights
	TY_{10-21}	TY_{22-25}	TY_{26-60}	S
H80	0.005	-0.023	0.011	18%
H145	0.024	-0.041	0.013	46%
M85	0.044	-0.052	0.008	72%

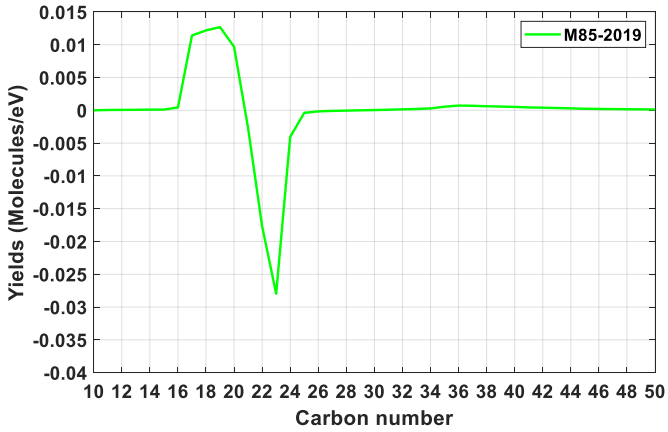

Figure 52: Hydrocarbon product selectivity in M85 Measured in 2019

Sample treated with methane (M85) was also analyzed on its yields and selectivity. Results were shown in figure 52. Total conversion and chain scission were both higher than samples irradiated with helium. Chain growth products were the lowest among all three samples. Therefore the selectivity was the highest. A high as 72% of the products were lights and survived the aging process. Also the total yield for lights was significantly (1.8x) higher, 4.4 molecules/100ev for M85 and 2.4 and 0.5 molecules/100 eV for the high and low temperature helium processing respectively. The M85 was not measured in 2016.

Product selectivity from this research is different from those found in literature. Results here indicated that the irradiation process with given conditions favors chain scission products over chain growth products even the irradiated hydrocarbons are heavy. This could be attributed to high dose rate and the use of bubbling gas. Our dose rate is 17 kGy/s, prior irradiation in the literature is 100 times lower typically with gamma and low power sources which do not have significant sample heating. For example Milinchuk [105] reported a low dose rate source and batch processing hexadecane in condensed state without any thermal control. Yields of light products in that process were 0.69

molecules/100eV, much lower than 2.4 or 4.4 molecules/100eV in our process. Yield of heavy products were 1.5 molecules/100eV, higher than 1.3 or 0.8 molecules/100eV in our process.

Sample M85 had the highest yields of chain scission products (4.4 molecules/100eV) and lowest yields of chain growth products (0.8 molecules/100eV). This feature might be due to a special property of methane under electron beam irradiation. Methane upon irradiation can produce very reactive species such as methyl (CH_3) and other radicals (CH_2 and CH). They will attack the alkane molecules and trigger chain reactions.

8.1.8 Conclusions of Irradiation of Mineral oil

Mineral oil was irradiated with the same electron beam under the continuous flow system at constant processing temperature. Conversion of reactants were on the order of 7%-12% at 350-500 kJ/kg. These overall yields are comparable to the literature. The selectivity to lights is higher than the literature. For helium gas processing at higher temperature had more stable light products, higher selectivity to light products, and a higher yield. Methane gas bubbling processing conditions lead to even more stable light products, higher selectivity to light products, and higher yield than the high temperature helium case. The better results with methane are likely due to the possibility for methane reactivity (e.g. hydrogen and methyl donors) compared to inert helium. These improvements compared to the literature are likely due to the gas addition and high dose rate, although there were other uncontrolled variables in comparing to the literature.

Comparing the results from irradiating mineral oils to those from irradiating crude oils, we are able to learn a few important things: first, high conversions was able to be achieved by irradiating oils with relatively low SEI; high conversion to light products was also achievable by irradiating heavy oils; ebeam is more effective to convert a certain type of heavy oils; ebeam irradiation method for heavy oils is very selective in terms of creating light products. Under the same system with similar SEI, conversion difference from irradiating mineral oil and two crude oils was resulted from the properties of the oil. Keep that in mind we could explore in details what exactly caused the difference. Mineral oil is a mixture of saturated alkanes and cycloalkanes distributed in the range of C15-C25 by boiling point. It has very low conductivity. Its density and viscosity are also lower than that of two crudes. Two crudes are a mixture of hydrocarbons and non-hydrocarbons (sulfur and metals) with extremely high concentration of asphaltene (7-8%) and aromatics. Significant differences between mineral oil and crudes could be attributed to physical properties (density, viscosity and conductively, et. al) and chemical properties (chemical composition and concentration of certain species). It seems that difference on physical properties between them is less dramatic than that of chemical properties. We believe that the primary factor that determine the irradiation results of heavy oils is its chemical composition and concentration of different compounds, which also has been reported in literature. In the next chapter, we irradiated eight different hydrocarbons and study their response under high energy ebeam. Conversion, yields and product selectivity were addressed and results were compared to those obtained from irradiation of crudes and mineral oil.

8.2 Irradiation of Pure Hydrocarbons with Different Structure

Before we introduce the experiment results, it is essential to point out a few points on how we select irradiating materials and what the selection rule is. Keep in mind that there are hundreds of type of hydrocarbons that could vary its property in multiple directions, for example, the type of chemical bonds that form the molecules and the physical size of the molecule such as length or radius of the molecules. Those are the most basic information that determines the physical and chemical property of a molecule. Undoubtedly, radiation responses of hydrocarbons will depend on those information. However it is impossible to study the effect of every single piece of physiochemical property of those hydrocarbons on their radiation responses. Therefore it is important to select parameters that exert the most significant influence on irradiation process. Those parameters need to be fundamental and are independent of hydrocarbons so that they could be used to completely characterize them. One of those parameters is the H/C value which has been used as a primary parameter to characterize crude oil samples. Low H/C ratio usually indicates a low value of crude oil and high refining cost. H/C values vary between 1 and 3 for most hydrocarbons. Alkanes which are saturated hydrocarbons have an H/C value larger than 2. Olefins that have unsaturated carbon bonds possess an H/C value slightly lower than 2 depending on the number of unsaturated bonds. Aromatics which are present in most of heavy crude oils have the lowest H/C values, e.g. H/C for benzene is 1. Both crude oils A and B have very low H/C ratio in the range of 1.47-1.48. In this

dissertation we proposed a similar parameter that could be more universally used to characterize different hydrocarbons. It is the saturation degree and could be calculated by:

$$satuDe = {(\frac{H}{C})_{real}} \Big/ {(\frac{H}{C})_{saturated}}$$

Saturation degree indicates the deficiency of hydrocarbon inside a molecules and have been used in chemistry field. It varies in the range of 0-1. Difference here is that we only consider carbon and hydrogen ignoring other atoms such as nitrogen, oxygen and halogen elements. It is very closely related to H/C values. Figure 53 shows a map of hydrocarbons with different H/C and satuDe values. H/C and satuDe have the same trend as the molecules grow in size. Three groups can be classified based on their values which separates alkanes, alkenes and aromatics. SatuDe values for saturated alkanes (group 1) is equal to 1. Group 2 includes alkenes and saturated alkanes with ring structures. Their satuDe values vary between 0.7-0.9. Group 3 are represented by benzene and toluene which are unsaturated hydrocarbons with ring structure. SatuDe values for them are in the range of 0.3-0.5. Note that satuDe value depends on the number of rings and side chains on the ring, for example, Tetralin has higher satuDe values than benzene and toluene because it has another saturated ring besides the benzene ring; ethylbenzene has higher satuDe value because it has a ethyl group attached to the benzene ring.

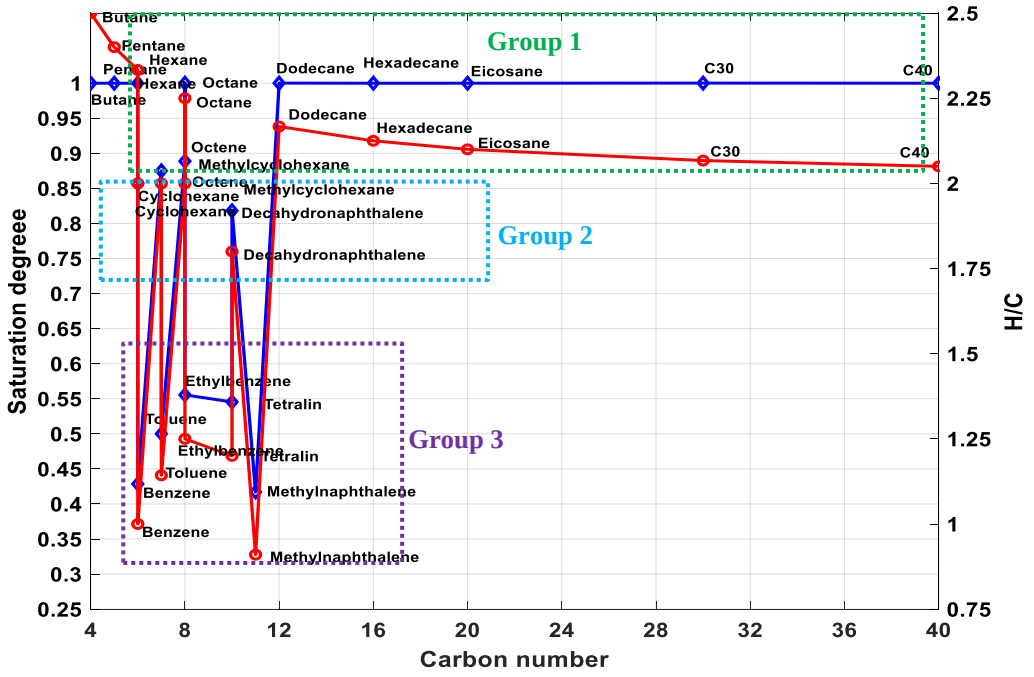

Figure 53: Saturation degree and H/C for multiple hydrocarbon compounds

One difference between H/C and satuDe on characterizing alkanes is that H/C value changes with molecular size and keeps decreasing as the molecules become larger, while satuDe remains constant. Molecular size is an important parameter when irradiating large hydrocarbons such as polymers[78,161].

The other parameter we selected is the average bond energy of all bonds (C-H, C-C and C=C) within one molecule:

$$E_{bond} = {}^{E_{total}}/_{N_{Bonds}}$$

Where E_{total} is the total energy of all bonds within a molecule and N_{Bonds} is the number of bonds. Chemical bonds form the basic structure of hydrocarbon molecules. Any chemical reaction involves at least one bond breakage or formation. In order to initiate a

chemical reaction either a thermal method or non-thermal method (radiation and non-thermal plasma method) could be used. Specifically for hydrocarbon cracking applications our goal is to break those carbon-carbon bonds. Conceptually, for a hydrocarbon molecule that has a certain number of carbon atoms, its stability should depend on its chemical bond strength which is represented by the bond energy. Reasonable to assume that more chemical bonds with small bond energy will favor the bond breakage. On the other hand, less chemical bonds with larger bond energy will make the molecule more stable under the same conditions. Similarly different type of hydrocarbons could be mapped out on a E_{bond} vs carbon number plot. Figure 54 shows three groups of hydrocarbons with their average bond energy. Typically average bond energy for straight alkanes is in the range of 390-400 kJ/mol. Olefins have slightly higher bond energy which might be in the range of 395-410 kJ/mol. Aromatics have the highest bond energy in the range of 410-440 kJ/mol. Note bond energy between group 1 and 2 might overlap due to the effect of molecule size since increasing the size of molecules in group 1 is able to reduce its bond energy that matches that of a molecule in group 2.

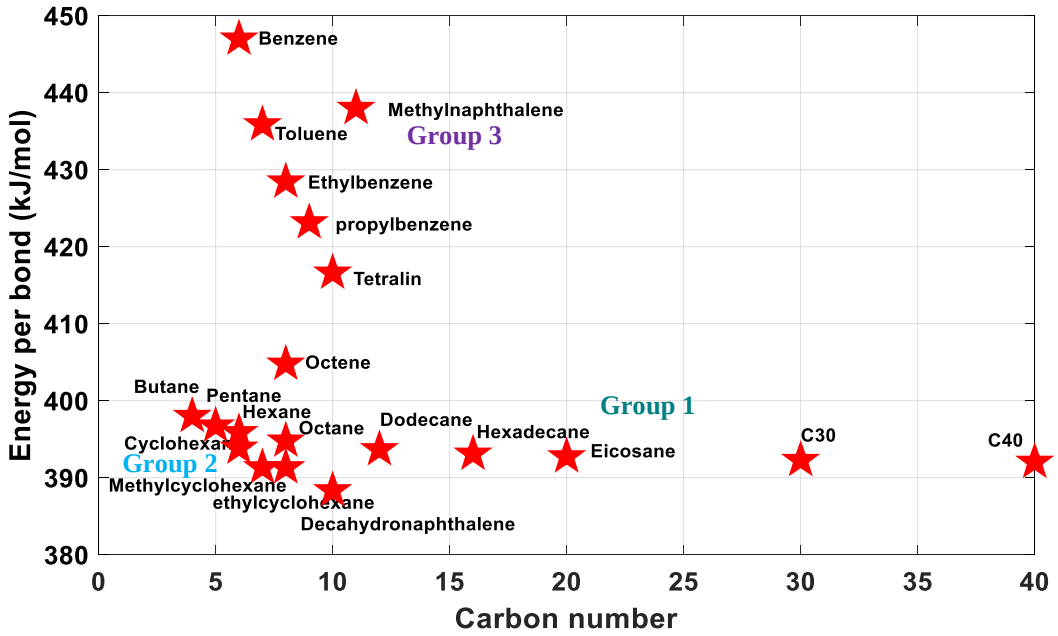

Figure 54: Average bond energy of multiple hydrocarbon compounds

Effect of saturation degree of a hydrocarbon molecule on its bond change behavior was explained by its mass spectrum under electron beams. Figure 55 represents the mass spectrum pattern of hydrocarbons with different saturation degree. In particular only fragments that are smaller than the original molecule was investigated. Then the total number of fragments was normalized by the total number of carbon-carbon bonds. Each group of hydrocarbons has a very distinctive mass spectrum pattern. Group 1 which represents straight alkanes has very high fragment number, but this number decreases very rapidly as the molecule size increases. Group 2 which is saturated alkanes with rings also shows high fragments number and this number decreases with an increased size of molecule. Group 3 shows the lowest tendency towards fragmentation with very fragment

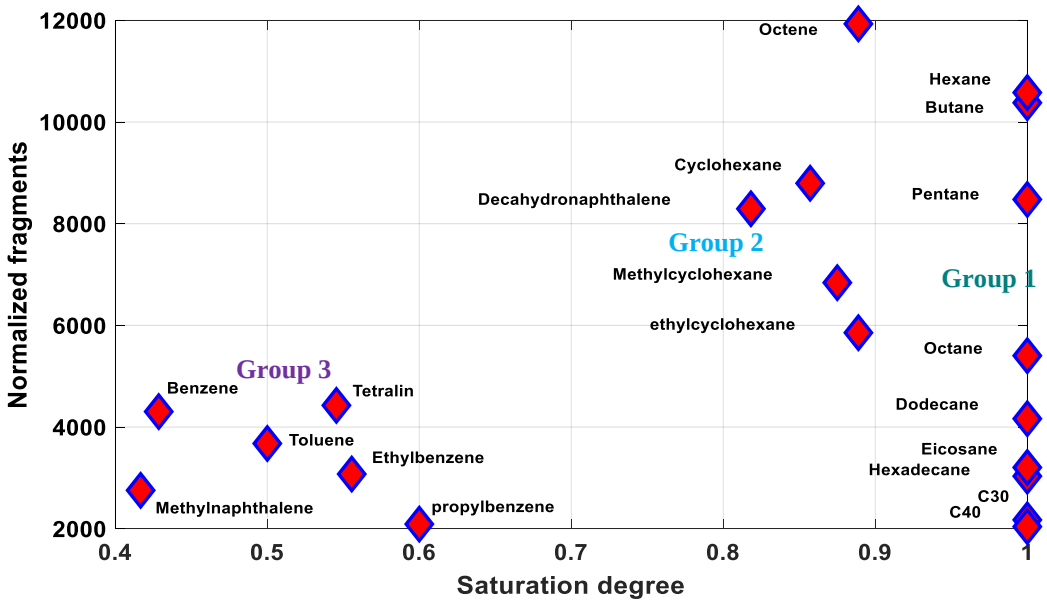

Figure 55: Normalized fragments dependence on saturation degree

number. Its saturation degree is only half of that of group 1 and 2. The number of fragments is also close to half of the fragments in group 1 and 2. Again increasing the size of a molecule mitigate its fragmentation property. For example adding branches (methyl, ethyl and propyl) on benzene molecule to form toluene, ethylbenzene and propylbenzene all reduced the fragments number.

Size of a molecules in terms of its carbon number was varied in group 1 in order to study its effect on fragmentation property. Results in figure 56 clearly showed that the number of fragments exponentially decayed as the molecular size increases. A two term exponential curve was used to fit the real results with 95% as the R^2 value. This is a counter intuitive phenomenon. When alkane molecules of larger size collides with high energy electrons, the chance of fragmenting the molecules should be higher due to a larger number

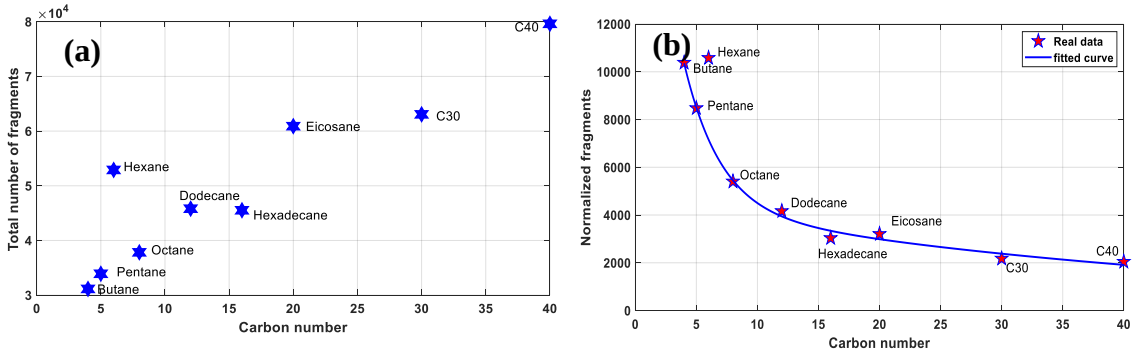

Figure 56: Total number (a) of fragments and normalized fragments (b) change with carbon number

of bonds on the molecule where fragmentation might happen. This may still be true and the abstract number of fragments when increases, it should also increase its susceptibility. But large hydrocarbon molecules also possess more energy states that allow them to absorb and store more energy without causing any bond breakage.

Despite saturation degree, average bond energy and molecular size, parameters such as geometry of the molecule may also play significant roles in irradiation of hydrocarbons[162]. Those parameters are part of the molecule properties and are considered intrinsic. There are external parameters that exert huge influence on radiation responses of those molecules. Parameters such as irradiation temperature and number density may completely change the radiation responses and cause significant deviation if those parameters are not controlled well. Since the goal of this chapter is to study the influence of intrinsic parameters, all external parameters remained the same for all samples.

Hydrocarbon samples were selected to represent saturated alkanes, alkanes with ring structure, aromatics, aromatics with branch of different length and polyaromatics. Three groups were classified based on their saturation degree (SatuDe). Saturation degree

of hydrocarbons indicates the hydrogen deficiency of a hydrocarbon inside its molecule and have been widely used in chemistry field. It affects the physicochemical properties of a molecule such as its molecular geometry, average chemical bond strength as well as electron density distribution. It varies in the range of 0-1. For example, SatuDe values for saturated alkanes (group 1) is equal to 1. Group 2 which includes alkenes and saturated alkanes with ring structures has a SatuDe values between 0.7-0.9. Group 3 are represented by benzene and toluene which are aromatics hydrocarbons. SatuDe values for them are in the range of 0.3-0.5. Effect of saturation degree (SatuDe) of a hydrocarbon molecule on its stability under high energy electron beam irradiation was studied. Before experiments, each sample was loaded into a new reactor at liquid state and sealed with argon to isolate air. During experiments, specific energy input (SEI) to all samples was controlled by controlling the irradiation time. SEI was estimated in the range of 350-450 kJ/kg. Both temperature and pressure inside the reactor were monitored remotely. Mass balance after experiment was conducted for all samples. Irradiated samples were analyzed by a series of techniques including thermal gravimetric (TG), GC-FID and GC-MS. Conversion, yields and product selectivity were estimated by those techniques and results were compared between each other based on the satuDe value.

Those samples are Cyclohexane, Methyl cyclohexane, Ethylbenzene, Tetralin, Toluene, Benzene and Methylnaphthalene. All were purchased from Sigma-Aldrich with more than 99% purity. Boiling point and chemical formula of all samples were shown in table 21.

Table 21: Boiling Point and Chemical Formula of Irradiated Samples

Samples	Pentane	Cyclohexane	Methylcyclohexane	Ethylbenzene	Tetralin	Toluene	Benzene	Methylnaphthalene
BP (ºC)	36	81	101	136	207	111	80	242
Chemical formula	C_5H_{12}	C_6H_{12}	C_7H_{14}	C_8H_{10}	$C_{10}H_{12}$	C_7H_8	C_6H_6	$C_{11}H_{10}$

H/C values and carbon bond numbers for all samples were shown in figure 57. Values of H/C decrease from 2 (cyclohexane and Methylcyclohexane) to 0.9 (methylnaphthalene). Because samples were selected based on H/C values, there are no samples that have identical H/C value. Carbon bond number changes when a branch was added to a ring hydrocarbon, e.g. Cyclohexane vs Methylcyclohexane and Benzene vs Toluene vs Ethylbenzene. So the effect of different branches on molecule radiation response will be studied.

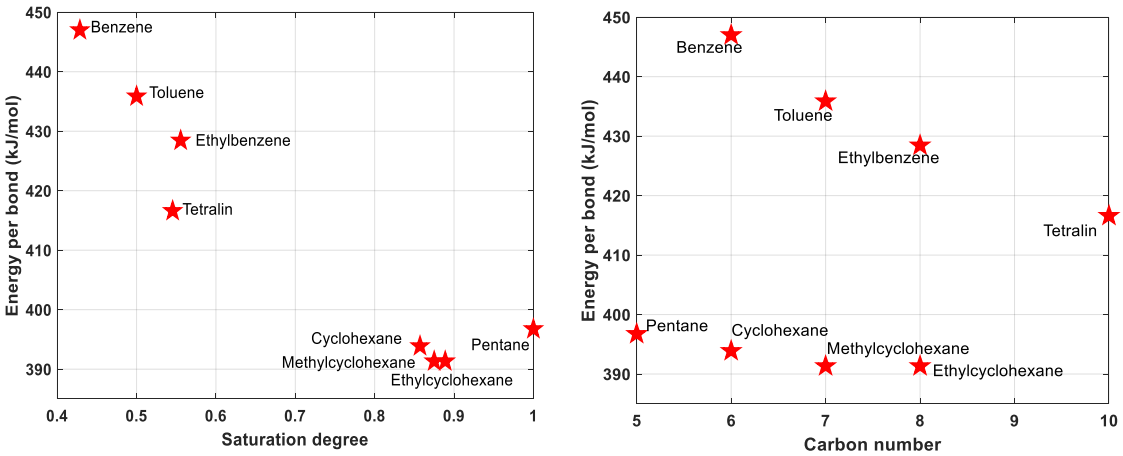

Figure 57: Saturation degree and average bond energy of irradiated hydrocarbons and their relationship

8.2.1 Experimental Method and Setup

Experiments were conducted with the setup shown below in figure 58. The reactor was made of ½ inch aluminum tubes with thin wall. The length of the tube is the same as the beam length which is 20 inches. Tube was sealed with a ball valve on one side and a pressure relief valve on the other side. One pressure gage was used to ensure a better sealing quality of the system. Before the ebeam test, pressure check was performed with argon gas and system was able to hold the pressure at 45 psi for more than ten hours. Pressure relief values setting point was 50 psi. After pentane samples was loaded into the reaction tube, trapped air needs to be removed from the system in order to avoid any flame or explosion caused by air-hydrocarbon reactions. To achieve this, argon was used to purge the system and after the purge trapped air concentration was below 0.01%. System was first pressurize by argon to 45 psi, then release the pressure to 5 psi and close the ball valve. This was repeated five times. Reactor with sample was weighed before and after the test.

Since samples needs to be irradiated at a condensed states for better results. This was achieved by irradiating the sample at low temperature to prevent phase change and pressure increase. Ice water bath was used to provide the desired cooling on the reactor. Ice water bath was inside a stainless steel container and a water pump helped move the water to increase the heat transfer coefficient. During the irradiation experiment, reactor was submerged into the ice water bath. Specific energy input (SEI) was also controlled by controlling the irradiation time. Only low (SEI) is the interest of this research to maximize the economic viability of this process. Characterizations techniques such as GC-

FID, GC-MS, FTIR and TGA will be used to study the irradiation effect. Mass balance was performed to determine the experiment uncertainly.

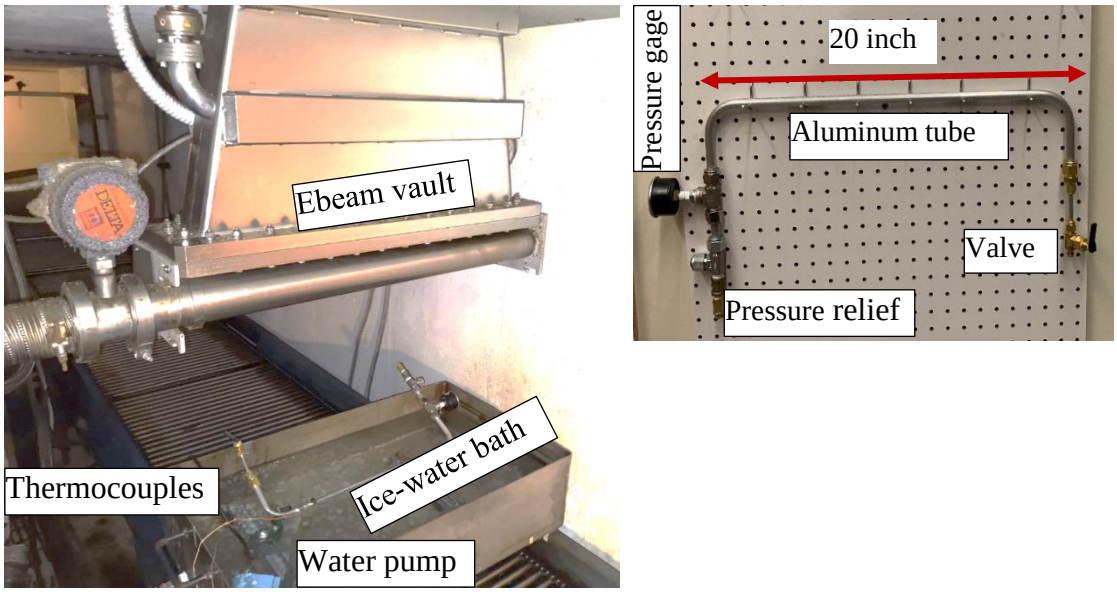

Figure 58: Setup for batch processing of pure hydrocarbons

Table 22 showed the irradiation parameters for all samples including irradiation time, dose rate and specific energy input. Because experimental setup is exactly the same for all samples and experiments were conducted at the same location under the beam, dose rate was identical. Dose (SEI) only depends on the irradiation time which was controlled by the beam operator. Irradiation time was in the range of 112-115 seconds, which indicates a dose range of 538-552 kJ/kg. Hydrocarbon samples were sealed inside an aluminum tube with a wall thickness about 1.5 mm. Cooling water was flowing on the

wall of the tube in order to maintain a low temperature on the reactor. High speed electrons had to penetrate both the aluminum and water before contacting the sample. Part of the ebeam energy was lost because of this. Real SEI of the sample had to compensate the loss due to this geometry. We estimated the SEI loss is about 10% because of 1.5 aluminum wall and 2 mm water stream.

Table 22: Experimental Parameters of Irradiation of Multiple Hydrocarbons

Samples	Measured dose rate (kGy/s)	Irradiation time (s)	Total SEI (kJ/kg)	Corrected SEI (kJ/kg)
Pentane	4.8	112	537.6	483.8
Methylcyclohexane	4.8	115	552.0	496.8
Cyclohexane	4.8	112	537.6	483.8
Ethylbenzene	4.8	113	542.4	488.2
Tetralin	4.8	114	547.2	492.5
Toluene	4.8	111	532.8	479.5
Benzene	4.8	110	528.0	475.2
Methylnaphthalene	4.8	110	528.0	475.2

8.2.2 Processing Temperature

Temperatures were measured from two locations to increase accuracy and reliability. One was in water and the other on the reactor wall. Temperature profiles were shown in figure 59 for all samples. Temperatures were able to be read and written in this high radiation identity environment except significant noise was recorded on both signals.

Overall samples were irradiated in the temperature range of 5 to 20 ^{o}C. This temperature range is below the boiling temperatures of all samples among which cyclohexane has the lowest boiling point (80 ^{o}C). It indicates that irradiation of samples occurred at liquid state with high number density.

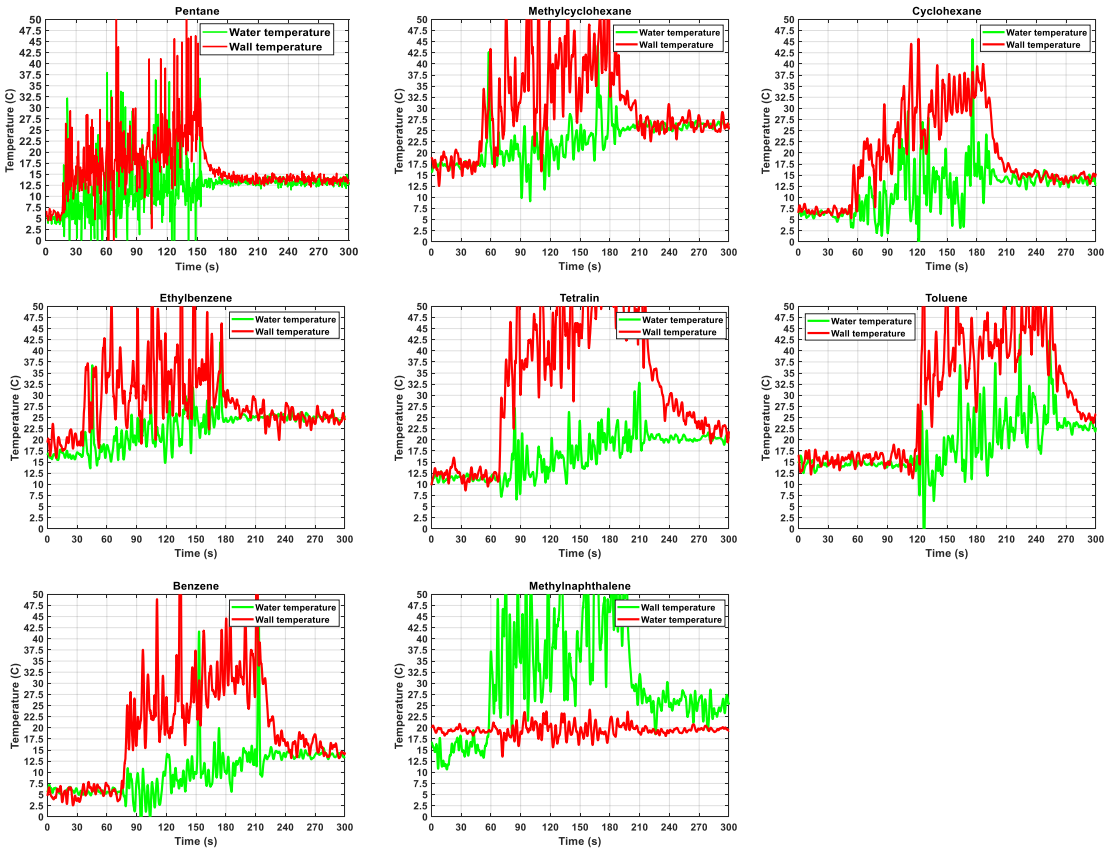

Figure 59: Temperature profiles for irradiation of all samples: green is reactor wall temperature; red is cooling water temperature

8.2.3 Mass Balance

Mass balance after tests was calculated for all samples and reported in table 23. Here mass balance results only shown the weight change from the sample and assume the weight of the reactor is constant. Weight of loaded reactor before and after irradiation was compared to calculate the mass loss. Mass loss could be due to two reasons. One is associated with the gaseous products from irradiating the sample. Gaseous species including hydrogen, methane, ethane and other small hydrocarbon molecules are common products from irradiating organic materials[116,117,134,163]. The other way to loss mass is due to evaporation of samples. Both the gaseous species and vapors were not collected or analyzed by either GC-FID or TGA but they are considered light products of the irradiation process. Liquid products were collected from the reactor and stored in glass jars. This dissertation research only focuses on characterizing irradiated liquid products and left the analysis of gaseous species for future work.

Table 23: Experimental Parameters for Irradiating all Hydrocarbon Samples

Samples	Treated mass (g)	Mass left (g)	Mass left percentage	Mass loss percentage	SEI corrected Mass loss
Pentane	16.00	15.73	98.31%	1.69%	1.69%
Methylcyclohexane	18.02	17.69	98.17%	1.93%	1.52%
Cyclohexane	17.58	17.22	97.95%	2.05%	1.72%
Ethylbenzene	18.79	18.58	98.88%	1.12%	0.84%
Tetralin	23.70	23.64	99.75%	0.25%	0.17%
Toluene	21.22	21.25	100.14%	-0.14%	0
Benzene	17.03	17.05	100.12%	-0.12%	0
Methylnaphthalene	28.34	28.2	99.51%	0.49%	0.32

Mass balance for all samples should be in the range of 100±0.5% if no species was lost. Figure 60 includes all mass balance results. Mass balance of first three samples including pentane, Methylcyclohexane and cyclohexane was significantly lower than 100%. It indicates that gaseous products have been produced with those three samples. It is also predicted that irradiation of straight alkanes, and saturated ring hydrocarbons gives higher yields of products. In particular, straight alkanes which have the highest H/C values, are the most reactive hydrocarbons under high energy irradiation. Compared to the first three samples, the rest of samples are different because they all have at least one unsaturated ring. More importantly, the H/C values of those samples are lower. Better mass balance were observed on them. It indicates that they are more stable under radiation or at least they are less prone to produce gaseous products. Mass balance results were correlated with saturation degree and average bond energy for all samples and shown in figure.

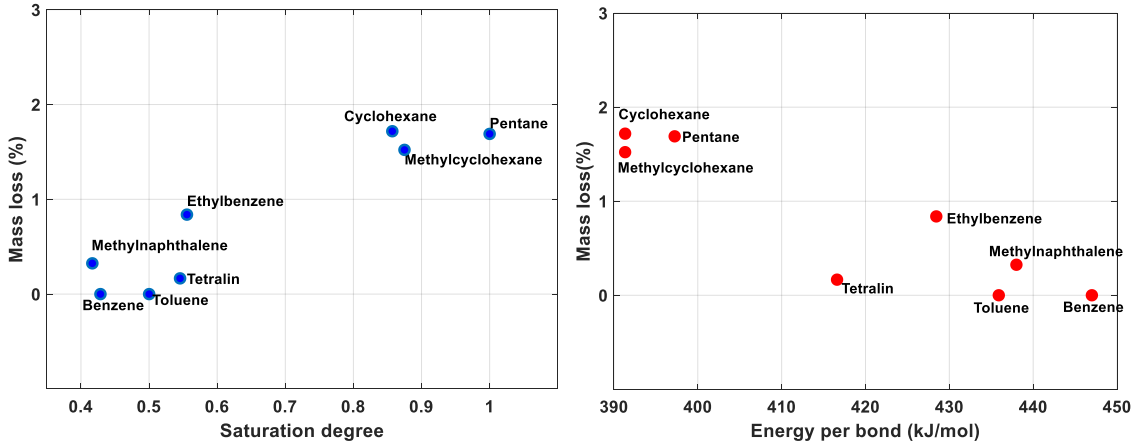

Figure 60: Mass loss during the irradiation process as a function of saturation degree

8.2.4 Color Change

Color change is another important indicator of hydrocarbons chemistry under high energy radiation and the radiation products. Figure 61 shows the color change before and after the radiation. All treated samples were referenced to an untreated sample (left) which is clear and transparent. Yellowness of those samples were analyzed by reading RGB on the photo of a sample under standard light conditions. Pentane did not show any change on its color after irradiation. All other samples shown increased yellowness after the irradiation. There is a close correlation between yellowness and H/C values from different molecular structure.

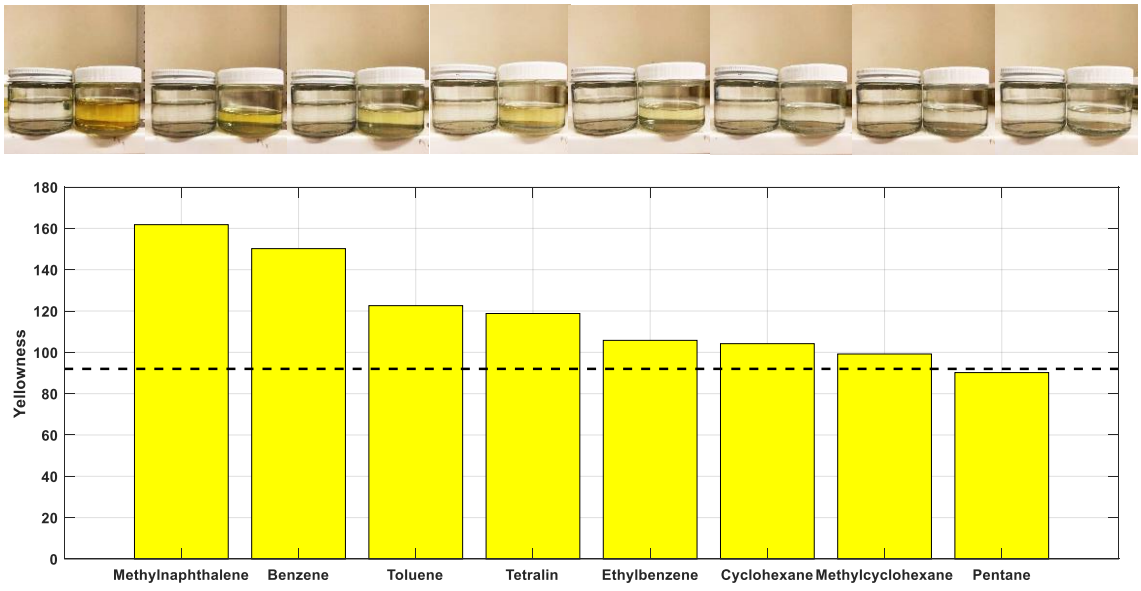

Figure 61: Color change of irradiated pure hydrocarbon samples

Yellowness of treated samples as a function of H/C values was plotted in figure 62. Yellowness is strongly bonded with the H/C values and keeps increasing when H/C value decreases from pentane, which represents saturated straight alkanes to methylnaphthalene, which represents hydrocarbons with unsaturated rings. It is worth noting that Methylcyclohexane and cyclohexane have the same H/C values but yellowness of Methylcyclohexane is lower than that of cyclohexane. This demonstrates the effect of a methyl branch on the molecule radiation stability. Theoretically the existence of a methyl group will make the hydrocarbon more susceptible to electron beam irradiation, because ethyl group is more reactive than methyl group under radiation. Results here are consistent with the theory. Similar trend was observed by comparing ethylbenzene, toluene and benzene. Ethylbenzene has an ethyl group which is longer than a methyl group and it shows lower yellowness. Another important result from the color detection is that Tetralin, which comprises one benzene ring and one saturated ring, shows less color change than that of methylnaphthalene, which has two unsaturated benzene rings and a methyl branch. Even though the methyl branch will make the molecule more susceptible to electron beam, but the effect was overturned by existence of a benzene ring. Benzene and cyclohexane has similar structure, but benzene shows much higher color change because of low H/C. The number of rings was also studied by comparing benzene and methylnaphthalene. It seems that higher number of unsaturated rings tend to change color more.

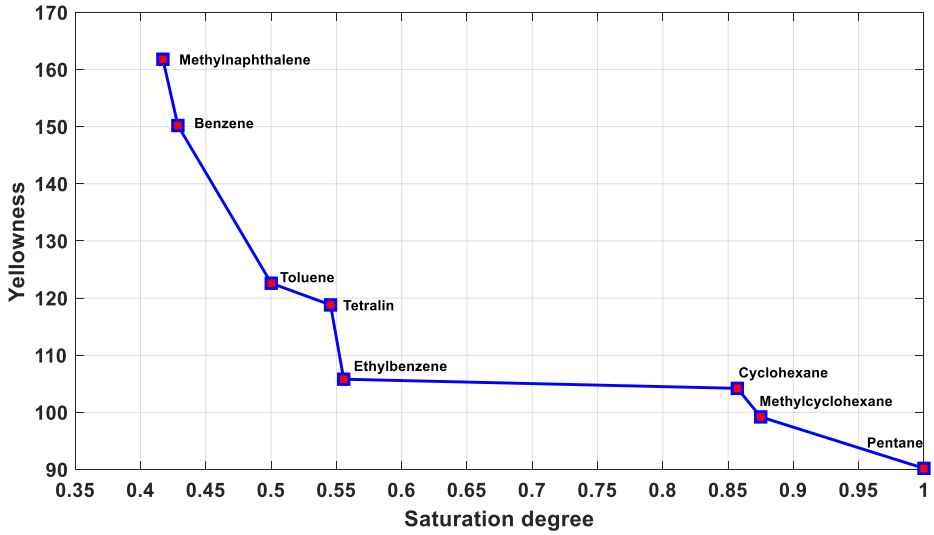

Figure 62: Yellowness as a function of saturation degree

8.2.5 GC-FID Analysis

Compounds change induced by high energy ebeam in all irradiated samples was studied by using GC-FID. Three figures for each sample were constructed to study the ebeam induced change and shown in figure 63. The first figure (a) included the raw GC-FID signals for both the original and irradiated compounds. The second figure (b) was integrated signal of the raw signal that represents a compound boiling curve. The third curve (c) showed the difference between the two boiling curves of raw sample and irradiated sample at different time.

GC-FID signals of irradiated pentane showed two important changes compared to the raw sample signal. Treated sample signal had at least three more distinguishable peaks after the primary peak corresponding to pentane compound. First two of those three peaks appeared at 0.74 min and 0.82 min, respectively, while pentane peak was at 0.65 min. The

retention time difference between them leads us to believe that those two peaks belong to pentane dimer and trimer products. The third peak occupied almost one minute in a range of 0.95-1.85 min. The width of a peak is a direct indicator of the concentration of the corresponded compound. The boiling-off curve of irradiated pentane shown that only 95% of the total mass was recovery after 0.72 minutes compared to 100% recovery of raw pentane. This demonstrates that there are about 5% hydrocarbons species that are heavier than pentane and are still in GC column. The other important change on the irradiated sample signal is its faster recovery before 0.72 min by about 4%. This indicates the existence of hydrocarbons that are lighter than pentane. That's why they showed up earlier on the GC signal. Because of the low pressure setup and relatively high processing temperature, it is impossible to trap hydrocarbons smaller than butane. Therefore the light hydrocarbons produced from irradiating pentane might be branched species such as iso-pentane. The third figure for pentane showed conversion to both light hydrocarbons and heavy hydrocarbons. It also showed the total reduction of raw pentane due to ebeam irradiation. About 8.5% of pentane was conversed to new hydrocarbon products. Among those products, 4.2% of them are light species and the rest of them are heavy species including dimers and trimers.

GC-FID signals of irradiated Methylcyclohexane clearly showed that there was a new peak from the irradiated sample at about 7.75 min. Because its retention time was much longer than that of raw Methylcyclohexane, This peak might be contributed to a dimer or trimer product of the Methylcyclohexane compound, but more molecular information is required to more accurately identify it. Boiling-off curve of the raw and irradiated sample

showed significant difference. The total mass of irradiated sample was recovered slower than that of raw sample and there was about 2% of the total mass in irradiated sample that could not be recovered before 20 min. This amount of mass was due to heavy compounds in the irradiated sample. Conversion plot show that more than 2% of Methylcyclohexane was converted to heavy compounds due to ebeam irradiation.

Irradiation of cyclohexane caused a similar change to the hydrocarbon compounds as Methylcyclohexane. New peaks were found on the GC curve after raw compound peak, which indicates that those new compounds are larger molecules such as dimers and trimers. Compared to Methylcyclohexane irradiation, which only produced significant amount of dimers, irradiation of cyclohexane produced both the dimer and trimer products which are labeled on near the peaks. This difference might be caused by the methyl group because all other conditions are identical. Boiling-off curve showed that mass recovery of irradiated sample was less than that of raw sample due to those heavy compounds. There was about 3.2% of total mass in irradiated sample that could not be boiled off after the

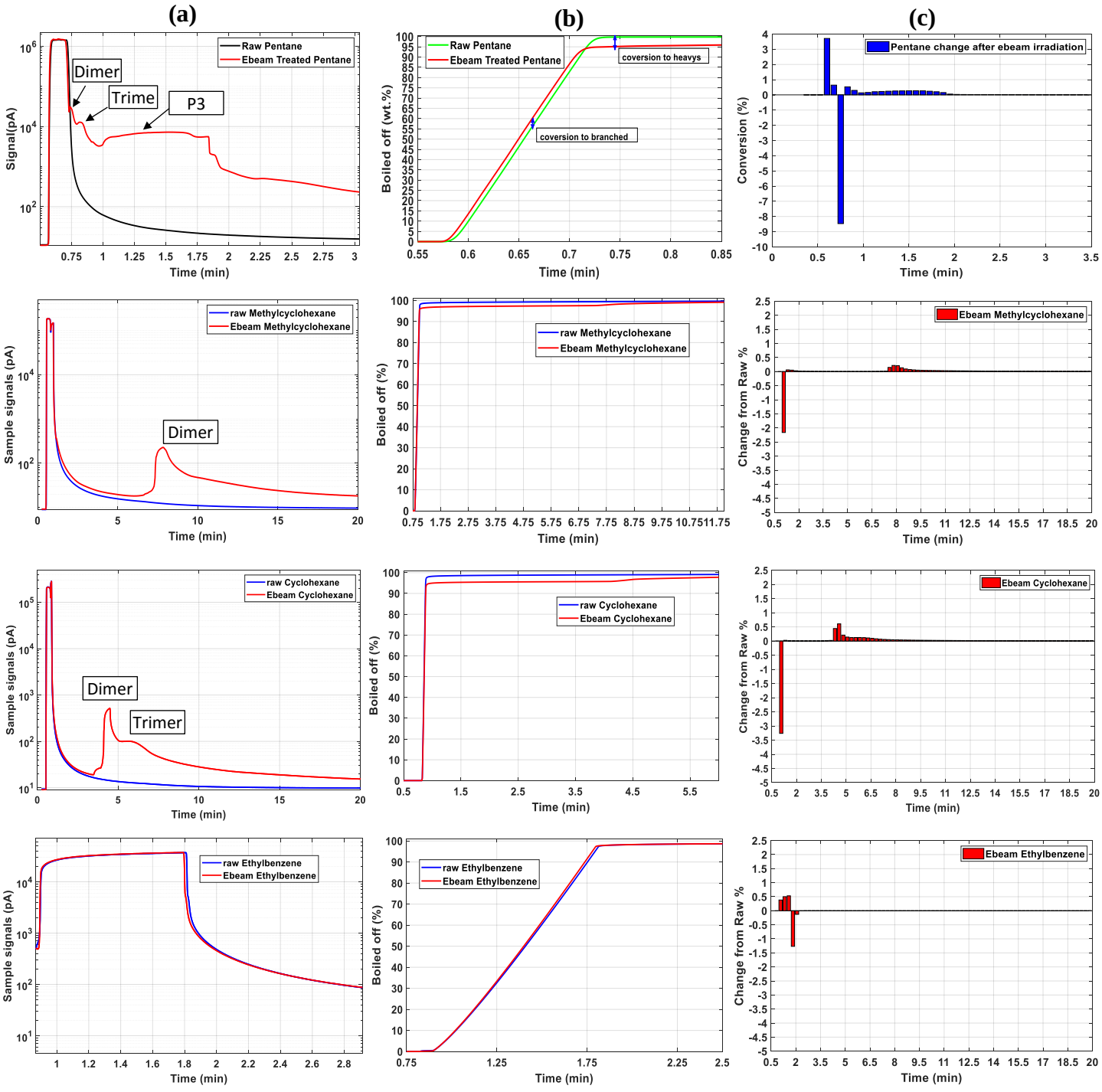

Figure 63: GC-FID analysis of Irradiated pentane, Methylcyclohexane, cyclohexane, ethylbenzene (from top to bottom): (a), raw signal, (b), Boiled-off signal, (c), conversion curve.

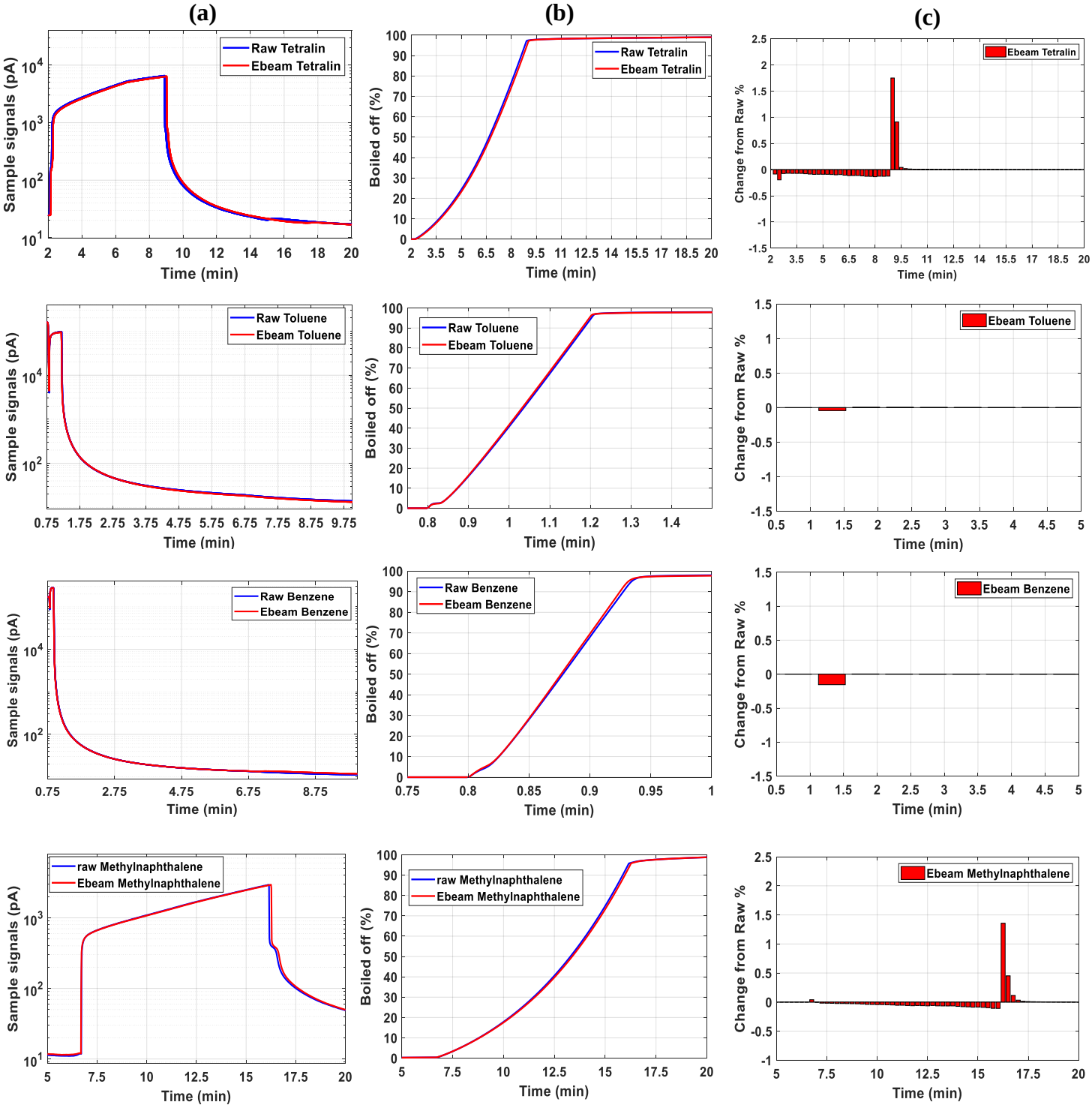

Figure 64: GC-FID analysis of Irradiated Tetralin, toluene, benzene and methylnaphthalene (from top to bottom): (a), raw signal, (b), Boiled-off signal and (c), conversion curve.

first minute. Conversion plot indicated that 3.2% of the raw cyclohexane was converted to heavy compounds by ebeam radiation. About 1.2% ethylbenzene was converted in irradiated sample by GC-FID. Ethylbenzene seems to be more stable than the previous three compounds. That might be due to its low saturation degree. GC-FID analysis was also performed on irradiated ethylbenzene, Tetralin, toluene, benzene and methylnaphthalene. Results were shown in figure 64. No significant conversions were detected except on Tetralin and methylnaphthalene, which all showed larger products due to polymerization. Overall GC-FID conversion depends on the saturation degree of each compound. Lower saturation degree makes the compound more stable and convert less to new products.

8.2.6 TG and DTG Analysis

Thermal analysis and differential thermal analysis on ebeam irradiated Methylcyclohexane, cyclohexane, ethylbenzene, Tetralin, toluene and methylnaphthalene were conducted. Results were compared between raw sample and the irradiated sample and shown in figure 65. Weight loss of irradiated Methylcyclohexane and cyclohexane are very different from those of raw samples due to the creation of new compounds. New compounds were identified as individual peaks by DTG analysis. Two peaks were found on irradiated Methylcyclohexane. The first DTG peak appeared after 5 min was attributed to Methylcyclohexane compound with a higher DTG rate. The second peak appeared slightly later than 10 min, which indicates the new compound is larger than

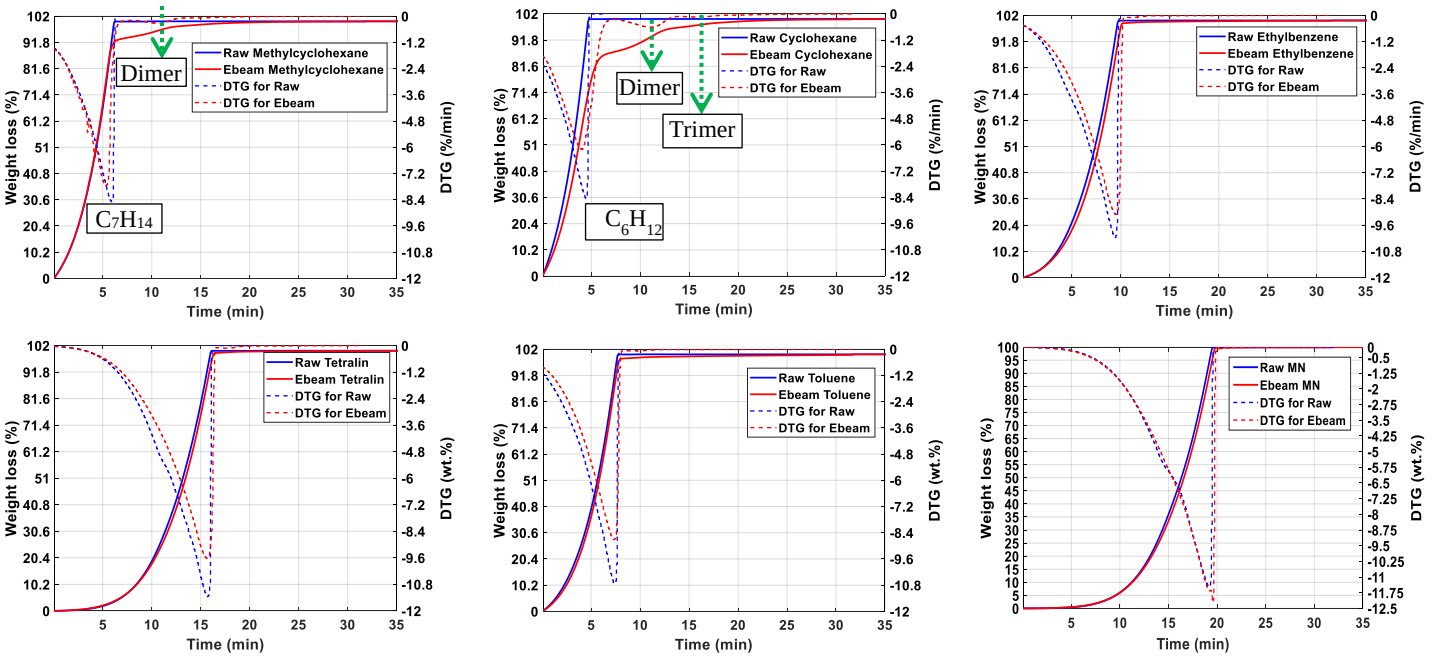

Figure 65: TG and DTG of Irradiated Methylcyclohexane, cyclohexane, ethylbenzene, Tetralin, toluene and methylnaphthalene

Methylcyclohexane molecules in terms of boiling point. Because it showed up at a time twice of that of raw Methylcyclohexane, it is reasonable to assume that this peak corresponds to a dimer product due to ebeam induced polymerization.

Three peaks were found on irradiated cyclohexane DTG curve. The first peak appeared at 4 min and represents a cyclohexane compound. The second and third peak are not present on raw sample DTG curve and represent new compounds. They showed up at 11.6 min and 16 min. We believe those two compounds are dimer and trimer products, respectively. The dimer and trimer products have lower DTG values compared to the original compound because of their low concentration in the irradiated samples. On contrary, ebeam irradiated ethylbenzene did not show significant change on both the TG

and DTG curves or the difference was below the thermal analysis detection limit. This demonstrated a higher molecular stability of ethylbenzene compound under high energy ebeam radiation.

TG and DTG analysis were also conducted on Tetralin, Toluene and methylnaphthalene to study ebeam effect on those compounds. TG curves of irradiated Tetralin and toluene samples are slightly lower than that of raw samples indicating that there were heavier species in irradiated samples. DTG peaks of Tetralin and toluene compound in irradiated samples were lower than those of raw compounds. But there was no additional peaks on the DTG curves from both compounds due to low concentration of new species. The TG and DTG curves of irradiated methylnaphthalene are almost identical with the raw sample. That provides evidence for a superior radiation stability of methylnaphthalene under high energy ebeam.

Those three compounds represent hydrocarbons with much lower saturation degree than the previous three (Methylcyclohexane, cyclohexane and ethylbenzene). Compounds with higher saturation degree are more susceptible to high energy ebeam and tend to produce more new species. It seems that hydrocarbon compound stability is very sensitive to its saturation degree under ebeam. More importantly, new compounds produced in ebeam irradiation are large molecule due to process such as polymerization or crosslinking.

Benzene was also irradiated with similar energy input by using the same setup. But samples were lost in a glass jar because of a sealing failure. Therefore we could not

Figure 66: Polymerized benzene due to ebeam irradiation after liquids all evaporated

perform thermal analysis on benzene. However, significant amount of solid product from benzene irradiation was observed on the bottom of the jar and shown in figure 66. It was a light brown color solid and accounted for 0.3% of the total mass. We believe that the product was also created through benzene polymerization induced by high energy ebeam.

8.2.7 GC-MS Analysis

GC-MS analysis were performed on the raw sample and irradiated sample. Mass spectrum corresponding to each compound was studied in details. Products in irradiated samples including isomers, dimers and trimers were identified based on the mass spectrum. GS-MS provide very useful information such as molecular structure and molecular weight for product yields and selectivity analysis. Results were shown in the next sections.

Figure 67a and b shows the GC-MS results of the original and irradiated Methylcyclohexane. Signals of irradiated sample are significantly different from that of the raw sample. Methylcyclohexane retention time was close to 2 min with two major peaks. All other peaks after 2 min are too small to be considered, which indicates a high purity of the original Methylcyclohexane sample. Signals of irradiated sample showed a few different features. More peaks were found with irradiated sample which indicates that new compounds were created in irradiated Methylcyclohexane by ebeam. Most of the new peaks are located on the GC curve between 8 and 9 min. There are a few peaks between 2 and 3 min. the peaks between 8 and 9 minutes were identified based on their mass spectrum. Most of them are Methylcyclohexane dimers that are formed through polymerization induced by ebeam. Three of those dimers with their exact molecular structure are identified as dimer 1-3. Their GC retention time was very close due to a similar chemical structure.

Baseline was subtracted on figure 65c and 65d to study only the new compounds resulted from ebeam polymerization. Area under each peak was first calculated to study its contribution to the total area of all accounted peaks. Raw sample had a few peaks that correspond to Methylcyclohexane molecules. Irradiated sample had a large number of new peaks that are formed by ebeam induced polymerization.

Area under peaks corresponding to raw compounds and new compounds are separated and compared in figure 65e. Area under Methylcyclohexane peak from raw sample contributed to almost 100% of the total area of all peaks. Whereas the contribution of area of Methylcyclohexane peak from the irradiated samples dropped to 94% and the

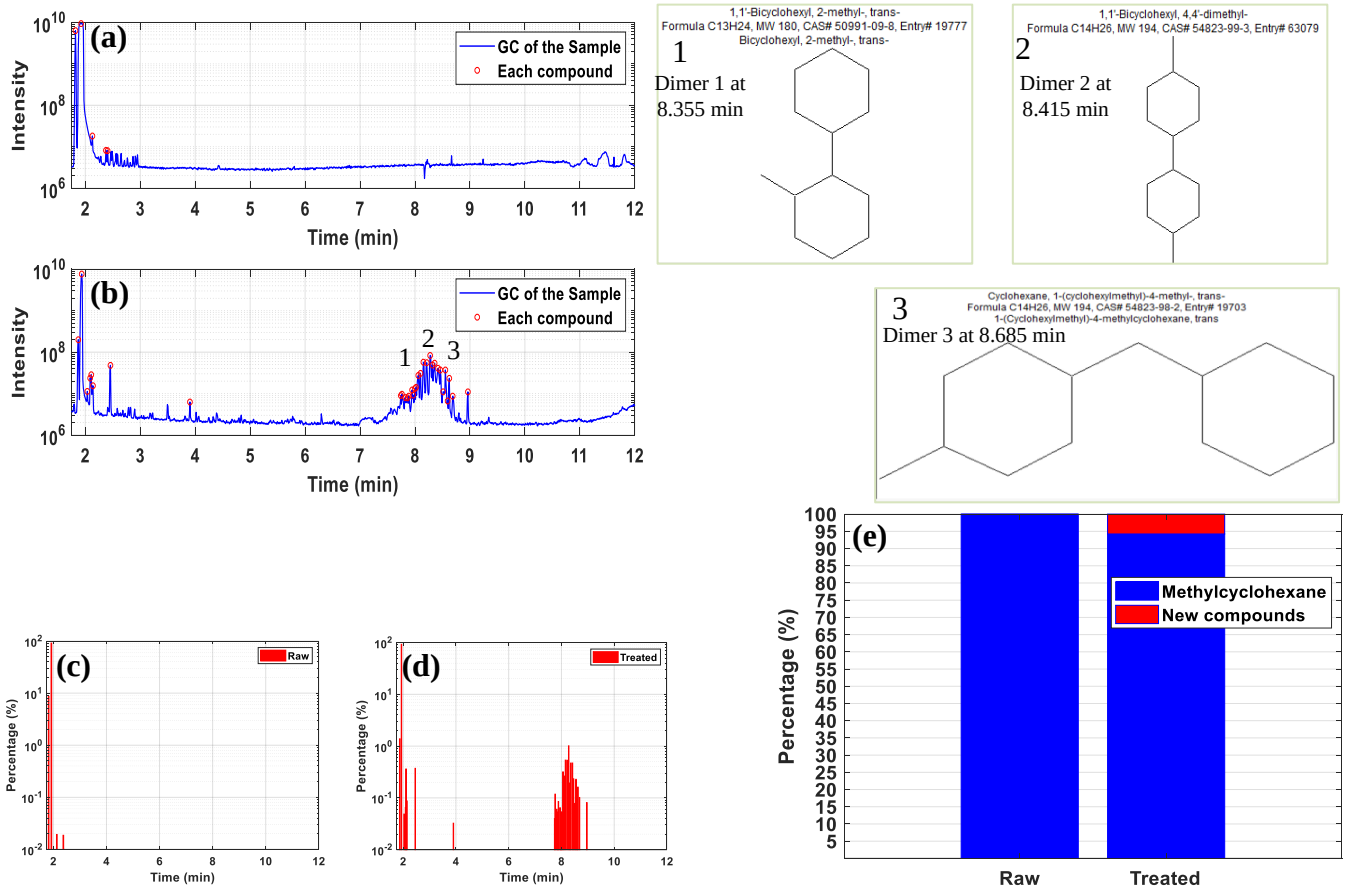

Figure 67: GC-MS analysis of irradiated Methylcyclohexane: (a), raw sample signal; (b), irradiated sample signal; (c), peak area of raw; (d), peak area of irradiated sample; (e), total area change. 1, 2 and 3 are dimer products

rest of the total area corresponds to new compounds created by ebeam. Previous analysis by GC-FID and TG have demonstrated that heavier compounds were produced by ebeam in Methylcyclohexane. GC-MS results were consistent with them. Those heavier compounds are dimers resulted from ebeam irradiation of Methylcyclohexane.

Figure 68 showed the GC-MS results of raw Cyclohexane and irradiated cyclohexane. GC signal of raw sample showed one peak at about 1.5 min which corresponds to the cyclohexane and no other peaks. GC signal of irradiated sample was

tremendously different. About 30 new peaks were identified in the range of 2-12 min. In particular the number of peaks was concentrated in the range of 7-8 min and 11-12 min. There was about 10 peaks in each of the one minute time window. Those peaks were identified based on their mass spectrum. Two of them are dimers. One is a trimer. Their molecular structure was shown in 1-4. It seems that molecule 1 was created by combining one cyclohexane molecule with another C6 molecule which is probably resulted from the ring opening of a cyclohexane molecule. Molecules 2 and 3 represent the dimer and trimer products from irradiating cyclohexane. Molecule 3 has longer retention time than that of molecule 2 because of its larger size. Molecule 4 is another trimer product that are produced by combining two cyclohexane molecules with rings and one C6 molecule without ring.

After baseline subtraction, only peaks were shown on the plot. Raw sample had only one peak corresponding to cyclohexane, while irradiated sample had more peaks corresponding to new compounds. Peak area was calculated for all peaks. Area change was compared in raw sample and irradiated sample. In raw sample, cyclohexane peak area accounts for 100% of the total area. This peak in irradiated sample, however only contributed to 75% of the total area. The other 25% of the total area was due to new compounds. Dimer products accounts for about 21% of the total area and trimer products

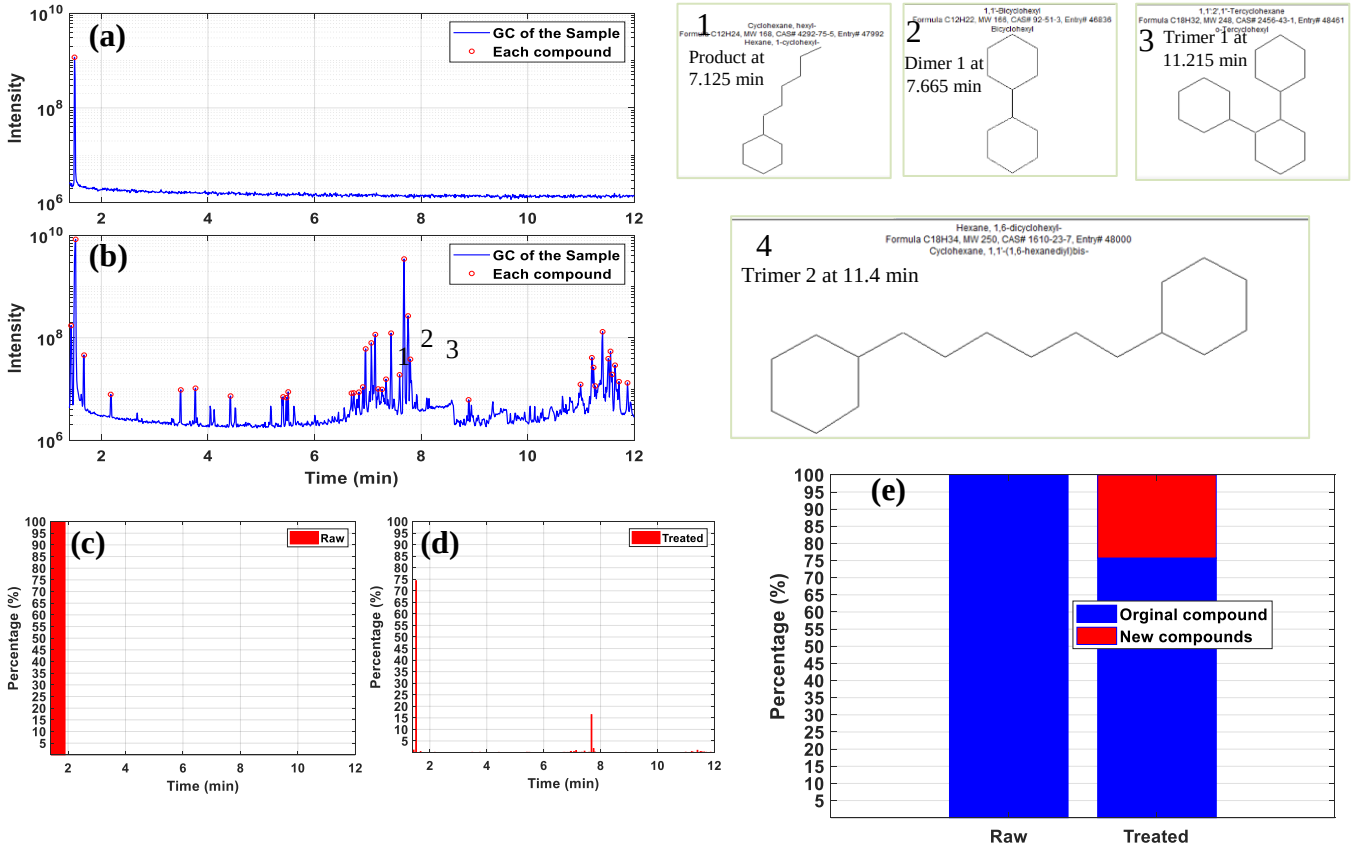

Figure 68: GC-MS analysis of irradiated cyclohexane: (a), raw sample signal; (b), irradiated sample signal; (c), peak area of raw; (d), peak area of irradiated sample; (e), total area change. 1, 2, 3 and 4 are dimer and trimer products

are responsible for 3% of the total area. Please note that there are also products in the range of 2-6 min. Those products might be resulted from the cyclohexane ring opening process. But mass spectrum data is required in order to identify them.

GC-MS analysis was conducted on raw ethylbenzene and ebeam irradiated ethylbenzene. Results were shown in figure 69. Raw ethylbenzene signal did not show any other peak except the ethylbenzene compound. But irradiated ethylbenzene showed lots of new peaks corresponding to new compounds. Ethylbenzene isomers and dimer products are found based on their mass spectrum. They are labeled as 1-4. Most dimer

products are found in the range of 9-10 min. There are a few other products in the range of 4-6 min. It seems that ethylbenzene was more stable under ebeam compared to Methylcyclohexane and cyclohexane, because less new species were found. Species resulted from opening of the benzene ring was not identified which also proves that ethylbenzene is a more stable compound under ebeam radiation.

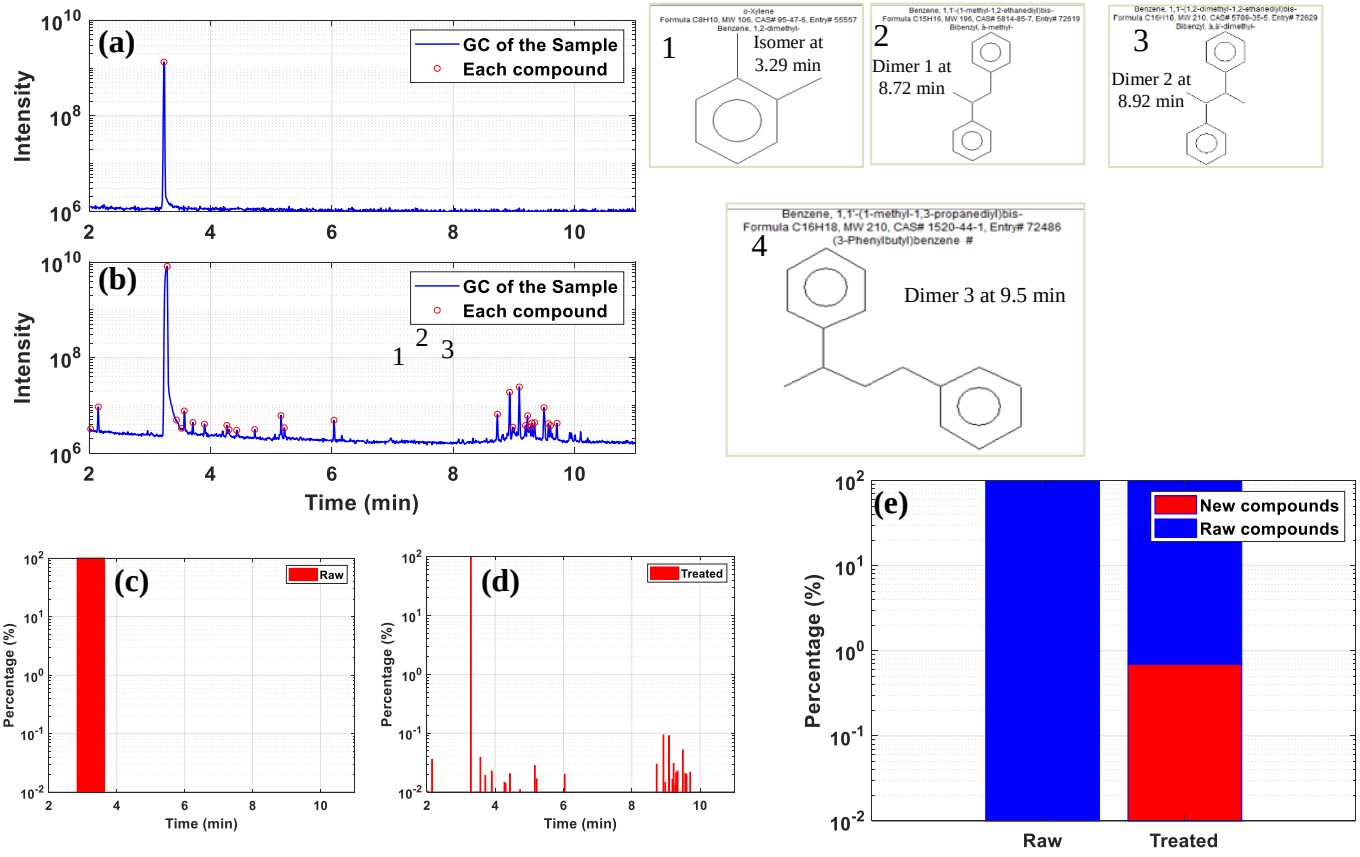

Figure 69: GC-MS analysis of irradiated ethylbenzene: (a), raw sample signal; (b), irradiated sample signal; (c), peak area of raw; (d), peak area of irradiated sample; (e), total area change. 1, 2, 3 and 4 are isomer and dimer products

Raw sample had only one peak corresponding to ethylbenzene. Irradiated sample had more peaks and those peaks are concentrated in the range of 9-10 min which are attributed to ethylbenzene dimers. Area of each peak was calculated. Ethylbenzene peak accounts for 100% of the area in raw sample. New species (isomers and dimers) created by ebeam irradiation contributed to 0.8% of the total area.

Tetralin GC-MS results were shown in figure 70 with both the raw sample and irradiated sample. Irradiated sample had more peaks in the range of 5-7 minutes. Majority of the new peaks in this range are attributed to compounds which are similar as Tetralin in their chemical structure and molecular weight, e.g. product 1 and product 2 are identified based on their exact mass spectrum. A few new peaks were also found between 12.5 and 13 min. We believe that those peaks corresponds to Tetralin dimers but more mass spectrum information is required in order to know its molecular structure. Figure 26 shows all the peaks after baseline subtraction. Raw Tetralin had four peaks in a narrow window between 5.5 and 6.2 min which are all related to the Tetralin compound. Peak area was calculated for each peak to study the product distribution in both raw and irradiated samples. Peak area at 6.13 min in raw sample accounts for 99.5 of the total area which demonstrates the high purity of raw sample. Irradiation of Tetralin produced a few new products which has a very similar retention time as the raw compound. Dimer products were also produced by ebeam irradiation but the centration of them is very low.

The overall conversion in irradiated Tetralin was calculated in figure 27. Area under peaks corresponding to new products in irradiated sample contributed to 0.8% of the total area. This number is higher than that of irradiated ethylbenzene.

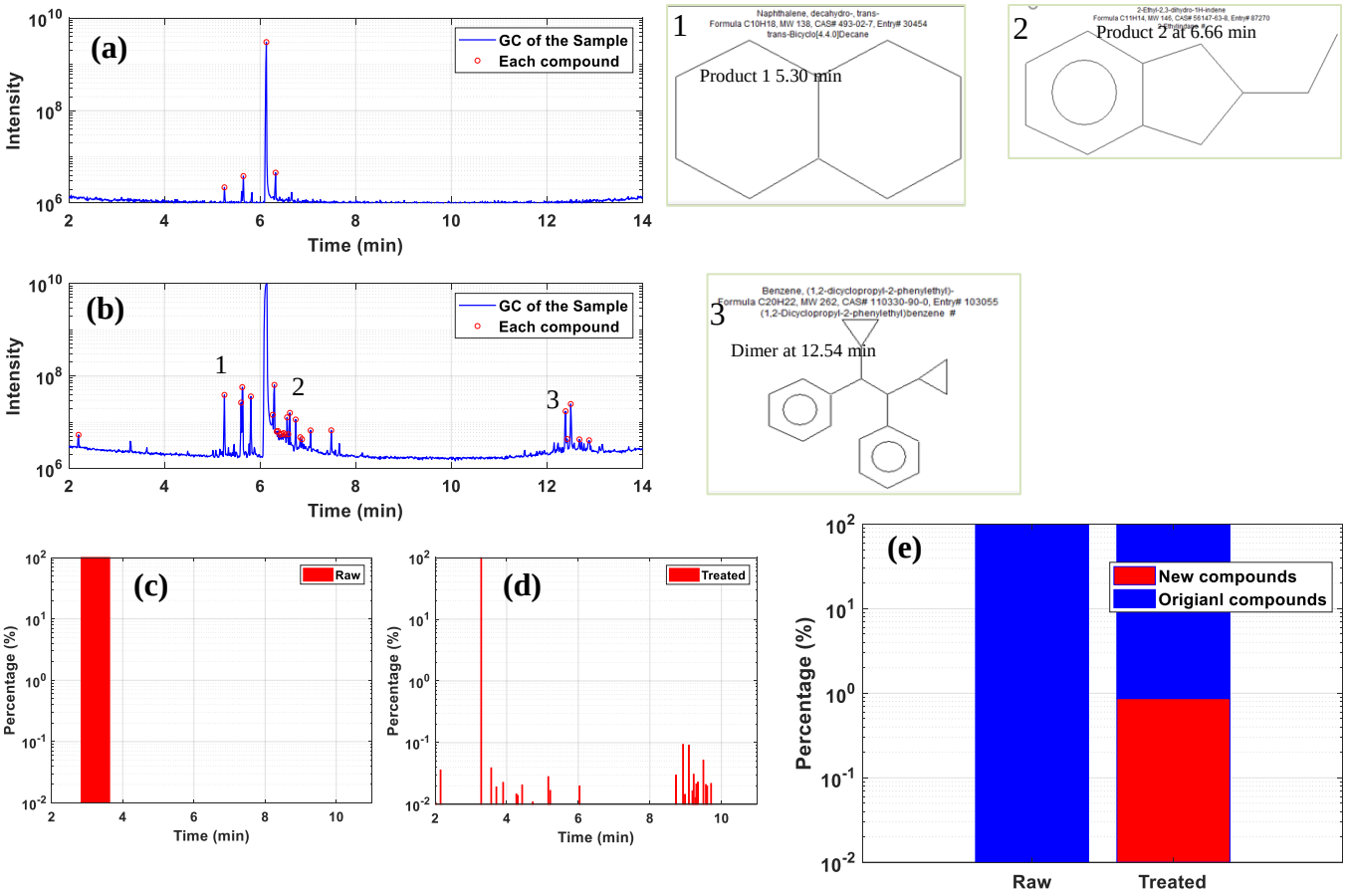

Figure 70: GC-MS analysis of irradiated Tetralin: (a), raw sample signal; (b), irradiated sample signal; (c), peak area of raw; (d), peak area of irradiated sample; (e), total area change. 1, 2 and 3 are new products

GC-MS results of irradiated toluene was shown in figure 71. There was only one single peak at 2.25 min on the raw toluene GC curve which belongs to the toluene compound. Irradiated toluene GC curve showed many other peaks other than the original one. Most of them are concentrated in a range of 8-9 min. Mass spectrum of those peaks revealed their molecular structure. Peak 1 to 3 are dimer products from irradiating raw toluene compounds and their structure were shown as 1-3. Area under each peak was calculated

after subtracting baseline from raw signal. There was only one peak on the raw toluene GC signal while more many other peaks were observed from the irradiated toluene sample. Most of those peaks are in the range of 8-9 min with a small peak area. Peak area difference was also compared between the raw and irradiated sample. Toluene peak from the raw sample accounts for 100% of the total area because no other peaks were observed. This area dropped by about 0.8-0.9% in irradiated sample because new compounds were created by

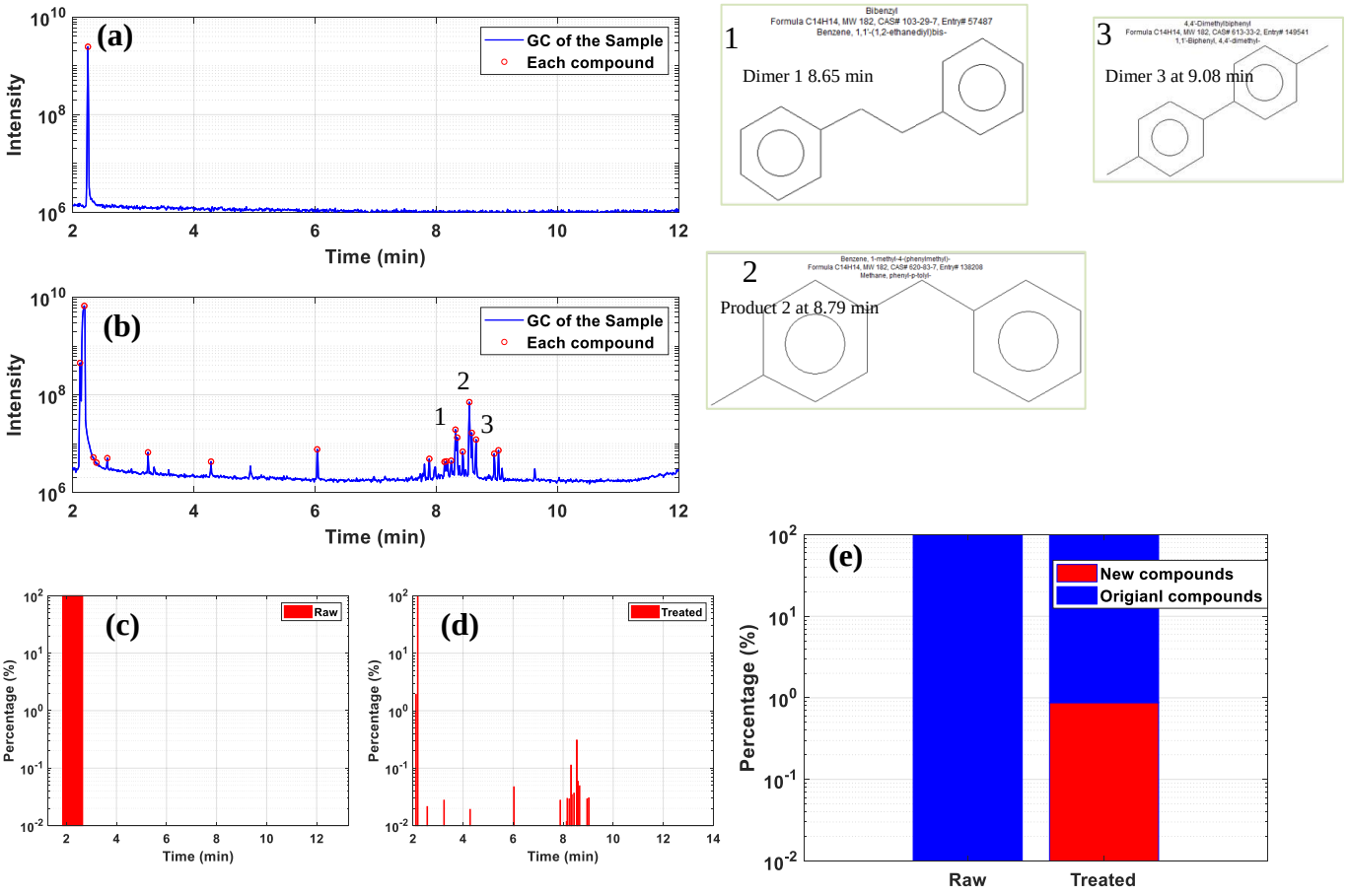

Figure 71: GC-MS analysis of irradiated toluene: (a), raw sample signal; (b), irradiated sample signal; (c), peak area of raw; (d), peak area of irradiated sample; (e), total area change. 1, 2 and 3 are dimer products

irradiating toluene. Dimer products in irradiated sample contribute 0.8% to the total area. GC-MS analysis was also conducted on irradiated Methylnaphthalene to study its radiation stability and products. Figure 72 showed the GC curve of both raw and irradiated methylnaphthalene. Raw sample has no other peaks other than the three peaks corresponding to the original compound. Irradiated sample shown many small peaks in the range of 7-8 min. Mass spectrum analysis shown that those peaks might be the isomer of methylnaphthalene, e.g. peak 1. Peak 2 was identified as another product whose molecular structure was also shown. No dimers or trimers were detected by GC-MS.

Area under each peak from both GC curves are calculated and showed in figure 32. There were many new peaks on the irradiated sample signal but those peaks have very small area in the range of 0.02 -0.03. Area distribution of the original compound and new compounds were shown in figure 33. In irradiated sample, new compounds created from irradiating the original methylnaphthalene compound contributed about 0.25% to the total area. This demonstrates that methylnaphthalene is a very stable chemical compound under ebeam radiation.

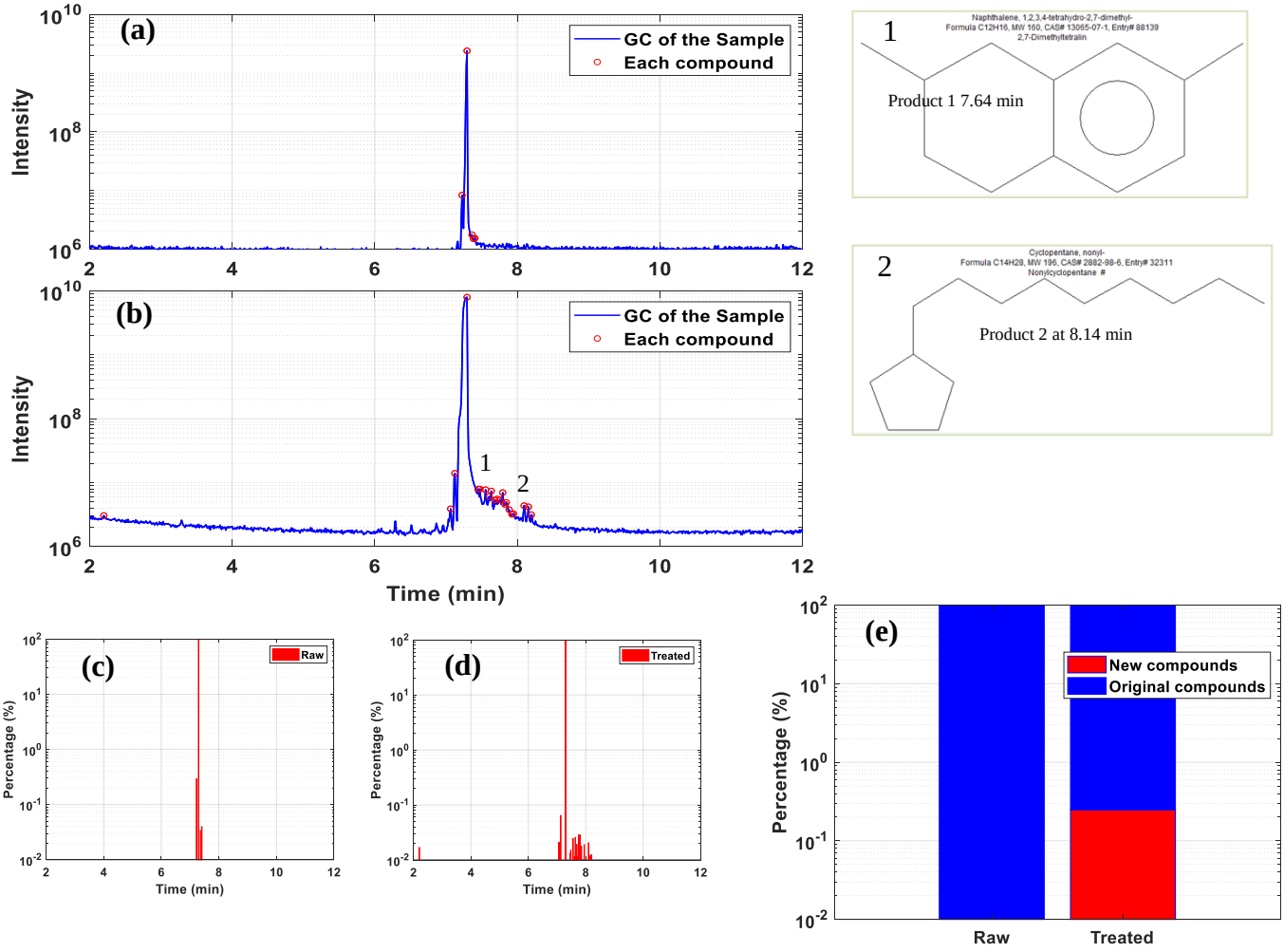

Figure 72: GC-MS analysis of irradiated methylnaphthalene: (a), raw signal of original; (b), raw signal of irradiated sample; (c), peak area of raw; (d), peak area of irradiated sample; (e), total area change. 1 and 2 are products

8.2.8 Conversion, Yields and Selectivity

The goal of conversion analysis was to quantify conversion of original chemical compounds to different products with known specific energy input. With conversion results from different compounds, we could study the effect of molecular structure and bond strength of each compound on its conversion to new species induced by high energy electron beam. Estimation of hydrocarbon conversion to new species, however, is very

challenging due to multiple reasons. One of the reasons is the lack of reliable techniques which could be used to separate different compounds and quantify them by different detectors. Due to the complexity of the job, there is tremendous risk if we only rely on one technique. Therefore we selected three different techniques (GC-FID, TG and GC-MS) from three different labs and use them to study conversion of irradiated samples. Results from different detectors could be used to verify each other and compensate each other as well. For example, GC-FID may tell us how much was converted to heavy species, but we are unable to know what those species are in terms of their molecular structure. In this case, GC-MS could be used to qualitatively characterize the new species. Results will be more accurate if we combine multiple techniques that could compensate each other.

To simplify conversion analysis we group new species based on their GC retention time: products that showed up before the original compound are called light product and products that showed up later are called heavy products. Conversion to small products caused by chain scission and ring opening of the original molecules induced by high energy ebeam irradiation. While conversion to heavy products are due to polymerization and chain crosslinking, e.g. dimers and trimers. Reduction of the original molecule in treated samples was a result of conversion to both of the products mentioned above. The value of reduction is equal to the sum of both light product conversion and heavy product conversion. Reduction of original compounds is also equal to the total conversion.

It is important to mention that light products quantified by both GC-FID and GC-MS did not include those that were lost as gas or vapor but were accounted for in mass balance results. Therefore the total conversion to light products will be a combination of

conversion by GC-FID or GC-MS and total mass losses. Similarly total conversion of the original compound in all treated samples also should be compensated by the mass losses.

In this paper we mainly rely on GC-FID results to study conversion and yields in the irradiation process. For example, we used the GC-FID total conversion. In order to include all possible products, we corrected the GC-FID results with GC-MS data for Tetralin and ethylbenzene. Table 24 and table 25 summarized the conversion results from both of the techniques. Note that conversion results are corrected by real specific energy input and referenced to the SEI of pentane.

Table 24: Conversion by GC-FID

Samples	Small Product (wt. %)	Reduction (wt. %)	Large Product (wt. %)
Pentane	3.64	-8.36	4.72
Methylcyclohexane	0.08	-1.80	1.71
Cyclohexane	0	-2.63	2.63
Ethylbenzene	0.37	-0.96	0.59
Tetralin	0	-1.66	1.66
Toluene	0	-0.04	0.04
Benzene	0	0.15	0.15
Methylnaphthalene	0.07	-1.25	1.18

Table 25: Conversion by GC-MS

Samples	Small Product (wt. %)	Reduction (wt. %)	Large Product (wt. %)
Methylcyclohexane	0	-5.5	5.5
Cyclohexane	0	-24*	24*
Ethylbenzene	0	-0.8	0.8
Tetralin	0.2	-0.8	0.6
Toluene	0	-0.8	0.8
Benzene	0	-0.2	0.2
Methylnaphthalene	0	-0.25	0.25

*GC-MS was done one month after GC-FID, significant amount of cyclohexane was evaporated from the glass jar

Relationship of total conversion or reduction of the original compounds with saturation degree and average bond energy was studied and shown in figure 73. There is a clear correlation between the total conversion of original compounds and saturation degree or average bond energy. It is very clear that hydrocarbon compounds with higher saturation degree or lower average bond energy tend to convert to other compounds more easily with the same specific energy input. Nearly 10% of Pentane was converted with about 450 kJ/kg SEI. Cyclohexane and Methylcyclohexane were also converted significantly by high energy ebeam radiation. Conversion values were about 4.2% and 3.2%, respectively, with similar SEI as pentane. The saturation degree of cyclohexane and Methylcyclohexane are 0.857 and 0.875, compared to unity saturation of pentane, but conversion values of those two compounds are lower by more than a factor of 2. This indicates a strong and nonlinear dependence of ebeam induced conversion on saturation

degree. Comparison between Tetralin & ethylbenzene conversion data with benzene & toluene data showed the same trend. At a saturation degree 0.55, about 1.8% of compounds were converted. When saturation degree was below 0.5 (benzene and toluene), less than 0.5% conversion was observed. It seems that Methylnaphthalene had higher conversion even with a lower saturation degree. This is due to the high conversion estimated by GC-FID. GC-MS conversion was actually close to that of benzene. Total conversion also depends on average bond energy. In general, conversion drops as average bond energy increases. A trend was observed between irradiated compounds: cyclohexane>Tetralin>ethylbenzene>methylnaphthalene>benzene. Pentane with slightly higher bond energy has a higher conversion, this might be due to its higher saturation degree. Methylcyclohexane and toluene had lower conversion compared to cyclohexane and benzene. This might be contributed to the methyl functional group. GC-MS and TGA data showed that there were less trimer products when irradiating compounds with a methyl group.

Similarly, the dependence of conversions to both light products and heavy products on saturation degree and average bond energy was studied. Conversion to light products was closely related to the saturation degree. More light products were produced from compounds with higher saturation degree. More than 5% of pentane was converted to lights with 300 kJ/kg SEI. Conversion to lights dropped to 1.5-1.7% with cyclohexane and Methylcyclohexane when saturation degree was in the range of 0.85-0.87. Conversion to lights continues to drop to below 0.5% when saturation degree is below 0.55. The effect of average bond energy on conversion to light product is similar as saturation degree. In

general, compounds with lower average bond tend to produce more lights under high energy ebeam irradiation. But dependence on those two parameters are not exactly the same. For example cyclohexane and Methylcyclohexane have lower average bond energy than pentane, but their conversions to lights are lower than pentane too. In this case, saturation degree is better correlated with the conversion to light products.

Large products production dependence on saturation degree and average bond energy was shown in figure 73 too. The trend is similar as light products. As the saturation degree increases, conversion to heavy products also increases for most studied compounds. We observed that conversion to heavy products was more sensitive to both the saturation degree and average bond energy. For example, cyclohexane and Methylcyclohexane, which have the same average bond energy and very close saturation degree, are converted with very different values. This may again be due to the functional group.

Conversion to heavy products from GC-MS data was also studied and its dependence on both saturation degree and average bond energy was shown in figure 73. It seems that GC-MS conversion to heavy products was more closely correlated with the saturation degree than the GC-FID data was. As saturation degree increases from benzene and methylnaphthalene to Methylcyclohexane and pentane, conversion also increases from less than 0.2% to more than 4%. Dependence of conversion to heavy products on average bond energy was less clear, although reducing the average bond energy generally increases the conversion.

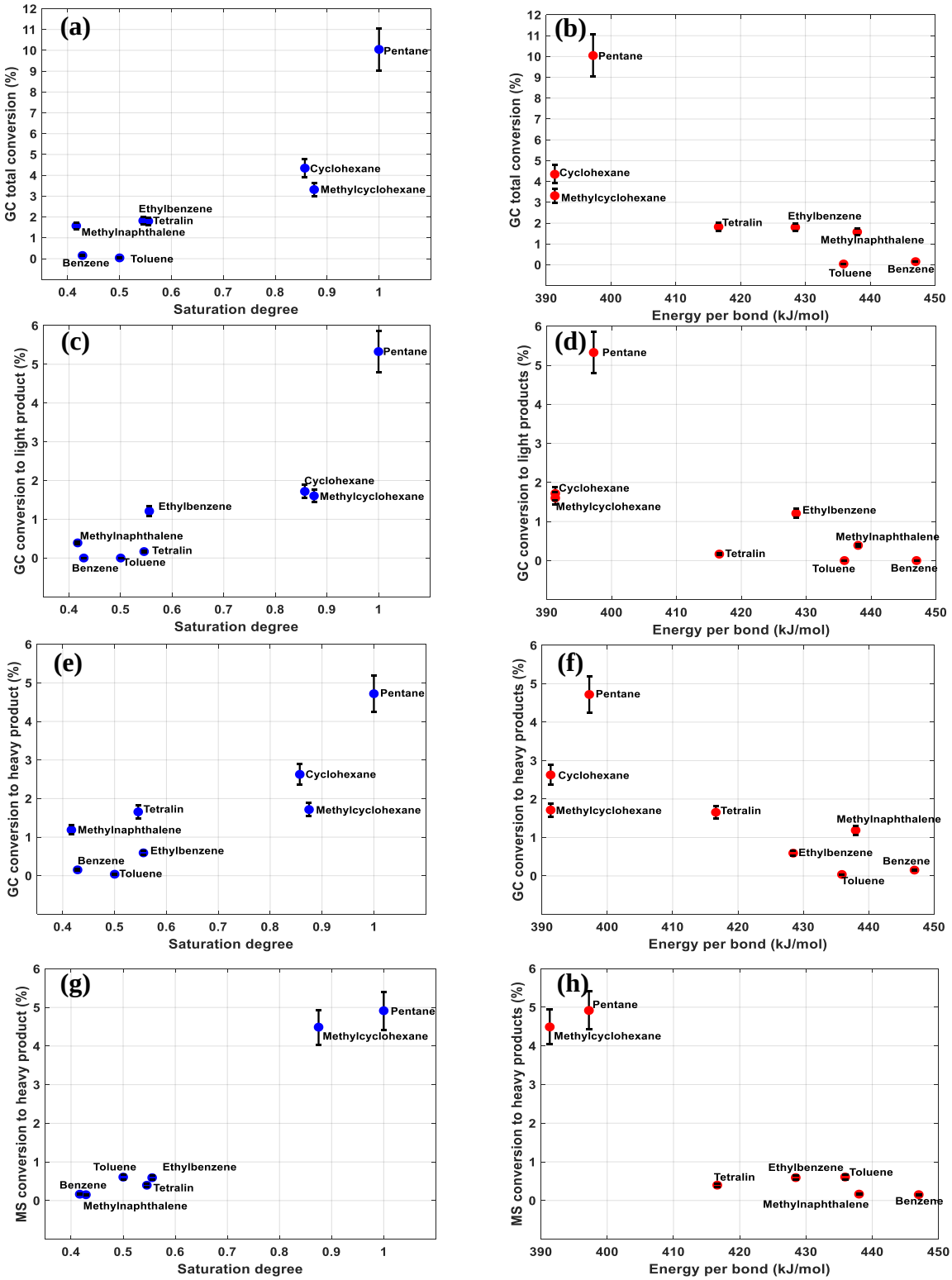

Figure 73: GC conversion dependence on saturation degree and average bond energy: (a) and (b), total conversion; (c) and (d), light products; (e) and (f), heavy products; (g) and (h), MS heavy product conversion

In order to estimate yield of each individual product from irradiating a different hydrocarbon sample, molecular weight of that product is required. In this case GC-MS and TGA analysis are extremely useful because it revealed the molecular structure of products in each irradiated sample. By using both of the techniques, we have identified the molecular structure of most of the heavy products in all of those irradiated hydrocarbons, which are predominately dimers and trimers from polymerizing the original hydrocarbon compound induced by high energy ebeam irradiation. Dimer products accounts for more than 90% of the total products by weight. The rest of them are trimers and isomers. Therefore, it is reasonable to assume that the molecular weight of heavy products in irradiated sample is equal to the molecular weight of a dimer compound:

$$MW_{HP} = MW_{dimer} = 2 * MW_{raw}$$

Where $\boldsymbol{MW_{HP}}$ is molecular weight of heavy product; $\boldsymbol{MW_{dimer}}$ and $\boldsymbol{MW_{raw}}$ are the molecular weight of a dimer and original compound.

Light product, however is not as well-known as heavy product due to two reasons. First, gaseous species produced from the irradiation process was not collected or analyzed. No information regarding those species was available. Second, although GC-FID analysis proved that there were light products, no molecular structure information was provided by this technique.

GC-MS data did not provide information on those products either. But extensive prior research have demonstrated that gaseous products from irradiating most non-alkane hydrocarbons are hydrogen and small hydrocarbons below C_3. Therefor the light product for yield analysis was assumed to be a medium gaseous hydrocarbon such as ethylene

(MW=30). Pentane is an exception because of its different response to ebeam irradiation. There is significant amount of liquid phase light product resulted from irradiating pentane. Because the GC signal of those products is very close to pentane, we assume that those products have similar molecular weight as pentane which is 72. Yields of light product from pentane irradiation will be based on two different molecular weight for analysis: 30 and 72.

Total reduction of original compounds by ebeam irradiation was first estimated for all samples in terms of number of molecules per 100 eV of specific energy input (SEI). Total reduction was studied as a function of both saturation degree and average bond energy which was shown in figure 74. Total reduction of pentane was close to 27 molecules/eV which seems unrealistically high. This might be partially due to the underestimation of SEI or overestimation of light product conversion. Reduction of Methylcyclohexane and cyclohexane due to ebeam irradiation was close to 7 and 12 molecules/100eV, respectively. Irradiation of methylnaphthalene, Tetralin and ethylbenzene also very efficiently reduced the original compounds at about 3-4 molecules/100eV, whereas benzene and toluene were very stable under ebeam radiation. The reduction of those compounds were 0.5 and 0.1 molecules/100eV, respectively.

Yields of both light products and heavy products were estimated based on their conversion and GC-MS product information. Yields were studied as a function of the saturation degree and average bond energy. Figure 74 showed the dependence of yields of light products on saturation degree and average bond energy. Overall yields of light products increase with increasing the saturation degree and decreasing the average bond

energy. Irradiation of pentane produced the largest amount of light products including both gaseous species (10 molecules/100eV) and liquid species (7 molecules/100eV). Light products from irradiating Methylcyclohexane and cyclohexane are comparable in the range of 16-17 molecules/100eV. Irradiation of ethylbenzene, methylnaphthalene and Tetralin also produce significant amount of light products which are 12, 4 and 2 molecule/100eV for each of them. Benzene and toluene are the most stable hydrocarbon compounds because no light products from them are detected.

Yield of heavy products from irradiating hydrocarbon samples were also estimated. Its dependence on saturation degree and average bond strength was shown in figure 74. Heavy products yields are more accurate due to their low evaporation tendency and more reliable GC-MS analysis results. There is a noticeable correlation between the heavy product yields and molecule saturation degree or bond energy. As the saturation degree increases or bond energy decreases, more heavy products are produced. Heavy product yields dependence on those two parameters is clearer than that of light product yields. Irradiation of pentane produces more heavy products (4.7 molecules/100eV) than cyclohexane (3 molecules/100eV) and Methylcyclohexane (2 molecules/100eV). Irradiation of Tetralin, methylnaphthalene and ethylbenzene also produced significant amount of heavy products, 2.5, 1.8 and 0.8 molecules/100eV, respectively. Yields of heavy products from irradiation of benzene and toluene are much lower than previous samples. The trend between them resemble that of cyclohexane and Methylcyclohexane. Cyclohexane and benzene tend to polymerized more than Methylcyclohexane and toluene. This might be related to a special function of methyl group.

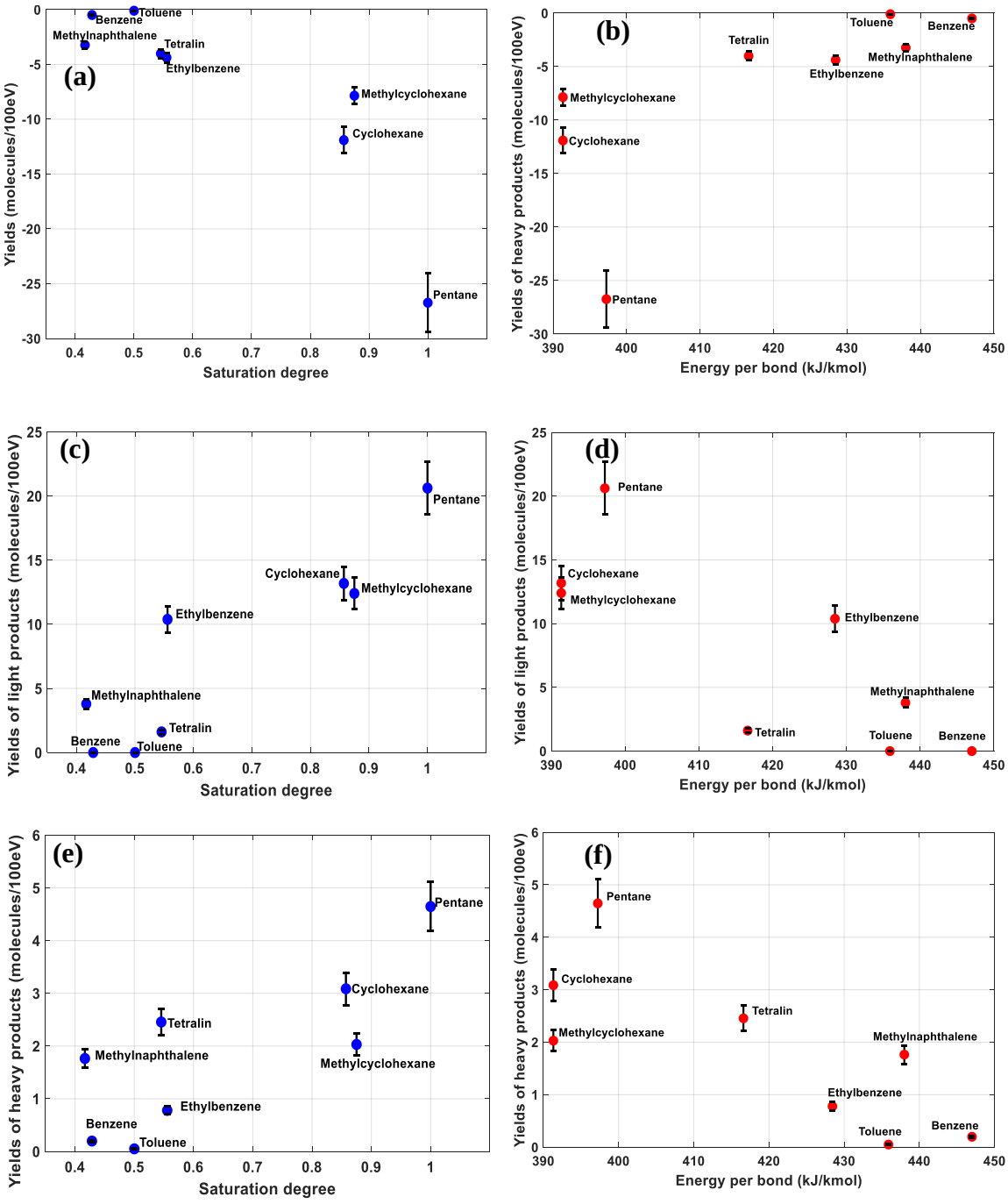

Figure 74: GC yields of different species and their dependence on saturation degree and average bond energy: (a) and (b), reduction of original compounds; (c) and (d), yields of light products; (e) and (f), yields of heavy products

Product selectivity defined as the ratio of total yields of light products over total yields of heavy products was estimated based on the calculated yields. Its dependence on both the saturation degree and average bond energy was studied and shown in figure 75. Results showed that product selectivity from irradiating different hydrocarbon compounds largely depends on the selected two parameters used to characterize the molecular structure. Saturation degree of one hydrocarbon molecule seems to be able to very clearly characterize the product selectivity of hydrocarbon irradiation by high energy ebeam. More specifically, compounds with higher saturation degree above 0.85 tend to produce more light products 4-6 times higher than heavy products. Those compounds include cyclohexane, Methylcyclohexane and pentane. Compounds with lower saturation degree below 0.55 have relatively low selectivity towards light products except ethylbenzene. The amount of light products produced from irradiation of Tetralin was only half of the quantity of its heavy products. Light product selectivity of irradiation of benzene and

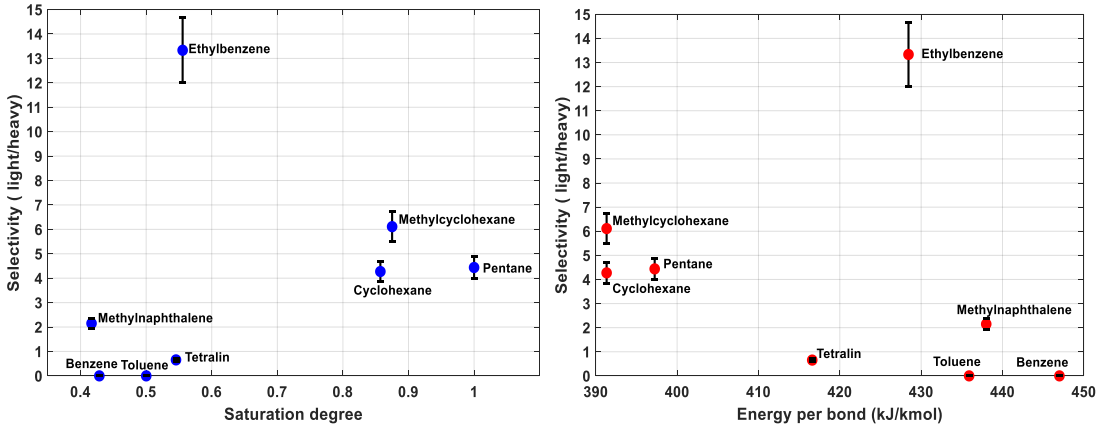

Figure 75: Selectivity (yields of light species over yields of heavy

toluene is close to zero because those two compounds only polymerize under ebeam to product heavy products, instead of chain scission to crack molecule.

8.2.9 Conclusions of Irradiation of Different Hydrocarbons

Irradiation of hydrocarbons with different saturation degree and average bond energy at low temperature showed several key features. Hydrocarbon responses to high energy electron beam irradiation in different ways. The differences could be illustrated by color change of irradiated sample, total conversion of irradiated sample, conversion to light products and heavy products, yield of each product and product selectivity. Each of the aspects depends on hydrocarbon properties including bulk fluids properties (density, viscosity and conductivity) and molecule properties (bond energy, H/C, saturation degree, molecular size, et al.). Neat samples are very similar on their bulk fluids properties. But results are extremely dissimilar from irradiating them due to the molecular property difference.

Irradiation of straight saturated alkanes represented by pentane caused the largest amount of conversion to both light and heavy products. Yields of products were very high due to a high conversion. Product selectivity is almost fifty lights to fifty heavies. But no color change was observed. Saturated alkanes with ring structure (Methylcyclohexane and cyclohexane) overall had lower conversion than pentane but tend to polymerize and produce significant amount of dimer and trimer products. Product selectivity to heavies is much higher than that of lights. Yields of the polymerized products are quite high. Hydrocarbons with unsaturated ring or rings are much less susceptible to electron beam and are not prone to conversion. GC-MS was able to detect polymerized products from

irradiating those hydrocarbons, but the conversion was less than 1% for most of the compounds. Very interestingly, those compounds all showed significant color change after irradiation. Yellowness could be used to quantify the color change of irradiated samples and it increased with increasing the compound saturation degree.

Conversion, yields and selectivity from irradiating those compounds were investigated as irradiation responses for their dependence on the saturation degree. Results were compared between different compounds. It seems that saturation degree directly affects those responses in a predicable way. For example, compounds with higher saturation degree tend to generate higher conversion and higher yields of products. Compounds with lower saturation degree, however, are more inert under high energy ebeam irradiation and only produce small amount of polymerized products.

Although multiple techniques were used to quantify conversion and characterize new products, there were still significantly uncertainties on the results. The biggest uncertainty is from gas and vapor products. Because they were not collected or analyzed by the GC-FID or GC-MS, we could not know the exact structure of those species. Analysis on them was purely based on assumptions and literature data. But it is important to point out that it is incredibly challenging to collect gas and vapors from this setup due to tremendous system design complexity and increased safety concerns. That does not mean it is impossible to achieve it, but only means that it will come with a more sophisticated system with more investment in safety measures.

It is very useful to compare results from irradiating different hydrocarbon mixtures with the same electron beam source. Conversion from each hydrocarbon mixture was

correlated with its saturation degree. For example, saturation degree of mineral oil was estimated to be in the range of 0.95-1 based on an average molecular carbon number 21. Similarly, saturation degrees of crude oil A and B were also estimated based on its known H/C ratio and average carbon number. Information regarding them was given in table 266. Note that there is significant difference on average carbon numbers estimated based on mass and mole distribution. Crude oil A has an average carbon number 46 based on mass and an average carbon number 29 based on moles. Crude oil B has an average carbon number 58 based on mass and average carbon number 36 based on moles. Mineral oil has an average carbon number 21 which does not change with mass or moles because of narrow hydrocarbon distribution with very similar compounds in the mixture.

Table 26: Saturation Degree of Hydrocarbon Mixtures

Oil	H/C	Average carbon Number		Saturation degree	
		Mass-based	Moles-based	Mass-based	Moles-based
Mineral oil	2	21	21	0.955-1	0.955-1
Crude oil A	1.49	46	29	0.729	0.720
Crude oil B	1.42	58	36	0.698	0.691

Conversion from different hydrocarbon mixtures was summarized on figure 76 at similar SEI (500-600 kJ/kg). First, mass-based conversion was compared for all samples and correlated with their mass-based on saturation degree in figure 76a. Oil A and mineral oil results were in the same trend obtained from irradiating pure hydrocarbon compounds.

Whereas crude oil B does not obey the same rule with a higher conversion than predicted. Mole-based conversion was also studied for all oils in figure 76b. Conversion based on moles was higher than conversion based on mass. For example, oil B conversion based on moles was about 13% compared to 11% based on mass. This could be attributed to the fact that saturation degree estimated based on moles was higher than that estimated based on mass.

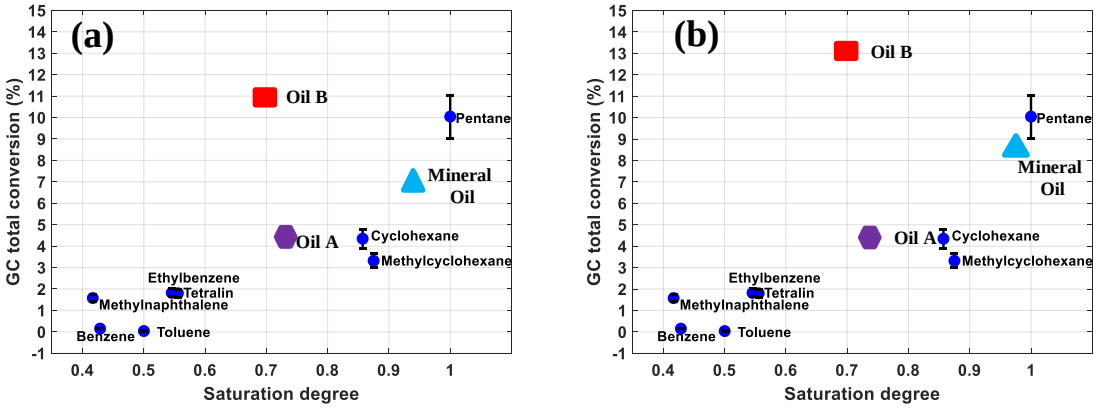

Figure 76: Conversion based on mass (a) and conversion based on mole numbers (b) for all hydrocarbon mixtures

In general, saturation degree of one hydrocarbon was closely related with its conversion induced by high dose rate electron beam irradiation. Higher saturation degree typically indicates higher conversion to light hydrocarbons. Saturation degree could vary with the method used to calculate it. Mass-based saturation degree of crude oils is usually smaller than mole-based saturation degree because of smaller molecular weight of light

hydrocarbons. This also explains why mole-based conversion is higher than mass-based conversion.

CHAPTER IX

IRRADIATION OF SMALL HYDROCARBONS FOR POLYMERIZAION AND HYDROCABRON VAPORS FOR CRACKING

Irradiation of mineral oil and hydrocarbons with ring structures were conducted in liquid form at relatively low temperatures. Results showed that both light and heavy compounds as products were produced from the irradiation process. More specifically, products from irradiating mineral oil are primarily light compounds initially and change over time to produce more heavy compounds. The product stability are both gas and temperature dependent. For example, higher irradiation temperature and supply of reactive gas help maintain the light product stability. But the irradiation process has to be aided with reactive gas and at relatively high temperature. Irradiation of hydrocarbons with rings at low temperatures tend to produce more polymerized products, especially those with saturated rings. It seems that polymerized products are more easily to be produced by irradiating multiple hydrocarbons at low temperatures, compared to light product which could also be produced but requires more delicate irradiation conditions because of their instability in nature.

Based on current results and our observations from irradiating different hydrocarbons, it is certainly viable to design a process with controlled conditions to achieve our goal. Two processes will be proposed here to accomplish two different goals. The first one is to grow the original hydrocarbon molecules by ebeam induced polymerization. Irradiated hydrocarbon compounds are small molecules below C_5. The

goal is to convert gaseous hydrocarbons to liquid fuels (GTL). The second process is to irradiate hydrocarbons at vapor states to enhance cracking and suppress recombination caused by polymerization. Vapors could be mixed with natural gas to change its chemical composition and partial pressure of the irradiated compound. The first process (GTL) has been investigated by a new irradiation experiment. Pentane was selected as a surrogate hydrocarbon for irradiation experiment. Results including experimental setup, irradiation parameters, hydrocarbon conversion and yields were studied in the previous chapter. The next session of this chapter will introduce more details about irradiation of small hydrocarbons for a gas to liquid (GTL) conversion process.

9.1 Irradiation of Small Hydrocarbons

Even though our goal is to convert natural gas to liquid fuels, it is not practical to irradiate natural gas with a simplistic setup like we have shown. To irradiate natural gas at a condensed state requires sophisticated reactor design and a series of safety measures to cope with extreme low temperature and potential high pressure. Therefore we followed the minimum viable product (MVP) concept and built our prototype setup to irradiate pentane. MVP provides us with sufficient features to satisfy early stage operation. Keep that in mind, the next and more complete set of features will be designed and developed after the knowledge we learned from the MVP. Irradiation of pentane with this setup allows us to study the mechanism of irradiating lighter hydrocarbons and learn important insights about the process. As a concept proof experiment, it provides us with sufficient knowledge and help us further develop the concept if necessary.

Beyond the adoption of a MVP concept, there are also important technical aspects why we select pentane as the first material. Propane is another candidate because of its abundance in natural gas and a larger industrial application potential. However it will pose great risk on the current system because of its high partial pressure at temperatures above 0 ^{o}C. What's worse, its partial pressure increases very rapidly as temperature increases due to energy addition from the beam. A comparison between of propane and pentane was made based on their thermal properties in a phase diagrams. Because irradiation tests are conducted in a batch reactor with constant volume, the irradiation process could be simulated as a constant volume heat addition process. Energy gain is due to electron molecule collision. Energy loss is due to water cooling. Therefore the final temperature and pressure of the system could be estimated with known energy addition rate and heat loss rate.

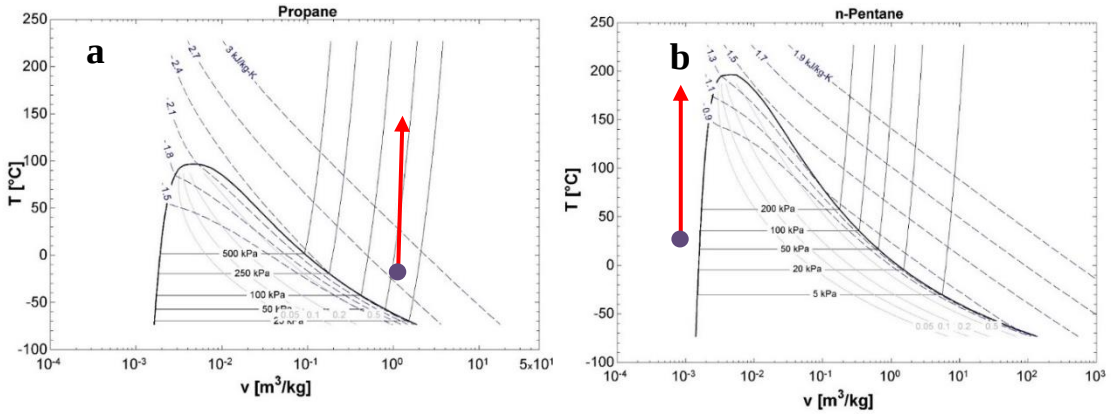

Figure 77: T-v diagram of propane (a) and pentane (b)

Figure 77a is the T-v diagram of propane and pentane at different pressures. On the diagram any constant volume process will be represented by a vertical line starting from the initial conditions. If temperature is 0 ^{o}C, propane is in gas phase in a wide range of pressures between 100 kPa and 250 kPa. Adding heat to it will increase the pressure very rapidly and eventually result in an over-pressure failure. In order to keep propane at a condensed state, either the pressure needs to be larger than 500 kPa or the temperature needs to be below its melting point (-42 ^{o}C). Both of those conditions are not achievable with the current system

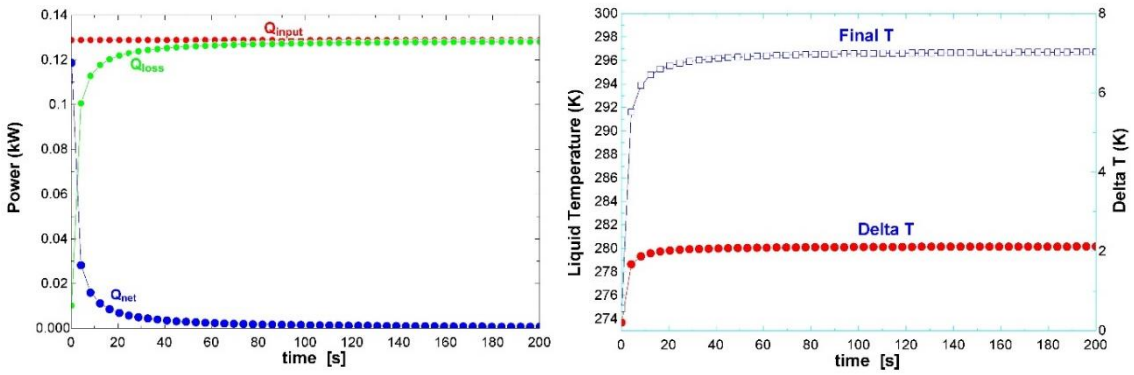

Figure 78: T-v diagram of propane (a) and pentane (b)

Figure 77b is the T-v diagram of pentane at different pressures. Similarly a constant volume heat addition process could be simulated. When temperature is 0 ^{o}C, pentane is at liquid state. What's more, it allows us to add a significant amount of heat before its pressure exceeds the limiting pressure of the system. Additional cooling with water will enhance the safety of our system.

Final temperature of the system was estimated with a heat transfer model. Results are shown in figure 78. Q_{in} was the heat addition rate and measured with dosimeters. Q_{loss} is the cooling power due to water. T is the temperature of the sample and $delta\ T$ is the temperature difference between sample and cooling water. The simulation results indicates that as energy is added into the system, a final steady state temperature will be reached due to a balance between the cooling power and heating power.

Another important reason we prefer to irradiate sample at a condensed states is related to the physiochemical process. Electron-molecule collision in a dense medium are much more efficient on creating reactive species because of high number density of molecules and high collision frequency. Molecule-molecule collision frequency is proportional to the number density of molecules: $\omega \propto n_i * n_j$. Increasing the number density of neutral molecules will increase the collision frequency significantly. The benefits of higher number density will be an enhanced conversion or yields with the sample specific energy input.

9.2 Irradiation of Natural Gas in GTL Process

It has been experimentally proved that high energy electron beam irradiation of small hydrocarbon compounds produces larger molecules with high yields. This definitely pushes the boundary of hydrocarbons that could be irradiated to produce products for different applications. Natural gas, one of the cleanest and abundant fossil fuel has lower carbon emissions and less impurities compared to other fuels. However, its market share among all energy resources has never been able to match its reserves and quality due to poor transportability and safety concerns. This might be addressed by converting natural

gas into high-quality liquid products (GTL) such as gasoline and diesel fuel through a similar process. It has very profound and broad impact on the energy industry. If natural gas could be successfully converted to gasoline in a cost effective manner, it will help transform the energy industry and save billions of dollars for our country and society.

Currently natural gasses are routinely cryogenically liquefied (called Liquefied Natural Gas - LNG) to ease transportation but this liquefaction is temporary. Permanently converting gaseous naturally occurring hydrocarbons (e.g. methane, ethane, propane, and butane) to liquids fuels would greatly improve their transportability. This process is referred to as Gas to Liquids (GTL). Such chemical conversion can occur through a crosslinking process. For natural gas crosslinking to chain length of N=2 to N=5 would produce condensed liquids at ambient temperatures and pressures. Irradiation of hydrocarbons is a known process to crosslink monomers. However, for the processing of light hydrocarbons it is very inefficient. Irradiation method might increase the yield and efficiency of light hydrocarbon crosslinking process. This is done by irradiating the natural gas in a high density state. The natural gas could be high pressure or low temperate (or a combination of both) to bring the density to levels comparable the liquid or solid density. Our processing permanently converts the natural gas to a liquid by irradiation chemistry. During irradiation radicals are generated and a polymerization chain reaction is initiated. One radical can lead several chain formation. Depending on the processing states and the addition of promoters the conversion can vary significantly. Irradiation at high density is unique in that the radical species is very short lived and will react with neutral species prior to being further excited. In low density processing multiple excitation would lead to

excessive decomposition, carbon nucleation, and yield of nano- and micro- particulate formation. Irradiation of natural gas at high density help to significantly increase the probability of radical induced reactions which lead to higher conversion to liquid products. For the condensed hydrocarbon conversions it will be highest when above the glass transition temperature and best when above the melting temperature but below the boiling temperature. The processing states thus must be carefully selected but will only have the most beneficial effects combined with the use of additives and a narrow range of energy input. This gas to liquid conversion process by high energy electron beam irradiation method is applicable to natural gas conversion to liquid fuels for better transportation and the product can also be used to produce diluent to help heavy crude oil transportation.

Unlike irradiation of mineral oils and pentane which are at liquid state during the irradiation experiments, irradiation of natural gas will be much more challenging and might encounter unprecedented issues related to process control and safety. First of all, natural gas is at gas state with extremely low density (0.7-0.9 kg/m^3) at ambient conditions. The density of most liquid hydrocarbons including mineral oil and pentane is three orders of magnitudes higher than that. This dramatic density difference limits the application of ebeam on irradiation of natural gas, because ebeam irradiation of materials is a volumetric method which will require tremendous volume flow rates in order to achieve a throughput at industrial scale. Natural gas could be liquefied before being irradiated. For example, methane will become liquids at temperature below -161^oC and start freezing at -182 ^oC. Irradiation experiment could be operated in this narrow window

when natural gas is at its liquid state. There might be additional challenge associated with irradiating natural gas in a very narrow operation window (-182 ^{o}C to 161 ^{o}C).

Experimental setup for irradiating natural gas will resemble the one used for irradiation of pentane but with several modifications to cope with thermodynamic difference between those two hydrocarbons. Natural gas has to be liquefied first before being irradiated. For lab scale test, liquefaction of natural gas could be achieved by contacting with liquid nitrogen in a closed system. Transporting the sample to ebeam facility will also require the use of liquid nitrogen. A liquid nitrogen bath similar as ice water bath could be deployed for both transportation process and for the irradiation experiment. Pressure relief valve and pressure gage needs to be upgraded for higher ratings to match natural gas pressure increase during the irradiation process. For industrial scale operation of this process, many optimizations on each component of the overall process need to be conducted, e.g. the liquefaction process could be completed in a separate plant which works the same way as a commercial LNG plan. High energy electron beam facility could be another separate unit. This facility should be built in a way that match the requirements of the production rate and power of the GTL process. Conceivably, the electron beam facility could be located near a well and real time convert natural gas to gasoline range fuels. The produced products could also be used as diluent to mix with crude oils and help meet the pipeline specs before transportation.

9.3 Irradiation of Hydrocarbon Vapors for Enhanced Cracking

In this section, I will try to lay out a theoretical background for the second process we proposed to enhance hydrocarbon cracking and suppress hydrocarbon recombination such as polymerization. I will also propose one setup that could be potential used to generate hydrocarbons vapors for irradiation purpose. Based on this setup irradiation could be implemented in a controlled manner. Partial pressure in a natural gas and hydrocarbon vapor mixture will be estimated. SEI in natural gas and hydrocarbon compound will be studied by a simulation with varied experimental parameters. Potential and limitations of this process will also be discussed with future improvement.

9.3.1 Theory about Cracking Hydrocarbons at Vapor States

Hydrocarbon cracking induced by electron beam irradiation has been discussed in CHAPTER II based on available literatures. In general, hydrocarbon molecules are activated by colliding with high energy electrons or photons. Activated molecules undertake a series of chemical reactions and produce different products. Two major reactions during the irradiation process compete with each other: cracking and polymerization. Radiation induced conversion and yields vary dramatically due to these two reactions. Both of the reaction depends on parameters in two categories. First category is the radiation source parameters including type of radiation, dose rate and total dose; the second category is irradiating material parameters including type of hydrocarbons, temperature, pressure, etc. If radiation source is a high energy electron beam with constant power, the first category parameters will be fixed. Therefore radiation yields and chemistry will only depend on the material properties. And we have proved that hydrocarbon material properties largely determine results of irradiation. However, the way

we vary the material properties was by changing the type of hydrocarbons. In real applications, we often do not have that freedom of changing the materials of irradiation. So the question that needs to be answered is how to improve the radiation yields by changing the material conditions given a certain type of hydrocarbons. So far we have observed from irradiating mineral oil that higher irradiation temperature and use of reactive gas helped producing more light products. Cold temperature and inert gas helped converting to heavy products. Hydrocarbon compounds with rings also produced more heavy products at low temperature. Those observations contributed to the initiation of the first process (GTL). Conceivably, if we reverse conditions in the GTL process, we will be able to create another process that favors conversion to small products (cracking). We already knew that high temperature and reactive gas mixing help this process. Another key of favoring hydrocarbon cracking is to reduce the number density of the molecules so that activated molecules will have less chance to collide with other molecules before they dissociate. Number density of the irradiating material can be easily reduced by three orders of magnitude if liquid turned into vapor. It is practical to combine those three parameters (high temperature, reactive gas mixing and vapor states) in one process to further enhance the cracking reactions.

Here we proposed a simple setup shown in figure 79 to study this process. Key components on this setup should include an oil tank, a heater, a chamber above the tank for irradiating the vapor, an oil trap, a pump and connecting lines between those elements. Natural gas might be recycled inside a closed loop and re-mix with the oil. Ideally, products from the irradiation chamber will be trapped in the oil trap which only allows

gaseous hydrocarbons to leave the system. The benefit of doing this is a better mass balance because most of the liquid hydrocarbons will be trapped. But it also increased the complexity of the system and could potentially encounter issues such as pump failure or leaking. To simplify this process, we could implement this without a close loop on the gas line and only focused on the trapped liquid. The wildly important goal is to prove that cracking products will be produced in the process and seen in the oil trap. Both systems are capable of doing that.

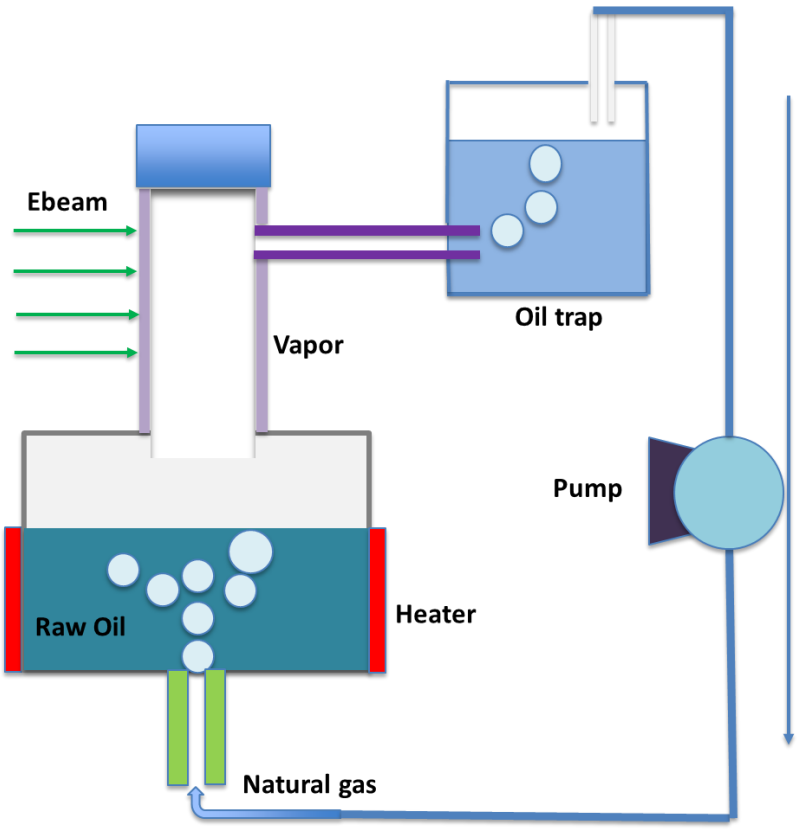

Figure 79: Experimental setup for irradiating vapors (concept)

9.3.2 Simulation of Hydrocarbon Partial Pressure and SEI in each Compound

Hydrocarbon vapor could be produced by a system mentioned above at a controlled temperature. When Natural gas is injected into the hydrocarbon liquids, it will help the evaporation process. More importantly, a natural gas and hydrocarbon vapor mixture will be created. Partial pressure of the hydrocarbon vapor is controllable by changing the temperature of the oil tank and natural gas flow rate. This is very viable without any complex device or parameter control. It provides us with great flexibility on control of partial pressure of irradiated hydrocarbons. Keep in mind that partial pressure is paramount in the hydrocarbon irradiation process.

Simulation was first conducted to study the partial pressure dependence of hydrocarbon on oil temperature and natural gas flow rate. Hexadecane was selected for this simulation with methane injection. Antoine Equation was used to estimate the partial pressure of hexadecane in the mixture[164,165]:

$$P = 10^{A-\frac{B}{C+T}}$$

Where A, B and C are component-specific constants. In this simulation constants are A=7.0287, B=1830.51 and C=154.45. Please note that Antoine equation was not experimentally verified. It was used to help us move forward with the idea of irradiating vapors. In this simulation, mass flow rate and mass percentage of hydrocarbons in the mixture were also estimated based on the partial pressure and given total flow rate. With partial pressure and mass flow rate, we are able to calculate the specific energy input to the hydrocarbon natural gas mixture by assuming the power of the ebeam source. Those

parameters depend on the oil temperature and showed different trend as temperature changes. Their dependence on temperature was shown in Figure 80.

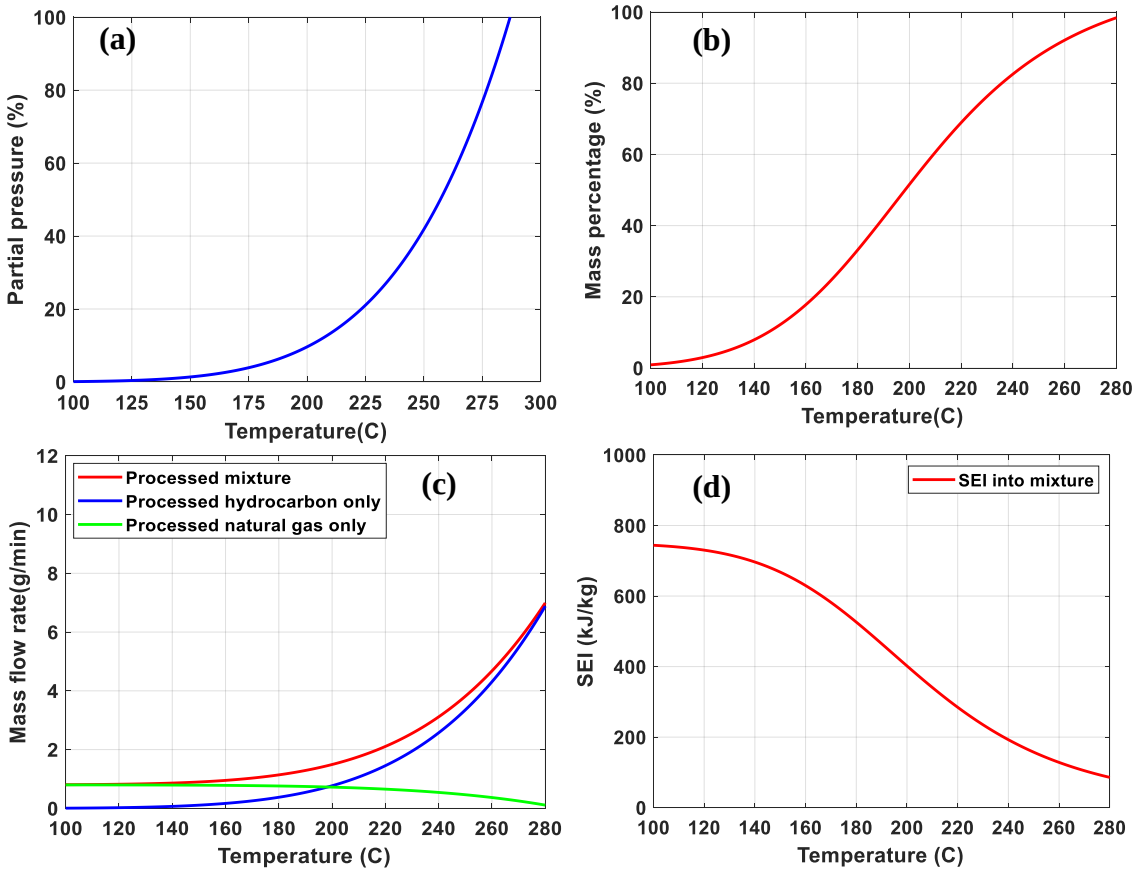

Figure 80: Estimated parameters for vapor irradiation process; (a) partial pressure vs Temperature; (b) mass percentage of irradiated hydrocarbons; (c) mass flow rates; (d) SEI of irradiated hydrocarbons

Basically, the simulation shows that partial pressure increased as oil temperature increased, which will also increase the mass percentage of hydrocarbon in the natural gas mixture. Mass flow rate of irradiated hydrocarbons increased very rapidly after 200 ^{o}C,

but natural gas mass flow rate kept dropping. Specific energy input (SEI) to the mixture was showed in Figure 78d. SEI to the mixture decreased with increasing the oil temperature, because of higher mass flow rate at constant ebeam power. If SEI target is 500 kJ/kg, the required temperature would be close to 185 ^{o}C.

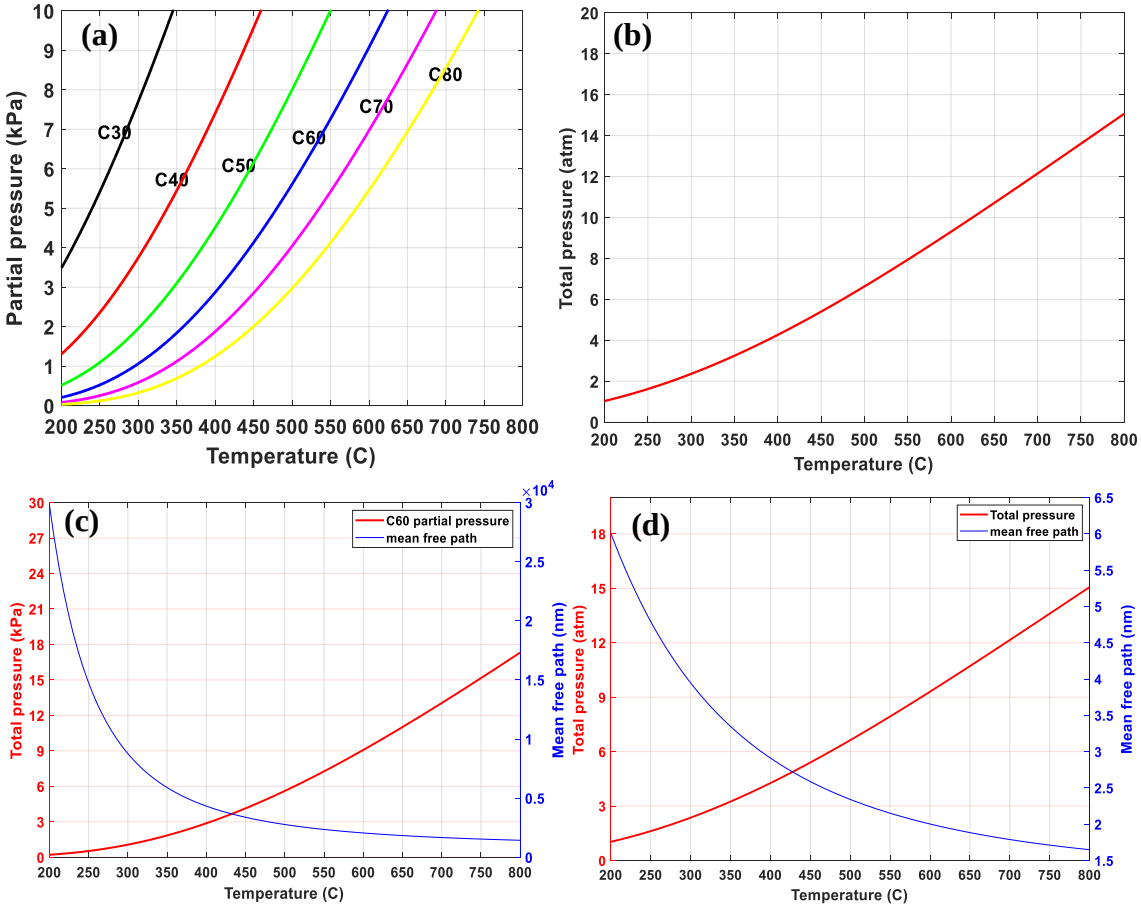

Figure 81: Estimation of partial pressure (a) and total pressure (b) of a series of hydrocarbons in the range of C20-C80; mean free path estimation based on the pressure by using ideal gas law

Antoine equation was also used to calculate partial pressure of a series of heavy hydrocarbons C20-C80 in a mixture and the total pressure at different temperatures. Antoine equation was able to accurately predict partial pressure of a single heavy hydrocarbon compound[165]. We assumed that Antoine equation is still valid in evaluating partial pressure of a hydrocarbon compound inside the mixture. Figure 81a showed the partial pressure of a few large compounds (C30-C80) with varied temperature. Partial pressure of them varies between 0.2 kPa to 7.5 kPa at 300 ^{o}C. It seems that pressure is very low and that might affect the throughput of a radiation system. However, petroleum is a mixture of many compounds. The total pressure of all hydrocarbons will be much higher if all partial pressures are combined. Total pressure was shown in figure 81b. It is more than 2 atmospheric pressure if we assume the mixture are comprised of C20-C80 compounds.

Mean free path is a fundamental parameter closely related to all reactions induced by electron beam radiation in the mixture. It was estimated based on an ideal gas law for both the pure substance system and a mixture system and shown in figure 81c and 81d. Mean free path in a pure substance system is close to a few tens of thousands of nanometer due to low pressure whereas its value is only a few nanometer in a system with hydrocarbon mixtures. For any radiation system with a size in the range of mm to m, the Knudsen number will be orders of magnitude smaller than 10, which means that we will not have a molecular flow where molecules only interact with the wall and don't see each other. But compared to a mean free path in liquids, those numbers are significantly larger.

Therefore molecules still strongly interact with each other but the interaction rate will be orders of magnitude lower than that in liquids.

We could relate the mean free path to reaction pathways in irradiated hydrocarbons induced by electron beam. More specifically, polymerization is a free radical combination process that is favored by smaller mean free path and higher collision frequency. Cracking is also a radical driven process but less depends on the collision frequency and mean free path because it is initiated from a single molecule. Then reactions propagate involving more collisions with other species to finally terminate the reaction. One extreme case is that when mean free path is too large without collisions, activated molecules will be terminated by colliding with the reactor wall, which leads to polymerized products. This is a typical semiconductor processing condition normally with very low energy efficiency. We are not interested in this operating region because of its low energy efficiency and polymerization occurred on the wall. The other extreme condition is irradiating hydrocarbons with too high collision frequency and small mean free path, for example irradiation of liquids or solids. Due to the high collision frequency, activated species have very high probability of recombining with each other and cause them to grow instead of decomposition.

So far the process of irradiating hydrocarbon vapors is still at a stage of idea initiation and system design. Even though simulation results provided significant theoretical support on its practical viability, more investment and efforts are required to finally implement this idea in a controlled manner to achieve our goal. It is also worth pointing out that results from irradiating petroleum vapors may not be as expected due to

incredible complexity of hydrocarbon irradiation. But it will provide important insight to the nature of irradiation of hydrocarbons under different conditions. Hopefully the map of radiation processing of hydrocarbons will be more complete by then.

CHAPTER X

CONCLUSIONS AND FUTURE WORK

10.1 Conclusions

Multiple experiments were conducted on irradiation of two heavy crude oils with high dose rate electron beam in a flow system. Parameters were varied during the experiments to study their effect on crude oil irradiation. A series of selected neat hydrocarbons were also irradiated by using the same electron beam source to understand the fundamental reaction mechanism of hydrocarbon irradiation. As illustrated in the dissertation motivations and objectives, the focus of this dissertation is to explore the feasibility of petroleum irradiation by understanding the fundamental mechanisms of irradiating different hydrocarbon compounds and characterize the chemical change induced by high dose rate electron beam.

Extensive literature review on petroleum refinery process and refining chemistry laid out the first foundation for this dissertation. Refining process in a refinery needs to work with specific feedstock and each refinery should vary with the feedstock. In general refinery processes could be divided into three major categories: separation, conversion and finishing. The scope of this dissertation is still a general refinery process, but it may have combined the categories in both an active way and passive way. For example the use of a separation chamber to trap evaporated species is to separates products from source materials being irradiated. Conversion occurs when hydrocarbon compounds in oils are activated by electron beam. Then chain reactions propagate to produce more radicals and

products. Multiple finishing processes may happen after hydrocarbon compounds are activated. Polymerization is one of the most common finishing processes in a refinery. It is possible that polymerization of activated compounds has led to the production of heavy products in irradiated oils, especially when oil temperature was within the range of polymerization. However, because of the broad scope of the research, it is possible that polymerization of activated compounds has led to the production of heavy products in irradiated oils, especially when oil temperature was in the range of polymerization window. This resulted in an overall low conversion.

Irradiation of petroleum as a potential refining technology in many ways is similar to a thermal method. Hydrocarbon cracking pathways are also identical. This implies that we could simply combine a thermal method with the irradiation method to achieve the same goal. Synergistic effect of radiation on petroleum thermal cracking has been observed. This demonstrates that the radiation method alone as a refining technology may not be enough, or it requires a very narrow operation parameters window, e.g. high dose rate.

The continuous flow system was designed and tested in the lab. It was composed of a few components including the processing box, high temperature pump, motor, channel, oil tank, separation chamber, heaters and insulation materials. A fire monitor and fire suppression system were also developed to work with the flow system. Real time videos were recorded and two fire extinguishers were targeted at the oil tank and processing box. Activation of the fire extinguishers were controlled in the control room based on the real time video. The remote control table was also located in the control room.

It was responsible for data logging and motor control. It also controlled air, water, gas and oil flow on the flow system. The entire system was designed in a way that is portable, independent and suitable with the electron beam facility at Texas A&M University. Flow system allows for irradiation of heavy or extra heavy oils at desirable conditions. Oil flow rate ranges from 0 to 3 LPM. Temperature ranges from 25 to 300 ^{o}C. Dose rate and dose are in the range of 0-20 kGy/s and 0 - ~3000 kGy. Multiple channels were designed and tested to achieve gas bubbling and constant oil temperature processing. One challenge was to combine gas bubbling and effective water cooling. Design of a water cooling jacket was able to successfully enable gas bubbling and effective water cooling at the same time.

Design of experiment (DOE) allowed us to screen important parameters in the irradiation of oil. The goal of DOE was to reduce the number of tests and used limited resources to achieve the best results. In this dissertation research, we investigated the effects of dose, temperature, gas bubbling and shear rate on irradiated oils. Parameters are not always independent from each other, e.g. temperature and shear rate. But we were still able to vary each parameter at once and kept others constant by slightly changing parameters that are known to have no effect or little effect on irradiation process.

Two heavy crude oils were irradiated at various conditions to study the effect of parameters mentioned above. Firstly, crude oil A was irradiated with very low dose (10-40 kGy) at different shear rates (10-100 s-1) to study the effect of shear rate and shear stress. It is known that large shear stress and shear rate can both change the particles' structure such as heavy oil structures and make them more susceptible to electron beam radiation. Results showed that there was no significant change on the viscosity of

irradiated oil A, which indicates that shear stress or shear rate were not able to change the fundamental structure of irradiated oil A with low energy input. Higher dose in irradiation of both oil A and oil B was more effective on viscosity reduction and heavy fraction conversion. Conversion to light products in both oil A and oil B was estimated by using the GC-FID analysis. About 3% to 7% conversion was achieved in oil A with medium energy input in the range of 300-600 kGy. Yields of light products in oil A were also estimated with known conversion and energy input. Total yields of light hydrocarbon products in the range of C10 to C25 are in the range of 2-3 molecules/100eV. Similarly conversion and yields were also calculated for irradiation of crude oil B. Conversion to light products in oil B could be as high as 12% with medium energy input. Yields of products were also higher than those of oil A. Total yields of light products are in the range 2.2-7.7 molecules/100eV. Yields of light products from irradiation of both crude oils are lower than those from irradiating a pure compounds, partially because products here are C10-C25, whose molecular weight is much larger than that of products from irradiating pure compounds. Note that products in this range are in the gasoline and diesel range which are the most valuable fractions in petroleum. More irradiation tests were performed with a specially designed water cooling jacket to reduce thermal effects of the beam. With the water cooling jacket, we were able to control oil temperature within ±20 ^{o}C to achieve radiation oil processing at constant temperature. This water cooling jacket was designed in way to maximize the cooling surface area between water and hot surfaces. Six tests were conducted with this jacket at various temperatures. In general, it was able to control the oil temperature in a broad window: 100-300 ^{o}C.

Important parameters including temperature, dose and condensates were compared based on their effect on for viscosity reduction for those two oils. There was an enhancing effect of temperature on viscosity reduction in the range of 200 and 250 ^{o}C for multiple energy input. Temperature effect during irradiation of oil B was not clear due to very limited number of runs. Dose was varied with a wide range between 100 kGy to 1500 kGy in irradiation of both oils. No clear trend was observed. Viscosity reduction in irradiated oil A highly depends on the total condensates. More condensates in irradiated oil means a higher viscosity reduction and vice versa. The trend was less clear between total condensates and viscosity reduction in irradiated oil B. This might be due to the very limited number of experiments.

Mineral oil was irradiated with about 300-500 kGy by passing 20 to 30 times down the channel at 18-24 kGy per pass. Temperature was controlled to be 80 oC or 150 ^{o}C +/- 10 ^{o}C. Three conditions are compared varying processing temperature and mixing gas, helium at 80 ^{o}C, methane at 80 ^{o}C and helium at 150 ^{o}C. The oil became yellow with irradiation and was darker for helium processing. Analysis by GC-FID showed 7%-12% conversion in treated samples and about 60% product selectivity of the converted products to light hydrocarbons right after the irradiation experiment. Stability of products was tested after two years and showed reduced conversion to light products, but heavy products remained the same. Initially 63%, after aging product selectivity to lights became 46% in sample irradiated at higher temperature and reduced from 62% to 18% in sample irradiated at lower temperature. Viscosity of treated samples with helium showed 6-8% increase compared to raw sample. Overall conversion yields in the flow system are 4 to 7

molecules/100eV higher than literature for batch processing of alkanes and cycloalkanes. Irradiation with methane had higher yields and higher selectivity to lighter products compared to helium. Product selectivity to light products is 72% after two years and total yield to lights is 4.4 molecules/100eV. Methane gas led to higher yield with almost no viscosity increase and less color change. These results indicate that oil conversion by irradiation is significant, can be long term and trend toward lighter molecules, and that gas and temperature plays a role in the electron beam induced conversion process and aging.

A series of hydrocarbons were irradiated by the same electron beam but with low dosees rate. Hydrocarbon samples were selected to represent saturated alkanes, alkanes with ring structure, aromatics, aromatics with branches of different lengths and polyaromatics. Three groups were classified based on their saturation degree (SatuDe). Saturation degree of hydrocarbons indicates the hydrogen deficiency of a hydrocarbon inside its molecule and have been widely used in chemistry field. It affects the physicochemical properties of a molecule such as its molecular geometry, average chemical bond strength as well as electron density distribution. It varies in the range of 0-1. The hydrocarbons were irradiated in a batch reactor submerged in a water bath in a temperature range of 5-20 ^{o}C. Dose rate in the range of 4.5 - 5 kGy/s was measured with calibrated dosimeters. Irradiation of straight saturated alkanes represented by pentane caused about 10% conversion to both light and heavy products. Yields of products were very high due to a high conversion, but no color change was observed. Product selectivity is almost 50% lights to 50% heavies. But no color change was observed. Saturated alkanes with ring structure (Methylcyclohexane and cyclohexane) overall had lower conversion than

pentane but tended to polymerize and produce significant amounts of dimer and trimer products. Product selectivity to heavies is much higher than that of lights. Yields of the polymerized products are quite high. Hydrocarbons with an unsaturated ring or rings are much less susceptible to electron beam irradiation and are not prone to conversion. GC-MS was able to detect polymerized products from irradiating those hydrocarbons, but the conversion was less than 1% for most of the compounds. Very interestingly, those compounds all showed significant color change after irradiation. Yellowness could be used to quantify the color change of irradiated samples and it increased with increasing the compound saturation degree.

Based on what we have learned and observed from doing this dissertation research, I would like to conclude this research topic with a few points regarding irradiation of petroleum:

1. Irradiation of petroleum depends on many parameters such as temperature, dose, use of gas donors and so on. It is hard to predict which one is more dominant in the process. In general, higher temperature, more reactive gas and higher dose favor the conversion of heavy oils.
2. Fraction or chemical composition of petroleum is probably more important than all the parameters mentioned above when predicting the conversion and products from irradiating a certain type of petroleum feedstock.
3. It is very challenging to predict conversion and products from irradiating crude oils due to unknown hydrocarbon distribution and chemistry, but it is possible to

estimate conversion and yields from irradiating a pure substance based on its physiochemical properties such as saturation degree.

4. Two chemical reaction pathways dominates the process of hydrocarbons irradiation: cracking and polymerization. External conditions such as gas supply, temperature and pressure could be altered to favor or suppress them, but the effect might be very limited unless creating extreme conditions, e.g. vacuum pressure or diluted with natural gas. More fundamentally, a certain type of hydrocarbon species may inherently favor one of the pathways because of its nature, for example, hydrocarbons with rings could polymerize a lot more easily than cracking.

5. To make irradiation of crude oils more effective, Irradiation of crude oils could be more effective if we might have to separate some certain fractions or species that favor cracking are separated and selectively irradiated without those that are in favor of cracking and avoid those that tend to polymerize. Conversion and yields will be optimized by using this strategy.

10.2 Future work

The results and efforts involved from conducting this dissertation research has led to the expansion of current research and a few new research directions. These include four major aspects: (1) better characterization techniques to study crude oil chemical composition and products; (2) irradiation of different crude oil fractions at different condition and their products distribution; (3) study of radiation chemistry, yields and

product selectivity; (4) economic analysis of irradiation of crude oil for industrial scale operation.

10.2.1 Better characterization techniques

To characterize tens of thousands of compounds in crude oil is tremendously challenging and often leads to confusing results. A limitation in this research with possible avenue for further explorations (though perhaps by an organic chemistry scientist and not a mechanical engineer) is the better characterization of petroleum, especially crude oil samples which were irradiated at different conditions. GC-FID and rheometer were the primary techniques used to study conversion and viscosity change in this research. Those two parameters, though very accurate and important, are not enough to fully characterize the chemical change in irradiated samples. GC-MS and TGA were used to quantitatively study the compounds change in pure hydrocarbons. Consistent results were observed from both of them. Those two techniques could also be used for crude oil analysis. Multiple GC columns equipped with different stationary phase are even more powerful for this purpose. For example GC-GC-FID or GC-GC-MS are both multiple dimensional techniques that could provide more detailed information regarding species in crude oils. Fourier transform infra-red (FTIR) spectroscopy could be performed on the petroleum compounds to determine some of the C-C and C-H bonding

10.2.2 Irradiation of different crude oil fractions

Irradiation of neat or pure hydrocarbons showed very different results from crude oil irradiation on conversion. Part of the reason is due to simpler characterization of the pure compounds after irradiation. More fundamentally, the difference was caused by the nature of irradiated samples. Irradiation of pure substance induces chemical reactions that only involve species resulted from the parent molecules. Those species share many common properties and might behave in a similar way during the irradiation process. However, crude oils are comprised of both hydrocarbons and non-hydrocarbons. Even hydrocarbons in crude oils vary dramatically in their response to radiation. Saturates are known to be very susceptible to electron beam irradiation and tend to produce many chain scission products. Aromatics and asphaltene, however are more stable and produce less products or polymerized products. In this research, crude oils were irradiated as bulk liquids without any separation, which indicates that all species will have equal chance to interact with other species. Higher concentration of aromatics and asphaltene might have greatly mitigated the effect of irradiation on other fractions such as saturates. This might have resulted in a significant loss on both conversion and yields. If fractions in crude oils are separated before irradiation, conversion and yield results will be different. It is highly possible that selective irradiation of saturated fraction and avoidance of asphaltene fraction will make this technology work better.

Separation of crude oil fractions is very energy intense and requires high temperature or low pressure system. The separation system needs to be compatible with the current electron beam irradiation system. Many system design and build work will be

different from our current system. Standard operating procedure and project safety analysis will be reinitiated and processed.

10.2.3 Radiation chemistry and yields of HC mixture

In this research dissertation, radiation chemistry of hydrocarbons was introduced quite comprehensively in the literature review section. Two fundamental chemical process induced by electron beam irradiation are polymerization and cracking. They coexist and compete in almost all hydrocarbons irradiation. This was demonstrated by yields of chain scission and polymerized products from different irradiated compounds. Yields from irradiating a certain compound provides information regarding whether this compound favors cracking or polymerization. It largely determines if this compound is suitable for applying this technology. But accurate yields calculation requires very detailed information about the product such as molecular structure and molecular weight. This is related to the first future work which is about radiation product characterization.

Chemistry in a pure substance might be well understood and well predicted on its products and yields. But petroleum is a mixture of tens of thousands of compounds with different properties. Chemistry in a mixture does not simply replicate chemistry from the pure substances. For example, yields from irradiating hydrocarbon mixtures are never a linear summation of yields from each compound in the mixture. Part of the reason is due to coupled chemistry when different compounds interact with each other. A binary mixture of alkane and aromatic could be irradiated and compared to the results from irradiating one of them. The fractions of each compound should vary to study the effect of mass ratio

on yields. It is possible that yields of a mixture like this scale up with the mass ratio by following an exponential or power law. And this phenomenon might be related to the electron density and distribution from two different species. Results will reveal how sensitive yields are to different compounds and their mass ratio in the mixture. This is very useful because we might be able to extrapolate the yields from irradiation crude oils based on yields and known mass ratio of each fraction.

10.2.4 Economics

Economic analysis of irradiation of petroleum could be a separate topic for future work. It needs to address the capital cost of accelerator, shielding and accessories inside an electron beam facility and any other accessories, operational cost of electricity, fuel and cooling air or water. Specific energy input into irradiated crude oils to achieve desired conversion and the price of the raw and product are both required information. After all these are known, the calculation of profitability could be performed by a *rate of return* (ROI) on investment method. ROI is the ratio of annual net profit to the total capital investment.

$$ROI = \frac{annual\ net\ profit}{total\ capital\ invesment}$$

ROI might be compared to a certain profitability standard and investment decisions should be made based on that. In general, higher ROI means that the process is desirable for the investment but might be risky.

The irradiation process uses electrical energy and convert low value fractions to high value fractions in crude oils. Therefore the price of treated oil becomes higher and

depends on the conversion and price differential between original feedstock and upgraded oil. Figure 82 shows the energy input and value change during the process. Feedstock was 20 $ per barrel. The upgrading process spent x $ and converted c% to product 2 at higher price.

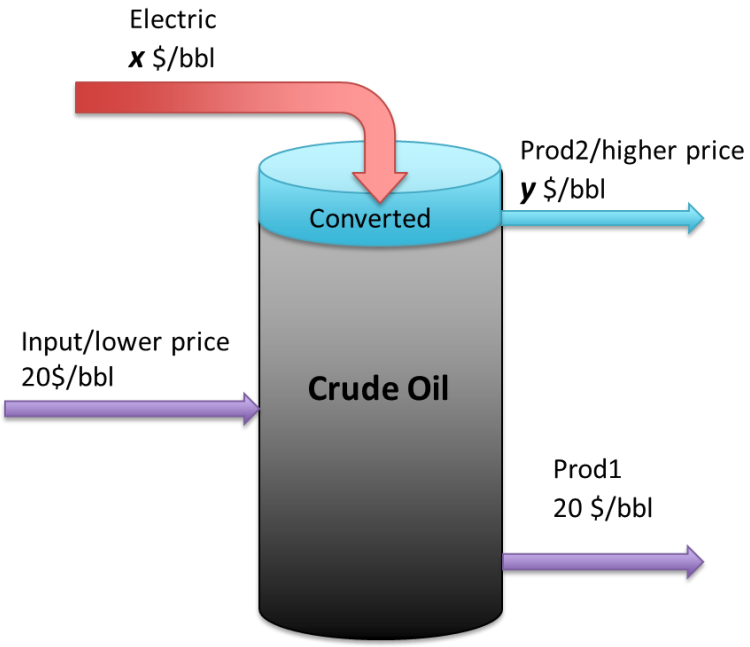

Figure 82: Oil upgrading process with energy input and price differential

We presented the relationship between the minimum required value added to processed oil and conversion at each specific energy input. We assumed that the power of accelerator was 500 kW and efficiency of it was 50%. Oil throughput was 5000 bbl/day. Natural gas was 95% recycled. Water was completely recycled and air cooled. Power required to recycle natural gas and water was assumed to be 10% of the power of accelerator. Total

operational costs were calculated. Figure 83 showed the results. If conversion caused by irradiation increases, the minimum required value added to oil will drop, which indicates a higher profitability of this process. Higher SEI compared to lower SEI requires higher conversion in order to make the process economical. For example, if breakeven price is at 30 $ between diluent and heavy crude, the required conversion will be higher than 8% in order to be profitable for SEI 500 kJ/kg. This means that process has a huge potential to be economically viable. While at the same energy input conversion has to be above 14% if this technology is used in refinery to process residuum and produce distillates. Results from processing both crude oils and mineral oil were showed on the process economics map. Oil A processing was not economically viable due to low conversion. Mineral oil economic results were on the border of profitability. Oil B results showed great profitability potential with high conversion with relatively low energy input. The minimum required price differential for Oil B is about 20 $ which is 10$ below the price differential between diluent and heavy oil. This indicates that electron beam irradiation of Oil B could be used in a partial upgrader.

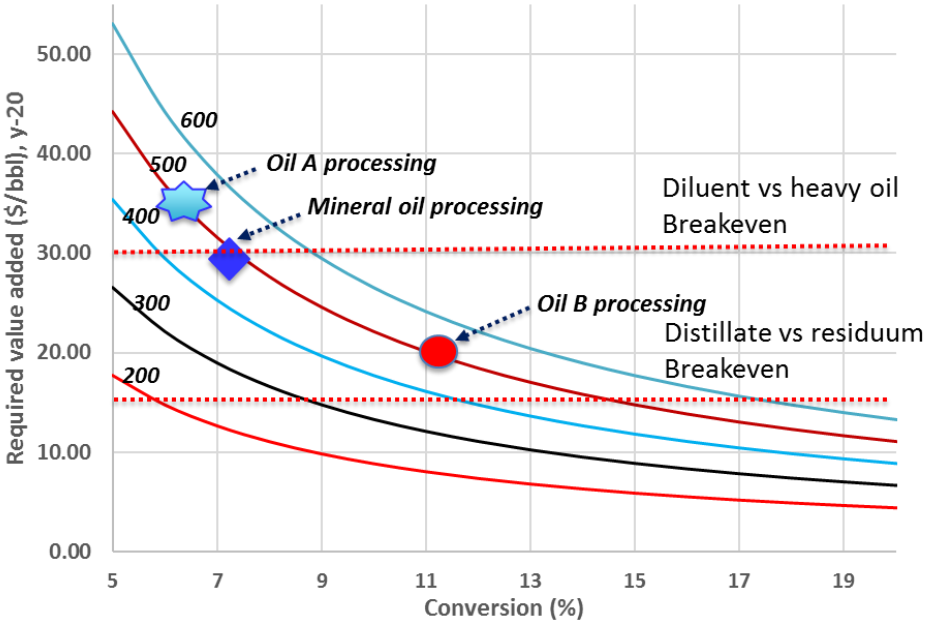

Figure 83: Minimum required value added to oil changes with conversion

REFERENCES

[1] Speight JG. Visbreaking: A technology of the past and the future. Scientia Iranica 2012;19:569–73. doi:10.1016/j.scient.2011.12.014.

[2] Rana MS, Sámano V, Ancheyta J, Diaz JAI. A review of recent advances on process technologies for upgrading of heavy oils and residua. Fuel 2007;86:1216–31. doi:10.1016/j.fuel.2006.08.004.

[3] Huc A-Y. Heavy Crude Oils: From Geology to Upgrading : an Overview. 2010.

[4] Grubb M. Who's afraid of atmospheric stabilisation? Making the link between energy resources and climate change. Energy Policy 2001;29:837–45. doi:10.1016/S0301-4215(00)00128-2.

[5] Boduszynski MM, Altgelt KH. Composition of Heavy Petroleums .4. Significance of the Extended Atmospheric Equivalent Boiling-Point (Aebp) Scale. Energy Fuels 1992;6:72–6. doi:10.1021/ef00031a011.

[6] Boduszynski MM. Composition of Heavy Petroleums. Molecular weight, hydrogen deficiency, and heteroatoms concentration as a function of atmospheric equivalent boiling point up to 1400°F. Energy & Fuels 1987;305:2–11. doi:10.1021/ef00001a001.

[7] Silva SL, Silva AMS, Ribeiro JC, Martins FG, Da Silva FA, Silva CM. Chromatographic and spectroscopic analysis of heavy crude oil mixtures with emphasis in nuclear magnetic resonance spectroscopy: A review. Analytica Chimica Acta 2011;707:18–37. doi:10.1016/j.aca.2011.09.010.

[8] Hasan SW, Ghannam MT, Esmail N. Heavy crude oil viscosity reduction and

rheology for pipeline transportation. Fuel 2010;89:1095–100. doi:10.1016/j.fuel.2009.12.021.

[9] Hart A. Advanced Studies of Catalytic Upgrading of Heavy Oils. 2014.

[10] Huc A-Y. Heavy Crude Oils - From Geology to Upgrading, an Overview. Editions Technip; 2011.

[11] Speight JG. Chemistry and Technology of Petroleum (5th Edition). 5th ed. CRC Press; 2014.

[12] Cheremisinoff NP. Handbook of Pollution Prevention and Cleaner Production. 2012. doi:10.1016/B978-1-4377-7815-1.00004-7.

[13] Scherzer J, Gruia AJ. Hydrocracking science and technology. 1996.

[14] Pines H. The Chemistry of Catalytic Hydrocarbons Conversions. Academic Press; 1981.

[15] Olah GA, Molnar A. Hydrocarbon chemistry. vol. Volume II: 2003.

[16] Sadrameli SM. Thermal/catalytic cracking of liquid hydrocarbons for the production of olefins: A state-of-the-art review II: Catalytic cracking review. Fuel 2016;173:285–97. doi:10.1016/j.fuel.2016.01.047.

[17] Rana MS, S??mano V, Ancheyta J, Diaz JAI. A review of recent advances on process technologies for upgrading of heavy oils and residua. Fuel 2007;86:1216–31. doi:10.1016/j.fuel.2006.08.004.

[18] Speight JG. Visbreaking: A technology of the past and the future. Scientia Iranica 2012;19:569–73. doi:10.1016/j.scient.2011.12.014.

[19] Joshi JB, Pandit AB, Kataria KL, Kulkarni RP, Sawarkar AN, Tandon D, et al.

Petroleum residue upgradation via visbreaking: A review. Industrial and Engineering Chemistry Research 2008;47:8960–88. doi:10.1021/ie0710871.

[20] Mohaddecy SRS, Sadighi S, Ghabuli O, Rashidzadeh M. Simulation of a visbreaking unit. Petroleum Technology Quarterly 2011;16.

[21] Chen QL, Yin QH, Wang SP, Hua B. Energy-use analysis and improvement for delayed coking units. Energy 2004;29:2225–37. doi:10.1016/j.energy.2004.03.021.

[22] Ikan R. Natural and Laboratory-Simulated Thermal Geochemical Processes 2003.

[23] Khorasheh F, Gray MR. High-pressure thermal cracking of n-hexadecane. Industrial & Engineering Chemistry Research 1993;32:1853–63. doi:10.1021/ie00021a008.

[24] Wu G, Katsumura Y, Matsuura C, Ishigure K. Comparison of Liquid-Phase and Gas-Phase Pure Thermal Cracking of n-Hexadecane. Industrial & Engineering Chemistry Research 1996;35:4747–54. doi:10.1021/ie960280k.

[25] Speight JG. The Chemistry and Technology of Petroleum, Fifth Edition. CRC Press; 2014. doi:10.1201/9781420008388.

[26] Biswas J, Maxwell IE. Recent process- and catalyst-related developments in fluid catalytic cracking. Applied Catalysis 1990;63:197–258. doi:10.1016/S0166-9834(00)81716-9.

[27] Rahimi N, Karimzadeh R. Catalytic cracking of hydrocarbons over modified ZSM-5 zeolites to produce light olefins: A review. Applied Catalysis A: General 2011;398:1–17. doi:10.1016/j.apcata.2011.03.009.

[28] Beds CF. Circulating Fluidized Beds. 1997.

[29] Nathan AJ, Scobell A. How China sees America. Foreign Affairs 2012;91. doi:10.1017/CBO9781107415324.004.

[30] Cortright RD, Dumesic JA. Kinetics of heterogeneous catalytic reactions: Analysis of reaction schemes. Advances in Catalysis 2001;46:161–264. doi:10.1016/S0360-0564(02)46023-3.

[31] Tominaga H, Tamaki M. Chemical Reaction and Reactor Desing. 1997.

[32] Choudhary N, Saraf DN. Hydrocracking: A Review. Industrial and Engineering Chemistry Product Research and Development 1975;14:74–83. doi:10.1021/i360054a002.

[33] Valavarasu G, Bhaskar M, Balaraman KS. Mild hydrocracking - A review of the process, catalysts, reactions, kinetics, and advantages. Petroleum Science and Technology 2003;21:1185–205. doi:10.1081/LFT-120017883.

[34] Ward JW. Hydrocracking processes and catalysts. Fuel Processing Technology 1993;35:55–85. doi:10.1016/0378-3820(93)90085-I.

[35] Oyekunle LO, Ikpekri OB, Jaiyeola A. Modelling of hydrodesulfurization catalysts: II. Effects of catalyst pore structures on deactivation by metal deposits. Catalysis Today 2005;109:128–34. doi:10.1016/j.cattod.2005.08.012.

[36] Weitkamp J. Catalytic Hydrocracking-Mechanisms and Versatility of the Process. ChemCatChem 2012;4:292–306. doi:10.1002/cctc.201100315.

[37] Chica A, Corma A. Hydroisomerization of pentane, hexane, and heptane for improving the octane number of gasoline. Journal of Catalysis 1999;187:167–76.

doi:10.1006/jcat.1999.2601.

[38] Mühl J, Srica V, Jednacak M. Determination of reformed gasoline octane 1989;68:201–3.

[39] Protić-Lovasić G, Jambrec N, Deur-Siftar D, Prostenik M V. Determination of catalytic reformed gasoline octane number by high resolution gas chromatography. Fuel 1990;69:525–8. doi:10.1016/0016-2361(90)90328-N.

[40] Carter JL, McVinker GB, Weissman W, Kmak MS, Sinfelt JH. Bimetallic catalysts; application in catalytic reforming. Applied Catalysis 1982;3:327–46. doi:10.1016/0166-9834(82)80267-4.

[41] Wei W, Chang S, Box P-. United States Patent [19] 1997.

[42] Rodríguez MA, Ancheyta J. Detailed description of kinetic and reactor modeling for naphtha catalytic reforming. Fuel 2011;90:3492–508. doi:10.1016/j.fuel.2011.05.022.

[43] Ciapetta FG, Wallace DN. Catalytic naphtha reforming. vol. 5. 1972. doi:10.1080/01614947208076866.

[44] Wang P, Zhang M, Zhang W, Yang C, Li C. Isomerization of n-Butane over SO_4^{2-} /Al_2O_3–ZrO_2 in a Circulated Fluidized Bed Reactor: Prospects for Commercial Application. Industrial and Engineering Chemistry Research 2017;56. doi:10.1021/acs.iecr.7b01858.

[45] Blekkan EA, Pham-Huu C, Ledoux MJ, Guille J. Isomerization of n-Heptane on an Oxygen-Modified Molybdenum Carbide Catalyst. Industrial and Engineering Chemistry Research 1994;33:1657–64. doi:10.1021/ie00031a003.

[46] Zhang A, Nakamura I, Aimoto K, Fujimoto K. Isomerization of n-Pentane and Other Light Hydrocarbons on Hybrid Catalyst. Effect of Hydrogen Spillover. Industrial and Engineering Chemistry Research 1995;34:1074–80. doi:10.1021/ie00043a008.

[47] Surla K, Vleeming H, Guillaume D, Galtier P. A single events kinetic model: N-butane isomerization. Chemical Engineering Science 2004;59:4773–9. doi:10.1016/j.ces.2004.07.036.

[48] Tran MT, Gnep NS, Szabo G, Guisnet M. Isomerization of n-butane over H-mordenites under nitrogen and hydrogen: Influence of the acid site density. Journal of Catalysis 1998;174:185–90. doi:10.1006/jcat.1998.1967.

[49] Van De Runstraat A, Kamp JA, Stobbelaar PJ, Van Grondelle J, Krijnen S, Van Santen RA. Kinetics of hydro-isomerization of n-hexane over platinum containing zeolites. Journal of Catalysis 1997;171:77–84. doi:10.1006/jcat.1997.1779.

[50] Wulfers MJ, Jentoft FC. Mechanism of n-butane skeletal isomerization on H-mordenite and Pt/H-mordenite. Journal of Catalysis 2015;330:507–19. doi:10.1016/j.jcat.2014.12.035.

[51] Chu HY, Rosynek MP, Lunsford JH. Skeletal isomerization of hexane over Pt/H-beta zeolites: Is the classical mechanism correct? Journal of Catalysis 1998;178:352–62. doi:10.1006/jcat.1998.2136.

[52] Benitez VM, Yori JC, Grau JM, Pieck CL, Vera CR. Hydroisomerization and cracking of n-octane and n-hexadecane over zirconia catalysts. Energy and Fuels 2006;20:422–6. doi:10.1021/ef050092j.

[53] Sinha AK, Sivasanker S, Ratnasamy P. Hydroisomerization of n -Alkanes over Pt - SAPO-11 and Pt - SAPO-31 Synthesized from Aqueous and Nonaqueous Media. Industrial & Engineering Chemistry Product Research and Development 1998;5885:2208–14. doi:10.1021/ie9707228.

[54] Kennedy JW. Principles of Polymer Chemistry. Journal of the American Chemical Society 1954;76:2854. doi:10.1021/ja01639a091.

[55] Jiang P, Wu X, Zhu L, Jin F, Liu J, Xia T, et al. Production of jet fuel range paraffins by low temperature polymerization of gaseous light olefins using ionic liquid. Energy Conversion and Management 2016;120:338–45. doi:10.1016/j.enconman.2016.05.010.

[56] Pfister D, Storti G, Tancini F, Costa LI, Morbidelli M. Synthesis and ring-opening polymerization of cyclic butylene 2,5-fFurandicarboxylate. Macromolecular Chemistry and Physics 2015;216:2141–6. doi:10.1002/macp.201500297.

[57] Xin R, Zhang J, Sun X, Li H, Ren Z, Yan S. Polymorphic behavior and phase transition of Poly(1-Butene) and its copolymers. Polymers 2018;10. doi:10.3390/polym10050556.

[58] Lee HK, Bang KT, Hess A, Grubbs RH, Choi TL. Multiple Olefin Metathesis Polymerization That Combines All Three Olefin Metathesis Transformations: Ring-Opening, Ring-Closing, and Cross Metathesis. Journal of the American Chemical Society 2015;137:9262–5. doi:10.1021/jacs.5b06033.

[59] Zhang Q, Jiang Y, Yao L, Jiang Q, Qiu Y. Hydrophobic surface modification of ramie fibers by plasma-induced addition polymerization of propylene. Journal of

Adhesion Science and Technology 2015;29:691–704. doi:10.1080/01694243.2014.997380.

[60] Luo L, Zhang N, Xia Z, Qiu T. Dynamics and stability analysis of gas-phase bulk polymerization of propylene. Chemical Engineering Science 2016;143:12–22. doi:10.1016/j.ces.2015.12.018.

[61] Shamiri A, Azlan Hussain M, Sabri Mjalli F, Mostoufi N, Saleh Shafeeyan M. Dynamic modeling of gas phase propylene homopolymerization in fluidized bed reactors. Chemical Engineering Science 2011;66:1189–99. doi:10.1016/j.ces.2010.12.030.

[62] Martins AR, Cancelas AJ, McKenna TFL. A Study of the Gas Phase Polymerization of Propylene: The Impact of Catalyst Treatment, Injection Conditions and the Presence of Alkanes on Polymerization and Polymer Properties. Macromolecular Reaction Engineering 2017;11:1–14. doi:10.1002/mren.201600011.

[63] Liu S, Chen C, Yu F, Li L, Liu Z, Yu S, et al. Alkylation of isobutane/isobutene using Bronsted-Lewis acidic ionic liquids as catalysts. Fuel 2015;159:803–9. doi:10.1016/j.fuel.2015.07.053.

[64] Gerzeliev IM, Ostroumova VA, Zhmylev VP, Khadzhiev SN. Comparative Evaluation of Zeolite Catalysts of Benzene Alkylation. Russian Journal of Applied Chemistry 2018;91:959–63. doi:10.1134/S1070427218060125.

[65] Kolesnikov IM, Vinokurov VA, Gushchin PA, Ivanov E V., Kolesnikov SI, Lyubimenko VA. Efficient catalysts for benzene alkylation with olefins. Catalysis

Communications 2016;82:1–6. doi:10.1016/j.catcom.2016.04.001.

[66] Ivashkina EN, Ivanchina ED, Nurmakanova AE, Boychenko SS, Ushakov AS, Dolganova IO. Mathematical Modeling Sulfuric Acid Catalyzed Alkylation of Isobutane with Olefins. Procedia Engineering 2016;152:81–6. doi:10.1016/j.proeng.2016.07.632.

[67] Omarov SO, Vlasov EA, Sladkovskiy DA, Semikin K V., Matveyeva AN, Fedorov SP, et al. Physico-chemical properties of MoO3/ZrO2catalysts prepared by dry mixing for isobutane alkylation and butene transformations. Applied Catalysis B: Environmental 2018;230:246–59. doi:10.1016/j.apcatb.2018.02.020.

[68] Gan P, Tang S. Research progress in ionic liquids catalyzed isobutane/butene alkylation. Chinese Journal of Chemical Engineering 2016;24:1497–504. doi:10.1016/j.cjche.2016.03.005.

[69] Woods R, Pikaev A. Applied radiation chemistry: radiation processing. 1994.

[70] Woo L, Sandford CL. Comparison of electron beam irradiation with gamma processing for medical packaging materials. Radiation Physics and Chemistry 2002;63:845–50. doi:10.1016/S0969-806X(01)00664-8.

[71] Berejka AJ, Cleland MR, Walo M. The evolution of and challenges for industrial radiation processing-2012. Radiation Physics and Chemistry 2014;94:141–6. doi:10.1016/j.radphyschem.2013.04.013.

[72] Cleland MR, Parks LA, Cheng S. Applications for radiation processing of materials. Nuclear Instruments and Methods in Physics Research, Section B: Beam Interactions with Materials and Atoms 2003;208:66–73.

doi:10.1016/S0168-583X(03)00655-4.

[73] Sang W, Speakmon M, Zhou L, Wang Y, Lei C, Pillai SD, et al. Detrimental effects of electron beam irradiation on the cowpea bruchid *Callosobruchus maculatus*. Pest Management Science 2016;72:787–95. doi:10.1002/ps.4053.

[74] Xiong C, Liu C, Liu W, Pan W, Ma F, Chen W, et al. Noninvasive discrimination and textural properties of E-beam irradiated shrimp. Journal of Food Engineering 2016;175:85–92. doi:10.1016/j.jfoodeng.2015.12.008.

[75] Smith B, Ortega A, Shayanfar S, Pillai SD. Preserving quality of fresh cut watermelon cubes for vending distribution by low-dose electron beam processing. Food Control 2016:1–5. doi:10.1016/j.foodcont.2016.02.017.

[76] Zhang Y, Rodrigue D, Ait-Kadi A, Liu IC, Chuang CK, Tsiang RCC, et al. Crosslinked polyethylene foams, via eb radiation. Radiation Physics and Chemistry 1998;52:197–200. doi:10.1016/S0969-806X(98)00139-X.

[77] Datta SK, Chaki TK, Khastgir D. Effect of electron beam radiation on mechanical and electrical properties of poly (ethy1ene-co-vinyl acetate) 1996;238:105–17.

[78] Salehi SM a, Mirjalili G, Amrollahi J. Effects of High-Energy Electron Beam on Low-Density Polyethylene Materials Containing EVA 2003;2:2–5.

[79] Zhang Y, Rodrigue D, Ait-Kadi A. High-Density Polyethylene Foams. I. Polymer and Foam Characterization. Journal of Applied Polymer Science 2003;90:2111–9. doi:10.1002/app.12821.

[80] Borhani Zarandi M, Amrollahi Bioki H. Thermal and mechanical properties of blends of LDPE and EVA crosslinked by electron beam radiation. The European

Physical Journal Applied Physics 2013;63:21101. doi:10.1051/epjap/2013130238.

[81] Silindir M, Özer AY. Sterilization methods and the comparison of E-beam sterilization with gamma radiation sterilization. Fabad Journal of Pharmaceutical Sciences 2009;34:43–53.

[82] Buchalla R, Schüttler C, Bögl KW. Radiation sterilization of medical devices. Effects of ionizing radiation on ultra-high molecular-weight polyethylene. Radiation Physics and Chemistry 1995;46:579–85. doi:10.1016/0969-806X(95)00222-J.

[83] Bang-Tai Tang, T-CH. Semiconductor device strusture with cap layer with top and bottom portions over gate electrode, 2018.

[84] Han B, Kyu Kim J, Kim Y, Seung Choi J, Young Jeong K. Operation of industrial-scale electron beam wastewater treatment plant. Radiation Physics and Chemistry 2012;81:1475–8. doi:10.1016/j.radphyschem.2012.01.030.

[85] Cleland MR, Parks LA. Medium and high-energy electron beam radiation processing equipment for commercial applications. Nuclear Instruments and Methods in Physics Research, Section B: Beam Interactions with Materials and Atoms 2003;208:74–89. doi:10.1016/S0168-583X(03)00672-4.

[86] Melorose J, Perroy R, Careas S. Reviews of Accelerator Science and Technology. Statewide Agricultural Land Use Baseline 2015 2015;1. doi:10.1017/CBO9781107415324.004.

[87] Melorose J, Perroy R, Careas S. No Title No Title. Statewide Agricultural Land Use Baseline 2015 2015;1. doi:10.1017/CBO9781107415324.004.

[88] Wiedemann H. Particle accelerator physics. Springer; 2015.

[89] Cleland MR. INDUSTRIAL ACCELERATORS AND THEIR APPLICATIONS., 2016.

[90] Itikawa Y. Molecular Processes in Plasmas. 2007. doi:10.1007/978-3-540-72580-0.

[91] David B. Williams CBC. Transmission Electron Microscopy. 2009. doi:doi:10.1201/9781420007800-c6.

[92] Pimblott SM, LaVerne JA. Production of low-energy electrons by ionizing radiation. Radiation Physics and Chemistry 2007;76:1244–7. doi:10.1016/j.radphyschem.2007.02.012.

[93] Schou J. Transport theory for kinetic emission of secondary electrons from solids by electron and ion bombardment. Nuclear Instruments and Methods 1980;170:317–20. doi:10.1016/0029-554X(80)91032-0.

[94] Opal CB, Peterson WK, Beaty EC. Measurements of Secondary-Electron Spectra Produced by Electron Impact Ionization of a Number of Simple Gases. The Journal of Chemical Physics 1971;55:4100–6. doi:10.1063/1.1676707.

[95] Jenkins TM, Nelson WR, Rindi A. Monte Carlo transport of electrons and photons. vol. 38. Springer Science & Business Media; 2012.

[96] Tartar A. Monte Carlo simulation of 10MV photon beams and beam profile validations. Measurement 2013;46:3026–31. doi:10.1016/j.measurement.2013.06.015.

[97] Hogstrom KR, Mills MD, Almond PR. Electron beam dose calculations. Physics

in Medicine and Biology 1981;26:445–59. doi:10.1088/0031-9155/26/3/008.

[98] Plante L, Cucinotta FA. Cross sections for the interactions of 1 eV-100 MeV electrons in liquid water and application to Monte-Carlo simulation of HZE radiation tracks. New Journal of Physics 2009;11. doi:10.1088/1367-2630/11/6/063047.

[99] Emfietzoglou D, Karava K, Papamichael G, Moscovitch M. Monte Carlo simulation of the energy loss of low-energy electrons in liquid water. Online 2003;48:2355–71.

[100] Kadri O, Ivanchenko VN, Gharbi F, Trabelsi A. GEANT4 simulation of electron energy deposition in extended media. Nuclear Instruments and Methods in Physics Research, Section B: Beam Interactions with Materials and Atoms 2007;258:381–7. doi:10.1016/j.nimb.2007.02.088.

[101] Llovet X, Powell CJ, Salvat F, Jablonski A. Cross Sections for Inner-Shell Ionization by Electron Impact. Journal of Physical and Chemical Reference Data 2014;43. doi:10.1063/1.4832851.

[102] Kurucz CN, Waite TD, Cooper WJ. The Miami Electron Beam Research Facility: a large scale wastewater treatment application. Radiat Phys Chem 1995;45:299–308.

[103] Gehringer P, Eschweiler H. Electron beam dosimetry in aqueous flow systems. Radiation Physics and Chemistry 2002;63:735–8. doi:10.1016/S0969-806X(01)00606-5.

[104] Woods, R. J., & Pikaev, A. K. (1993). Applied radiation chemistry: radiation

processing. John Wiley & Sons.

[105] Milinchuk VK (Viktor K, Tupikov VI (Valentin I, Kemp TJ (Terence J. Organic Radiation Chemistry Handbook. E. Horwood; 1989.

[106] Kimura A, Osawa M, Taguchi M. Decomposition of persistent pharmaceuticals in wastewater by ionizing radiation. Radiation Physics and Chemistry 2012;81:1508–12. doi:10.1016/j.radphyschem.2011.11.032.

[107] Lin K, Cooper WJ, Nickelsen MG, Kurucz CN, Waite TD. Decomposition of aqueous solutions of phenol using high energy electron beam irradiation - a large scale study. Appl Radiat Isot 1995;46:1307–16. doi:10.1016/0969-8043(95)00236-7.

[108] Duarte CL, Sampa MHO, Rela PR, Oikawa H, Silveira CG, Azevedo AL. Advanced oxidation process by electron-beam-irradiation-induced decomposition of pollutants in industrial effluents. Radiation Physics and Chemistry 2002;63:647–51. doi:10.1016/S0969-806X(01)00560-6.

[109] Schwarz HA, Draganić IG, Draganić ZD, Draganic IG, Draganic ZD. The Radiation Chemistry of Water. Radiation Research 1972;51:209. doi:10.2307/3573657.

[110] Wu MH, Liu N, Xu G, Ma J, Tang L, Wang L, et al. Kinetics and mechanisms studies on dimethyl phthalate degradation in aqueous solutions by pulse radiolysis and electron beam radiolysis. Radiation Physics and Chemistry 2011;80:420–5. doi:10.1016/j.radphyschem.2010.10.008.

[111] El Omar AK, Schmidhammer U, Jeunesse P, Larbre J-P, Lin M, Muroya Y, et al.

Time-Dependent Radiolytic Yield of OH • Radical Studied by Picosecond Pulse Radiolysis. The Journal of Physical Chemistry A 2011;115:12212–6. doi:10.1021/jp208075v.

[112] Lukes P, Locke B, Brisset J. Aqueous- Phase Chemistry of Electrical Discharge Plasma in Water and in Gas–Liquid Environments. Plasma Chemistry and … 2012.

[113] Benziger SB. Reaction of Hydroxyl Radical With Aromatic Hydrocarbons 2010.

[114] Orlovskii VM. Modification of Liquid Hydrocarbons Irradiated by a Nanosecond E-Beam n.d.:272–4.

[115] Dewhurst HA. Radiation Chemistry of Organic Compounds. I. n-Alkane Liquids 1957;61:1466–71.

[116] Manion J, Burton M. Radiolysis of Hydrocarbon Mixtures. Journal of Physical Chemistry 1952;56:560–9.

[117] Tabuse S, Izumi Y, Kojima T, Yoshida Y, Kozawa T, Miki M, et al. Radiation protection effects by addition of aromatic compounds to n -dodecane. Radiation Physics and Chemistry 2001;62:179–87.

[118] LaVerne JA, Dowling-Medley J. Combinations of Aromatic and Aliphatic Radiolysis. Journal of Physical Chemistry A 2015;119:10125–9. doi:10.1021/acs.jpca.5b07414.

[119] T. Gaumann JH. Aspects of Hydrocarbon Radiolysis. 1968.

[120] Butler J. Radiation chemistry of hydrocarbons. International Journal of Radiation Biology 1982;41:701–2. doi:10.1080/09553008214550821.

[121] Kondoh T, Yang J, Norizawa K, Kan K, Yoshida Y. Femtosecond pulse radiolysis study on geminate ion recombination in n-dodecane. Radiation Physics and Chemistry 2011;80:286–90. doi:10.1016/j.radphyschem.2010.07.049.

[122] Wu G, Katsumura Y, Matsuura C, Ishigure K, Kubo J. Radiation Effect on the Thermal Cracking of n -Hexadecane. 1. Products from Radiation-Thermal Cracking. Industrial & Engineering Chemistry Research 1997;36:3498–504. doi:10.1021/ie970025f.

[123] Mirkin G, Zaykina RF, Zaykin YA. Radiation methods for upgrading and refining of feedstock for oil chemistry. Radiation Physics and Chemistry 2003;67:311–4. doi:10.1016/S0969-806X(03)00058-6.

[124] Jonah CD, Rao BSM. Radiation chemistry: present status and future trends. vol. 87. Elsevier; 2001.

[125] Zaikin YA. Low-temperature radiation-induced cracking of liquid hydrocarbons. Radiation Physics and Chemistry 2008;77:1069–73. doi:10.1016/j.radphyschem.2008.07.001.

[126] Zaikin Y, Zaikina R. Petroleum radiation processing. CRC Press; 2013.

[127] Makuuchi K, Cheng S. Radiation processing of polymer materials and its industrial applications. John Wiley & Sons; 2012.

[128] Cardoso ECL, Lugão AB, Andrade E Silva LG. Crosslinked polyethylene foams, via eb radiation. Radiation Physics and Chemistry, vol. 52, 1998, p. 197–200. doi:10.1016/S0969-806X(98)00139-X.

[129] Dias DB, de Andrade e Silva LG. Polyethylene foams cross-linked by electron

beam. Radiation Physics and Chemistry 2007;76:1696–7. doi:10.1016/j.radphyschem.2007.02.089.

[130] T. Gaumann JH. Aspects of Hydrocarbon Radiolysis. New York: Academic Press; 1968.

[131] Arai H, Nagai S, Matsuda K, Hatada M. Radiolysis of methane by electron beam irradiation over wide ranges of dose and dose rate. Radiation Physics and Chemistry 1981;17:217–21. doi:10.1016/0146-5724(81)90334-4.

[132] Arai H, Nagai S, Matsuda K, Hatada M. Effect of irradiation temperature on the radiolysis of methane. Radiation Physics and Chemistry 1981;17:151–7. doi:10.1016/0146-5724(81)90265-X.

[133] Wu G, Katsumura Y, Matsuura C, Ishigure K, Kubo J. Radiation Effect on the Thermal Cracking of n -Hexadecane. 2. A Kinetic Approach to Chain Reaction. Industrial & Engineering Chemistry Research 1997;36:3498–504. doi:10.1021/ie970025f.

[134] Technical C, Company NO. PROTECTION IN RADIOLYSIS OF n-HEXADECANE-2 . RADIOLYSIS OF n-HEXADECANE IN THE PRESENCE OF ADDITIVES 1992;40:451–9.

[135] Aske N, Kallevik H, Sjöblom J. Determination of saturate, aromatic, resin, and asphaltenic (SARA) components in crude oils by means of infrared and near-infrared spectroscopy. Energy and Fuels 2001;15:1304–12. doi:10.1021/ef010088h.

[136] Trejo F, Centeno G, Ancheyta J. Precipitation, fractionation and characterization

of asphaltenes from heavy and light crude oils. Fuel 2004;83:2169–75. doi:10.1016/j.fuel.2004.06.008.

[137] Pereira JSF, Moraes DP, Antes FG, Diehl LO, Santos MFP, Guimarães RCL, et al. Determination of metals and metalloids in light and heavy crude oil by ICP-MS after digestion by microwave-induced combustion. Microchemical Journal 2010;96:4–11. doi:10.1016/j.microc.2009.12.016.

[138] Duyck C, Miekeley N, Porto da Silveira CL, Aucélio RQ, Campos RC, Grinberg P, et al. The determination of trace elements in crude oil and its heavy fractions by atomic spectrometry. Spectrochimica Acta - Part B Atomic Spectroscopy 2007;62:939–51. doi:10.1016/j.sab.2007.04.013.

[139] Alfi M, Barrufet MA, Moreira RG, Da Silva PF, Mullins OC. An efficient treatment of ultra-heavy asphaltic crude oil using electron beam technology. Fuel 2015;154:152–60. doi:10.1016/j.fuel.2015.03.040.

[140] Nadirov NK, Zaykin YA, Zaykina RF. Progress in high viscosity oil and natural bitumen refining by ionizing irradiation. Proceedings of the International Conference on Oil and Bitumens, Kazan, vol. 4, 1994, p. 1638–42.

[141] Zaykina RF, Zaykin YA, Mirkin G, Nadirov NK. Prospects for irradiation processing in the petroleum industry. Radiation Physics and Chemistry 2002;63:617–20. doi:10.1016/S0969-806X(01)00653-3.

[142] Thesis A, Yang D. Heavy Oil Upgrading From Electron Beam (E-Beam) Irradiation Heavy Oil Upgrading From Electron Beam (E-Beam) Irradiation 2009.

[143] Laboratory NET. A Literature Review on Cold Cracking of Petroleum Crude Oil Energy Policy Act of 2005 Section 1406 2006:30.

[144] Zaki AA, El-Gendy NA. Removal of metal ions from wastewater using EB irradiation in combination with HA/TiO2/UV treatment. Journal of Hazardous Materials 2014;271:275–82. doi:10.1016/j.jhazmat.2014.02.025.

[145] Mason RL, Gunst RF, Hess JL. Statistical design and analysis of experiments: with applications to engineering and science. vol. 474. John Wiley & Sons; 2003.

[146] Design E. Statistics – Textbook Experimental Design 2015.

[147] Anderson JE, Kim BR, Mueller SA, Lofton T V. Composition and analysis of mineral oils and other organic compounds in metalworking and hydraulic fluids. Critical Reviews in Environmental Science and Technology 2003;33:73–109. doi:10.1080/10643380390814460.

[148] Mehrotra AK. A generalized viscosity equation for liquid hydrocarbons: Application to oil-sand bitumens. Fluid Phase Equilibria 1992;75:257–68. doi:10.1016/0378-3812(92)87022-F.

[149] Ely JF, Hanley HJM. Prediction of transport properties. 1. Viscosity of fluids and mixtures. Industrial & Engineering Chemistry Fundamentals 1981;20:323–32. doi:10.1021/i100004a004.

[150] Clough RL, Gillen KT, Malone GM, Wallace JS. Color formation in irradiated polymers 1996;48:583–94.

[151] Toriyama K, Iwasaki M, Nunome K. ESR studies of irradiated methane and ethane at 4.2 K and mechanism of pairwise trapping of radicals in irradiated

alkanes. The Journal of Chemical Physics 1979;71:1698–705. doi:10.1063/1.438508.

[152] Raghuvanshi SK, Ahmad B, Siddhartha, Srivastava AK, Krishna JBM, Wahab MA. Effect of gamma irradiation on the optical properties of UHMWPE (Ultra-high-molecular-weight-polyethylene) polymer. Nuclear Instruments and Methods in Physics Research, Section B: Beam Interactions with Materials and Atoms 2012;271:44–7. doi:10.1016/j.nimb.2011.11.001.

[153] Wallace JS, Sinclair MB, Gillen KT, Clough RL. Color center annealing in gamma-irradiated polystyrene under vacuum and air atmospheres. Radiat Phys Chem 1993;41:85–100.

[154] Jess A. Mechanisms and kinetics of thermal reactions of aromatic hydrocarbons from pyrolysis of solid fuels. Fuel 1996;75:1441–8.

[155] Li CZ, Nelson PF. Fate of aromatic ring systems during thermal cracking of tars in a fluidized-bed reactor. Energy and Fuels 1996;10:1083–90. doi:10.1021/ef960054n.

[156] Data JCE, Doi AA, Caudwell DR, Trusler JPM, Vesovic V, Wakeham W a. Viscosity and Density of Five Hydrocarbon Liquids at Pressures up to 200 MPa and Temperatures up to 473 K Viscosity and Density of Five Hydrocarbon Liquids at Pressures up to 200 MPa and Temperatures up to 473 K † 2009:359–66. doi:10.1021/je800417q.

[157] Hogenboom DL. Viscosity of Several Liquid Hydrocarbons as a Function of Temperature, Pressure, and Free Volume. The Journal of Chemical Physics

1967;46:2586. doi:10.1063/1.1841088.

[158] Bair S. The high pressure rheology of some simple model hydrocarbons. Proceedings of the Institution of Mechanical Engineers, Part J: Journal of Engineering Tribology 2002;216:139–49. doi:10.1243/1350650021543960.

[159] Kierstead HA, Turkevich J. Viscosity and structure of pure hydrocarbons. The Journal of Chemical Physics 1944;12:24–7. doi:10.1063/1.1723875.

[160] Kanti M, Zhou H, Ye S, Boned C, Lagourette B, Saint-Guirons H, et al. Viscosity of liquid hydrocarbons, mixtures and petroleum cuts, as a function of pressure and temperature. The Journal of Physical Chemistry 1989;93:3860–4. doi:10.1021/j100346a097.

[161] Keizo and Cheng SM. Radiation Processing of Polymer Materials and Its Industrial Applications. 2012. doi:10.1002/9781118162798.ch1.

[162] Bader RFW, MacDougall PJ, Lau CDH. Bonded and Nonbonded Charge Concentrations and Their Relation to Molecular Geometry and Reactivity. Journal of the American Chemical Society 1984;106:1594–605. doi:10.1021/ja00318a009.

[163] Kubo, J., & Otsuhata, K. (1992). Inhibition of radiation degradation of polyolefins by hydroaromatics. International Journal of Radiation Applications and Instrumentation. Part C. Radiation Physics and Chemistry, 39(3), 261-268.

[164] Rodgers RC, Hill GE. Equations for vapour pressure versus temperature: Derivation and use of the antoine equation on a hand-held programmable calculator. British Journal of Anaesthesia 1978;50:415–24.

doi:10.1093/bja/50.5.415.

[165] Kudchadker AP, Zwolinski BJ. Vapor Pressures and Boiling Points of Normal Alkanes, C21 to C100. Journal of Chemical and Engineering Data 1966;11:253–5. doi:10.1021/je60029a039.

APPENDIX

MATLAB code to process GC-FID data and generate Sim Dist, conversion and yields plots are presented in appendix. Code used to process GC-MS data and TGA data are also attached here in this appendix. The rest of the plots are photos either taken with camera or cited from literature.

GC-FID data processing

```
%% load calibration data
clc;
close all;
clear;
Calnew=xlsread('new calibration 2019.xlsx');
CNo=Calnew(:,3);
T=Calnew(:,1);
BP=429.24*log(CNo)-631.55;
plot(T,CNo,'x-','linewidth',2)
% title ('GC Calibration')
ylabel('Carbon Number')
xlabel('time (min)')
set(gca,'xtick',[0:4:45])
set(gca,'ytick',[0:6:120])
set(gca,'fontweight','bold','fontsize',16);
grid on

%% load data
oldraw=xlsread('Treated 2016.xlsx','11082016','A:C');
Ebeam1_2016=xlsread('Treated 2016.xlsx','11082016','D:F');
Ebeam2_2016=xlsread('Treated 2016.xlsx','11292016','D:F');
newraw=xlsread('MO 2019.csv');
Ebeam1_2019=xlsread('Treated1108_2019.csv');
Ebeam2_2019=xlsread('Treated1129_2019.csv');
Ebeam3_2019=xlsread('Treated1213_2019.csv');
L=length(oldraw);
M(:,:,1) = oldraw(:,[1 3]);
M(:,:,2) = Ebeam1_2016(:,[1 3]);
```

```
M(:,:,3) = Ebeam2_2016(:,[1 3]);
M(:,:,4)=newraw(1:L,:);
M(:,:,5)=Ebeam1_2019(1:L,:);
M(:,:,6)=Ebeam2_2019(1:L,:);
M(:,:,7)=Ebeam3_2019(1:L,:);
names = {'Raw-2016','H80-2016','H145-2016','Raw-2019','H80-2019','H145-
2019','M85-2019'};
colors ={'k';'r';'b';'k';'r';'b';'g'};
figure
plot(oldraw(:,1),oldraw(:,3),newraw(:,1),newraw(:,2),'linewidth',2)
legend('raw-2016','raw-2019')
xlim([0 35])
%%
dt = 0.05;
Time = [5:dt/10:35];
dcmfactor=[1;1;1;1;1;1;1;1;1;1;1];
for j = 1:7;
    if j<=3
    x = M(:,1,j)+1.2;
    y = M(:,2,j);
    y2= interp1(x,y,Time);
    y2(isnan(y2)) = 0;
    y2(y2<=0)==0;
    M3(:,j) = y2;
    else
    x = M(:,1,j);
    y = M(:,2,j);
    y2= interp1(x,y,Time);
    y2(isnan(y2)) = 0;
    y2(y2<=0)==0;
    M3(:,j) = y2;
    end
end
figure
plot(Time,M3(:,:),'Linewidth',2)
legend(names)
xlabel('Time (min)')
ylabel('Mineral oil sample signal (pA)')
xlim([5,35])
ylim([0,12000])
```

```
set(gca,'fontweight','bold','fontsize',16)
grid on
%%
figure
CarbNo = interp1(T,CNo,Time);
h=plot(CarbNo,M3,'linewidth',2);
set(h,{'color'},colors)
xlim([10,60])
xticks(10:5:60)
ylim([0,12000])
xlabel('Carbon Number');
ylabel('Sample signal (pA)');
legend(names)
set(gca,'fontweight','bold','fontsize',16);
set(gcf,'Position',[100 100 600 400])
grid on
%% integration

TimeToStartIntegration =5; % min
TimeToEndIntegration=35; % min
ind1 = min(find(Time>TimeToStartIntegration));
ind2=max(find(Time<TimeToEndIntegration));
CarbNo = interp1(T,CNo,Time(1:ind2));
CNStartInt = interp1(T,CNo,TimeToStartIntegration);
CNEndInt=interp1(T,CNo,TimeToEndIntegration);
Int = cumtrapz(Time(1:ind2),M3(1:ind2,:));
Int2 = Int - Int(ind1,:);
TotalInt = Int2(end,:);
IntNorm = Int2./TotalInt;
IntNorm(Time<TimeToStartIntegration,:) = 0;
IntNorm(isnan(IntNorm))=0;
figure
h=plot(Time(1:ind2),IntNorm(:,:)*100,'linewidth',2)
% hold on
% plot([0 80],[1 1],'--')
set(h,{'color'},colors);
xlabel('Time (min)')
ylabel('percentage boiled off')
ylim([-.1,101])
legend(names)
```

```
set(gca,'fontweight','bold','fontsize',14);
grid on

err=IntNorm(:,1)-IntNorm(:,4);
plot(Time(1:ind2),err)
IntNorm(:,1:3)=IntNorm(:,1:3)-0.5*err;
IntNorm(:,4:7)=IntNorm(:,4:7)+0.5*err;
IntNorm(IntNorm<=0)==0;
%% Sim Dist plot
BP=(429.24*log(CarbNo)-631.55-32)/1.8;
figure
h=plot(CarbNo,IntNorm*100,'linewidth',2)
set(h,{'color'},colors)
xlabel('Carbon number')
ylabel('Boiled off (wt.%)')
ylim([0,101])
yticks(0:10:100)
xlim([5, 60])
legend(names)
set(gca,'fontweight','bold','fontsize',14);
set(gcf,'Position',[100 100 600 400])
grid on
figure
i=1;
j=3;

h=plot(BP,IntNorm(:,i:j)*100,'linewidth',2);
set(h,{'color'},colors(i:j))
xlabel('Boiling point (C)')
ylabel('Boiled off (wt.%)')
ylim([0,101])
yticks(0:10:100)
xlim([150, 600])
xticks(150:50:600)
legend(names(i:j));
set(gca,'fontweight','bold','fontsize',14);
set(gcf,'Position',[100 100 600 400])
grid on
%% distribution
Cval = [10:1:80];
```

```
for ii = 2:length(Cval)
   m=0;
   for jj =1:7
      m=m+1;
      y = IntNorm(:,jj);
      v1 = interp1(CarbNo,y,Cval(ii-1));
      v2 = interp1(CarbNo,y,Cval(ii));
      pctbelowCN(ii,m) = v2-v1;
   end
end
tval=[5:0.25:35];
for ii = 2:length(tval)
   m=0;
   for jj = 1:7
      m=m+1;
      y = IntNorm(:,jj);
      v1 = interp1(Time(1:ind2),y,tval(ii-1));
      v2 = interp1(Time(1:ind2),y,tval(ii));
      pctbelowt(ii,m) = v2-v1;
   end
end

i=1;
j=3;
figure
h=bar(Cval,pctbelowCN(:,i:j)*100)
set(h,{'facecolor'},colors(i:j))
legend(names(i:j))
xlim([10,45])
xticks(10:5:45);
yticks(0:2.5:22.5);
ylim([0,22.5])
xlabel('Carbon number')
ylabel('Percentage (wt.%)')
set(gca,'fontweight','bold','fontsize',14);
set(gcf,'Position',[100 100 1000 400]);
grid on
%% conversion plot
c={'r';'b';'g';'k'};
figure
```

```
h=bar(Cval,(pctbelowCN(:,2)-pctbelowCN(:,1))*100,'facecolor','r')
legend(names(2))
ylabel('Change (wt.%)')
xlim([10,60])
xticks([10:5:60])
xlabel('Carbon number');
ylim([-8,3])
yticks(-8:1:3)
set(gca,'fontweight','bold','fontsize',14)
set(gcf,'Position',[100 100 600 400]);
grid on
figure
h=bar(Cval,(pctbelowCN(:,3)-pctbelowCN(:,1))*100,'facecolor','b')
legend(names(3))
ylabel('Change ( wt.%)')
xlim([5,60])
xticks([5:5:60])
xlabel('Carbon number');
ylim([-8,3])
yticks(-8:1:3)
set(gca,'fontweight','bold','fontsize',14)
set(gcf,'Position',[100 100 600 400]);
grid on
figure
bar_handle=bar(Cval,(pctbelowCN(:,7)-pctbelowCN(:,4))*100,'facecolor','g')
legend(names(7))
ylabel('Change ( wt.%)')
xlim([5,60])
xticks([5:5:60])
xlabel('Carbon number');
ylim([-8,3])
yticks(-8:1:3)
set(gca,'fontweight','bold','fontsize',14)
set(gcf,'Position',[100 100 600 400]);
grid on

%% yields
N1=10;
N2=80;
SE=[0 500 530 0 500 530 300]; % kJ/kg
```

```
Mass=[0 0.97145 1.825 0 0.97145 1.825 1.83];% kg
Q=SE.*Mass; %kJ
E_eV=Q.*6.242e21; %eV
for ii=1:7
   if ii<=3
changefromraw(:,ii)=(pctbelowCN(:,ii)-pctbelowCN(:,1))*100;
   else
changefromraw(:,ii)=(pctbelowCN(:,ii)-pctbelowCN(:,4))*100;
   end
end
figure
plot(Cval,changefromraw(:,2:3),'Linewidth',2);
xlabel('Carbon number');
ylabel('Change from raw (%)');
ylim([-7.5,5]);
yticks(-7.5:0.75:5);
xlim([N1,N2]);
legend(names(2:3));
set(gca,'fontweight','bold','fontsize',16);
set(gcf,'Position',[100 100 600 500]);
grid on
figure
plot(Cval,changefromraw(:,5:7),'Linewidth',2);
xlabel('Carbon number');
ylabel('Change from raw (%)');
ylim([-7.5,5]);
yticks(-7.5:0.75:5);
xlim([N1,N2]);
legend(names(2:3));
set(gca,'fontweight','bold','fontsize',16);
set(gcf,'Position',[100 100 600 500]);
grid on

C_CC=N1:1:N2;
MW=(C_CC*12+(2*C_CC+2))';
for ii=1:7
change_CC(:,ii)=interp1(Cval,changefromraw(:,ii),C_CC);
conversion(:,ii)=sum(change_CC(:,ii));
end
for ii=1:7
```

```
    yields(:,ii) = 0.01*change_CC(:,ii).*Mass(1,ii)./MW.*6.022e26./E_eV(:,ii);
end
for ii=1:7
    totalsci(:,ii)=sum(yields(1:12,ii));
    totalgrow(:,ii)=sum(yields(17:68,ii));
    totalreduc(:,ii)=sum(yields(13:16,ii))
end
smallcarbon=sum(pctbelowCN(1:12,:))*100;
midcarbon=sum(pctbelowCN(13:16,:))*100;
largecarbon=sum(pctbelowCN(17:68,:))*100;
%% yields plot

figure
h=plot(C_CC,yields(:,7),'-','Linewidth',2);
xlabel('Carbon number');
ylabel('Yields (Molecules/eV)');
set(h,{'color'},colors(7));
xlim([10 50])
xticks(10:2:50)
ylim([-0.04,0.015]);
yticks(-0.04:0.005:0.015);
legend(names(7));
set(gca,'fontweight','bold','fontsize',16);
set(gcf,'Position',[100 100 800 500]);
grid on
```

GC-MS data processing

```
%% load data
clc
clear
close all

[~,sheets1] = xlsfinfo('Raw GCMS.xlsx');
[~,sheets2] = xlsfinfo('Ebeam GCMS.xlsx');
num_sheets1 = length(sheets1);
num_sheets2=length(sheets2);
data1 = cell(num_sheets1, 1);
for K = 1 : num_sheets1
```

```
  data1{K} = xlsread('Raw GCMS.xlsx', sheets1{K});
end
data2 = cell(num_sheets2, 1);
for K = 1 : num_sheets2
  data2{K} = xlsread('Ebeam GCMS.xlsx', sheets2{K});
end
names={'Raw';'Treated'};
mames={'Cyclohexane';'New compounds'};
%% GC data
GC_raw=data1{7};
GC_em=data2{1};
figure
plot(GC_raw(:,1),GC_raw(:,2),'b','linewidth',2)
xlabel('Time (min)')
ylabel('Intensity')

legend('Raw Cyclohexane')
%ylim([2e6 1e10])
xlim([1 12])
hold on
plot(GC_em(:,1),GC_em(:,2),'r','linewidth',2)
set(gca,'fontweight','bold','fontsize',14)
set(gcf,'Position',[100 100 600 400])
ylim([2e6 1e10])
xlim([1.25 12])
xticks(1.25:0.25:12)
legend('Ebeam Cyclohexane')
%% find GC peaks
time1=linspace(1.25,12,10/0.01);
GC(:,1)=interp1(GC_raw(:,1),GC_raw(:,2),time1,'pchip');
GC(:,2)=interp1(GC_em(:,1),GC_em(:,2),time1+0.55,'pchip');
for i=1:2
[pk,lk,w,p]=findpeaks(GC(:,i),time1,'MinPeakHeight',1e7,'MinPeakDistance',0.02
);
Peaks{:,i}=pk;
Lks{:,i}=lk;
Widths{:,i}=w;
Proms{:,i}=p;
   parea{:,i}=pk.*w';

end
```

```
for i=1:2
  for j=1:length(Peaks{:,i})
   PKstart(j,i)=Lks{1,i}(1,j)-2*Widths{1,i}(1,j);
   PKend(j,i)=Lks{1,i}(1,j)+2*Widths{1,i}(1,j);
  end
end
for i=1:2
   for j=1:length(Peaks{:,i})
      t{j,i}=linspace(PKstart(j,i),PKend(j,i),(PKend(j,i)-PKstart(j,i))/0.001);
      baselinestart(j,i)=interp1(time1,GC(:,i),PKstart(j,i));
      baselineend(j,i)=interp1(time1,GC(:,i),PKend(j,i));
   end
end
for i=1:2
   for j=1:length(Peaks{:,i})
     eachpeak{j,i}=interp1(time1,GC(:,i),t{j,i});
   end
end
for i=1:2
tarea(:,i)=sum(parea{:,i});
perarea{:,i}=parea{:,i}./tarea(:,i)*100 % area percent of each peak
if i==2
rawarea(:,i)=sum(perarea{:,i}(1:2));
newarea(:,i)=100-rawarea(:,i);
else
rawarea(:,i)=sum(perarea{:,i});
newarea(:,i)=100-rawarea(:,i);
end
end
%% plot GC peaks
for i=1:2
subplot(2,1,i)
plot(time1,GC(:,i),'color','b','Linewidth',1)
hold on
plot(Lks{:,i},Peaks{:,i},'o','markersize',4,'color','r')
% for j=1:length(Peaks{1,i})
% plot([PKstart(j,i) PKend(j,i)],[baselinestart(j,i) baselineend(j,i)],'r')
% end
 ylim([1e6 1e10])
```

```
xlim([1.25 12])
xlabel('Time (min)')
ylabel('Intensity')
legend('GC of the Sample ','Each compound')
set(gca,'fontweight','bold','fontsize',14)
set(gcf,'Position',[100 100 800 600])
grid on
end


figure
bar(Lks{:,1},perarea{:,1},'edgecolor','r','facecolor','r')
%bar(Lks{:,2},perarea{:,2},'edgecolor','r','facecolor','r')
xlim([1.25 12])
xlabel('Time (min)')
ylabel('Percentage (%)')
ylim([0.01 100])
yticks(0:5:100)
set(gca,'fontweight','bold','fontsize',14)
%set(gca,'yscale','log')
legend(names(1))
grid on


matrix=[rawarea;newarea]';
figure
h=bar(matrix,'stacked','edgecolor','b')
set(h,{'facecolor'},{'b';'r'})
hold on
%xlabel('Compouds')
ylabel('Percentage (%)')
ylim([0.01 100])
yticks(0:5:100)
set(gca,'fontweight','bold','fontsize',14)
set(gca,'xticklabel',names)
set(gcf,'Position',[100 100 600 400])
legend(mames)
grid on
```

TG and DTG data processing

```
%% load data
clc;
close all;
clear;

RawMChexane=xlsread('raw methylcyclohexane 05102019.xlsx','A41:C500');
RawChexane=xlsread('raw cyclohexane 05082019.xlsx','A41:C500');
RawEbenzene=xlsread('raw ethylbenzene 05102019.xlsx','A41:C500');
RawTetralin=xlsread('raw Tetralin 05102019.xlsx','A41:C500');
RawToluene=xlsread('raw Toluene 05102019.xlsx','A41:C500');
% RawBenzene=xlsread('raw Benzene 05102019.xlsx','A41:C500');
RawMnaphthalene=xlsread('raw Methylnaphthalene 05102019.xlsx','A41:C500');

EbeamMChexane=xlsread('Ebeam methylcyclohexane
05102019.xlsx','A41:C500');
EbeamChexane=xlsread('Ebeam Cyclohexane 05102019.xlsx','A41:C500');
EbeamEbenzene=xlsread('Ebeam ethylbenzene 05102019.xlsx','A41:C500');
EbeamTetralin=xlsread('Ebeam Tetralin 05102019.xlsx','A41:C500');
EbeamToluene=xlsread('Ebeam Toluene 05102019.xlsx','A41:C500');
EbeamMnaphthalene=xlsread('Ebeam Methylnaphthalene
05102019.xlsx','A41:C500');

M{:,1}=RawMChexane;
M{:,2}=RawChexane;
M{:,3}=RawEbenzene;
M{:,4}=RawTetralin;
M{:,5}=RawToluene;
M{:,6}=RawMnaphthalene;

N{:,1}=EbeamMChexane;
N{:,2}=EbeamChexane;
N{:,3}=EbeamEbenzene;
N{:,4}=EbeamTetralin;
N{:,5}=EbeamToluene;
N{:,6}=EbeamMnaphthalene;
names1 = {'Raw Methylcyclohexane','Raw Cyclohexane','Raw
Ethylbenzene','Raw Tetralin','Raw Toluene','Raw Methylnaphthalene'};
names2 = {'Ebeam Methylcyclohexane','Ebeam Cyclohexane','Ebeam
Ethylbenzene','Ebeam Tetralin','Ebeam Toluene','Ebeam Methylnaphthalene'};
```

```
colors ={'r';'g';'b';'c';'y';'m'};

plot(M{:,2}(:,1),M{:,2}(:,3));
hold on
plot(N{:,2}(:,1),N{:,2}(:,3));
%% interpolate data

for i=1:6
   y = M{:,i}(:,2);
   inx=find(y>=31)
   S(i)=min(inx)
   time1{:,i}=M{:,i}(S(i):end,1)-M{:,i}(S(i),1);
   Tp1{:,i}=M{:,i}(S(i):end,2);
   w1{:,i}=M{:,i}(S(i):end,3);
end
dt = 0.05;
Time = [0.01:dt/10:36]';
for i=1:6
   x = time1{:,i};
   y = Tp1{:,i};
   z=w1{:,i};
   y2= interp1(x,y,Time);
   y2(isnan(y2)) = 0;
      z2= interp1(x,z,Time);
      z2(isnan(z2)) = 0;
Temp1(:,i) = y2;
Wt1(:,i)=z2;
end

for i=1:6
DTG1(:,i)=diff(Wt1(:,i))./diff(Time);
InitWeight1(i)=max(Wt1(1:P(i),i));
end

for i=1:6
   y = N{:,i}(:,2);
   inx=find(y>=31)
   S(i)=min(inx)
   time2{:,i}=N{:,i}(S(i):end,1)-N{:,i}(S(i),1);
   Tp2{:,i}=N{:,i}(S(i):end,2);
   w2{:,i}=N{:,i}(S(i):end,3);
```

```
end
for i=1:6
    x = time2{:,i};
    y = Tp2{:,i};
    z=w2{:,i};
    y2= interp1(x,y,Time);
    y2(isnan(y2)) = 0;
       z2= interp1(x,z,Time);
       z2(isnan(z2)) = 0;
Temp2(:,i) = y2;
Wt2(:,i)=z2;
end
InitWeight2=max(Wt2,[],1);
for i=1:6
DTG2(:,i)=diff(Wt2(:,i))./diff(Time);
end
for j=1:6
   inx1=find(Temp1(:,j)==0);
  inx2=find(Temp2(:,j)==0);
   P(j)=min(inx1)-1;
  Q(j)=min(inx2)-1;
end
for j=1:6
   inx3=find(DTG1(:,j)==0);
   inx4=find(DTG2(:,j)==0);
   R(j)=min(inx3)-5;
   V(j)=min(inx4)-5;
end
%% TG plot

for i=6
figure
yyaxis left
plot(Time,100-Wt1(:,i)./InitWeight1(i)*100,'-b','Linewidth',2)
hold on
plot(Time,100-Wt2(:,i)./InitWeight2(i)*100,'-r','Linewidth',2)
xlabel('Time (min)')
ylabel('Weight loss (%)')
xlim([0.1 35])
ylim([0,102])
```

```
yticks(linspace(0,102,11))
set(gca,'fontweight','bold','fontsize',16,'ycolor','k')
yyaxis right
plot(Time(1:P(i)),Temp1(1:P(i),i),'--b','Linewidth',1.5)
hold on
plot(Time(1:Q(i)),Temp2(1:Q(i),i),'--r','Linewidth',1.5)
ylabel('Temperature (C)')
legend([names1(i),names2(i),'Temperature for Raw','Temperature for Ebeam'])
xlim([0.1,35])
ylim([20,350])
set(gca,'fontweight','bold','fontsize',16,'ycolor','k')
grid on
set(gcf,'Position',[100 100 700 500])
end

for i=6
figure
yyaxis left
plot(Time,100-Wt1(:,i)./InitWeight1(i)*100,'-b','Linewidth',2)
hold on
plot(Time,100-Wt2(:,i)./InitWeight2(i)*100,'-r','Linewidth',2)
xlabel('Time (min)')
ylabel('Weight loss (%)')
xlim([0.1,35])
ylim([0,102])
yticks(linspace(0,102,11))
set(gca,'fontweight','bold','fontsize',16,'ycolor','k')
yyaxis right
plot(Time(1:R(i)),DTG1(1:R(i),i),'--b','Linewidth',1.5)
hold on
plot(Time(1:V(i)),DTG2(1:V(i),i),'--r','Linewidth',1.5)
ylabel('DTG (wt.%)')
legend([names1(i),names2(i),'DTG for Raw','DTG for Ebeam'])
xlim([0.1,35])
ylim([-12 0])
yticks(linspace(-12,0,11))
set(gca,'fontweight','bold','fontsize',16,'ycolor','k')
grid on
set(gcf,'Position',[100 100 700 500])
end
```

```
%% DTG plot
for i=1:6
   pct1(:,i)=100-Wt1(:,i)./InitWeight1(i)*100 ;
   pct2(:,i)=100-Wt2(:,i)./InitWeight2(i)*100  ;
end
tval=[0.01:0.25:35];
for ii = 2:length(tval)
    m=0;
    for jj = 1:6
        m=m+1;
        y1 = pct1(:,jj);
        y2 = pct2(:,jj);
        v1 = interp1(Time,y1,tval(ii-1));
        v2 = interp1(Time,y1,tval(ii));
        pctbelowt1(ii,m) = v2-v1;
        v3 = interp1(Time,y2,tval(ii-1));
        v4 = interp1(Time,y2,tval(ii));
        pctbelowt2(ii,m) = v4-v3;

    end
end
for i=1:6
changet(:,i)=(pctbelowt2(:,i)-pctbelowt1(:,i));
inx=find(changet==0);
end
for i=1:6
figure
h=bar(tval,changet(:,i))
h.FaceColor='red';
legend(names2(i))
ylabel('Change from Raw %')
xlabel('Time (min)');
xlim([0,35])
xticks([0:2:35])
ylim([-3,5])
yticks(-3:0.5:5)
set(gca,'fontweight','bold','fontsize',16)
set(gcf,'Position',[100 100 700 500])
grid on
end
```

```
%% yields and conversion plot
SE=400; % kJ/kg
Mass=[18 17.58 18.79 23.7 21.22 28.34];% kg
Q=SE.*Mass; %kJ
E_eV=Q.*6.242e21; %eV

for ii=4
figure
bar(tval,changet(:,ii));
xlabel('Time (min)');
ylabel('Change from raw (%)');
ylim([-5,5]);
yticks(-5:0.5:5);
xlim([0.8 35]);
xticks(0.8:1:35)
legend(names1(ii));
set(gca,'fontweight','bold','fontsize',16);
grid on
inx(:,1)=[22 26];
inx(:,2)=[20];
inx(:,3)=[39];
inx(:,4)=[23 65];
inx(:,5)=[31];
inx(:,6)=[78];
end
HCratio=[2.5 2 2 1.25 1.2 1.14 0.91];
setuDe=[1 0.875 0.8571 0.5556 0.5455 0.5001 0.4171];
reduction=[-10 -9.3 -27.1 -8.24 -5.2 -4.45 -5];
production1=[3.5 1.6 0 0.05 0.24 0 0.07 ];
production2=[4 7.73 27.1 8.1 5.1 4.2 4.9];
carbons=[5 7 6 8 10 7 11];
normprod=production2./carbons;
plot(setuDe,production1,'p','markersize',15,'markerfacecolor','k');
text(setuDe,production1,['Pentane',names2],'fontsize',14,'fontweight','bold')
hold on
xlabel('Saturation degree');
ylabel('Production of small products (wt.%)');
ylim([0 3.5]);
yticks(0:0.35:3.5);
xlim([0.35 1.1]);
```

```
xticks(0.35:0.1:1)
set(gca,'fontweight','bold','fontsize',16);
set(gcf,'Position',[100 100 700 500])
grid on
```